The molecular basis of enhanced glucose transporter, SGLT1, expression in the diabetic intestine

Thesis submitted in accordance with the requirements of the University of Liverpool for the degree of Doctor in Philosophy

Rasha Abdulrahman Alshali

January 2014

CONTENTS

LIST OF FIGURES

Chapter 1:

Chapter 3:

Chapter 4:

Chapter 5:

Chapter 6:

LIST OF TABLES

LIST OF ABBREVIATIONS

APS	Ammonium persulphate
ATP	Adenosine triphosphate
BBM	Brush border membrane
BBMV	Brush border membrane vesicles
BLM	Basolateral membrane
bp	base pair
BSA	Bovine serum albumin
cAMP	3',5'-cyclic adenosine monophosphate
CCK	Cholecystokinin
cDNA	Complementary DNA
CHO	Carbohydrate
cpm	counts per minute
Cy3	Cyanine dye 3
DAPI	4'6-diamidino-2-phenylindole
ddH_2O	"Double-distilled" water - nuclease free
DM	Diabetes mellitus
DMSO	Dimethyl sulphoxide
DNA	deoxyribonucleic acid
DNase	deoxyribonuclease
dNTP	Deoxyribose nucleotide triphosphate
DTT	Dithiothreitol
ECL	Enhanced chemiluminescence
EDTA	Ethylene diamine tetraacetic acid
EE cell	Enteroendocrine cell
FITC	Fluorescein isothiocyanate
GGM	Glucose-galactose malabsorption
GI	Gastrointestinal
GIP	Glucose-dependent insulinotropic peptide
GLP-1	Glucagon-like peptide 1
GLP-2	Glucagon-like peptide 2
GLP-2R	Glucagon-like peptide 2 receptor
GLUT	Facilitated glucose transporter
GPCR	G-protein coupled receptor
HEPES	4-(2-hydroxyethyl)-1-piperazineethanesulfonic acid
IPTG	Isopropyl β-D-1-thiogalactopyranoside
Kbp	Kilobase pair
kDa	kiloDalton
LB	Lysogeny Broth
mRNA	Messenger RNA
NADP	Nicotinamide adenine dinucleotide phosphate
NADPH	Reduced nicotinamide adenine dinucleotide phosphate
NCBI	National Center for Biotechnology Information
PAC1	PACAP receptor 1
PACAP	Pituitary adenylate cyclase-activating peptide

PBS	Phosphate buffered saline
*p*CMB	*p*-Chloromercuribenzoate
PCR	Polymerase chain reaction
PLCβ2	Phospholipase C-β2
PMSF	Phenylmethanesulfonyl fluoride
PNMF	post-nuclear membrane fractions
PVDF	Polyvinyl difluoride
PYY	Peptide YY
qPCR	Quantitative PCR (i.e. real-time PCR)
RNA	ribonucleic acid
RNase	ribonuclease
RP2	RNA Polymerase 2
rpm	Revolutions per minute
rRNA	Ribosomal RNA
RT	Reverse transcriptase
RT-PCR	Reverse transcriptase polymerase chain reaction
SDS	Sodium dodecyl sulphate
SDS-PAGE	Sodium dodecyl sulphate polyacrylamide gel electrophoresis
SEM	standard error of the mean
SGLT1	Sodium/glucose cotransporter 1
SI	Small intestine
SOB	Super optimal broth
SOC	Super optimal broth, modified for “catabolite repression”
T1R1	Type 1 taste receptor, member 1
T1R2	Type 1 taste receptor, member 2
T1R3	Type 1 taste receptor, member 3
T2R	Type 2 taste receptor
Taq	DNA polymerase originally isolated from *Thermus aquaticus*
TEMED	Tetramethylethylenediamine
Tm	Melting temperature
Tris	Tris (hydroxymethyl) aminomethane
Triton X-100	octyl phenoxy polyethoxyethanol
TRPM5	Transient receptor potential melastatin 5
TTE	Tris-TAPS-EDTA
Tween-20	polyxyethylene (20) sorbitan monolaureate
UV	ultraviolet
VIP	Vasoactive Intestinal Polypeptide
V_{max}	Maximum velocity
VPAC1	VIP/PACAP receptor 1
X-gal	5-bromo-4-chloro-3-indolyl-β-D-galactoside

ACKNOWLEDGEMENTS

I would never have been able to finish my thesis without the guidance of my supervisor, help from friends and support from my family and my husband.

It gives me a great pleasure in acknowledging my PhD supervisor Professor *Soraya Shirazi-Beechey* for all her help, advice and encouragement and for assisting me to achieve my goals and for her willingness and patience to read and correct my writing. She has been my caring friend and guide in social life and academic career.

My thanks go to my second supervisor Dr *A. Ellis*, the Consultant Gastroenterologists (The Royal Liverpool Hospitals) for providing the human intestinal biopsies and for clinical advice; and the Consultants in Surgery at the Department of Gastroenterology (The University Hospital, Jeddah, Saudi Arabia) Dr. Sibiany, Dr. Fallata, Dr. Akbar and the other staff for proving the human duodenal samples. Thanks also go to Dr. Djouhri, and Miss Dermody (The University of Liverpool) for providing the rats.

I would like to thank the financial support from the Saudi Ministry of Higher Education and King Abdulaziz University for funding this study.

I would like to express my deepest gratitude to my lab colleagues: *Drs. Kristian Daly, Andi Moran, Sheila Ryan, Galina Burdyga, Dan Batchelor, Daleep Arora, Miran Al-Rammahi* and fellow PhD student *Darren Weatherburn* for their academic and technical assistance with my research and their welcoming friendship. Special thanks goes to contributors to this thesis: *Andi* for some data on RNA assessment using quantitative PCR, *Galina* for some of the immunohistochemical work, and *Kristian* for all his counsel.

I dedicate this thesis to my husband, *Ahmed Alnowailaty*, for his love, encouragement whenever I needed for achieving success, despite difficulties and being away during my years of study. Most importantly, I am most grateful to my parents, *Sameera* and *Abdulrahman*, for their warm support and prayers, and my kids, Jana and Aboody, for their love and patience during my stressful times, my brothers *Raed* and *Rayan*, and my sister *Shatha* for their affection.

ABSTRACT

Background:

Dietary carbohydrates are hydrolyzed in the small intestine ultimately, by the brush-border membrane disaccharidases (sucrase, maltase and lactase) into monosaccharides: D-glucose, D-galactose and D-fructose. D-glucose and D-galactose are transported across the brush border membrane (BBM) from the intestinal lumen into enterocytes by the Na^+- dependent glucose transporter 1, SGLT1, while D-fructose is transported by GLUT5. These monosaccharides, exit the cell across the baso-lateral membrane (BLM) into the systemic circulation via the facilitated monosaccharide transporter, GLUT2. SGLT1 regulation is vital for the provision of glucose to the body and for maintaining glucose homoeostasis. The expression and activity of SGLT1 are adaptively regulated by dietary sugars in most species studied. The intestinal capacity to absorb glucose is maintained via basal level of SGLT1 expression. However, this capacity becomes limited when the luminal carbohydrates exceed a threshold level, leading to up-regulation of SGLT1.

Previous work in our laboratory has shown that luminal sugar concentration, when above a threshold, is detected by the intestinal glucose sensor, consisting of two subunits, Taste 1 receptor 2 (T1R2) and 3 (T1R3) expressed in enteroendocrine L-cells. This activates a pathway, in endocrine cells, leading to secretion of the gut hormone glucagon like peptide 2 (GLP-2), known to up-regulate SGLT1 expression. Binding of GLP-2 to its receptor on the enteric neurons induces a neuronal response evoking secretion of vasoactive intestinal peptide (VIP) and/or Pituitary adenylate cyclase-activating polypeptide (PACAP) by sub-mucosal plexus. Binding of VIP/PACAP to their receptor VPAC1 (VIP and PACAP receptor type 1) on the basolateral membrane of absorptive enterocytes leads to increased concentration of intracellular cAMP which in turn enhances the half-life of *SGLT1* mRNA, increasing the number of SGLT1 proteins per enterocytes.

In diabetes, the intestinal capacity for glucose absorption is enhanced complicating the aetiology of the disease. This enhanced expression is independent of either luminal sugar and blood glucose concentrations or insulin levels.

The work in this thesis was aimed at identify molecular basis of enhanced SGLT1 expression in the diabetic intestine using intestinal tissues from rats with experimentally induced diabetes and biopsies from the intestine of human diabetics. The data indicate that increased SGLT1 expression is due to dysregulation of pathway controlling SGLT1 expression.

Summary of work carried out in this thesis:

In the duodenum of diabetic patients, maltase activity was higher by 2 fold, and *SGLT1* mRNA expression was increased by 3-fold compared to that in healthy individuals. SGLT1 protein was expressed on the BBM of enterocytes on the entire villus in the duodenum of both diabetics and healthy subjects, with relatively stronger staining on the BBM lining the villi of the diabetic intestine. However, no expression was observed in the crypts. The experimental data support that the enhanced SGLT1 expression and glucose absorption in the intestine of diabetic humans with non-insulin dependent diabetes mellitus (NIDDM) is attributable to more enterocytes expressing SGLT1, but mostly due to a specific increase in the number of SGLT1 protein per each enterocyte.

The changes in body and small intestinal parameters brought about by diabetes were assessed in streptozotocin-induced diabetic rats. They had a loss in body weight, while showed an increase in the small intestinal weight and length compared to that in control rats. Intestinal villi were longer in the diabetic rats compared to that in controls. This was accompanied by higher activities of intestinal BBM enzymes (maltase, sucrase and alkaline phosphatase) compared to that in the controls. These changes were more pronounced in the mid and distal small intestine.

Rat intestinal SGLT1 activity and expression were determined using glucose transport studies, western blot analysis, quantitative RT-PCR and immunohistochemistry. There was a significant increase in SGLT1 activity and expression, at mRNA and protein levels, in the diabetic intestine compared to that in controls. In the proximal intestine of control and diabetic rats, SGLT1 protein was expressed on the BBM of enterocytes of entire villus, whereas, in the mid and distal small intestine, SGLT1 expression was limited to the upper villus region in control rats; the expression was extended to the lower villus in diabetics. However, in both groups negligible SGLT1 detection was found in the crypts.

The basolateral membrane monosaccharide transporter, GLUT2 was exclusively expressed on the BLM of enterocytes in the intestine of both control and diabetic rats. GLUT2 protein was absent in BBMV isolated from the intestine of control and diabetic rats rejecting the controversial proposition that GLUT2 protein is trafficked to the BBM in the diabetic intestine. The data however, demonstrated the exclusive role of GLUT2 in glucose transport across the BLM. *GLUT2* mRNA expression was significantly elevated in the intestine of diabetic rats compared to that in controls, suggesting that there is an enhanced increase in trans-cellular glucose transport from the intestinal lumen into circulation in diabetes.

The magnitude of changes in the villus length and the activity of BBM marker enzymes were not entirely correlated with the enhanced expression and function of SGLT1 in the diabetic rat intestine; suggesting that the enhanced glucose absorption in the mid and lower villus of diabetic intestine is due to a combination of more SGLT1 expression per cell, and more cells supporting SGLT1 expression; the latter being due to additional SGLT1 transporters being expressed on the BBM of immature enterocytes of lower villus.

Potential changes in key signaling molecules involved in SGLT1 upregulation were investigated, whenever possible in human and rat intestinal tissues. In the diabetic intestine, the intestinal glucose sensor, T1R2-T1R3 was expressed in the enteroendocrine cells, with no change in the expression pattern at either mRNA or protein levels. The pro-glucagon gene, encoding for gut hormones GLP-1 and -2, was also unchanged, as well as the expression of the receptor for GLP-2 on the enteric neurons. However, GLP-2 secretion was significantly higher in the intestine of diabetic rats, and was independent of the concentration of luminal glucose. In the diabetic intestine of both humans and rats there were significant increases in the expression of the neuropeptides VIP and PACAP at mRNA and protein levels, compared to that in controls.

Conclusion:

The expression of intestinal glucose transporter, SGLT1, is enhanced in the diabetic intestine due to increased secretion of i) GLP-2 from enteroendocrine cells (diabetic rat) and ii) VIP from enteric neurons (diabetic rats and humans).

Chapter 1

Introduction

INTRODUCTION

For healthy living of all organisms, oxygen and nutrition are the basic requisites for growth and function. What we consume from the natural dietary resources is converted into simple molecules to nourish, energize, protect, build and renew cells and tissues of our body. Carbohydrates, proteins, fats, vitamins and minerals provide the body with energy and building blocks. However, glucose is the basic fuel-supplying nutrient, which is the most required, other essential nutrients like fatty acids, amino acids, purine and pyrimidine bases have structural roles, while minerals and vitamins are needed in minute amounts. For the utilization of these ingested dietary components, the digestive system transfers the food into gastrointestinal lumen to be digested with the help of enzymes and hormones. Then, nutrients are absorbed across the intestinal wall to the systemic circulation to be delivered to body tissues and cells.

1. The human digestive system:

1.1. The gross anatomy of the digestive system

The digestive system is composed of two groups of organs: the gastrointestinal tract (GIT) and the accessory organs. The GIT, or alimentary canal, is a tube consists of connected hollow organs extending from the oral cavity to the anus. The GIT includes: mouth, pharynx, oesophagus, stomach, small intestine and large intestine ending at the anal canal. These structures have overlapping functions, but each region has distinctive histological characteristics for specialized role. The accessory organs include: teeth and tongue, salivary glands, liver, gallbladder and pancreas. Apart from the tongue and teeth, these organs are not in direct contact with the food contents but they assist in food digestion by producing and delevering their secretions and hormones into the GIT.

In the mouth, or the oral cavity, the teeth help in chewing the foodstuff and the tongue manipulates food for mastication before swallowing and its upper surface is covered by the sensory taste buds. The salivary glands produce saliva, which lubricates the mouth and secrete salivary amylase, which mixed with food to start the digestion of carbohydrates. Food bolus passes through the pharynx and esophagus to reach the stomach, which further mixes and grinds food along with some food digestion by pepsin and hydrochloric acid. The stomach releases the mixed gastric chyme into the intestine at a rate appropriate for digestion and absorption.

The small intestine

The small intestine (SI) is a convoluted narrow canal, which can be as long as 9 metres in adult human cadaver, but it is shorter in living human due to the smooth muscular tone. It extends from the pylorus of the stomach to the ileocaecal valve and subdivided into three structural segments: duodenum, jejunum and ileum. There is no distinct demarcation between the jejunum and ileum, but characteristic changes appear gradually between regions.

The small intestine is the major site of digestion and absorption, where the luminal contents are mixed with the pancreatic juice, bile and mucosal digestive enzymes. The mechanical peristalsis moves the content through the small intestinal length toward the large intestine.

- The duodenum constitutes the proximal 25-30 cm that is the widest and shortest region of the SI occupied between the pylorus to the ligament of Treitz. Mucus secreting glands (Brunner's glands) are exclusively found in the duodenum to facilitate the mechanical breakdown of nutrients. Anatomically, the duodenum has C-shape that is divided into four portions: superior, descending, horizontal, and ascending. The secretions from the pancreas, liver and gall bladder are released via the pancreatic and the bile ducts, which join the second part of the duodenum.
- The jejunum is around 2.5 meters long in the mid intestine. It has wider luminal diameter and more vascular and thicker wall than the ileum due to the mucosal membrane folding (*Plicae circularis*, or valves of Kerckring), which becomes smaller and less numerous distally in the small intestine and totally absent in the distal ileum (Ross *et al.*, 2003).
- The ileum is two-to-three meters long of freely mobile coils attached to the posterior abdominal wall by the mesentery, like the jejunum, but it is less vascular and narrower than the jejunum. It ends by joining the large intestine at the ileocecal junction (Tortora and Derrickson, 2006).

1.2. Specialized histological features of the small intestine

The wall of the gastrointestinal tract from the lower oesophagus to the anal canal is basically composed of four-layered tissues, as shown in figure 1. They are arranged from inner to outer (deep to superficial) surface: mucosa, submucosa, muscularis externa and serosa. However, there are some local characteristic differences for each functional region along the small intestinal length (Tortora and Derrickson, 2006).

***Figure 1:* Three-dimension view of the four tissue layers of the small intestinal wall**

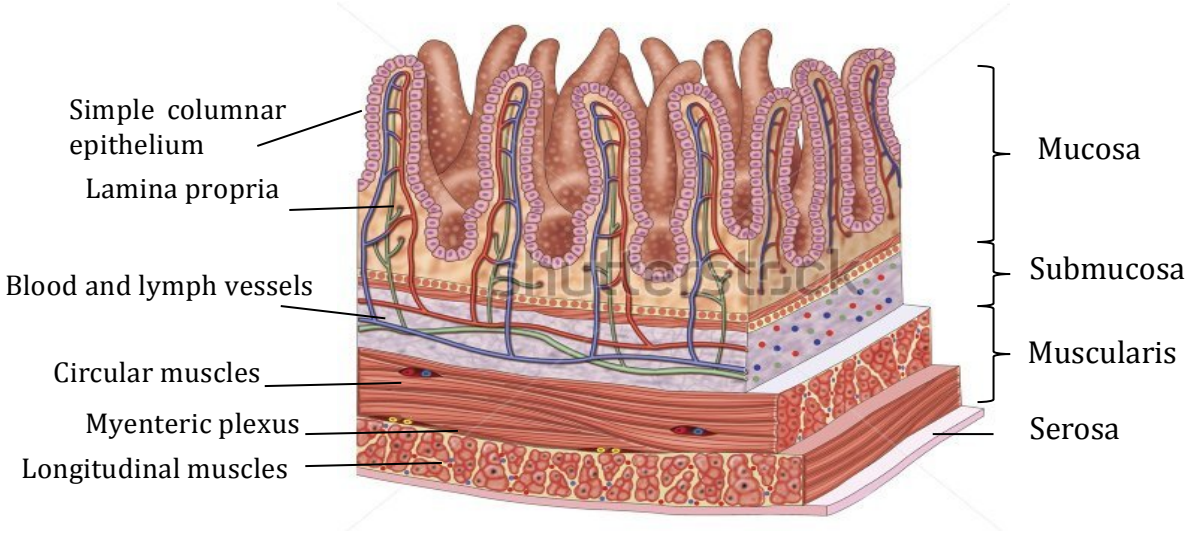

The wall of the small intestine is composed of four layers of tissues: deep (luminal) to superficial surface: mucosa, submucosa, muscularis and serosa (taken with permission from Tortora and Derrickson, 2006).

The layers of the small intestinal wall:

1. The mucosa is the innermost mucus membrane consisting of simple columnar epithelium layer including the absorptive enterocytes, the enteroendocrine cells and the goblet cells. The lamina propria is loose connective tissue contains blood and lymphatic vessels plus the mucus and a thin layer of smooth muscles. It also contains secretory cells of the Brunner's glands in the duodenum for moisturising (Martini *et al.*, 2001), and the mucosa-associated lymphatic tissue (MALT) cells, which has a role in protection and immunity (Tortora and Derrickson, 2006). The muscularis mucosa is a thin layer of smooth muscle fibres arranged in two sheets: inner-circular layer (encircles the lumen) and outer-longitudinal layer (oriented parallel to the long axis of the GIT). The contractions of those muscles alter the shape of the lumen and move the epithelial folds.
2. The submucosa is a dense connective tissue layer containing blood and lymphatic vessels plus the submucosal neuronal network of sensory and autonomic nerve fibers known as the submucosal Meissner's plexus .
3. The muscularis externa are two sheets of smooth muscle layers: inner-circular and outer-longitudinal muscles fibres. They are innervated by the myenteric plexus (Auerbach's) of autonomic nerves to perform involuntary contractions for the movement of the luminal contents along the tract toward the distal ileum.
4. The serosa is the outermost thin layer of serous membrane covering the whole tract except the oesophagus and the distal rectum (Martini *et al.*, 2001, Ganong, 2003).

The luminal surface of the small intestine has special features characterized by circular mucosal folds (*plicae circulares*), 10 mm long, and finger-like projections protruding into the gut lumen (villi), 0.5 to 1 mm long with a number of 20-40 per mm^2. Additionally, the microvilli on the apical side of each absorptive cell massively expand the epithelial surface area about 600 times for the adaptation of intestinal nutrient absorption. Each villus is covered by epithelial cells and has a core of lamina propria, smooth muscle cells, and lacteal lymphatic and blood capillary networks. These villi vary in their length and shape in different regions; they are leaf-like in the duodenum, while they are larger and more numerous in the jejunum. Therefore, the absorptive surface area is much greater in the duodenum and jejunum than the ileum. The ileum is also characterized by Peyer's patches, which are consisting of aggregated lymphatic nodules. These nodules originate in the lymph tissues of the lamina propria and reach the mucosal surface where the villi are absent (Atlas of human histology by Fiore, M., 1981). These villi are separated from each other by simple tubular crypts (crypts of Lieberkühn).

1.3. The Microstructure of the small intestinal epithelial cells

The intestinal epithelium is capable of fast repair and regeneration to replace the damaged cells due to the harsh luminal environment. Progenitor undifferentiated stem cells in the intestinal crypts proliferate and differentiate into subtypes of epithelial cells covering the villi. The four main cell lineages include: absorptive enterocytes, secretory enteroendocrine cells, mucus-secreting goblet cells and Paneth cells (Schmidt *et al.*, 1985, Freeman, 2008). Figure 2 displays the different cell types of intestinal epithelium, their shapes and distribution along the crypt/villus axis. Near the base of the crypts, in between the villi, the Paneth cells migrate downward to the crypt base, whereas, other cells migrate upward to the villus tip where they undergo apoptosis and shed into the lumen of the intestine. This leads to complete cell renewal every 2-3 days in mice (Ferraris and Diamond, 1993), 3-4 days in sheep (Attaix and Meslin, 1991) and 3-5 days in human small intestine (Junqueira and Carneiro, 1971).

***Figure 2:* The shape and distribution of epithelial cell types lining the small intestine**

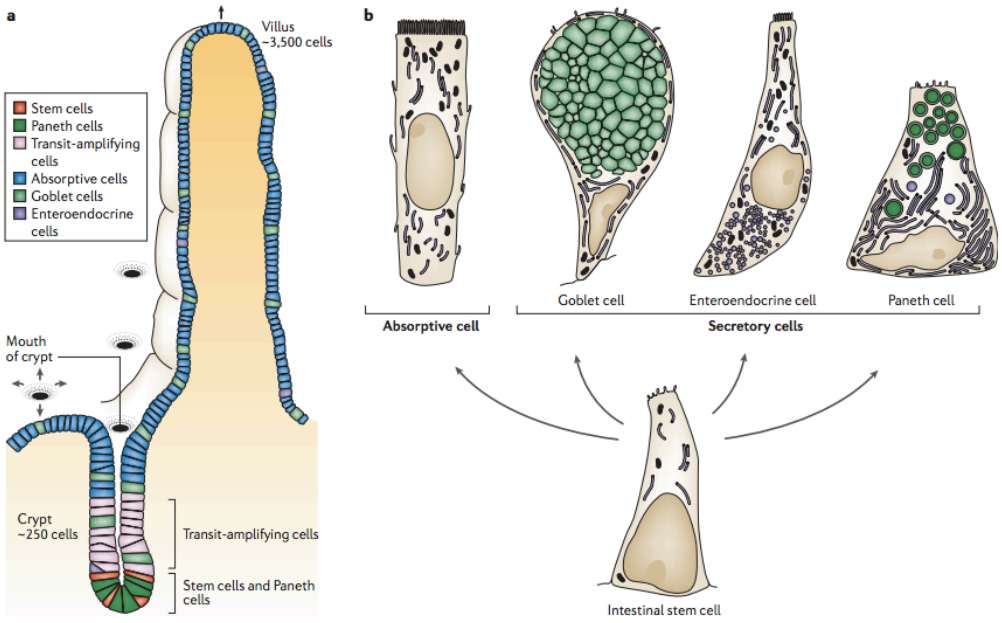

The stem cell near the crypt base gives rise into microarrays of intestinal epithelial cells. a) the distribution of the cell types along the villus. b) the shape of different mucosal cell types in the small intestine (taken with permission from Crosnier et al., 2006).

1.3.1 The absorptive cells (enterocytes)

The absorptive cells (enterocytes) are the predominant cell type of the intestinal mucosal lining, comprising 90 % of the total epithelial population. The enterocytes are simple columnar cells responsible for the absorption of digested nutrients and ions from the gut lumen into the bloodstream (Cheng and Leblond, 1974b). Adjacent enterocytes are firmly oriented and closely apposed with tight junctions, where the membranes actually fuse and no gaps between cells at the apical part. However, membranes appear adjacent or separated at the basal side of the cells. Figure 3 shows the structure of the enterocytes, the nucleus and Golgi apparatus occupy the basal part of the cell, while the rough endoplasmic reticulum and the lysosomes are in the apical part. The cytoplasmic membrane of the enterocyte has two domains, which are separated by tight junctions: the luminal/apical and the basal domains.

The brush-border membrane (BBM) is on the apical side of the cell having microvilli on its surface and facing the intestinal lumen. While the basolateral membrane (BLM) is on the serosal and lateral sides of the cell facing the systemic circulation (Madara *et al.*, 1981). The BBM exhibits distinctive packed array of microvilli, each about 1 µm in high and 0.1-0.2 µm in width, which serve a huge

expanded surface area for intestinal absorption. The microvilli are covered by glycocalyx and stiffened by fibrils bundle. Enterocytes contain blood vessels and lacteal lymphatic capillary inside, and enzymes and nutrient transporters are implemented on the luminal side of the membrane. The low fluidity of this membrane increases its stability and reduces the passive permeability. On the opposite side, the BLM is similar to the plasma membrane of other cells. It differs from the BBM in its cholesterol/lipid composition.

These membranes have different thickness, about 1 or 1.5 µm thick, different surface charges and properties that facilitate the pure isolation of brush-border and basolateral membrane vesicles (Shirazi-Beechey *et al.*, 1990), as discussed in a later section.

About 300 cells to each villus per day are newly generated from the stem cells in the intestinal crypt (Wright, 2006). These cells migrate along the crypt/villus axis to reach the villus tip during their lifespan for continuous turnover of the enterocyte (Thomson *et al.*, 1994, Cheng and Leblond, 1974b). During the migration of the enterocyte, it undergoes maturation and differentiation, which result in modification in the structure and composition of the cytoplasmic membrane. Hence, the cell becomes able to maintain an electrochemical gradient to develop its digestive and absorptive activity.

***Figure 3:* A diagram of the absorptive cell in the small intestine (Enterocyte)**

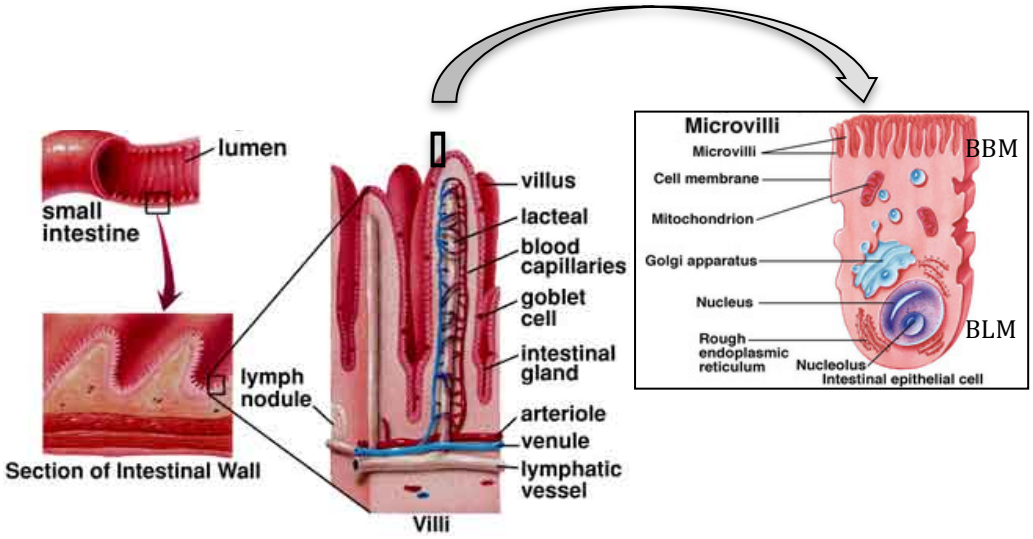

Diagram shows the histological structure of enterocytes lining the intestinal mucosa. (taken with permission from After L. R. Johnson, ed., Physiology of the Gastrointestinal Tract, Raven Press, 1981).

1.3.2 The goblet cells

These goblet-shaped cells are glandular simple columnar cells having microvilli on their apical membrane and found scattered along the villi between the enterocytes. They secrete glycoproteins, known as mucins, to moisturize the mucosal epithelial surface and to protect the microvilli from abrasion. They are more abundant in the ileum than the duodenum, but also present in the large intestine (Specian and Oliver, 1991, Ross *et al.*, 2003).

1.3.3 The enteroendocrine cells (EECs)

These are specialised epithelial cells sparsely distributed along the villus between the enterocytes. In total, they form the largest endocrine organ in the body although they only represent < 1% of the intestinal epithelium (Sternini *et al.*, 2008). The EECs are flask shaped with a prolonged narrow apical domain that is directly in contact with the luminal contents. More than twenty subtypes of the EECs have been identified according to their endocrine secretions 'peptide hormones' which are produced in response to the changes in the luminal components. These secretions either influence neighbouring enterocytes or exert effects on distant tissues or activate the vagal and enteric afferents neurons to control the gastrointestinal physiological functions and gut-brain sensing for the coordination of food intake. Some of these hormones act distally and are known as incretins that promote pancreatic insulin secretion and regulate food intake (Cheng and Leblond, 1974a, Rehfeld, 1998, Rindi *et al.*, 2004, Miguel-Aliaga, 2012). Enteroendocrine cells are known to be responsible for the chemosensing pathways of the intestinal tract, as discussed later.

There are various types of endocrine cells, for examples: K-cells, I-cells, L-cells, S-cells, G-cells and others. K-cells are predominantly found in the duodenum and secrete glucagon-dependent insulinotrophic peptide (GIP). L-cells are found scattered throughout the small and large intestine, highly numerous in the distal ileum and colon than the jejunum and duodenum (Mortensen *et al.*, 2003, Eissele *et al.*, 1992), they secrete glucagon-like peptides (GLP-1 and GLP-2) and hormone peptide YY (PYY). I-cells secrete cholecystokinin (CCK) and S-cells or the enterochromaffin cells secrete serotonin (Breer *et al.*, 2012).

However, the EECs are classified into 'open type' and 'closed type' cells. The 'closed type' cells are not in direct contact with the luminal environment due to the epithelial tight junctions. In contrast, 'open type' cells are considered the key intestinal chemosensory cells as they have apical microvilli allowing them to detect and recognize the dietary constitutes in the lumen.

1.3.4 The Paneth cells

These are pyramidal-shaped cells with large coarse granules pushing the nucleus toward the cell base. Paneth cells are found in the base of the crypts throughout the intestine. They secrete antimicrobial substances like peptidases, α-defensins, zinc, lysosomal enzymes e.g lysozyme, which regulate the microbial population of the intestinal microflora (Ouellette *et al.*, 2000, Shirazi-Beechey *et al.*, 2011a).

1.4. The enteric nervous system (ENS)

The enteric nervous system (ENS) is a broad network of neurons in the wall of the gastrointestinal tract from the oesophagus to the anus. In the small intestine, as seen in figure 4, the ENS is subdivided into two plexuses: the submucosal plexus, which lies within the submucosa, and the myenteric plexus, which is located between the two muscle sheets of the muscularis layer (Sasselli *et al.*, 2012). The ENS is the main division of the autonomic nervous system that governs the function of the digestive tract independently of the central nervous system, although, it normally communicates with the central nervous system through the vagus nerve and the prevertebral ganglia (Furness, 2008). The ENS coordinates gut reflexes and motility, controls exocrine and endocrine secretions and gut hormones, blood flow, water and electrolyte transport, and regulates the immune and inflammatory processes (Hansen, 2003).

More than 30 functional types of enteric neurons are present that secrete an intimidating array of about 25 different neurotransmitters. Most neurons utilize several transmitters and neuromodulators like acetylcholine and norepinephrine, which have stimulatory and inhibitory effects, respectively, on the gut functions and activity. Others include: serotonin, dopamine, cholecystokinin, substance P, vasoactive intestinal polypeptide and somatostatin (McConalogue and Furness, 1994, Galligan *et al.*, 2000).

***Figure 4:* The ENS is subdivided into two plexuses in the small intestine**

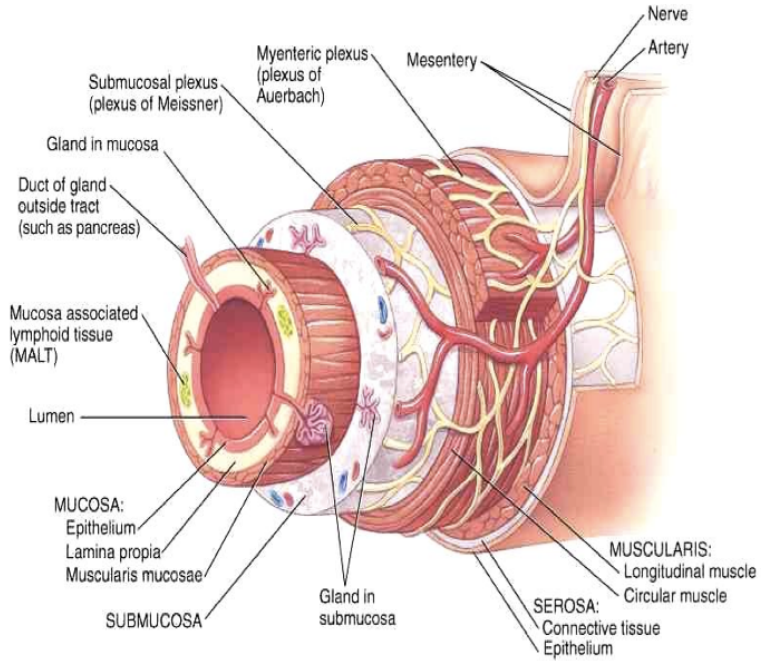

The enteric nervous sysytem includes two main plexi. An inner submucosal plexus resides within the submucosal layer; and an outer myenteric plexus lies between the longitudinal and circular muscle layers (taken with permission from Tortora and Derrickson, 2006).

2. Functions of the small intestine

2.1. Digestion of dietary components:

Different nutritional materials have energetic and structural roles supplying the body with fuel for energy-needed activities and providing the building blocks for tissue growth and repair processes. Carbohydrates are needed for body energy storage like starch and glycogen; provide structural support like cellulose in the plants and chitin in the extra-skeleton of arthropods, spiders, fungi and yeast (Hamid *et al.*, 2013) and serve as a blood major carbohydrate energy storage like trehalose in the insects (Becker *et al.*, 1996). To obtain the benefit of nutrition, the digestive system extracts the nutrients from what we eat through digestion and absorption processes.

2.1.1. Carbohydrate digestion

Dietary carbohydrates (CHO) are organic compounds also known as saccharides. They are divided, depending on the backbone number of sugar molecules, into monosaccharides, disaccharides, oligosaccharides and polysaccharides. Monosaccharides naturally exist as sugars: glucose in honey, galactose in dairy products and fructose in many fruits. Disaccharides include: maltose, sucrose and lactose. Maltose is found in germinating grain; sucrose is

present in sugar beet, table sugar and sugar cane, while lactose is the main carbohydrate in human and other mammalian milk. Polysaccharide like starch is found in bread, corn and potatoes, while the cellulose is a complex indigestible plant fibre.

Among monosaccharides, glucose is a principle metabolite in nutrition; it forms the unit component of all the other short and long chain polysaccharides. It's chemical formula is $C_6H_{12}O_6$ that is mainly abundant as natural sugars in grape, honey, starch and some fruits. Glucose is the main essential carbohydrate metabolite, especially for the glucose-dependent tissues like the brain and red blood cells. Hence, it is required for normal physiological functions in all the living organisms. Glucose is metabolized by the cells to generate ATP (the energy generating molecule). However, glucose can also be provided by gluconeogenesis or from the breakdown of glycogen.

Digestion is the mixing of food with enzymes and the mechanical and chemical breakdown of the nutrients into their smallest molecular structures capable of being absorbed. In the mouth, starch digestion begins where it is broken down into maltose by the salivary α-amylase secreted from the salivary glands, although its action is inhibited by the low pH in the stomach. In the duodenum, the presence of fats and proteins evokes the release of cholecystokinin (CCK) that stimulates the release of pancreatic α-amylase to breakdown carbohydrates by hydrolysing α-1,4 linkages. This completes the digestion process of starch and oligosaccharides into disaccharides. In the small intestinal lumen, where the final stages of carbohydrate digestion occur, disaccharides are further hydrolysed by the brush-border membrane disaccharidases (maltase, sucrase and lactase) into their absorbable monosaccharides units (glucose, galactose and fructose). However, the plant cellulose is hydrolysed in the large intestine by the microbiota.

2.1.2. The digestive enzymes:

- **Disaccharidases:**

These are specific digestive enzymes synthesized by mucosal cells lining the intestinal wall. Intestinal disaccharidases are synthesized then anchored and expressed on the brush border membrane (BBM) of the enterocytes, therefore, they are considered BBM markers. Disaccharidases are glycoside hydrolases 'α-glucosidases' that catalyse disaccharides into the simplest sugar form, monosaccharide, to be absorbed via monosaccharide transporters. However, higher disaccharidase activities have been reported during pregnancy and lactation to adapt to the energy demands (Prieto *et al.*, 1994), and in diabetic animals when compared to normal non-diabetic groups (Martinez *et al.*, 2003).

Maltase enzyme (EC 3.2.1.20) is known by different names such as maltase-glucoamylase and alpha-1,4-glucosidase, and is encoded by the *MGAM* gene located on chromosome 7 (Nichols *et al.*, 2003). Maltase is synthesized as a single polypeptide chain and cleaved post-translationally by pancreatic proteases. It is predominantly present as a homodimeric complex that is anchored by the NH_2-terminal segment to the brush border membrane (Noren *et al.*, 1986).

Maltase splits maltose into the two constituent D-glucose molecules by breaking the glycosidic bond (α 1-4 bond) between the 'first' carbon of one glucose molecule and the 'fourth' carbon of the other glucose molecule. The hydrolysis rate is slower with increasing substrate size, thus it hydrolyses 1,6-α-D-glucose linkage at a slower rate (Sorensen *et al.*, 1982). Intestinal maltase also hydrolyses polysaccharides. The activity of mucosal maltase-glucoamylase and mucosal sucrase-isomaltase constitute the final steps of small intestinal digestion of the linear starch oligosaccharides to glucose. Thus, these enzymes play crucial role in starch digestion and prandial glucose homeostasis (Quezada-Calvillo *et al.*, 2007, Nichols *et al.*, 2009, Nichols *et al.*, 2003).

Sucrase enzyme (EC 3.2.1.48), also known as sucrose alpha-glucosidase, is encoded by the *SI* gene, which resides on chromosome 3q26 (Nichols *et al.*, 2003). Sucrase-isomaltase (SI) is synthesized intracellularly as a single-chain precursor protein (pro-sucrase-isomaltase) that undergoes rapid trimming in the rough endoplasmic reticulum, then, slowly transported to the Golgi where complex glycosylation occurs. Finally, when destined for the luminal side of the microvillus membrane, SI is cleaved extracellularly by the pancreatic proteases, trypsin or elastase, into its enzymatically active subunits sucrase and isomaltase (Hauri *et al.*, 1979, Hauri *et al.*, 1982, Conklin *et al.*, 1975). The two mature subunits are highly homologous and remain closely associated with each other by strong non-covalent ionic interactions (Naim *et al.*, 1988). Those two domains of the enzyme complex are folded similarly, which both reside on the same polypeptide, and the native folded state is referred to as a pseudo-dimer. Sucrase splits sucrose by hydrolysing the α-1,2 glycosidic linkages between glucose and fructose monomers (Hertel *et al.*, 2000).

Lactase enzyme (EC 3.2.1.23-62), also known as β-glycosidase complex or lactase-phlorizin hydrolase (LPH), is a member of the β-galactosidase family of enzymes. It is present predominantly along the brush border membrane of the enterocytes lining the small intestinal mucosa. It can be divided into five domains: (i) a 19 amino acid cleaved signal sequence; (ii) a large pro-domain that is not present in mature lactase; (iii) the mature lactase fragment; (iv) a hydrophobic anchor spanning the membrane; and (v) a short hydrophilic carboxyl terminus

(Mantei *et al.*, 1988). In humans, lactase is encoded by the LCT gene, which is localized to the second chromosome 2q21 (Harvey *et al.*, 1993). LPH is synthesized as a single-chain polypeptide precursor, prepro-LPH, that is cleaved in two sequential steps: firstly, amino acid signal sequence is cleaved in the endoplasmic reticulum resulting in pro-LPH (215-kDa), which is sent to the Golgi apparatus for terminal glycosylation. Secondly, two amino acids are cleaved by the luminal pancreatic protease, trypsin, to form mature LPH (160-kDa). It is anchored via the NH_2-terminal segment to the brush border membrane and oriented with an intracellular C-terminus and an extracellular N-terminus on the luminal surface of the membrane (Naim *et al.*, 1994, Zecca *et al.*, 1998).

The mature human enzyme comprises two catalytic glutamic acid sites: one for lactose hydrolysis, connected to Glu-1749, and one for phlorizin hydrolysis, connected to Glu-1273 (Skovbjerg *et al.*, 1981, Zecca *et al.*, 1998). Lactase is essential in the hydrolysis of lactose in milk into glucose and galactose monomers, as well as other beta-galactosides and beta-glucosides (Noren *et al.*, 1986, Conklin *et al.*, 1975).

Newborn humans have high levels of lactase expression that is down-regulated after weaning resulting in lower lactase expression in the small intestine. However, lactase deficiency causes the common symptoms of hypolactasia, or lactose intolerance. Some adults exhibit lactase persistence that is characterized by lactase activity that remains high in adulthood, in which mutation occurs outside the LCT gene, in the control region regulating its expression.

- **Alkaline phosphatase:**

Alkaline phosphatase (ALP) (EC 3.1.3.1) is a hydrolase enzyme responsible for the dephosphorylation (removing phosphate groups) of its substrate molecules including: proteins, nucleotides and alkaloids. It works in alkaline environment (Komoda *et al.*, 1981, Benham and Harris, 1979) and found in all body tissues but concentrated in bone, liver, bile duct, kidney, placenta and intestine.

The intestinal alkaline phosphatase (IAP) is anchored to the brush-border membrane of the enterocytes through a phosphatidylinositolglycan attached covalently to the C-terminal amino acid (Engle *et al.*, 1995). IAP has a crucial defense function in the gut by limiting bacterial trans-epithelial invasion and detoxifying luminal bacterial lipopolysaccharide (LPS). ALP prevents the bacterial endotoxin-induced inflammation by dephosphorylating and detoxifying the endotoxin component of LPS. LPS are found in the outer membrane of Gram-

negative bacteria and elicit strong immune responses in animals (Bates *et al.*, 2007, Vaishnava and Hooper, 2007). ALP enzyme has also a role in regulating the secretion of bicarbonate and adjusting the duodenal pH. It maintains intestinal homeostasis and monitors the absorption of lipids across the luminal membrane of enterocytes. Some dietary molecules like fat, protein, and carbohydrate modulate the expression and activity of intestinal ALP (Lalles, 2010, Goldberg *et al.*, 2008, Chen *et al.*, 2010).

2.1.3. Brush-border membrane markers and the use of Brush-border membrane vesicles (BBMV):

The brush border membrane (BBM) differs from the basolateral membrane (BLM) in its structure and composition of lipids and proteins. The BBM has characteristic arrays of transporters and digestive proteins, which can be used as specific membrane markers. The classical markers are listed in table 1.1, which can be assessed to identify the membrane domain and confirm the purity of membrane preparations.

Transport mechanisms of different nutrients across the membrane domains of the enterocytes, using *in vitro* techniques, can be accomplished by using purified BBM and the BLM selectively. These membranes form right-side-out vesicles (BBM) and mixed population of right-side-out and inside out vesicles (BLM). The pure isolation of membrane vesicles helps to characterize the role of the serosal and luminal surfaces of the intestinal mucosal lining.

***Table 1.1:* Some proteins of the brush border and the basolateral membranes in the small intestine:**

Membrane	***Protein***	***Function***
Brush-border membrane (BBM)	Sucrase Lactase Maltase Trehalase	Glycosidase
	Aminopeptidase A, N, W Carboxypeptidase γ-Glutamyl transferase	Peptidase
	Alkaline phosphatase Phosphodiesterase 1	Phosphatase
	Villin Glycoprotein	Structural
	Glucose/Galactose transporter (SGLT1)	Na^+-dependent transporter
	Fructose transporters (GLUT5) Cl^- transporter ATP-dependent H^+ & HCO_3 Neutral & basic amino acids transporter	Na^+-independent transporter
	Peptide transporters (PepT1)	H^+-dependent transporter
	Amino acid transporters	
	Na^+/H^+ exchanger and Na^+/SO_4^{2-} co-transporter (Gunther *et al.*, 1983)	
Basolateral membrane (BLM)	Na^+/K^+ ATPase Ca^{2+} ATPase	ATPase
	Ca^{2+}/Cl^- transporter	Ca^+-dependent transporter
	Neutral amino acids Monosaccharide transporter (GLUT2)	Na^+-independent transporter

Advantages of this BBMV isolation technique over other procedures used before:

Nutrient transport across the small intestinal epithelium has been studied using several *in vitro* methods employing segments of intestinal loops, everted sacs, inverted sleeves, sheets of intestinal tissue or isolated mucosal enterocytes (Fisher and Parsons, 1949, Wilson and Wiseman, 1954, Emoto *et al.*, 2000).

The study of intestinal transport mechanism was motivated with the ability to isolate separately pure cell membranes, which overcame the limitations of the previously used methods. The technique of isolating brush border membrane vesicles (BBMV) offers experimental benefits over the use of isolated intact whole cells or tissues as the latter lose their functional polarity upon isolation. Hence, it becomes possible to validate the role of each membrane in various intra- and extra-cellular conditions (Stevens *et al.*, 1984, Murer and Kinne, 1980, Hopfer *et al.*, 1973). The most important advantages of membrane vesicle preparation include:

1) Vesicles are almost free of cellular contamination by other organelles, facilitating the studies to identify the structure and function of pure membranes.
2) Vesicles are not 'alive' avoiding the restrictions of tissue survival, hence allowing transport studies across the BBM in the absence of oxygen.
3) Vesicles have negligible unstirred water layers as the mucus coat is removed from the membrane surface during vesicle preparation; that is very helpful for the study of active transport systems because they depend on the substrate concentration adjacent to the membrane (Barry and Diamond, 1984).
4) Membrane vesicles can be stored for long time in liquid nitrogen without detectable loss of transport activity, also short incubation time can be enough for the measurement of substrate uptake (Berteloot and Semenza, 1990).
5) Using vesicles enable to change and control the intra- and extra- cellular environment in experiments like the substrate and electrochemical gradients, unlike intact tissues and cells.
6) Pure BBMV eliminates the effect of sugar metabolism within the tissue and its paracellular shunt, which interfere with the results of transport studies (Stevens *et al.*, 1984).
7) When using difficult to obtain and limited human biopsies or animal samples, membrane vesicles reduce the number of experimental animals or human volunteers required, because little biological material is needed in each experiment, and more experiments can be performed and directly compared to obtain data for given enquiries.

In this study, brush border-membrane vesicles (BBMV) and post-nuclear membrane fractions (PNMF) were used. The method of selective purification of BBM from cellular homogenates of intestinal tissue was done by the cation precipitation procedure, as described by Schmitz *et al.* (1973) and Kessler *et al.* (1978), depending on the difference in surface membrane charge densities between the BBM, BLM and organelle membranes (Schmitz *et al.*, 1973, Kessler *et al.*, 1978). This is achieved by the incubation of the cellular suspension with Mg^{2+} or Ca^{2+}. The BBM surface has a negative charge density that allows the accommodation of both positive charges of the bivalent cations, like Mg^{2+} and Ca^{2+}. This property minimizes the Mg^{+2} cross-linking and hence reduces the aggregation of BBM fragments and their precipitation. The BLM and intracellular membranes, however, have a surface charge density that can incorporate only one of the positive charges of the bivalent cations, leading to cross-linking between two fractions and subsequent aggregation of the BLM fragments. By differential centrifugation, the intracellular and basolateral membranes are precipitated and separated from the brush border membranes.

Under optimized conditions of this rapid, simple and reliable procedure, BBM forms tightly sealed, oriented right-side-out vesicles with a diameter of 100-150 nm (Hearn *et al.*, 1981). These vesicles separate the intravesicular aqueous space from the suspending extravesicular medium and are impermeable to high-molecular weight compounds. Essentially the BBMV are stable, pure and free of contamination by basolateral, cytosolic and mitochondrial membranes. In studies of Na^{+}- dependent glucose uptake into BBMV, the lipid-permeable anion thiocyanate (SCN^{-}) is used to provide a membrane potential creating intravesicular negative charge to force the influx of Na^{+} ions, which co-transported with glucose molecules via SGLT1.

Previous studies have confirmed the characterisation and the integrity of the prepared vesicles by several independent methods like D-glucose uptake, electron-microscopic technique and immunological methods. The uptake studies with different conditions demonstrated that the vesicles retain the glucose carrier system in a sodium-dependent manner, which occurs in purified brush-border membranes (Hopfer *et al.*, 1973). Using the electron-microscope freeze-fracture method, asymmetrical distribution of particles was distinct on the two membranes allowing the orientation of the isolated membrane vesicles to be assessed (Haase *et al.*, 1978b, Aubry *et al.*, 1988, Venien *et al.*, 1988).

2.2. Absorption (carbohydrates):

Food passes from the stomach to the duodenum and is then moved along the small intestine by peristalsis. Absorption is the transport processes of the digested nutrients from the gut lumen into the bloodstream across the intestinal wall through the luminal and the serosal sides of the epithelial absorptive cells 'enterocytes'. Absorption of almost all nutrients, including water and electrolytes, minerals and vitamins and all the organic molecules like (monosaccharides, amino acids and fatty acids), takes place in the small intestine. They are absorbed either by passive facilitated diffusion or by active transport mechanisms via specific carrier proteins that are incorporated into the lipid bilayer membranes on the BBM and the BLM of the enterocytes.

2.2.1. Monosaccharide transporters (SGLT and GLUT families)

The transport of monosaccharide (glucose, galactose and fructose) across the lipid bilayer of the plasma membrane is mediated by two distinctive groups: the SGLT family (sodium-dependent glucose transporters) and the GLUT family (sodium-independent glucose transporters) (Wood and Trayhurn, 2003, Scheepers *et al.*, 2004).

SGLT family: More than 450 members of this gene family (sodium-dependent glucose transporters; encoded by gene *SLC5A*), also known as the sodium/substrate symporter family (SSSF), are now recognized in many species. This family of transporters are responsible for the classical model of active nutrient transport, energy-dependent, against their concentration gradient and with co-transportation of Na^+ ions. SGLT family members are expressed in different tissues to transport specific substrates with varying affinities (Turk and Wright, 1997). They include: the glucose transporters SGLT1 and SGLT2 and a glucose sensor SGLT3 (which transport glucose but not galactose in pigs)(Diez-Sampedro *et al.*, 2003), the transporters for myo-inositols and vitamins SGLT 4 and 6, anions (proteins SLC5A5 and SLC5A8), plus the mannose and fructose transporter SGLT5 and the high-affinity choline transporter (protein SLC5A7) (Michel *et al.*, 2006, Scheepers *et al.*, 2004, Wood and Trayhurn, 2003).

SGLT transporters are integral membrane proteins sharing a common core of 14 membrane-spanning α-helices with hydrophobic extracellularly located N- and C-termini (Turk and Wright, 1997). They are all approximately 60-80 kDa proteins. In humans, there are 11 recognized members of *SLC5* genes (Wright and Turk, 2004).

- SGLT1 (encoded by gene *SLC5A1*) is highly expressed in the small intestine for glucose/galactose absorption; it will be discussed in a separate section in details.

- SGLT2 is more abundant on the BBM in the S1 and S2 segments in the proximal convoluted tubules of the kidney; it is responsible for renal glucose reabsorption (Wright, 2001, Yang *et al.*, 2010). SGLT2 (encoded by gene *SLC5A2*) is located on chromosome 16, close to the centromere (Wells *et al.*, 1993). In contrast to SGLT1, SGLT2 co-transports glucose only in lower affinity but higher capacity with a sodium to glucose coupling ratio of 1:1 (Kanai *et al.*, 1994). Both SGLT 1 and 2 activities can be blocked by Phlorizin (Phloretin-2`-β-glucoside) (Gerardi-Laffin *et al.*, 1993).
- Human SGLT3, unlike SGLT 1 and 2, is considered a glucose sensor rather than a glucose transporter because the binding of sugars to hSGLT3 causes membrane depolarization and not sugar transport. Hence it conducts informing signals to cells about the extracellular glucose concentration when expressed in *Xenopus laevis* oocytes, acting as a glucose-gated ion channel (Diez-Sampedro *et al.*, 2003). It co-localizes with the acetylcholine receptor in the plasma membrane of cholinergic neurons at the neuromuscular junction and is abundant in the enteric nervous system. It is expressed in the skeletal muscles, small intestine, kidney, uterus and testes (Kong *et al.*, 1993, Diez-Sampedro *et al.*, 2003). hSGLT3 (encoded by gene *SLC5A4*) composed of 659 amino acids with 70% identity to the human SGLT1. However, a single amino acid mutation, substitution of glutamate by glutamine at position 457, shifts this SGLT3 glucose sensor into a glucose transporter resembles SGLT1, as in pigs where it is a sodium/glucose cotransporter (Wright, 2001, Bianchi and Diez-Sampedro, 2010).
- SGLT4 (encoded by gene *SLC5A9*) is the low affinity glucose and mannose transporter. It is expressed mainly in the small intestine and kidney playing a role in the absorption and reabsorption of mannose, 1,5-Anhydroglucitol and fructose in addition to the glucose and galactose (Tazawa *et al.*, 2005, Koga *et al.*, 2010).
- SGLT5 (encoded by gene *SLC5A10*) is a kidney mannose and fructose transporter that is exclusively expressed in the renal brush border membrane, but its function is unknown (Fukuzawa *et al.*, 2013). SGLT5 is an orphan sodium-dependent transporter with poorly recognized function. It consists of 597 amino acids with protein molecular weight of approximately 65 kDa (Zhao *et al.*, 2005).
- SGLT6 (encoded by gene *SLC5A11*) is a high-affinity myo-inositol transporter with sodium beside its responsibility to transport glucose in the intestine, brain and kidney (Wright *et al.*, 2007).

- Other members of the SLC5 family in humans include:

- The sodium/myoinositol co-transporter (SMIT) (encoded by gene *SLC5A3*), it is expressed in brain, heart, kidney and lung that may also transport sugars with low affinity.
- The sodium/iodide co-transporter (NIS) (encoded by gene *SLC5A5*), found mainly in the cells of the thyroid gland.
- The apical iodide transporter (AIT) (encoded by gene *SLC5A11*), another Na^+/iodide cotransporter, also found in the thyroid gland (Wright and Turk, 2004).
- The sodium/multivitamin cotransporter (SMVT) (encoded by gene *SLC5A6*), also transports other essential cofactors such as biotin, pantothenic acid and lipoic acid. It is expressed in kidney, brain, heart, lung and placenta but with some uncertainty as to its function (Vadlapudi *et al.*, 2012, Wright and Turk, 2004).
- The high affinity choline transporter CHT (encoded by gene *SLC5A7*), found in the spinal cord and medulla, a Cl^- and Na^+-dependent choline cotransporter that mediates the uptake of choline for acetylcholine synthesis in cholinergic neurons (Bazalakova and Blakely, 2006).

GLUT family: this family of facilitated transporters (sodium-independent or energy-independent glucose transporters; gene *SLC2A*) mediates passive sugar transport down their concentration gradient across the cell membrane (Shirazi-Beechey, 1995, Wilson-O'Brien *et al.*, 2010). This family belongs to the Major Facilitator Superfamily (MFS) of membrane transporters (Thorens and Mueckler, 2010). They are predicted to share a structural 12 membrane-spanning α-helical segments with intracellularly located N- and C-termini. However, they differ in their functional properties, mainly the binding affinity to the inhibitory ligand Cytochalasin B, and exhibit tissue-specific distribution pattern (Scheepers *et al.*, 2004, Seatter and Gould, 1999, Augustin, 2010, Pessin and Bell, 1992). GLUT family involves 14 putative members in humans, which are subdivided based on sequence similarity into three classes:

I. Class I group (GLUTs 1-4 and GLUT14) known as glucose transporters which are inhibited by Cytochalasin B with different affinities (Bell *et al.*, 1993). This class includes:

- GLUT1 has an intermediate glucose affinity, in relation to other isoforms in class I. It is known as the glucose transporter in erythrocytes, across the blood-brain barrier and the basolateral membrane of the renal epithelium (Mueckler, 1994). It is also proposed to transport a vitamin C precursor (Dehydroascorbic acid) (Vera *et al.*, 1993, Rose *et al.*, 1988, Gould and Holman, 1993).

- GLUT2 is the facilitative glucose, galactose and fructose transporter that is inhibited by both Cytochalasin B and phloretin (Joost *et al.*, 2002). It is expressed in liver and pancreas plus in the small intestine and kidney epithelial cells (Kramer *et al.*, 2009). It will be discussed in more details separately.
- GLUT3 isoform has similar properties and glucose uptake activity to GLUT1 (Asano *et al.*, 1992, Olson and Pessin, 1996). GLUT3 is a brain-type glucose transporter and is expressed in tissues with high glucose demand like neurones and brain more than skeletal muscles and kidney (Gould and Holman, 1993). It is believed that *SLC2A3* gene duplication results in the GLUT14 isoform (*SLC2A14* gene), which maps to chromosome 12p13.3 and is expressed mainly in the testis (Wu and Freeze, 2002).
- GLUT4 is one of the insulin-mediated glucose transporters among GLUT family with a high glucose affinity. Therefore, it is highly abundant in insulin-responsive tissues like the skeletal and cardiac muscles and adipose tissues (Olson and Pessin, 1996). When these cells are exposed to insulin, the GLUT4 transporter is translocated from the intracellular compartment into the plasma membrane (Asahi *et al.*, 1999, Haney *et al.*, 1991, Li and McNeill, 1997).

II. Class II group (GLUTs 5, 7, 9, 11 and 13 or HMIT), which are known as fructose transporters. They are, in contrast to Class I, insensitivite to Cytochalasin B and Phloretin. This class involves:

- GLUT5 is the fructose specific transporter across the BBM of the intestinal enterocytes, and other tissues, with no ability to transport glucose or galactose (Douard and Ferraris, 2008). It will be discussed shortly in a separate section.
- GLUT7 gene has been cloned from human intestine hGLUT7 encoding 524 residues sharing 68 % similarity and 53 % identity with its closer GLUT5 isoform. GLUT7 is primarily expressed in the apical domain of the small intestine and colon, although mRNA has been detected in the prostate and testis. When GLUT7 is expressed in Xenopus oocytes, it exhibits high-affinity for glucose and fructose but not galactose transport (Li *et al.*, 2004). However, its physiological substrate probably has not been identified yet (Cheeseman, 2008). GLUT7 is also a known hepatic microsomal Glucose-transporter protein (Waddell *et al.*, 1992, Bell *et al.*, 1993).
- Human GLUT9 (encoded by gene *SLC2A9*) isoform was initially identified as GLUTX, which maps to chromosome 4p15.3-p16. It encodes 540 amino acids sharing a sequence identity of 44 % to GLUT5 and 38 % to GLUT1 (Joost *et al.*, 2002, Phay *et al.*, 2000, Doege *et al.*, 2000). It was unexpectedly discovered to be a facilitative uric acid transporter in liver and kidney (Preitner *et al.*, 2009).

- GLUT11 (encoded by gene *SLC2A11*) is a novel member of GLUT family showing 40-42 % identity to GLUT5. It has been suggested that fructose may be the most specific substrate for GLUT11, (Joost and Thorens, 2001, Wu *et al.*, 2002b). The human *SLC2A11* gene generates three GLUT11 isoforms, which are found in a tissue specific manner like heart, pancreas, kidney, placenta and skeletal muscles, but their function is not yet certain (Scheepers *et al.*, 2005).
- GLUT13, also called HMIT (H^+-coupled myoinositol transporter), is a recently cloned proton-myoinositol symporter included in the GLUT family. It is expressed in brain tissues regulating the myo-inositol metabolism, and in neurons sustaining the inositol signalling at synapses (Uldry *et al.*, 2001, Di Daniel *et al.*, 2009).

III. Class III group comprises (GLUTs 6, 8, 10, 12, and 14), which comprises poorly identified and structurally atypical isoforms of GLUT family. Comparatively, little is known about these GLUT transporters whose members are characterized by their glycosylation site in extracellular loop 9, rather than on loop 1. This class involves:

- GLUT6 is considered a pseudogene, as it is not expressed at the protein level. It was cloned from leucocytes (white blood cells) and also found in the brain and spleen (Zhao and Keating, 2007b). It revealed a 79.6 % sequence identity with GLUT3 (Kayano *et al.*, 1990, Gould and Holman, 1993). GLUT 6, 8 and 12 have intracellular retention motifs, though they are found at both the N- and C-termini.
- GLUT8 (gene *SLC2A8*) is a recently identified high-affinity glucose transporter regulated in a hormonal-dependent manner in various tissues. It shows insulin-induced expression and translocation, trafficked to the plasma membranes in response to insulin, which are critical for embryonic blastocyst survival (Pinto *et al.*, 2002, Carayannopoulos *et al.*, 2000). It is also expressed in the acrosomal region of human spermatozoa in a gonadotropin-dependent manner, while expressed in the lactating mammary gland in response to lactogenic hormones (Schurmann *et al.*, 2002, Zhao *et al.*, 2004).
- Human GLUT10 is encoded by gene *SLC2A10* that is mapped to chromosome 20q12-q13.1, a region linked to non insulin-dependent diabetes mellitus (NIDDM), and hence it is a candidate gene for type 2 diabetes (McVie-Wylie *et al.*, 2001). It is a high-affinity glucose transporter, but also recognized as mitochondrial dehydroascorbic acid (DHA) transporter playing a protective role from oxidative cellular injury (Segade *et al.*, 2005, Bento *et al.*, 2005, Andersen *et al.*, 2003, Mohlke *et al.*, 2005, Lee *et al.*, 2010).

- A newly defined GLUT12 mediates the glucose reabsorption in the renal distal and collecting tubules. Its protein level is increased in diabetic nephropathy and hypertension (Miller *et al.*, 2005, Linden *et al.*, 2006). GLUT12 is also found in insulin-responsive tissues suggesting its complementary role in glucose homeostasis before the appearance of GLUT4 in those tissues.
- GLUT14 is expressed in the testis, but its precise roles are unknown (Thorens and Mueckler, 2010). GLUT14 maps to chromosome 12p13.3 (17.1M), which shares remarkable identity to GLUT3 with a similar genomic organization. GLUT14 likely resulted from a duplication of GLUT3, but, in contrast to GLUT3, the putative glycosylation sites of GLUT14 are present in loop 1 of the membrane spanning domain (Wu and Freeze, 2002).

a) Monosaccharide transporter GLUT2

GLUT2 is a bidirectional, high capacity but low affinity, transporter that passively diffuses monosaccharides (glucose, galactose and, with lower affinity, fructose) with their concentration gradient across the cell membranes (Zhao and Keating, 2007b). GLUT2 is the key facilitative glucose transporter isoform expressed mainly in the hepatocytes and insulin-secreting pancreatic β-cells, plus the basolateral membrane of absorptive cells in the small intestine and the kidney (Gould and Holman, 1993).

In the small intestine, GLUT2 facilitates the exit of glucose, galactose and fructose, with highest affinity to glucose, out of enterocytes across the basolateral membrane to the blood stream (Kellett and Helliwell, 2000, Shirazi-Beechey, 1995, Thorens *et al.*, 1990a). Furthermore, it is responsible for glucose reabsorption through the basolateral membrane of the proximal convoluted tubules in the kidney (Goestemeyer *et al.*, 2007, Takata, 1996, Thorens *et al.*, 1990b). In the liver, GLUT2 mediates glucose uptake through the sinusoidal membrane of the hepatocytes. Hepatic *GLUT2* mRNA and protein expression is up-regulated by thyroid hormone which increases the hepatic output of glucose synthesized by gluconeogenesis into the blood (Weinstein *et al.*, 1994, Thorens *et al.*, 1990b). In addition, GLUT2 has other physiological roles including the regulation of a glucose-induced insulin secretion from pancreatic β-cells (Tiedge and Lenzen, 1991). It also provides a glucose-sensing function in the hypothalamus and participates in cerebral glucose sensing, as shown in rat brain studies (Arluison *et al.*, 2004).

Indeed, GLUT2 has a much higher affinity for glucosamine than for glucose (Uldry *et al.*, 2002). It also transports 3-O-methyl-D-glucopyranoside (3-OMD) and 2-deoxy-D- glucopyranoside (2-DG), but not α-methyl-D-glucose (α- MG).

In humans, the GLUT2 protein is composed of 524 amino acids and shares ~55% identity with GLUT1 isoform (Gould and Bell, 1990, Fukumoto *et al.*, 1988). The amino acid sequence of GLUT2 displays 81% identity between human, rat and mouse (Zhao and Keating, 2007b). Its secondary structure is similar to the other isoforms of GLUT family, comprising 12 transmembrane domains with intracellular C- and N- termini (Takeda *et al.*, 1993). It is encoded by the *SLC2A2* gene, which was cloned, sequenced and mapped to chromosome 3q26.1-26.3 (Matsutani *et al.*, 1992). Defects in this gene cause the rare glycogen storage disease Fanconi-Bickel syndrome (Santer *et al.*, 2002).

In this laboratory, two GLUT2 antibodies have been raised to two different epitopes of GLUT2 (see Figure 5), the details about these antibodies are mentioned in the Methods section.

One antibody has been raised to a synthetic peptide corresponding to amino acid residues 40-55 of rat GLUT2. Alignment of this region of rat with that of pig and horse shows that it has 87.5% and 71.4% identity with pig and horse GLUT2, respectively (Figure 5A). The other antibody was raised to a synthetic peptide corresponding to the C-terminus region of the equine GLUT2. Alignment of this region of horse and pig GLUT2 shows 92.9% identity (Figure 5B). Both antibodies have been used, in previous work, in immunohistochemistry to identify the membrane location of GLUT2 protein in enterocytes of pig and horse intestinal tissues (Stearns *et al.*, 2010), and presented in this thesis in rat tissue (Chapter 4).

<u>Figure 5</u>: Alignment of GLUT2 amino acid sequence in different species

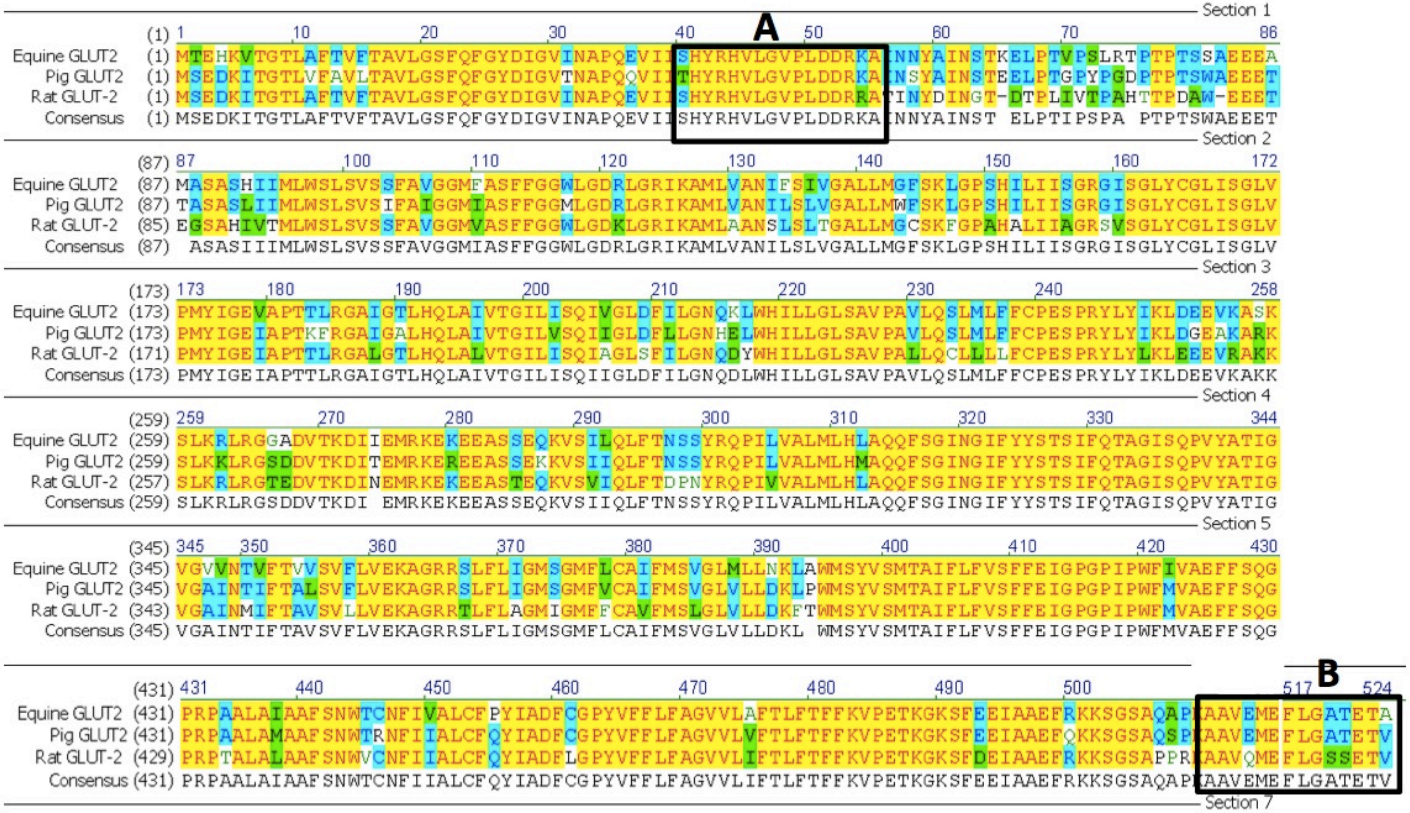

Alignment of amino acid sequences of GLUT2 in three species: rat, pig and horse. The boxed areas A (from 40-55 residues) and B (from 511-524 residues, C-terminus) show the two regions to which the anti-peptide antibodies were raised. (Alignment was processed and captured from Vector NTI software).

Does GLUT2 traffic to the BBM of enterocytes?

It has been claimed, by Kellett and his colleagues, that under certain conditions, when luminal glucose or fructose concentrations are increased, GLUT2 is activated and rapidly inserted into the BBM of the enterocytes, and glucose absorption by GLUT2 across the BBM is 3-fold greater than that by SGLT1 (Kellett and Helliwell, 2000, Kellett *et al.*, 2008, Kellett and Brot-Laroche, 2005, Kellett, 2001, Helliwell *et al.*, 2000). It has been proposed that, in high luminal sugars, glucose uptake by SGLT1 increases the volume of enterocyte, (due to high osmolarity and the co-transport of water molecules by SGLT1), which trigger Ca^{2+} entry to activate PKCβII. Subsequently, via PKCβII and MAP kinase-dependent pathways, this promotes the rapid trafficking of cytosolic GLUT2 into the apical membrane (Affleck *et al.*, 2003, Mace *et al.*, 2007).

The immunohistochemical expression of GLUT2 on the enterocyte apical membrane was detected using an antibody to a sequence within the large extracellular loop of GLUT2 that permits the localization of GLUT2 at the BBM (Affleck *et al.*, 2003). However, using one of the two antibodies is puzzling because that was only observed in rats, *in vivo,* but it could not be proven in any other species. The two anti-GLUT2 antibodies were used, with various approaches, by other investigators who showed that GLUT2 is exclusively localized to the BLM of enterocytes with no protein expression on the BBM in fructose- and glucose-perfused intestines of neonatal rats (Cui *et al.*, 2005), horses (Dyer *et al.*, 2009), dogs and cats (Batchelor *et al.*, 2011) and piglets (Moran *et al.*, 2010b).

Other authors also strongly argued that GLUT2 does not participate in the transport of monosaccharides across the BBM. Although, it has been shown that fructose transport is reduced by half in the BBM of *GLUT2*-knockout mice, suggesting that 50% of luminal fructose transport is mediated by apical GLUT2 (Gouyon *et al.*, 2003), but, in GLUT2-null mice and humans with inactivating mutations in GLUT2 (Fanconi-Bickel syndrome), there was no evidence of impaired intestinal glucose transport (Santer *et al.*, 2003, Stumpel *et al.*, 2001). Other findings declined the presence of GLUT2 on the luminal intestinal domain that, if exist, should allow fructose absorption when GLUT5 is absence in *GLUT5*-knockout mice, which are unable to absorb fructose at all (Barone *et al.*, 2009), or when GLUT5 activity is limiting, as in healthy human volunteers who show symptoms of malabsorption and a positive breath hydrogen test following ingestion of excessive (50g) fructose (Montes *et al.*, 1992), indicating limited capacity of fructose absorption via GLUT5 in humans. Furthermore, the lethal phenotype of glucose-galactose malabsorption argues against the presence of apical GLUT2 that should

compensate glucose and galactose absorption when SGLT1 is mutated in humans (Gorboulev *et al.*, 2012). Finally, the presence of GLUT2 in the BBM would allow the transported glucose and galactose by SGLT1 to escape back into the lumen, only to be absorbed again by SGLT1 in a useless cycle (Wright *et al.*, 2003, Wright and Turk, 2004). Collectively, there is comprehensive evidence (from those findings plus our Results in chapter 4) indicating that GLUT2 is exclusively located on the BLM and is not existing on the apical membrane of enterocytes, indicating that SGLT1 is the major route for dietary glucose (and galactose) absorption from the intestinal lumen into the enterocytes across the BBM.

b) Fructose transporter GLUT5

GLUT5 is a high-affinity facilitative transporter that is the sole isoform of GLUT family specific for fructose, but not glucose or galactose. It is an integral membrane transporter across epithelial membranes found in different fructose consuming tissues. The greatest amount of GLUT5 is expressed in the small intestine, where it passively facilitates the absorption of luminal fructose into enterocytes across the apical membrane (BBM) in human (Blakemore *et al.*, 1995), horse (Merediz *et al.*, 2004), rabbit (Miyamoto *et al.*, 1994), rat and mouse (Corpe *et al.*, 2002). GLUT5 is also found abundantly in the testis, where it was first discovered, in human mature spermatozoa to mediate uptake of fructose for use as an energy source (Burant *et al.*, 1992) as well as in the brush-border membrane of the kidney, skeletal muscle, adipocytes (Hajduch *et al.*, 1998), heart and brain (Douard and Ferraris, 2008, Shepherd *et al.*, 1992).

Human *SLC2A5* gene is situated on the short arm of chromosome 1 encoding GLUT5 protein with 501 amino acids sharing ~40% identity with the other GLUT family members (Kayano *et al.*, 1990). The expression and localization patterns of human *GLUT5* are regionally modified showing the highest mRNA level in small intestinal BBM, mainly the mature enterocytes of the jejunum. However, it has been claimed that GLUT5 can be expressed on the BLM with lower levels (Davidson *et al.*, 1992, Blakemore *et al.*, 1995). This expression and activity seems to be also regulated by developmental stage, increased after 1 year in humans (Nobigrot *et al.*, 1997) and after weaning in rats (Toloza and Diamond, 1992). Studies on rats revealed that increasing dietary fructose rapidly upregulates the expression of intestinal *GLUT5* mRNA and GLUT5 protein mainly in the BBM of the jejunum along the whole villus enterocytes (Inukai *et al.*, 1993, Jiang *et al.*, 2001). Although *GLUT5* mRNA transcription and protein activity follow circadian influences, it is potentially affected by intracellular cAMP and by thyroid hormone. In some tissues, GLUT5 expression is insulin-mediated as seen in skeletal muscles in response to insulin

hormone secretion from the pancreas (Mahraoui *et al.*, 1994, Castello *et al.*, 1995, Mochizuki *et al.*, 2007, Hajduch *et al.*, 2003).

However, GLUT5 expression levels and fructose uptake rates are increased in diabetes (Burant *et al.*, 1994, Dyer *et al.*, 2002a), and significantly affected by hypertension (Mate *et al.*, 2001), obesity (Litherland *et al.*, 2004), and inflammation; and appear to be induced during cancers, especially in the mammary glands (Douard and Ferraris, 2008).

c) Sodium/ glucose co-transporter 1, SGLT1

The sodium/glucose co-transporter (SGLT1) is the most studied isoform of SLC5 family. It was first recognised in 1987 by Hediger *et al.*, who identified the primary structure of rabbit SGLT1 by cloning and cDNA sequencing from rabbit intestine (Hediger *et al.*, 1987). Then, human SGLT1 was cloned and sequenced in 1989 (Hediger *et al.*, 1989b), with significant homology in SGLT1 sequence in a number of species including mouse, rat, cow, sheep, dog, cat, pig and horse (Dyer *et al.*, 2002a, Hediger and Rhoads, 1994, Shirazi-Beechey, 1995, Tarpey *et al.*, 1995, Batchelor *et al.*, 2011).

Human intestinal *SGLT1* gene, named (*SLC5A1*), has been cloned and sequenced and the chromosomal localization studies mapped the gene to reside on the distal arm of chromosome 22q13.1 (Turk *et al.*, 1993, Hediger *et al.*, 1989a, Hediger *et al.*, 1989b). In most mammals, the SGLT1 gene encodes a polypeptide consisting of 662-664 amino acids (Shirazi-Beechey, 1995) with a molecular mass of 72-85 kDa, glycosylation adds about 15 kDa (73-75 kDa in human) (Turk *et al.*, 1993, Turk *et al.*, 1994). SGLT1 is predicted to comprise 12 trans-membrane helices with 15 spanning exons. Gene defects in *SGLT1* cause the known disorder 'glucose and galactose malabsorption' (Turk *et al.*, 1991).

As demonstrated in Figure 6, the secondary structure model of SGLT1 protein comprises 14-15 exons; it shows 12-14 transmembrane α-helices spans with hydrophilic amino terminus and hydrophobic carboxyl terminus, both facing the extracellular side of the plasma membrane. SGLT1 carrier has the glycosylation site (SGLT1 motifs) and the putative glucose-binding sites in the C-terminal half of the truncated protein (Wright and Turk, 2004, Turk and Wright, 1997, Wright *et al.*, 1998, Zhao *et al.*, 2005, Wright *et al.*, 1992, Wright *et al.*, 2007, Turk *et al.*, 1993, Wright *et al.*, 2004). However, the Na^+-binding site of SGLT1 remains undefined.

Figure 6: A modified membrane topological model of SGLT1.

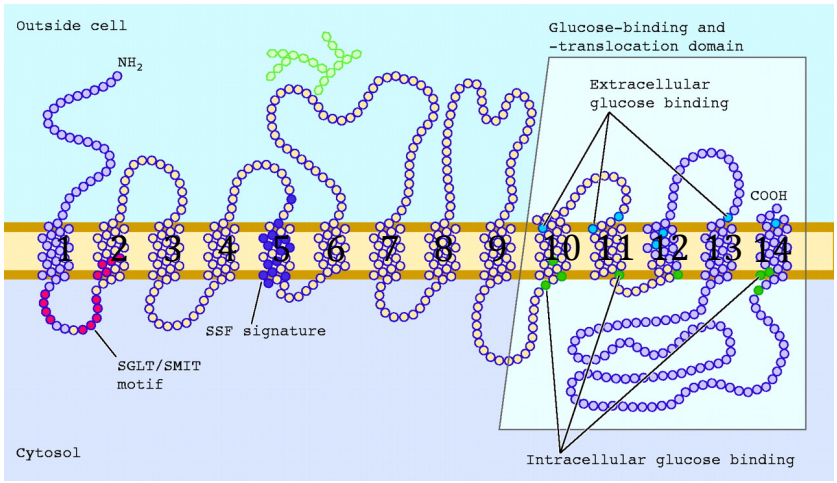

The topological model of SGLT1 gene shows: the transmembrane segments/helices are numbered, the exons are depicted in circles and the N- and C- termini face extracellularlly and are indicated by "NH_2" and "COOH," respectively. The D-glucose binding sites are illustrated in the boxed area. (taken with permission from Wright et al., 2004)

SGLT1 is a sodium-coupled glucose symporter that actively transports glucose/galactose in Na^+-dependent manner across the cytoplasmic membrane. It has higher affinity to glucose than galactose, but low capacity with a Na^+ to glucose ratio of 2:1 (Shirazi-Beechey, 1995). It is mainly expressed in the BBM of intestinal enterocytes, where it is responsible for the luminal absorption of D-glucose and D-galactose in many species with similar functional characteristics (Takata *et al.*, 1992, Hediger and Rhoads, 1994, Wright, 1993).

It has previously been reported that along the vertical crypt-villus axis, SGLT1 mRNA and protein are detected only in the villus, highest levels in the villus-tip, but not in the crypts. Conversely, along the horizontal axis of small intestinal length, SGLT1 protein is more abundant in the proximal regions and declined gradually with distal progression (Hwang *et al.*, 1991, Freeman *et al.*, 1993). During development, studies on neonatal pigs revealed that SGLT1 activity and protein expression is high along the entire crypt-villus axis at birth and during suckling period (Yang *et al.*, 2011).

SGLT1 is also highly expressed on the apical membrane (BBM) of the proximal tubular cells of S3 segment in the kidney where it mediates 10% of the reabsorption of filtered glucose, while the majority is reabsorbed by SGLT2 (Mather and Pollock, 2011; Pajor *et al.*, 1992). Unexpectedly, it was observed that SGLT1 expression in human heart was about 10-fold higher than that observed in kidney tissue (Zhou *et al.*, 2003). It is also found to increase glucose permeability in the

blood-brain barrier (Elfeber *et al.*, 2004), testis, prostate, and parotid gland (Tarpey *et al.*, 1995, Wright *et al.*, 2007) and its expression is affected by lactation in the mammary glands (Zhao and Keating, 2007a). Interestingly, SGLT1 is multifunctional; it can also act as a water pump (Loo *et al.*, 2002), a sodium unipolar or a urea transporter.

Alignment of the SGLT1 amino acid sequence showed that rabbit SGLT1 shares a high degree of homology with other species. The polyclonal antibody to SGLT1 used in this study was raised to a synthetic peptide corresponding to amino acids 402-420; a region shown in Figure 7. As seen, there is a high degree of homology in amino acids 402-420 sequence amongst various species; having 84.2% to 100% identity and 89.5% to 100% similarity to other species.

***Figure 7:* Alignment of SGLT1 amino acid sequence in different species**

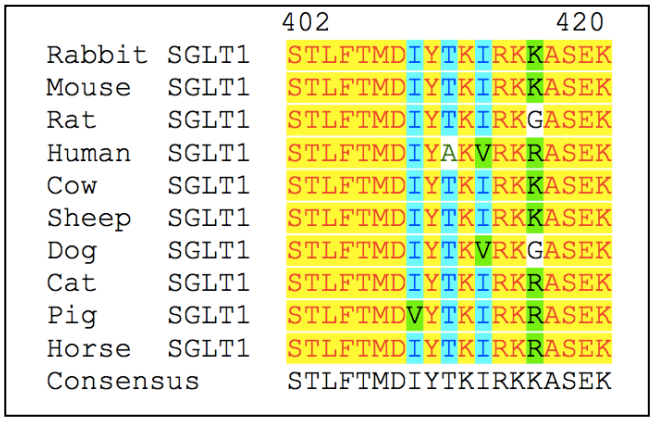

Alignment of amino acid sequences (from 402-420 residues) of rabbit SGLT1 with the same region of sequence of several other species. Very high homology is seen in this region to which the anti-peptide antibodies were raised. (Alignment was processed and captured from Vector NTI software).

Operational mechanism of SGLT1

SGLT1 binds to a couple of Na^+ ions at the extracellular surface, which promote a conformational adaptation allowing one glucose molecules to occupy glucose-binding site at the receptor's external surface. The co-transporter switches its conformational state facing both substrates bound near the intracellular compartment to release Na^+ and glucose into the cytoplasm. Subsequently, transport is resumed again after exposing the binding sites on the extracellular surface of the membrane. Thus, taking the optimal conformational state for further extracellular substrate binding (Wright *et al.*, 2007, Stevens *et al.*, 1990, Loo *et al.*, 1998, Loo *et al.*, 2006).

The co-transport of Na^+ and sugar by SGLT1, on the BBM, is described as a secondary active transport because the driving force of the Na^+ gradient is maintained by the primary active Na^+/K^+-pump or Na^+/K^+-ATPase, located on the

BLM. The rate of glucose transport by SGLT1 is organized by the direction and magnitude of the Na^+-gradients across the plasma membrane, which is set by the Na^+/K^+/ATPase (Zhao and Keating, 2007b). Na^+ is the physiological cation driving sugar transport by SGLT1; otherwise, it can be driven to a lesser extent by H^+ and Li^+ ions (Wright *et al.*, 2003, Hirayama *et al.*, 1994). The apparent affinity of SGLT1 for sugar is 25 times higher for Na^+-sugar cotransport than that for H^+ -sugar cotransport. However, H^+/glucose cotransport is potentially relevant in the duodenum, where the luminal content has a high glucose concentration in acidic media (Wright, 2006). SGLT1 activity is inhibited by the non-transported competitive blocker phlorizin (phloretin-2'-beta-glucoside).

2.2.2. Trans-epithelial transport of monosaccharide, sugar absorption

Previously, it was hypothesized that glucose can be passively transported via paracellular route, known as solvent drag, in high glucose concentrations. However, the transport route for glucose, galactose and fructose is mainly via the transcellular pathway, known as transporter-mediated absorption. The glucose transport mechanism across the intestinal wall occurs via the enterocytes that is mediated by integrated carriers in the cell membrane known as ‘‘glucose transporters’’ (Takata, 1996). The rate and affinity of these transporters regulate the precise substrate uptake to be used by different tissues according to their requirements.

A model for monosaccharide absorption across a mature enterocyte of the small intestine is shown in Figure 8. The transport of dietary glucose/galactose across the brush-border membrane (BBM) from the lumen into the enterocyte is mediated by SGLT1, while fructose is passively diffused via GLUT5. On the basal side of the cell, accumulated glucose, galactose and fructose within the cell diffuse out into bloodstream across the basolateral membrane (BLM) through GLUT2 (Drozdowski and Thomson, 2006, Wood and Trayhurn, 2003, Burant *et al.*, 1992). Intracellular Na^+ ions are transported out across the BLM by the Na^+/K^+-ATPase, which generates the energy from ATP and maintains the electrochemical gradient needed for active glucose transport. Therefore, SGLT1 is considered a second active transport, dependent on the action of the Na^+/K^+-ATPase. This model of absorption is almost universally accepted (Ferraris and Diamond, 1989, Ferraris *et al.*, 1990).

However, others showed that paracellular shunts have a minor transport role not exceeding 2-7% of total intestinal absorption, even in high luminal concentrations of nutrients (Lane *et al.*, 1999). It is suggested that some glucose is phosphorylated within the cell and accumulated in endosomes, then, delivered to the lateral spaces by exocytosis at the BLM (Stumpel *et al.*, 2001).

***Figure 8*: Sugar transporters via the enterocyte in the small intestine.**

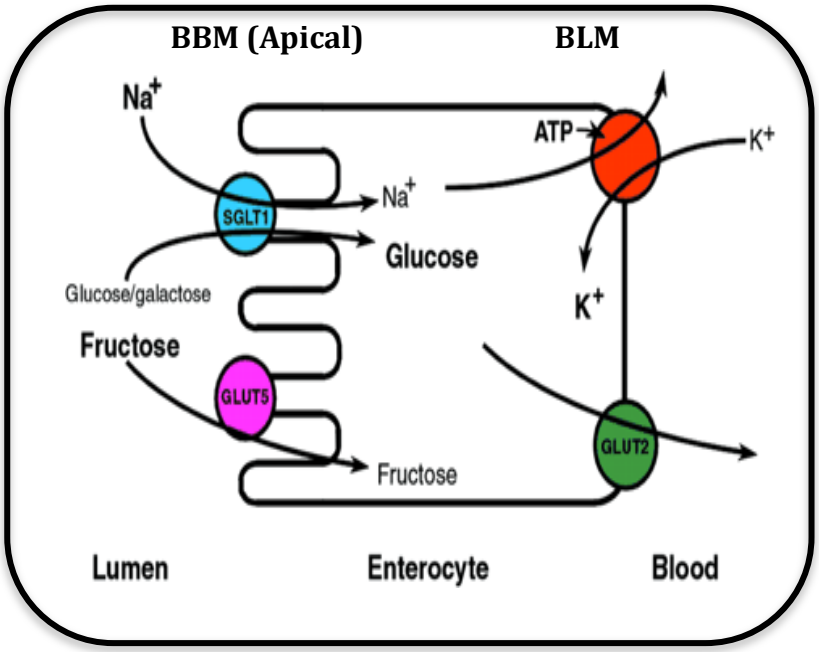

The diagram shows mature enterocyte with the sugar transporters. On the brush-border membrane (BBM): SGLT1 transports glucose and galactose, and GLUT5 enters fructose from the gut lumen into the cell. On the basolateral membrane (BLM): GLUT2 diffuses glucose, galactose and fructose out the cell to the blood. Na^+/K^+-ATPase on the BLM generates the Na^+ concentration gradient required for SGLT1 function. (adapted with permission from Wright, 1998).

2.2.3. Regulation of intestinal sugar transport:

It is vital to sustain an effective blood glucose level for healthy and normal physiological processes. The maintenance of glucose homeostasis is affected by the dietary sugar transport from the intestinal lumen into the blood stream and subsequently to be taken up by the utilizing tissues. Blood glucose is also controlled by insulin and glucagon, which is a complementary role of the endocrine pancreas.

In general, the absorption of all nutrients across the small intestinal wall is carried out through the absorptive enterocytes. Hence, this transport is affected by the structural and the physiological properties of these cells beside other important non-specific and specific mechanisms.

Non-specific mechanisms regulate the absorption of sugar as well as other different nutrients, including: the modification of the intestinal structure such as expanding its absorptive surface area resulting in alteration of the cell number (hyperplasia) or size (hypertrophy) or the length of the microvilli and thus more enterocytes per villus (Smith *et al.*, 1991). Another significant non-specific factor is the maturity of enterocytes. Mature enterocytes, which migrate up to villus tip,

exhibit improved transport function as the BBM alters its fluidity and lipid composition, being more rigid and capable for accelerating sugar transport rate (Meddings *et al.*, 1990, Brasitus and Dudeja, 1985, Vazquez *et al.*, 1997). Furthermore, the mucosal clearance and the blood flow rate plus the gastric emptying and the gut motility have great impact on nutrient absorption. Shifting the ratio of transporting to non-transporting cells also affects absorption, plus the changes in intestinal mass that occurs during development and aging or in adaptation to physiological stress like pregnancy and lactation (Valenkevich and Iakhontova, 1996, Vincenzini *et al.*, 1989). In addition, pathological conditions such as obesity and diabetes mellitus have dramatic effect on glucose transport (Ciaraldi *et al.*, 1981).

Other suggested but not proven indirect mechanisms affecting the Na^+ -dependant glucose transport are: changing the transmembrane electrochemical gradient of Na^+ (Thompson and Debnam, 1986, Murer and Hopfer, 1974), altering the transmembrane potential caused by ions like Na^+ and K^+ providing driving force controlling the rate of glucose intracellular accumulation by causing cation-induced differences in the affinity of transporters on both sides of the BBM (Kimmich and Carter-Su, 1978, Kimmich *et al.*, 1977).

The specific mechanisms regulating the absorption of sugar but not necessarily changing the absorption of another nutrient, include: changing the turnover state of the small intestinal cells and the number of existing transporters in the membrane, by switching their status from ‘inactive’ to ‘active’ forms (Wright *et al.*, 1997), or changing the rate of synthesis or rate of degradation or the site density of glucose transporter. Modulating the substrate-binding affinity of the sugar transporters, affinity constant, which is increased by ATP, but reduced by adenosine (Lachaal *et al.*, 2001, Ferraris and Diamond, 1997).

Importantly, specific apical glucose transport is primarily regulated by the intrinsic activity of SGLT1 transporter and its actual amount of protein in the membrane (Dyer *et al.*, 2009) (The regulation of SGLT1, is discussed separately). Moreover, the consumed dietary levels of carbohydrates, fibres, fats and electrolytes have a potential regulatory effect on intestinal sugar transport (Dyer *et al.*, 1997b, Ferraris, 2001). The ratio of unsaturated to saturated fats in diets can alter the lipid composition of the BBM during cell maturation and affect sodium-dependent glucose transport (Alessandri *et al.*, 1990).

2.2.4. Regulation of SGLT1:

Expression of SGLT1 is consequently regulated at the levels of transcription (Korn *et al.*, 2001, Vayro *et al.*, 2001) mRNA accumulation (which is most likely a result of activation of *SGLT1* gene transcription) and mRNA stability (Loflin and Lever, 2001), posttranslational intracellular trafficking (Delezay *et al.*, 1995), membrane expression and activity. SGLT1 is initially synthesized in the lower villus, and during cellular maturation and migration up the villus, SGLT1 protein is incorporated into the brush-border membrane according to the density site on the membrane. Functional SGLT1 is expressed with much higher activity in the mature villus cells in rodents (Freeman *et al.*, 1987) and rabbits (Meddings *et al.*, 1990).

Several studies revealed no correlation between the expression profile of *SGLT1* mRNA and SGLT1 protein or its function. The transport rate and protein expression are increased when the amounts of *SGLT1* mRNA are reduced, in 25-50 h old enterocytes. It appears that this change in mRNA translational efficiency depends on the age of the enterocytes but not on their villus position, and enterocytes are around that age when they leave the crypts (Dong *et al.*, 1997).

Further work on mice demonstrated that irreversibly programmed SGLT1 expression is related to the maturity status of enterocytes. Cells migrate along the vertical crypt/villus axis, then they shed from the villus tip, this takes about two days in rat intestine (Junqueira and Carneiro, 1971) and 4-6 days in human intestine (Thomson *et al.*, 1994). Owing to that, the intestinal glucose transport activity increased within 1-3 days after switching from low to high-CHO diet, this time lag is sufficient to increase the site density of glucose transporters. This also corresponds to the time taken by the crypt enterocytes to migrate to villi, and the functional SGLT1 is observed in the newly formed mature enterocytes (Ferraris and Diamond, 1992, Ferraris *et al.*, 1992, Ferraris and Diamond, 1993). Hence, immunohistochemical expression of SGLT1 protein is detected on the BBM of the entire villus but not the crypt cells in the studied species: rabbits, rats, piglets, horses, dogs and cats (Batchelor *et al.*, 2011, Dyer *et al.*, 2009, Dyer *et al.*, 2007, Moran *et al.*, 2010b, Hwang *et al.*, 1991, Takata *et al.*, 1992) . Moreover, sugar transport activity of SGLT1 in intestinal enterocyte mediated by cyclic AMP has been proposed to lead to significant hyperpolarization of the potential difference across the BBM, a crucial driving force for Na^+/sugar transport (Sharp and Debnam, 1994).

Intestinal glucose uptake follows a circadian rhythm related to periodic insulin secretion, which is interrupted by prolonged fasting or continuous intestinal glucose infusion in animals (Van Cauter *et al.*, 1997). There is a maintained basal level of intestinal SGLT1 expression and activity in order to sustain a regular blood glucose concentration. However, this expression is modified by several factors: luminal dietary carbohydrates, perinatal development, enterocyte maturation plus

physiological factors (lactation, pregnancy and starvation) and pathological conditions (diabetic and obesity) (Moran *et al.*, 2010b, Ferraris, 2001). Different species demonstrate dietary and developmental regulation of the intestinal glucose absorption. The intestine of ruminant animals is a model that is naturally exposed to significant changes in luminal carbohydrates during developmental progression from pre-ruminant to ruminant stages. It has been shown that intestinal SGLT1 expression is controlled at the post-transcriptional level. This expression declines dramatically in ruminant sheep correlates with the sugar feed selectivity as animals shift from milk lactose to grass and variable sugar diet (Wood *et al.*, 2000).

Other studies on lambs and swine also show that intestinal SGLT1 activity is modified by fluctuating dietary carbohydrate (Dyer *et al.*, 1997a, Moran *et al.*, 2010b). Similar findings were observed in rat intestine and revealed that the enhanced carbohydrate diet-regulated SGLT1 expression occurs at transcriptional level, leading to more glucose transport. In pigs, *SGLT1* mRNA, protein abundance and glucose uptake activity remained constant when the weaned piglets were fed low carbohydrate-containing diets, while increasing the dietary carbohydrate content above 50% rapidly enhanced intestinal SGLT1 expression. Interestingly, when the low carbohydrate -containing diets were supplemented with artificial sweeteners, the intestinal expression of SGLT1 was increased to the levels of high-carbohydrate diets. However, intestinal morphometric analysis denied the structural trophic effect on the SGLT1 expression, as no changes were observed in the crypt depth or villus high among animals fed low and high carbohydrate diets (Moran *et al.*, 2010b, Moran *et al.*, 2010a).

In general, SGLT1 expression is reported to match the carbohydrate content in natural diet of a number of different species including rats, humans, fish, horses, pigs (Buddington, 1987, Buddington and Diamond, 1992, Dyer *et al.*, 2009, Dyer *et al.*, 1997b, Miyamoto *et al.*, 1993, Moran *et al.*, 2010b), and glucose absorption tends to be higher in herbivores than in carnivores (Buddington *et al.*, 1987). Considering the substrate-dependent regulation of SGLT1, a low salt-diet decreases the glucose uptake rate (V_{max}) by reducing the electrical potential of BBM, due to less available Na^+ molecules (Jaso *et al.*, 1995).

2.3 Absorption of water and electrolytes:

Glucose, amino acids and ions trigger water transport via cotransporters. SGLT1 acts as water pump accounting for about 50 % of the total water transport across the human intestinal BBM (Loo *et al.*, 2002). It is a secondary active water transporter along with Na^+ and glucose in variable ratios of (2 Na^+: 1 glucose : 249 water molecules relates to *Xenopus* oocytes expressing SGLT1, 260 water molecules for human BBM and 424 for rabbit BBM) (Loo *et al.,* 2002, Loo *et al.*, 1996, Meinild *et al.*, 1998, Zeuthen *et al.*, 1997). Ratio and transport rate will vary dependant on

osmotic gradient/luminal content tonicity (or experimental medium). Also altered by temperature, external Na^+ and sugar levels and any alteration in membrane potential (Meinild *et al.,* 1998).

Subsequently, across the basolateral membrane, intracellular Na^+ is exported out towards the blood by Na^+/K^+-ATPAse, and glucose passively diffuses out by the facilitated transporter, GLUT2. It is commonly thought that Na^+ transport increases the local osmotic pressure in the lateral intercellular spaces, and that creates osmotic water flow across the epithelial BLM (Wright and Loo, 2000).

Sodium is co-transported with glucose and amino acids. Other ions and electrolytes are either transported via specific carriers (uni-porter) or co-transported with other nutrients (co-transporter). For example: the apical anion channel, a basolateral membrane K^+ channel and NaK2Cl cotransporter (Field, 2003).

2.4 Intestine as an endocrine system: secretion and protection

The gastrointestinal tract has the ability to defend against toxins and poisons as well as to resist infection and inflammation. The mucosal chemosensation can detect harmful components in the gut lumen and evoke protective reactions like vomiting, inhibit gastric empting or diarrhea. In addition, the paneth cells secrete antimicrobial substances as part of the defense mechanism; and goblet cells release mucus for lubrication to protect the epithelium from mechanical damage.

After dietary ingestion, the digestion and absorption of nutrients are accompanied by stimulated secretion of multiple gut hormones, which are peptides synthesized by specialized enteroendocrine cells. Digestion is processed by GIT functions including: gastric empty and GI motility, stimulating pancreatic secretions like insulin, controlling appetite and food intake to maintain metabolic homeostasis (Tolhurst *et al.*, 2012). These GIT functions are controlled by hormones produced by many endocrine glands, but most pronounced, by hormones secreted within the GIT itself. The digestive system is the largest endocrine organ in the body, constituting the endocrine cells (EEC) within the gut, which collectively referred to as the enteric endocrine system. Various endocrine cell types may express different hormonally active fragments of the same prohormone according to cell-specific posttranslational processing.

The GI produces more than 20 hormones that act either locally as a paracrine factors interacting with neighbouring cells and nerve endings or distally as classical circulating hormones (Rehfeld, 2004; Rehfeld, 1998). These hormones activate neural communication with peripheral organs, involving the liver, adipose tissue, muscles and the pancreas, to coordinate energy intake and storage (Drucker, 2007).

The most studied gut hormones include GIP, GLP-1, GLP-2, gastrin, somatostatin, CCK and serotonin; their actions are listed in table 1.2 (Breer *et al.*, 2012, Bryant and Bloom, 1979, Sjolund *et al.*, 1983, Dockray, 2012, Batterham and Bloom, 2003, Phillips and Prins, 2011, Jang *et al.*, 2007). These gut hormones affect glucose metabolism in different complementary ways: by regulating appetite and food intake, affecting gastric emptying and gut motility, and modulating meal-related fluctuations in plasma glucose levels by released incretins that enhance pancreatic insulin release and affecting tissue specific insulin sensitivity (Ashley Blackshaw and Young, 2011, Rasoamanana *et al.*, 2012, Holst and Orskov, 2001, Heijboer *et al.*, 2006, Kokrashvili *et al.*, 2009).

Table 1.2: Gut hormones secreted by enteroendocrine cells:

Cell Type	Location	Hormone	Function
G-cell	Stomach antrum, duodenum	Gastrin	- Controls gastric acid secretion
D-cell	Stomach, Duodenum, Pancreas	Somatostatin	- Inhibits gastrin and hydrochloric acid release - Inhibits Secretin and CCK - Inhibits glucagon - Inhibits gut smooth muscle motility - Stimulate gastric sphincters
S-cell	Proximal intestine	Secretin	- Inhibits gastric acid secretion - Stimulates secretion of bicarbonate fluids from the pancreas and liver into the gut.
X/A like cells	Stomach	Ghrelin	- Act on hypothalamus to stimulate food intake
K-cell	Proximal intestine	GIP	- Promotes insulin secretion
I-cell	Proximal intestine	CCK	- Stimulates secretion of pancreatic enzyme and gallbladder contraction - Inhibits food intake
M-cell	Proximal intestine	Motilin	- Motivates gut motility
L-cell	Distal ileum and colon	GLP-1, GLP-2, PYY	- Trigger bile and insulin secretion - Suppress food intake - Inhibit gut secretion and motility GLP-2: discussed shortly

CCK: cholecystokinin, GIP: glucose-dependent insulinotropic peptide, GLP: glucagon-like peptide, PYY: peptide tyrosyl tyrosine.

2.4.1. Gut hormones: GIP, GLP-1 and GLP-2

Intestinal enteroendocrine cells secrete GLP-1, GLP-2 and GIP, plus other GI hormones, from the basal side of the cell. GLP-1 and GLP-2 are hormonal peptides released from the intestinal L-cells, while GIP is secreted by K-cells of the EEC. GLP -1 and -2 are synthesized by the common precursor proglucagon peptide, composed of 160 amino acids, which is expressed in several tissues and gives a diversification of peptides depending on a tissue-specific post-translational processing. The proglucagon gene produces GLP-2 and GLP-1 hormones in the intestinal EEC and the brain, whereas it evokes glucagon secretion in pancreatic α-cells (Drucker *et al.*, 1986, Kieffer and Habener, 1999, Mojsov *et al.*, 1986).

Both GLP-1 and GIP are incretins, while GLP-2 is an intestinotrophic factor. The two incretins GLP-1 and GIP influence insulin release in different ways: they promote insulin biosynthesis and stimulate glucose-dependent insulin secretion; plus, they increase the proliferation (neogenesis) and survival of the pancreatic islet β-cell (Abraham *et al.*, 2002). Incretins also facilitate glucose uptake by muscles and adipose tissues (Drucker, 2003, Drucker, 2006, Fehmann *et al.*, 1995). Most hormones in the glucagon superfamily, including GLP-1, GLP-2 and GIP are rapidly inactivated by the enzyme dipeptidyl peptidase-4 (DPP-4), and cleared by the kidney (Kieffer *et al.*, 1995, Tavares *et al.*, 2000, Deacon, 2004).

Additionally, GLP-1 exerts extra roles in glucose homeostasis including suppression of glucagon release from α-cells of the Islets of Langerhans, resulting in reduced endogenous production of glucose by the liver. It also slows gastric emptying and reduces the rate of nutrient absorption. GLP-1 can affect the hypothalamus to induce satiety and reduce food intake, thus controlling body weight (Drucker, 2007, Yabe and Seino, 2011).

GIP is derived from a 153- residue precursor, preproGIP, and circulates as a 42-amino acid peptide. It has an insulinotropic action and also known as gastric inhibitory peptide because it was originally identified to inhibit gastric motility (Cho and Kieffer, 2010, Takeda *et al.*, 1987).

Glucagon-like peptide 2 (GLP-2) is a 33-amino acid peptide hormone produced by the EEC in response to dietary intake especially carbohydrates and lipids (Xiao *et al.*, 1999, Drucker, 2001a). GLP-2 has both intestinotrophic effects and physiological actions on the GIT. It enhances intestinal mucosal growth by stimulating crypt cell proliferation and suppressing villus cell apoptosis (Drucker *et al.*, 1996, Thulesen, 2004). This adapts the gut epithelium to luminal nutrients (Burrin *et al.*, 2003, Drucker, 1999, Shin *et al.*, 2005) or repairs intestinal hypoplasia, mucosal injury and atrophy associated with conditions like total parenteral nutrition or intestinal resection (Ljungmann *et al.*, 2001, Munroe *et al.*, 1999). Moreover,

GLP-2 promotes nutrient absorption by inhibiting gastric motility and gastric acid secretion and stimulating intestinal basolateral membrane glucose transport (Cheeseman and Tsang, 1996). In addition, it modulates intestinal blood flow, increases the barrier function of the gut epithelium, reduces gut permeability and bacterial translocation in cases of intestinal inflammation; and stimulates the expression of digestive enzymes (Burrin *et al.*, 2003, Drucker, 1999, Drucker, 2001b, Drucker, 2002, Estall and Drucker, 2006). Interestingly, GLP-2 up-regulates the expression of SGLT1 via neurohormonal signals involving the enteric nervous system (Cheeseman, 1997).

2.4.2. Neuropeptides: VIP, PACAP and Substance P

Neuropeptides are small protein-like molecules (peptides) synthesized in the nervous system to modulate intercellular communication between neurons. They convey neuronal signals to target cells that express the binding receptors of these peptides; hence, they are known as neurotransmitters or neuromodulators. Neuropeptides are stored in large granular vesicles (LGV) in the nerve cells and are released in a regulated secretory pathway (Merighi *et al.*, 2011). In the gut, the most released neuropeptides by the enteric nervous system are acetylcholine, vasoactive intestinal peptide (VIP), pituitary adenylate cyclase-activating polypeptide (PACAP) and substance P (SP).

- VIP: VIP is a neuropeptide produced in the central and peripheral nervous systems, including the neuronal networks of the GI tract (Gozes and Brenneman, 1989). In the CNS, VIP-containing nerve fibres are concentrated particularly in the cerebral cortex, and specific areas of hippocampus, amygdala and hypothalamus (Loren *et al.*, 1979). In the GI tract, VIP is primarily localized to tiny nerve fibres and nerve terminals of the muscle layer, found throughout the gut ranging from esophagus to rectum including the pancreas (Bryant *et al.*, 1976). A study reported that VIP expression is also found in all the layers of the colon (muscle plus mucosa), but with highest concentrations in the submucosal and myenteric plexus (Bryant and Bloom, 1979). However, it has been documented in man that VIP is also present in secretory cells of the mucosal layer, as well as the immune cells (de Jonge, 2013).

VIP was originally identified in the porcine duodenum as a 28 amino acid residue peptide, and named for its potent vasodilator actions (Mutt and Said, 1974, Schaaper and Beyerman, 1984). It has pleiotropic effects on gut functions: 1) it greatly stimulates the mucosal secretion of water and electrolyte (Barbezat and Grossman, 1971, Schwartz *et al.*, 1974); 2) it regulates gut motility by inhibiting the peristaltic reflex (mediates inhibitory motor neurons in the gut) and stimulating contractions of the circular smooth muscle layer (Grider and Makhlouf, 1990, Grider and Makhlouf, 1988); 3) dilates peripheral blood vessels and controls intestinal

blood flow (Theodorsson *et al.*, 1991); 4) promotes secretion of pancreatic bicarbonate-rich fluids and glucagon, while inhibits gastric acid secretion (Holst *et al.*, 1984, Nassar *et al.*, 1995); 5) modulates the immune response to mucosal infection and inflammation (Surrenti *et al.*, 1993).

The physiological action of VIP as a neurotransmitter or a possible paracrine or local hormone varies greatly depending on its tissue location. As VIP is widely distributed in the respiratory and urogenital tracts, exocrine glands, the thyroid and adrenal glands, it is involved in the enhanced mucosal secretions, relaxation of smooth muscle activity, hyperventilation, enhanced myocardial contractility and cardiac output, as well as its vasodilatation role to regulate the blood flow in those organs (Fahrenkrug and Emson, 1982). In addition, VIP has anti-inflammatory action and modulates the cellular functions in the immune system of the body (Delgado and Ganea, 2013, Delgado *et al.*, 2004a). VIP exerts its actions by binding to two G-protein-coupled receptors, VPAC1 and VPAC2, which also recognize, with a similar high affinity, another neuropeptide named pituitary adenylate cyclase-activating polypeptide (PACAP) (Laburthe *et al.*, 2007).

- **PACAP:** PACAP, like VIP, is multifunctional neuropeptide acting as a prominent neurotransmitter/ neuromodulator in the central and peripheral nervous systems, as well as the pituitary gland. It is also a potent hormone regulating the paracrine and autocrine secretions of various peripheral tissues including the adrenal gland and organs of the digestive, respiratory, urinary and reproductive systems (Arimura and Shioda, 1995, Sundler *et al.*, 1992, Uddman *et al.*, 1991). Two forms of PACAP were identified with 27 and 38 amino acid residues that are generated from the same precursor gene (Miyata *et al.*, 1989, Miyata *et al.*, 1990).

In the CNS, it is most abundant in the hypothalamus, with lower levels in other brain regions (Ghatei *et al.*, 1993). In pancreatic islets, PACAP acts as an insulinotropic factor, at minute concentrations, stimulating insulin secretion in a glucose-dependent manner (Yada *et al.*, 1994), beside its parasympathetic and sensory neurotransmitter effects. Additionally, it is considered as an immunomodulatory and anti-inflammatory agents acting through diverse mechanisms in the immune system (Delgado *et al.*, 2004b, Ganea and Delgado, 2002, Leceta *et al.*, 2000).

- **Substance P:** Substance P (SP): is a short 11 amino acid neuropeptide known as a brain/gut peptide, which is found predominantly in the dorsal root ganglia and sensory neurons, as well as in the gut and other tissues. SP has variable roles, mainly, it is an important element in pain perception and as a regulator of

neuroimmune interactions (Harrison and Geppetti, 2001), it also promotes epithelial cell growth (Reid *et al.*, 1993), and has proinflammatory properties involved in inflammatory diseases (O'Connor *et al.*, 2004). Moreover, it has a significant role in glucose homeostasis as it affects insulin secretion and its resistance (Brown and Vale, 1976). SP mediates its effects through 3 neurokinin (NK) receptors, belonging to the G-protein coupled-receptor family. The high-affinity receptor for SP is NK-1, while NK-2 and NK-3 bind with much lower affinity to this neuropeptide (Bellucci *et al.*, 2002).

In the gut, SP is released by neurons of the myenteric and submucosal plexus and other cells like enteroendocrine cells, eosinophils and macrophages. Activation of both NK-2 and NK-3 receptors affects GI motility, whereas activation of NK-1R stimulates chloride secretion, reduces smooth muscle function, modulates immune responses and induces intestinal inflammation (Gross and Pothoulakis, 2007, Koon and Pothoulakis, 2006).

The precursor of SP is Protachykinin-1 protein that is encoded by the *TAC1* gene in human. The common precursor preprotachykinin encodes four peptide of the tachykinin hormone family: substance P, neurokinin A, neuropeptide K and neuropeptide gamma, depending on differential precursor RNA splicing and posttranslational processing (Krause *et al.*, 1989). These hormones are thought to function as neurotransmitters interacting with nerve receptors and smooth muscle cells (Carter and Krause, 1990).

G protein-coupled receptor family (GPCR):

The superfamily of GPCR are also known as 7 transmembrane domain receptors because they pass through the cell membrane seven times. GPCRs involve the mentioned receptors such as: VPAC1, VPAC2, PAC1 and GLP-2R. Molecules outside the cell bind to these receptors as ligands and activate them to induce tissue-specific responses by acting through two principal signal transduction pathways: the cAMP signaling pathway and the phosphatidylinositol signaling pathway (Gilman, 1987). These ligands include nutrients, light-sensitive compounds, odours, hormones and neurotransmitters; the latter are peptides or large proteins.

GPCRs are engaged in a wide variety of physiological processes, they mediate our sense of vision, smell, taste, and pain (Vaidehi *et al.*, 2002), as well as many automatic functions of the body such as blood pressure, heart rate and digestive processes (Harris *et al.*, 2008). In addition, they regulate activity of the immune system and inflammation (Lombardi *et al.*, 2002). However, over 90% of nonsensory GPCRs are expressed in the brain, where they are involved in various vital neuronal functions including behavioral and mood regulation (Gainetdinov *et al.*, 2004).

3. Nutrient sensing in the gastrointestinal tract

3.1. Types of taste receptors, and the mediated intracellular pathway:

Two types of taste receptors have been identified, type 1 (T1Rs) and type 2 (T2Rs) that belong to the G protein–coupled receptors (GPCRs) superfamily (Bachmanov and Beauchamp, 2007). The T1R family involves three characterized members: T1R1, T1R2 and T1R3, whereas the T2R family includes many members of the 43 human *TAS2R* genes, five of which are pseudogenes (Rozengurt, 2006, Andres-Barquin and Conte, 2004, Bachmanov and Beauchamp, 2007). The T1R2/T1R3 combination was identified as a broad-specificity sweet sensor, while the T1R1/T1R3 combination acts as a broad-spectrum L-amino acid sensor (Li *et al.*, 2002, Nelson *et al.*, 2001).

These taste receptors are highly expressed on the epithelium covering the tongue located on the apical surface of taste cells in the taste buds. However, their expression, for the first time was detected in enteroendocrine cells of the intestine (Dyer *et al.*, 2005). They are also found in other tissues, including pancreas (Nakagawa *et al.*, 2009), brain (Ren *et al.*, 2011, Singh *et al.*, 2011) and several cell types of the airway epithelium (Folwaczny *et al.*, 1999a, Pilch, 2008, Tizzano *et al.*, 2010). Generally, these receptors detect similar stimuli using similar signaling effectors, but prompt different responses in different tissues.

In the taste cell, nutrient tastant molecules bind to taste receptors to activate serial intracellular transducers involving the G-protein α-gustducin, phospholipase Cβ2 (PLCβ2) and the second messengers IP3 and its receptor IP3R3, which mediates the release of Ca^{2+} from intracellular stores. Subsequently, the Ca^{2+}-dependent activation of TRPM5 channels, on the cell membrane, leads to cell membrane depolarization, generation of action potentials and release of ATP neurotransmitters at the synapse to stimulate gustatory afferent neurons (Finger *et al.*, 2005, Kaske *et al.*, 2007, Kinnamon, 2012, Martin *et al.*, 1997, Sabino-Silva *et al.*, 2010), thus, delivering the information from the tongue or the gut to the brain.

Concerning the sense of taste by the lingual epithelium, taste receptors have a role in selection, evaluation and satiation of food (Folwaczny *et al.*, 1999b). They interact with the taste stimuli “ligand”, to initiate the transmission of neuronal signals to the brain resulting in taste perception. Subsequently, they either initiate a protection response (as a warning signal induced by bitter-tasting toxic substance) or mediate food intake and gut absorption through triggering the gut-brain neural pathway (Sternini *et al.*, 2008).

In the gut mucosa, those specialized nutrient sensors on the EECs function as chemoreceptors involved in satiation, mainly transmitted by vagal afferents, and the regulation of intestinal transports as discussed later.

3.2. The five taste modalities:

The distinctive five basic taste modalities are: sweet, umami, bitter, sour and salty. All other tastes come from a combination of these basic tastes. They are explained as following:

- Sweet taste: This pleasant taste is sensed by T1R family receptors that function as heterodimer combined subunits: T1R2/T1R3 for the sweet perception. These receptors detect the presence of carbohydrates, natural sugars and artificial sweeteners in the oral cavity as well as in the intestinal lumen (Nelson *et al.*, 2001, Dyer *et al.*, 2005).

- Umami taste: This is described as the hearty or savoury taste. It is detected by the heterodimer combined GPCR subunits: T1R1/T1R3 which are stimulated by glutamic acids like monosodium glutamate, L-amino acids and peptides like 5`-ribonucleotides (Kinnamon and Vandenbeuch, 2009, Li *et al.*, 2002).

- Salt taste: Salty flavour is sensed by salt receptors that are ion channels admitting Na^+ ions into the cells resulting in cell depolarization and Ca^{2+} entry. Hence, it regulates the intake of Na^+ and other salts important for fluid and electrolyte balance (DeSimone and Lyall, 2006).

- Sour taste: Sourness is the taste that detects the acidity of food and drinks. It helps to avoid the ingestion of spoiled food and maintaining the acid–base balance of the body. The candidate sour receptors, PKD2L1, govern H^+ ions entering the cell, playing a role as pH detectors (Ishii *et al.*, 2009, Kataoka *et al.*, 2008, DeSimone and Lyall, 2006).

- Bitter taste: This is the unpleasant, sharp, or disagreeable taste of bitter characteristic of many toxic compounds. Bitter taste receptors are the T2R family that recognizes harmful toxins and noxious foods. Hence, bitter sensing alerts humans and limits the intestinal absorption of these substances by modifying the gut membrane transporters (Wu *et al.*, 2002a, Rozengurt, 2006, Li *et al.*, 2011).

On the tongue, each taste bud is a pack of aggregated 50-150 polarized neuroepithelial taste cells forming clusters of columnar pseudostratified epithelium in the oral cavity (Uchida *et al.*, 2012). Taste buds are distributed as “tongue map” on the superior surface of the tongue, the soft palate and the epiglottis (Zhang *et al.*, 2003). Various taste modalities are mediated via different mechanisms according to the primary taste receptor and transduction pathway expressed in a given taste cell. As seen in Figure 9, it is believed recently that all tongue areas are responsiveness to the five basic modalities in varying degree of intensity, as modality-specific receptors (response to one taste over the others) are widely expressed in discrete subpopulations of taste cells. The 'gustotopic' map of the tongue can be seen in other tissues of the gut (e.g. stomach, gallbladder, small

intestine, colon, etc), with taste receptors at different locations. Also true for the naso-tracheal epithelium. The brain also maps in its response to taste (Chen *et al.,* 2011, Huang *et al.,* 2006).

***Figure 9:* Diagram of human tongue showing the 'gustotopic' map to different tastant**

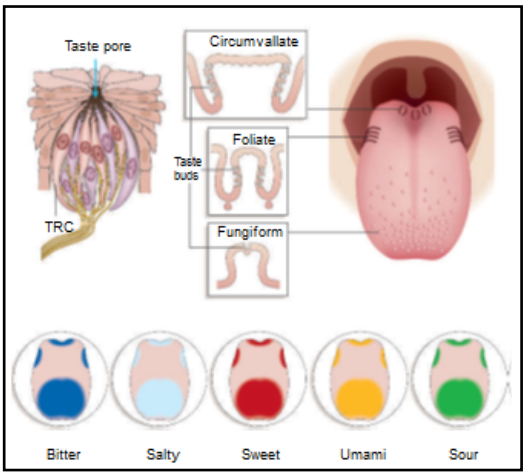

Diagram demonstrating the functional anatomy of human tongue, it shows that all areas of the tongue sense all taste modalities bitter, sour, sweet, salty and umami. (Taken with permission from Chandrashekar et al. Nature 2006, 444: 288-294).

3.3. Glucose sensing and signalling in the gut:

In a similar taste signalling mechanism to that of the tongue, if not the same, the small intestine has the ability to sense luminal nutrients via taste-receptors (nutrient sensors) located on the EECs, which are in direct contact with the gut contents. Upon activation of these receptors, they trigger intrinsic and extrinsic signalling pathways, communicating with the intestinal sensory, endocrine and absorptive cells, and evoking neuronal circuits through the enteric nerve endings, which do not penetrate the mucosal epithelium to reach the gut lumen (Breer *et al.*, 2012, Shirazi-Beechey *et al.*, 2011a, Powley *et al.*, 2011). The chemo-sensation promotes the secretory granules near the BLM of the EEC to release peptides (stimulating local nerves and neighbouring cells) or classical circulating hormones (affecting distal tissues) (Janssen and Depoortere, 2013, Tolhurst *et al.*, 2012). These secretions are involved in glucose hemostasis (Drucker, 2007) and gene expression (Moran *et al.*, 2010a), plus other roles as discussed previously (gut hormones and neuropeptides).

Importantly, intestinal sensing enables the gut to regulate nutrient transporters, providing an adaptive absorptive function to match luminal nutrient concentrations. This chemo-sensing concept of the GI system became first evident when Bayliss and Starling observed that a gut hormone (secretin) was released in response to increased luminal acids (Bayliss and Starling, 1902).

4. The pathway of intestinal glucose sensing mediating SGLT1 expression

Expression of SGLT1 has been shown to be upregulated in response to increased luminal monosaccharides, although, the metabolism of monosaccharides is not required for this response (Shirazi-Beechey *et al.*, 1991, Dyer *et al.*, 1997b). Moreover, the introduction of a membrane impermeable glucose-analogue also stimulated SGLT1 up-regulation, indicating that monosaccharide-induced SGLT1 expression is mediated by luminal sensing, and is independent of glucose metabolism or absorption (Shirazi-Beechey *et al.*, 2011b, Dyer *et al.*, 2003). These data suggest that there is a glucose sensor, distinct from SGLT1, which detects luminal glucose and initiates a signaling pathway resulting in enhancement of SGLT1 expression (Dyer *et al.*, 2003). In 2005, our laboratory was the first to show that taste receptor T1R family members are expressed in the intestinal enteroendocrine cells (Dyer *et al.*, 2005).

Studies using *T1R3*- and gustducin-knockout mice provided convincing evidence that the gut-expressed glucose receptor T1R2-T1R3 and Gα-gustducin act as the intestinal glucose sensor involved in sweet taste transduction (Margolskee *et al.*, 2007). In *T1R3*-and gustducin-knockout mice, no change was observed in SGLT1 expression and function on either low- or high-carbohydrate diet (1.9% and 70% sucrose). Indicating that the deletion of either α-gustducin or T1R3 in mice abolished sweet transduction and prevented the intestinal up-regulation of SGLT1 expression in response to increased dietary carbohydrates, which was observed in wild type mice. However, the expression of SGLT1 in both types of knockout mice was identical to that in wild type animals on the low-carbohydrate diet. This suggests that the intestinal capacity to absorb glucose is maintained via basal levels of SGLT1 expression, independent of luminal sugar sensing by T1R3 and gustducin, although, this capacity becomes limiting when luminal carbohydrate exceeds a threshold level that activates an inducible signaling pathway, dependent on T1R3 and gustducin to up-regulate SGLT1 expression in response to luminal sugars (Margolskee *et al.*, 2007).

Further experiments using cat intestine as a naturally occurring T1R2-deficient model show that T1R2-T1R3, should be co-expressed as a heterodimer on the endocrine cells to sense luminal glucose concentration for SGLT1 upregulation (Batchelor *et al.*, 2011).

Dietary monosaccharides as well as artificial sweeteners activate glucose sensors (T1R2/T1R3), on luminal surface of the enteroendocrine cells (Moran *et al.*, 2010a, Shirazi-Beechey *et al.*, 2011b). Activated receptors engage α-gustducin and provoke intracellular signaling pathways, involving elevated calcium levels,

membrane depolarization and second messenger cascades, to promote the secretion of gut hormones: GLP-1, GLP-2 and GIP (Rasoamanana *et al.*, 2012). In response to luminal carbohydrates, EECs secrete GLP-2 hormone, which is involved in the up-regulation of SGLT1 expression (Drucker, 2001a, Moran *et al.*, 2010a). GLP-2 interacts with its receptors (GLP-2R), residing on afferent enteric neurons, to elicit neuronal signals transmitted through the submucosal myenteric plexus and promotes the release of neuropeptides at the nerve ending (Stoner, 2005). Consequently, neuropeptides PACAP and VIP bind to their VPAC1 receptors, stimulatory G-protein receptors, on the BLM of the absorptive enterocytes.

This results in elevated levels of intracellular mediator cAMP and hence, increases the post-transcriptional cAMP-dependent stability of *SGLT1* mRNA (Sharp and Debnam, 1994, Sternini *et al.*, 2008). Eventually, enhances the expression of functional SGLT1 protein, which is synthesized and inserted into the BBM to increase glucose uptake rate (Dyer *et al.*, 2007, Raybould, 2007, Shirazi-Beechey *et al.,* 20011b*)*. This stabilization is mediated by cytoplasmic protein interacting with a uridine-rich element (URE) in the 3' untranslated region (UTR) of *SGLT1* mRNA (Lee *et al.*, 2000, Loflin and Lever, 2001). One study suggested that cyclic AMP has a role in the physiological modulation of intestinal sugar transport, through hyperpolarization of the potential difference across the BBM, an important driving force for SGLT1 in intestinal enterocyte.

It has been demonstrated that GIP also participate in intestinal glucose absorption, as it helps intracellular accumulation of cAMP and thus up-regulates SGLT-1 expression (Singh *et al.*, 2008). However, work in our laboratory has shown that GIP receptor knockout mice do not upregulate SGLT1 expression in response to high carbohydrate diets, refuting the role of GIP in dietary-induced SGLT1 regulation (Shirazi-Beechey *et al.*, 2011a).

5. Disorders related to monosaccharide transporters and digestive enzymes:

5.1. Glucose/Galactose malabsorption (GGM)

GGM is a rare autosomal recessive metabolic disorder caused by combined mutations in *SGLT1* gene. However, several missense mutations have been identified in different sequences of the gene in GGM, either in the transmembrane helix or in the extracellular loop (e.g. Gly318Arg and Ala468Val), (Leu147Arg and Cys355Ser) and (Ala304Val and Arg499His) (Wright *et al.*, 2002, Turk *et al.*, 1991, Martin *et al.*, 1996). *SGLT1* mutations do not affect protein synthesis, insertion into the endoplasmic reticulum or glycosylation, but they severely impair protein processing through the Golgi apparatus and lead to defective trafficking of the

mutant protein from the endoplasmic reticulum to the BBM of the enterocytes. The mis-trafficking could be due to protein misfolding or aggregation (Martin *et al.*, 1997, Lam *et al.*, 1999).

GGM is characterized by a defect in glucose transporter (SGLT1) resulting in impaired intestinal absorption of glucose and galactose as well as water molecules. Hence, patients with GGM present with neonatal onset of life-threatening osmotic diarrhoea and dehydration, which is potentially fatal unless these monosaccharides are removed from the diet (Turk *et al.*, 1991, Boisen and Hjelt, 1999, Schneider *et al.*, 1966). The diarrhoea is caused by the intestinal accumulation of glucose/galactose, which attracts water by their osmotic effect. Moreover, the loss of the SGLT1 function as a water pump, due to impaired glucose-stimulated water absorption, leads to more accumulation of luminal water and over-loading the intestine with fluids promoting peristalsis. This diarrhoea ceases once intake of lactose, sucrose, glucose and galactose are withdrawn from the diet, but promptly resumes if they are re-introduced. However, children with GGM are treated with oral rehydration therapy (ORT) and thrive normally depending on fructose-based replacement-diet (Wright, 1998, Naftalin, 2008).

5.2. Congenital Lactase deficiency (CLD)

CLD is a common enzyme deficiency disorder that is inherited as an autosomal recessive. It is due to mutation in the lactase enzyme coding gene, affecting the protein structure and trafficking pathway (Uchida *et al.*, 2012). Therefore, lactase enzyme activity is severely diminished to 5-10% in the small intestinal epithelium resulting in impaired lactose digestion and it will not be absorbed, and hence its accumulation creates a luminal osmotic effect leading to water retention. CLD is also characterized by watery diarrhoea in newborns when they start breast-feeding or are fed lactose-containing formulas. It is mandatory to switch their nutrition to lactose-hydrolyzed human milk, and then to a gluten-free diet (Torniainen *et al.*, 2009, Kuokkanen *et al.*, 2006, Simila *et al.*, 1982).

5.3. Diabetes Mellitus (DM)

- Definition and types:

Diabetes mellitus (DM) is a common metabolic disorder characterized by disturbance in the metabolism of carbohydrates, fat and proteins, resulting in uncontrolled hyperglycaemia. DM is classified by the World Health Organization (WHO) according to etiological criteria into three common clinical types: type 1, type 2 and type 3. Type 1 is the insulin-dependent diabetes mellitus (IDDM), which is common in children due to autoimmune-mediated pancreatic β cells destruction

leading to absolute insulin hormone deficiency. Type 2 is the non-insulin dependent diabetes mellitus (NIDDM), which is the most common form of DM and mostly affects adults over 40 years of age (discussed later). Type 3 is known as gestational diabetes that affects pregnant mothers and can be resolved after delivery. Both type 2 and type 3 are characterized by peripheral tissue resistance to insulin, although there is normal insulin levels (Alberti and Zimmet, 1998).

- **Clinical features and diagnosis:**

It is a common heterogenic disease in the developing countries with increased incidence and threatening complications. It is strongly affected by genetic predisposition plus causative environmental factors that impair the tissue insulin-sensitivity, like consuming high carbohydrate diets and central obesity (Otieno *et al.*, 2008, Alberti and Zimmet, 1998). Patients with NIDDM present with the classic symptoms of diabetes (ie, polyuria, polydipsia, polyphagia, fatigability and weight loss). Upper gastrointestinal dysfunctions are common among diabetic patients, such as abdominal pain, vomiting, constipation, diarrhea, which could indicate diabetic autonomic neuropathy involving the GIT (Alwakeel *et al.*, 2009, Schlienger, 2013, Palmer, 2004). Other worse symptoms manifesting hyperglycemia include blurred vision, paresthesias, and recurrent infections and delayed healing. However, many patients with type 2 diabetes are asymptomatic and remain undiagnosed for several years till they complain of various clinical aspects.

The diagnosis of diabetes is based on the history of the classical symptoms (as above) plus diagnostic tests including (Puavilai *et al.*, 1999):

1- Fasting blood glucose level of ≥ 126 mg/dL (7 mmol/L) on two separate tests.

2- Random blood glucose level of ≥ 200 mg/dL (11.1 mmol/L).

3- Oral glucose tolerance test (OGTT) is the measuring of plasma glucose concentration before the test (fasting) and after drinking 75g glucose syrup. The record of ≥ 7 mmol/l in fasting, or ≥ 11.1 mmol/l two hours after the OGTT indicates diabetes.

4- The glycated hemoglobin (HbA1C) test is a blood test monitoring the average blood sugar level for the past two to three months. Level of 6.5 % or higher on two separate tests indicate diabetes mellitus (Christophi *et al.*, 2013, Ingram and Bachrach, 2012).

- **Complications of NIDDM:**

Complications of diabetes mellitus vary between progressive chronic to dangerous acute situations due to uncontrolled, i.e. extremely high or very low, blood glucose levels. Acute complications include: diabetic ketoacidosis, hyperglycemia hyperosmolar state, hypoglycemia, which are considered as a medical emergency leading to diabetic coma or death if there is inadequate or delayed treatment (Liu *et al.*, 2012, Palmer, 2004, Stoner, 2005). While, chronic complications involve: microvascular or macrovascular complications. Microvascular damage (microangiopathy) can affect various body tissues and could lead to organ failure. It can cause cardiomyopathy, nephropathy, retinopathy (presented as vision loss) and neuropathy (presented as diabetic foot and skin, nail and hair changes) (Alwakeel *et al.*, 2009, Schlienger, 2013, Sima, 2006). Macrovascular damage leads to brain stroke, cardiovascular disease (heart attack) and diabetic myonecrosis (muscle wasting). Additionally, impaired immune response in diabetic individuals can lead to severe infection and inflammation with slower recovery than normal response (O'Connor *et al.*, 2006).

- Managements of DM:

Diabetes mellitus is effectively managed by multimodal intensive therapies to maintain glucose homeostasis and to minimize the risk of complications. In type 1 (IDDM), insulin injections are the chief line of treatment, or pancreatic transplants in severe uncontrolled diabetic cases (Folwaczny *et al.*, 1999b). However, in patients with type 2 (NIDDM), treatment starts with controlling blood pressure, consuming a carbohydrate-restricted diet, encouraging physical exercise and reducing body weight. Insulin injections and oral hypoglycaemic drugs (OHD) have been also used as standard medical approaches, prescribed either alone or in combination. OHD mainly act by enhancing endogenous insulin release (insulin sensitizers: metformin and the thiazolidinediones), or increasing its action (sulfonylureas and meglitinides), minimizing insulin resistance, reducing hepatic gluoconeogenesis (biguanides), limiting glucose absorption through inhibiting sugars hydrolysis by the intestinal BBM disaccharidases (alpha-glucosidase inhibitors), or lipolysis inhibitors (Bell, 2004, Wagman and Nuss, 2001).

However, due to the limited efficacy and side effects of insulin and OHD, the development of new therapeutic alternatives has become mandatory. Recently, researchers shifted their attention to manipulate the intestinal capacity for dietary sugar absorption by investigating glucose transporter expression, their regulation and inhibition. This work gave rise to a newly innovative drug Thioglycosides, which control hyperglycaemia by inhibiting hSGLT1 (Castaneda *et al.*, 2007). Although, it is not clear how its accompanied osmotic diarrhoea will be tolerated, due to the blocking of water pump action by SGLT1.

a) SGLT1 and diabetes mellitus:

Previous studies on human patients with non-insulin dependent diabetes mellitus (NIDDM) showed that the enhanced expression of intestinal monosaccharide transporters SGLT1 leads to the increased capacity of intestinal glucose absorption (Dyer *et al.*, 2002b). These results were also observed in diabetic rats (Lorenz-Meyer *et al.*, 1977). It was also found that SGLT1 transporter activity is significantly higher in duodenal biopsies of diabetic patients compared to that in control subjects. Abundance of SGLT1 protein and mRNA is increased in diabetics by 4-fold and 3-fold, respectively. This enhanced expression and activity of SGLT1 was independent of fluctuations in the dietary carbohydrate content, as documented in healthy individuals, and was not responsive to changes in blood glucose and insulin levels (Dyer *et al.*, 2002b, Burant *et al.*, 1994).

Hence, new strategies can be designed to manage postprandial hyperglycemia by reducing the absorption of dietary sugars from the gut, resulting in lower blood glucose levels. Researchers can contribute by identifying the factors and pathways involved in the regulation of intestinal glucose transport. Interest is focused recently on the expression of the chief glucose transporter (SGLT1), from the gut lumen into the enterocyte, as a new therapeutic target for diabetic patients (Castaneda-Sceppa and Castaneda, 2011).

Some innovative drugs are under clinical trail, for treatment of type II diabetes with minimal risk of hypoglycemia, such as inhibitors of SGLT1 and SGLT2 to reduce renal glucose reabsorption as well as to promote urinary glucose excretion (Kinne and Castaneda, 2011, Washburn, 2012, Tahrani *et al.,* 2013). LX4211, is a dual inhibitor of SGLT1 and SGLT2 that is also modulating intestinal glucose absorption (Lapuerta *et al.*, 2013, Zambrowicz *et al*., 2012).

Additionally, the use of glucose analogues Thioglycosides has shown promising therapeutic potential to control hyperglycemia (Castaneda *et al.*, 2007). The first drug developed was the phlorizin analogue T-1095, which blocks SGLT2 to reduce glucose reabsorption in the proximal convoluted tubules in the kidney (Arakawa *et al.*, 2001, Oku *et al.*, 2000). T-1095 significantly improved hyperglycemia and prevented diabetic neuropathy (Ueta *et al.*, 2005). Other examples of specific SGLT2 inhibitors include Dapagliflozin (BMS-512148), which reduces blood glucose by 55% after 5 hours of a single dose and is extremely selective for SGLT2 than SGLT1 (Han *et al.*, 2008, Meng *et al.*, 2008), Sergliflozin (KGT-1251) that prevent the development of glomerulosclerosis and nephropathy (Jabbour and Goldstein, 2008).

b) Insulin signalling and regulation of glucose transport:

Insulin is the most potent hormone regulating the metabolism of lipids, proteins and carbohydrates, by promoting their synthesis and storage while inhibiting their breakdown and release into the blood (Khan and Pessin, 2002). Its main anabolic action is stimulating the uptake of glucose, amino acids and fatty acids into the insulin-responsive cells like fat tissues and striated muscles. Additionally, it promotes cell growth and differentiation by acting on genes involved in the production of certain growth factors (Saltiel and Kahn, 2001).

Insulin is synthesized by the islets of β cells of the pancreas and secreted into the blood stream in response to postprandial elevation of blood sugar concentration. It maintains glucose homeostasis in two ways:

1- It stimulates glucose uptake from the blood into the fat and muscle cells, to promote its intracellular storage as triglycerides,
2- It inhibits glucose production and output from the liver to the circulation by inhibiting pancreatic α-cells to secrete glucagon (supressing gluconeogenesis and glycogenolysis), and by promoting liver glycogenesis (Cherrington *et al.*, 2007, Wilcox, 2005).

The main insulin-regulated glucose transporter is the facilitative glucose transporter GLUT4 that is expressed abundantly in adipocytes and skeletal muscle cells (James *et al.*, 1988). Insulin increases glucose uptake in these cells by stimulating the translocation of GLUT4 from intracellular compartments, where it is sequestered in GLUT4 storage vesicles (GSV) in low insulin state, to the functional site on the surface of the cytoplasmic membrane (Pilch, 2008). This GLUT4 translocation is a complex process initiated by the binding of insulin to its receptor (IR), which has two extracellular α-subunits (hormone-binding domain) that auto-phosphorylates the transmembrane β-subunits and activates the tyrosine kinase domain (Gammeltoft and Van Obberghen, 1986, Kido *et al.*, 2001). In response to insulin–receptor binding, intracellular proteins known as insulin responsive substrates (IRS) are phosphorylated, which in turn, interacts with other insulin signaling molecules to promote further cascades. Eventually, this leads to the trafficking of GLUT4 vesicles by mediating the tethering, docking and fusion of GLUT4 protein to the cell membrane (Govers *et al.*, 2004, Karylowski *et al.*, 2004). Finally, after achieving the effect of insulin-regulated glucose transport, GLUT4 is removed from the cell surface by endocytosis of the insulin-receptor complex (Chang *et al.*, 2004, Larance *et al.*, 2008, Rowland *et al.*, 2011), and insulin is inactivated and degraded by insulin degrading enzymes mostly by liver cells (Duckworth *et al.*, 1998).

In NIDDM, insulin has normal levels but the peripheral target tissues have reduced sensitivity to insulin (partial or complete insulin resistance). This resistance is either due to defects in some of the IRS members (Sesti *et al.*, 2001) or due to mis-trafficking of the insulin-stimulated GLUT4 translocation affecting GLUT4 expression on the cell surface of the adipocytes and myocytes (Miura *et al.*, 2001). This prevents glucose uptake by these cells and pooling of high glucose in the circulation.

6. Streptozotocin and its use:

Streptozotocin (STZ) is a compound that was identified originally in the late 1950s as a naturally occurring broad-spectrum antibiotic derived from *Streptomyces achromogenes* (Vavra *et al.*, 1959). However, in the mid-1960s, it was realized to be a genotoxic chemical that particularly targeting the pancreatic insulin-producing beta cells. Therefore, it was used as chemotherapy for treating certain cases of pancreatic islet insulinomas. However, due to its toxic and carcinogenic effect, its use is limited to the metastatic or unremovable neuroendocrine pancreatic tumours (Turner *et al.*, 2010, Murray-Lyon *et al.*, 1968, Brentjens and Saltz, 2001, Herbai and Lundin, 1976). Recently, it is widely used as a potent diabetogenic agent in research to induce experimental diabetes in rats since it causes insulin deficiency and hyperglycaemia, producing an animal model of insulin-dependent diabetes mellitus (type 1 DM)(Ito *et al.*, 1999).

STZ is a glucosamine-nitrosourea molecule that has a similar structure to glucose, enough to compete with glucose, to be taken up by the glucose transporter GLUT2 into the pancreatic β cell. STZ is not recognized by other glucose transporters, demonstrating its selective cytotoxicity to the pancreatic beta cells because these cells have relatively higher levels of GLUT2, the target for STZ (Gai *et al.*, 2004, Schnedl *et al.*, 1994, Wang and Gleichmann, 1995, Wang and Gleichmann, 1998). Upon entrance of the STZ into the cells, it causes irreversible cell damage by alkylating and directly methylating the DNA. The damaged DNA (single-strand breaks) induce the crucial step for the diabetogenic effect of STZ, activating poly ADP-ribosylation resulting in the reduction of NAD^+ and ATP. The enhanced phosphorylation of ATP provides a substrate for xanthine oxidase to form superoxide radicals, subsequently, generating hydrogen peroxidase and hydroxyl radicals. As a result after STZ treatment, insulin-producing beta cells are destroyed by necrosis. Superimposed on these effects is the immune reaction evoked against the β-cell destruction (Wang and Gleichmann, 1998, Szkudelski, 2001, Bolzan and Bianchi, 2002, Junod *et al.*, 1967, Wilson *et al.*, 1984).

This diabetogenic agent has a remodeling effect on the morphological parameters and probably the biological properties in the small intestine, which are similar to that seen in diabetic humans with the classical signs of diabetes mellitus (Zhao *et al.*, 2003, Gajdosik *et al.*, 1999). Animals with STZ-induced diabetes show hyperphagia, altered intestinal functions, and arrested body weight gain, but promoted intestinal growth and mucosal proliferation (Miller *et al.*, 1977). These animal models are used to investigate the changes in the diabetic intestine and the underlying mechanisms up-regulating SGLT1 to enhance glucose absorption.

Aims of this study

General aim:

To investigate potential changes in morphology and carbohydrate digestive and absorptive functions of the small intestine of control and diabetic subjects. Streptozotocin-induced diabetic rats were used as a model to identify the detailed mechanism(s) underlying the enhanced expression of SGLT1 in the diabetic intestine.

Specific aims:

To determine potential changes in:

1. Morphology, activity of disaccharidases and expression of SGLT1 (at levels of mRNA, protein and function) in the small intestine of diabetic rats compared to controls.
2. The activity of disaccharidases and SGLT1 expression in duodenal biopsies obtained from diabetic subjects compared with those obtained from healthy controls.
3. Key signalling molecules participating in pathways regulating SGLT1 expression.

Ultimate aim:

To identify the molecular mechanisms involved in enhanced SGLT1 expression in the diabetic intestine.

Chapter 2

Materials and methods

Materials

1. Antibodies

Antibodies used in immunohistochemistry or western immunoblotting were:

Primary antibodies:

- SGLT1 polyclonal antibody: raised in rabbit (custom synthesis) to a synthetic peptide corresponding to amino acids 402-420 (STLFTMDIYTKIRKKASEK), a conserved intracellular loop of SGLT1 (Dyer *et al.,* 2009).
- GLUT2 polyclonal antibody: two antibodies were used:
  1-A commercial antibody raised in rabbit against a peptide sequence of rat GLUT2 (residues 40-55), (clone 07-1402, Millipore Ltd, Watford, UK),
  2- Antibody raised in rabbits (custom synthesis) to a synthetic peptide corresponding to amino acids 523–536 (AAVEMEFLGATETA) of equine GLUT2 C-terminus region (Stearns *et al.,* 2010).
- T1R2 and T1R3 polyclonal antibodies: T1R2 (H-90):sc-50305 and T1R3 (H-145):sc-50353, commercial antibodies raised in rabbit and were purchased from Santa Cruz Biotechnology, INC., CA, USA.
- Mouse monoclonal antibody against β-Actin (clone AC-15) was purchased from Sigma-Aldrich Ltd, Poole, Dorset, UK.
- VIP polyclonal antibody: raised in rabbit (AB982, Merck Millipore, Deutschland, Germany).
- Substance P affinity purified mouse monoclonal antibody: purchased from (Neuromics, Edina, USA).

Secondary antibodies:

- FITC (Fluorescein isothiocyanate) secondary antibodies: FITC-conjugated donkey anti-rabbit and anti-mouse IgG were used as appropriate in immunohistochemistry, they were purchased from Jackson ImmunoResearch Laboratories, West Grove, USA.
- Affinity purified peroxidase-linked swine anti-rabbit and rabbit anti-mouse IgG conjugated to horseradish peroxidase secondary antibodies were purchased from Dako, Stockport, UK.

2. Bacterial strains, plasmids and primers

For the cloning of cDNA sequences, the bacterial strains *E.coli* J M 109 and the recombinant plasmid pGEM-Teasy Vector System were purchased from Promega Ltd., Southampton, UK.

The primers for quantitative real-time PCR were designed using Pubmed website (http://www.ncbi.nlm.nih.gov/nuccore/) and Vector NTI software, then, ordered and manufactured by Eurogentec (Germany).

3. Chemicals and commercial kits

- Bio-Rad protein assay kit was obtained from Bio-Rad Laboratories Ltd., Hemel Hempstead, Hertfordshire, UK.
- D-Glucose UV Assay kit was purchased from R-Biopharm Rhône Ltd., Glasgow, Scotland, UK.
- In western blotting technique, PVDF membrane (0.2 µm) for protein blotting was supplied by Bio-Rad Laboratories. Western blots were developed using the Enhanced ChemiLuminescence kit (ECL) purchased from Amersham-Biosciences Ltd., Buckinghamshire, UK, and the spray (WEST-one Western Blot Detection System, iNtRON) was obtained from Biotechnology, UK. Western blot membranes were exposed to Kodak Biomax Light film purchased from Sigma-Aldrich.
- For RNA isolation, RNeasy Mini Kit was supplied by Qiagen Ltd., Crawley, West Sussex, UK. The purification of cDNA was carried out using QIAquick™ PCR purification kit obtained from Qiagen, as before.
- For gel running purposes, the 100 bp Gene ruler DNA ladder plus, the protein ladder and the Orange Loading Dye solutions were purchased from MBI Fermentas, Hanover, MD, USA, as was the 100 mM nucleotide NTP set.
- pGEM-Teasy Vector System for PCR products cloning was purchased from Promega Ltd., Sunderland, Tyne and Wear, UK, as was the AMV Reverse transcriptase.
- The radioisotopes D-[U ^{14}C]-glucose used for the transport studies were purchased from Amersham-Pharmacia Biotechnology Ltd., Little Chalfont, UK.

All other chemicals and solutions were obtained from Bio-Rad Laboratories Ltd. Fisher Scientific (Leicestershire, UK) and Sigma-Aldrich Ltd. unless otherwise mentioned.

Methods

2.1. Animals and tissue collection:

All animal procedures were carried out under the regulations of approved UK Home Office project licence. All Home Office permissions were in place and work was in accordance to the Animals (Scientific Procedures) Act 1986. The Establishment license number (Home Office permission for Liverpool University) is 40/2408. The use of intestinal tissues from diabetic and control rats were under project license number 40/3144, PPL holder Dr Laiche Djouhri. Rodents were provided by the University of Liverpool Biomedical Sciences Unit, and they were sacrificed by schedule 1 of the UK Home Office Regulation. Pigs were provided by the University of Liverpool Farm Animal Division, they were maintained on commercial diets and were sacrificed by an overdose of anaesthetics by the University veterinary surgeons under schedule 1 of UK Home Office regulation. The use of animals and all procedures used were reviewed and approved by Mr Ewan Birnie, Animal Health Officer BVMS, FRCVS of the University of Liverpool acting on behalf of the Home Office.

Mice: Adult male mice (C57BL/6) wild-type, 8 weeks age, were maintained on 40 % carbohydrate diet for 5 to 8 days (diets were obtained from Purina Mills, Richmond, IN, USA). They were housed in a room kept at 21±2°C and was on a 12-hour light/dark schedule. They were sacrificed by cervical dislocation and the entire small intestine was removed immediately. It was cut into 3 equal sections corresponding to proximal, mid and distal parts. The intestinal loops were cut open and rinsed clean with cold saline (0.9 % NaCl, pH 7.4). Then, tissues for brush-border membrane vesicle preparation were wrapped in aluminium foil and frozen immediately in liquid nitrogen and stored at -80 °C until use. Pieces of tissue, 2-3 cm, were placed into PBS containing 4% paraformaldehyde for 4 hours at 4°C for subsequent fixing as described below for histological assessments and immunohistochemical studies.

Pigs: Male and female pigs were used in this study (Landrace X Large White). Weaned pigs were 43 days old, whilst suckling pigs aged 28 days. They were housed in a room kept at 21±2°C and was on a 12-hour reverse light schedule. They were sacrificed with an intravenous injection of 20 ml Penobarbitone (200 mg/ml, Pentoject, Animal care Ltd, York, UK) into the cranial vena cava in the chest. The small intestine was removed from animals and divided into sections of duodenum (distal to the pylorus), jejunum (half way along the small intestine) and ileum (proximal to the ileocaecal junction). The tissue sections were everted and cleaned with cold saline, cut open and wrapped in aluminium foil and frozen in liquid nitrogen and subsequently stored at -80 °C until used for vesicles preparation.

Rats: Adult male (Sprague-Dawley) rats were divided into two groups: controls and diabetics. They were housed in standard environmental conditions with temperature of (21 ± 2 °C), humidity (55 ± 10 %), and a 12 hour light-dark cycle, with available access to water and food. After killing by cervical dislocation, the small intestinal tissues were removed and divided into proximal, mid and distal parts. They were collected and treated similar to mouse intestinal tissues described above for immunohistochemical studies, while the BBMVs were prepared freshly on the same day. In addition, small intestinal samples were also collected from the three sections for RNA isolation, which were placed in screw-capped cryotubes and frozen immediately in liquid nitrogen then stored at -80 °C until use.

Humans: procedures were performed under approvals of Ethics Committee of both hospitals for the work and sample collection for this study. Liverpool researh ethics committee (MREC 02/11/228/A 2K/128) and King Abdulaziz university hospital ethics approval (KAU 358/2766-GE). Written consents from the patients were secured before tissue biopsy removal. Tissue biopsies were transferred from KSA to UK in dry ice package using FedEx by express post.

Tissue biopsies from the second part of the duodenum were taken during routine gastrointestinal investigation for possible GIT disorders. However, all tissues used as control were shown to be normal by histological analysis. Type 2 diabetes was assessed by measuring the fasting blood glucose concentration having values of > 5.5 mmol/L, or random blood glucose level of > 10.5 mmol/L. Three diabetic patients were on controlled carbohydrate diets, seven were on anti-diabetic medications and eight were with uncontrolled diabetes.

Tissue samples were collected from male (12 non-diabetics and 11 diabetics) and female (8 non-diabetics and 7 diabetics) human subjects. Biopsies were either frozen immediately in liquid nitrogen then stored at -80 °C for BBMV, PNMF preparations and RNA isolation or fixed in Paraformaldehyde for immunohistochemical studies. Some samples were collected at the Royal Liverpool University Hospital (Liverpool, UK) by Dr Anthony Ellis, consultant gastroenterologist. While some other samples were collected at King Abdulaziz University Hospital (Jeddah, Saudi Arabia) by consultant gastroenterologists and surgeons: Dr. A. Sibiany, Dr. H. Fallata, Dr. H. Akbar and Dr. S. Bazara'a.

2.2. Inducing diabetes mellitus in rats:

Diabetes mellitus in rats was induced experimentally by Streptozotocin injection (STZ, Sigma Aldrich S0130). Rats were kept fasting for 18-24 hours before the intra-peritoneal injection of a single dose (60 mg/kg body weight). STZ was dissolved in physiological saline immediately prior to injection (60 mg/ml per kg), and the animals were injected with STZ under fume hood.

After 3 to 7 days of STZ administration, a random blood glucose concentration was determined in tail vein blood using a glucometer (the Bayer Contour test meter and strips, Bayer plc, Berkshire, UK), under Isofluorane and O_2 anaesthesia. Rats that had blood glucose of 11.1 mmol/L or more were considered diabetic and were utilized in the study. Most of the diabetic rats had values of at least 20 mmol/L. Some had blood glucose concentration values greater than 34 mmol/L, which is too high to be measured by the available devices.

2.3. Preparation of membrane vesicles:

2.3.1. Preparation of brush-border membrane vesicles (BBMV) from animal tissue:

Solutions:

- Buffer 1

Mannitol (Sigma)	100 mM
HEPES/Tris, pH 7.1 (Fisher Scientific)	2 mM

- Buffer 2

Mannitol	100 mM
HEPES/Tris, pH 7.4	2 mM
$MgSO_4$	0.1 mM

- Buffer 3

Mannitol	300 mM
HEPES/Tris, pH 7.4	20 mM
$MgSO_4$	0.1 mM
NaN_3 (Sigma)	0.02% (w/v)

The method of isolating brush-border membrane vesicles is based on the differential centrifugation and cation precipitation techniques as described by Kessler *et al.1978* and Biber *et al.*1981.

All steps of the procedure were carried out at 4 °C and following the method of Shirazi-Beechey *et al.*, 1990. Protease inhibitors were added to the hypotonic buffer 1, either Protease Inhibitor Cocktail (one tablet of PIC (Roche) per 50 ml of buffer 1) for proximal small intestinal samples, or mixture of several protease inhibitors: 0.5 mM benzamidine (Sigma), 0.5 mM 1,4-dithiothreitol 'DTT' (Sigma) and 0.2 mM phenylmethylsulfonyl fluoride 'PMSF' (Fluka) for the mid and distal tissue samples.

Intestinal tissues 5-10 g were thawed, or used freshly, in 30 ml of ice-cold buffer 1, and were cut into small pieces by sharp scissors. In a thick-walled glass tube, mucosal enterocytes were removed from the tissue using a VIBRO-mixer EI™ with a 23 mm diameter head (Chemap AG, CH-8604 Volketswil, Switzerland) on the highest sitting for 1 minute or until muscle pieces appeared smooth. Vibromixing time was for 30 seconds with an interval rest on ice to avoid heating the tissue, then

vibromixed for further 30 seconds. The cell suspension was filtered through a Büchner funnel, to remove tissue debris and mucus, and its volume was brought up to 25 ml with buffer 1. After mixing, 1 ml samples of homogenate were removed and stored at -20 °C as a control for later studies.

To remove soluble membranes and organelles from the cell suspension, $MgCl_2$ was added to a final concentration of 10 mM and stirred on ice for 20 minutes. For the sedimentation of the large cell organelles and nuclei, the cell suspension was centrifuged at 3000 x g for 10 minutes at 4 °C (SS-34 fixed angle rotor, Sorvall RC-5C centrifuge, Kendro Laboratory Product, USA). The pellet, containing the precipitated nuclei, was discarded, while the supernatant was collected and centrifuged at 30,000 x g for 30 minutes at 4 °C.

The supernatant was discarded and the pellet was re-suspended in Buffer 2 by applying about 10 strokes with a Dounce homogenizer. Again, the suspension was centrifuged at 30,000 x g for 30 minutes. The supernatant was discarded and the final pellet, containing the precipitated purified BBM vesicles, was re-suspended in an appropriate small amount of isotonic Buffer 3 to produce a final concentration of 20-30 mg/ml. The sample was homogenized by passing through a 27-gauge needle or Hamilton syringe several times. Aliquots of the brush-border membrane vesicles were divided and some were stored in liquid nitrogen for uptake tests, while other aliquots were stored at -20 °C for Western blotting and enzyme assays.

For the diabetic and control rats, the BBMVs were prepared using the freshly removed small intestinal tissue as soon as possible after animals were killed. D-glucose uptake assays were carried out on the same day as the use of fresh tissue showed better results. Aliquots were mixed with sample buffer for SDS-PAGE electrophoresis before freezing to avoid freezing/thaw, which leads to protein degradation.

2.3.2. Preparation of brush-border membrane vesicles (BBMV) from human duodenal biopsies

Brush-border membrane vesicles (BBMV) were isolated from frozen human duodenal biopsies using the microscale technique of BBMV preparation as described by Shirazi-Beechey *et al.,* (1990)

Protease Inhibitor Cocktail was added to buffer 1. In 2 ml tube, human biopsy tissue was thawed in 1 ml of ice-cold buffer 1 and homogenized using a Polytron X-10/25 Rotor-Stator device for 30 seconds. The Polytron was rinsed with 1 ml of buffer 1 to collect all cell suspension. 50-100 µl of homogenate was preserved for later use. $MgCl_2$ was added to the cell suspension to a final concentration of 10 mM and mixed for 20 minutes in a rotary mixer in a cold room. After mixing, the cell suspension was centrifuged at 3000 x g for 10 minutes at 4°C (rotor SS-34). The pellet was discarded while the supernatant was collected and centrifuged at 30,000

x g for 30 minutes at 4°C. Next, the supernatant was discarded and the pellet was re-suspended gently in 10-20 µl of Buffer 3 and homogenized by passing through a Hamilton syringe several times. Aliquots of the BBMV samples were stored at -20 °C for Western blotting and enzyme assays.

2.3.3. Preparation of post-nuclear membrane fractions (PNMF) from human biopsies:

Using the method described by Lambert *et al.*, (2002) and Klett *et al.*, (2004). Post-nuclear membrane fractions were prepared from human duodenal biopsies and all steps were carried out at 4°C.

Human biopsies were placed on a glass plate resting on ice and cut into small pieces using a sterile scalpel blade. Tissue pieces were immediately transferred into 120 µl of hypotonic Buffer 1 containing protease inhibitor cocktail (1 tablet of PIC per 50 ml of buffer 1). Using a hand-held homogenizer, tissues were disrupted manually 3-5 times and the homogenizer was then rinsed with 30 µl of Buffer 1 to collect all suspension in the tube. The suspension was mixed in a vibromixer at the highest speed for 2 minutes to remove the epithelial cells. The vibromixer was then rinsed with 1 ml of Buffer 1 and collected into the suspension tube. The suspension sample was mixed and any visible connective tissue was removed with a sterile pipette tip. 50 µl of homogenate was reserved and stored at -20 °C to be used as a control for later studies. The suspension was centrifuged at 500 x g for 10 minutes at 4 °C (rotor SS-34, Sorvall RC-5C centrifuge, Kendro Laboratory Product, USA) to sediment the nuclei. The nuclei pellet was discarded and the supernatant was centrifuged at 30,000 x g for 30 minutes at 4 °C. The final pellet, containing the purified post-nuclear membrane fractions, was resuspended in 20-50 µl of isotonic Buffer 3. The cellular suspension was well-homogenised using a Hamilton glass syringe. Human PNMF were stored at -20 °C until use.

2.4. Quantification of protein concentration

The Bio-Rad assay technique was used to determine the protein concentration, in the BBM vesicles and homogenates, according to the procedure of Tarpey *et al.*, (1995). The assay is based on the Bradford method (Bradford, 1976), where the absorbance is detected by a spectrophotometer when the protein binds to Coomassie blue under acidic conditions.

2.4.1. Micro Protein Assay

Beside protein samples, a standard curve for calibration was prepared using bovine γ-globulin (1.5 mg/ml) ranging from 0 to 24 µg protein, each in 800 µl Buffer 3. Protein samples were diluted 1:800 in Buffer 3. 200 µl of the Bio-Rad protein dye (BioRad, Herts, UK) was added to all samples and standards used for the calibration

curve. Tubes were mixed and incubated for 10 minutes at room temperature before reading the absorbance.

2.4.2. Macro Protein Assay

Similar to the micro protein assay but scaled up by preparing a standard curve for calibration using bovine γ-globulin (1.5 mg/ml) ranging from 0 to 150 µg protein, each in 100 µl Buffer 3 in tubes. In sample tubes, 5 µl of protein sample was diluted (5:100) in Buffer 3 were placed. The Bio-Rad protein dye was diluted 1:5 and filtered through Whatman filter paper. Then, 5 ml were added to the tubes of all samples and standards of the calibration curve, mixed and incubated for 10 minutes at room temperature.

For both micro and macro assays, the absorbance of all reactions was measured against a no-protein blank at 595 nm using a spectrophotometer (Hitachi U-2000, UK). Absorbance readings were plotted alongside standard protein concentrations. The unknown values of protein concentrations of the samples were determined from the standard calibration curve.

2.5. Transport study of D-glucose into brush-border membrane vesicles

The transport rate of D-glucose into the intestinal BBMVs was estimated by using the rapid filtration technique as described by Shirazi *et al.,* (1981a) D-glucose transport study was carried out on the same day of animals being sacrificed and used freshly prepared BBMVs isolated from the proximal, mid and distal regions of the small intestine.

The following solutions were prepared previously and stored at 4 °C:

2X Glucose Solution:

0.2 mM	D-glucose
0.02 % (w/v)	NaN_3

Uptake Buffer:

200 mM	NaSCN or KSCN
200 mM	Mannitol
0.2 mM	$MgSO_4$
0.02 % (w/v)	NaN_3
40 mM	HEPES/Tris, pH 7.4

Stop Buffer*:*

150 mM	KCl
0.1 mM	$MgSO_4$
0.02 % (w/v)	NaN_3
20 mM	HEPES/Tris, pH 7.4

0.1 mM of Phlorizin was dissolved in ethanol just before use.

On the day of the experiment, Millipore filters of 25 mm diameter (0.22 µm pore size, cellulose acetate/nitrate filters, Millipore, GSTF02500 Millipore, Herts., UK) were soaked in double distilled water before use. Before starting the assay, incubation medium was prepared by mixing equal volumes of 2X glucose solution and uptake buffer. 25 µl of D-[U ^{14}C]-glucose (30,000 cpm) per 1 ml of incubation medium were added and mixed well.

Using the freshly prepared BBMVs, 20 µg of protein per assay was aliquoted in test tubes and kept on ice. For each sample, the assay was carried out in triplicate plus two blanks using the uptake buffer containing sodium thiocyanate (NaSCN) and triplicate plus two blanks using the uptake buffer containing potassium thiocyanate (KSCN). Before starting the reaction, the test tubes with the aliquoted BBMV samples were incubated at 37 °C for 5 minutes.

The reaction was started by adding 100 µl of incubation medium, containing either 100 mM NaSCN or 100 mM KSCN, to 20 µg protein and incubated at 37 °C for 3 seconds. The reaction was rapidly stopped by adding 1 ml of ice-cold stop buffer, containing Phlorizin, to the tube and mixed by vortexing. 900 µl of the reaction mixture was removed and filtered immediately through the pre-wetted Millipore filters under suction with vacuum. The filter was washed five times with 1 ml of ice-cold stop solution to remove excess radio-labelled D-glucose. The washed filters were then placed into scintillation vials and dissolved in 4 ml of scintillation fluid (OptiPhase 'hiSafe' 2 Liquid Scintillation Cocktail, PerkinElmer, Leics, UK), and counted for radioactivity in a scintillation counter (LS 6500 Multi-purpose Scintillation Counter, Beckman Coulter, USA).

Internal standards were also performed using the unfiltered incubation medium (containing either NaSCN or KSCN) that was selected randomly from the samples. 50 µl of the unfiltered incubation medium was mixed with 4 ml of liquid scintillation cocktail. To account for the non-specific binding of the radio-labelled D-glucose to the BBM vesicles, zero-time blanks were performed alongside. In the blank tubes, 1 ml of ice-cold stop buffer was added to the BBMV samples before the addition of 100 µl of incubation medium. The obtained values of the blanks were subtracted from the values of uptake results.

In order to calculate the Na^+ -dependent D-glucose transport rate into the BBM vesicles, Na^+ and K^+ -based uptake buffers were used. Results obtained in presence of K^+ were subtracted from those measured in the presence of Na^+ -containing buffer to obtain the values representing the D-glucose transport rate that is Na^+ -dependent.

2.6. Enzyme Assays

Solutions to start the reactions:

- Sucrase assay buffer

Na^+ Maleate, pH 6 (Hopkins and Williams)	100 mM
Sucrose (Sigma)	56 mM

- Maltase assay buffer

Na^+ Maleate, pH 6	100 mM
Maltose (Sigma)	56 mM

- Lactase assay buffer

Na^+ Maleate, pH 6	100 mM
Lactose (Sigma)	56 mM
p-Chloromercuribenzoate (*p*CMB)	200 mM

*Note: p*CMB was added to the Lactase Assay Mix to inhibit the activity of any contaminating lysosomal β-galactosidases.

2.6.1. Determination of disaccharidases enzyme specific activity:

Maltase, sucrase, lactase and alkaline phosphatase are all digestive enzymes and markers for the brush-border membrane. Disaccharidase assays were carried out based on the method of Dahlqvist (1964). The specific enzyme activities were measured, at the physiological temperature of 37 °C, in the brush-border membrane vesicles (BBMV) and their corresponding homogenate to calculate the enrichment and recovery of the samples.

BBMV were thawed and re-homogenized using a 27-gauge needle prior to dilution with Buffer 3 (appropriate dilution for each sample). While the homogenate samples were either diluted or used neat. Each sample was carried out in triplicate.

Of each dilution, 50 µl were placed in a glass test tube and were incubated at 37 °C for 2 minutes. The reaction was started by adding 50 µl of Enzyme Assay Mix at every 10 seconds, to maintain exact incubation time, subsequently the tubes were incubated at 37 °C for 15 minutes. The reaction was stopped by transferring the tubes into a boiling water bath for 2 minutes. Then, reaction tubes were cooled to room temperature for 30 minutes.

After that, a commercial D-glucose Assay Kit was used as instructed by the manufacturer using the supplied solution 1 and suspension 2. To each sample reaction tube, 1.9 ml of ddH_2O and 1 ml of Solution 1 (mixture of powder consisting of NADP, ATP, $MgSO_4$ and Triethanolamine buffer, pH 7.6, diluted in 45 ml of ddH_2O) was added. The reaction was started by the addition of 20 µl of Suspension 2 (contains: Hexoquinase, glucose-6-phosphate dehydrogenase). They were mixed and incubated at room temperature for 15 minutes. Finally, the absorbance was measured at 340 nm against a no-sample buffer blank using a Hitachi U-2000 spectrophotometer.

Calculation of enzyme activity:

The enzyme activity in a sample was calculated using the following equations:

- Activity (µmol/ml/min) = $\frac{\text{final volume (ml)} \times \text{Dilution factor} \times \text{Absorbance at 340 (nm)}}{\varepsilon \times \text{Sample volume (ml)} \times \text{Time (min.)}}$

- Specific enzyme activity (micromol/min/mg protein)= $\frac{\text{activity (µmol/ml/ min)}}{\text{Protein concentration (mg/ml)}}$

ε is the E_{mM} Extinction coefficient of NADPH at 340 nm; it is 6.3 for maltase, sucrase and lactase.

In sucrase assay, the released D-glucose is the product of sucrose hydrolysis by sucrase into fructose and glucose molecules. In lactase assay, it is the product of lactose hydrolysis by lactase into galactose and glucose molecules. In maltase assay, it is the product of maltose hydrolysis by maltase into two glucose molecules.

Sucrase

Sucrose ----------> Fructose + Glucose

Lactase

Lactose ----------> Galactose + Glucose

Maltase

Maltose ----------> Glucose + Glucose

However, the activity of maltase was divided by two, because a single reaction of maltose hydrolysis gives two D-glucose molecules.

The released D-glucose in the reaction was determined using the commercial D-glucose Assay Kit by measuring the absorbance of NADPH at 340 nm in a spectrophotometer.

The basic principle of the method is the phosphorylation of D-glucose to D-glucose-6-phosphate in the presence of ATP and hexokinase with the formation of ADP. In the presence of glucose-6-phosphate dehydrogenase, $NADP^+$ specifically oxidases D-glucose-6-phosphate to D-gluconate-6-phosphate with the formation of the final products NADPH and H^+.

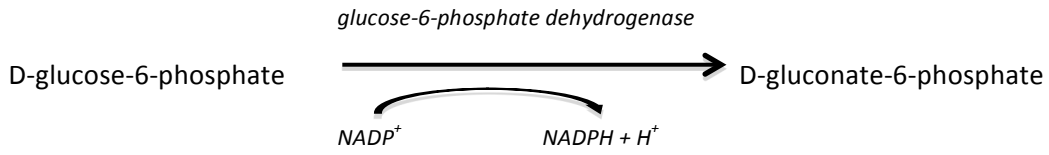

The amount of released NADPH during the reaction is proportionally to the amount of D-glucose present in the sample.

2.6.2. Determination of alkaline phosphatase specific activity:

p-Nitrophenylphosphate (*p*NPP) was used as a chromogenic substrate for alkaline phosphatase in the enzyme assay, according to the method of Shirazi *et al.,* (1981b). A reaction buffer was made containing: 10 mM disodium carbonate (Na_2CO_3), 10 mM sodium bicarbonate ($NaHCO_3$), 0.1 mM magnesium sulphate ($MgSO_4$). The enzyme assay mix was prepared freshly, prior to starting the reaction, by mixing the reaction buffer with 10 mM *p*-Nitrophenyl Phosphate (*p*NPP) solution in a ratio of 9:1, according to Shirazi *et al.*, (1981a).

The samples were diluted appropriately with buffer 3, 50 µl aliquot were placed in plastic tubes and incubated at 37 °C for 2 minutes along with a buffer blank. The reaction was started by the addition of 1 ml enzyme assay mix and was staggered by 10 seconds to maintain exact incubation time. The tubes were incubated at 37 °C for 10 minutes. The reaction was stopped by the addition of 1 ml of 0.5 M NaOH before cooling to room temperature.

The following reaction will occur:

$$pNPP + H_2O \xrightarrow{\text{ALK Phosphatase}} pNP + P_i$$

When water is added to *p*NPP in the presence of alkaline phosphatase enzyme, in alkaline pH buffer, yellow *p*-nitrophenol (*p*NP) is catalysed. This released product can be determined by measuring its absorbance at 400 nm with a Hitachi U-2000 spectrophotometer.

Specific enzyme activity in the samples was calculated using the following equation:

$$\text{- Activity (µmol/ml/min)} = \frac{\text{final volume (ml)} \times \text{Dilution factor} \times \text{Absorbance at 400 (nm)}}{\varepsilon \times \text{Sample volume (ml)} \times \text{Time (min.)}}$$

$$\text{- Specific enzyme activity (µmol/min/mg protein)} = \frac{\text{activity (µmol/ml/ min)}}{\text{Protein concentration (mg/ml)}}$$

ε is the E_{mM} Extinction coefficient of NADPH; it is 17 for alkaline phosphatase.

2.7. SDS-polyacrylamide gel electrophoresis (SDS-PAGE) and Western Blotting

2.7.1. Preparation of gels

The Bio-Rad Mini-PROTEIN II dual slab cell apparatus (Bio-Rad, Herts., UK) was used for gel casting. The glass front plate and 1 mm-thick glass spacer plate were ethanol-cleaned and assembled alongside each other in a holding device. All reagents for polyacrylamide gels were warmed to room temperature before use. Ammonium persulphate (APS) solution was prepared immediately before use.

Running gel (8 % acrylamide) for proteins 40-100 kDa, and 4 % stacking gel were prepared by mixing the following components in a Büchner flask in the listed order:

Running gel:

ddH_2O	4.73 ml
Running gel buffer (Tris/HCl 1.5 M, pH 8.8)	2.5 ml
30 % (v/v) Acrylamide/BIS 37.5:1 (Promega)	2.67 ml
20 % (w/v) SDS	50 µl
TEMED (BioRad)	5 µl
20 % (w/v) APS (Sigma)	50 µl

Stacking gel:

ddH_2O	6 ml
Stacking gel buffer (Tris/HCl 0.5 M, pH 6.8)	2.5 ml
30 % (v/v) Acrylamide/BIS 37.5:1 (Promega)	1.35 ml
20 % (w/v) SDS	50 µl
TEMED (BioRad)	10 µl
20 % (w/v) APS (Sigma)	50 µl

Running/separating gel mixture was poured by pipette between the two layers of glass plates, avoiding bubbles, up to 2 cm below the top edge. 5-7 drops of water-saturated butanol were added on top forming a thin layer, and the gel was allowed to polymerise for 30-40 minutes. Then, the layer of water-saturated butanol was removed with absorbent filter paper just before pouring the stacking gel by pipette over the polymerised running gel. A plastic comb was inserted between the glass plates and aligned avoiding the formation of air bubbles in the gel and kept to polymerise for 30 minutes.

The gels were either used immediately, or wrapped in wet tissue covered by suran wrap to be stored at 4 °C up to one week till use.

2.7.2. Preparation of solutions and protein samples for SDS-PAGE

Tank Buffer:

Glycine	1.44 % (w/v)
SDS	0.1 % (w/v)
Tris base	0.3 % (w/v)

Transfer Buffer:

Methanol	20 % (v/v)
Glycine	150 mM
Trizma base	20 mM

2X sample buffer:

SDS	2 % (w/v)
Glycerol	10 % (v/v)
β-mercaptoethanol	5 % (v/v)
Bromophenol blue	0.01 % (w/v)
Tris/HCl, pH 6.8	62.5 mM

Protein samples:

Constant amounts in µg of protein samples were diluted at least 1:3 ratio (v/v) with denaturing 2X sample buffer. For the immunoblotting of samples from pig intestine, 20 µg of protein was used. While, for the immunoblotting of samples from rat intestine, 10 µg of protein was used and loaded onto the gel. Smaller amounts were used in rat intestinal samples, as this showed better blots. Samples were prepared before loading onto the gel for pig intestinal samples. But they were prepared and mixed with sample buffer on the same day of BBMVs preparation for rat samples, and aliquots were stored at -20 °C in order to avoid protein degradation.

2.7.3. Separation of the protein samples on SDS-PAGE gels

The gels were assembled into Mini-PROTEIN II electrophoresis chamber and inserted into a tank (BioRad, UK). The inner chamber of the tank was filled with Tank Buffer to reach the cathode and cover the wells at the top of the gel with the removal of the plastic comb. The outer chamber was filled only to cover the bottom of the gel.

Then, the prepared diluted protein samples were loaded onto the gel along with 5 µl of molecular weight marker (PageRular, Prestained Protein Ladder, Fermentas). Electrophoresis was run at a constant current of 12 mA/gel, for 60 to 90 minutes, until the Bromophenol blue dye had reached the bottom of the gel.

2.7.4. Electrotransferring of proteins to PVDF membrane

After gel electrophoresis, the gel was removed from the electrical rig, the glass plates were separated gently and the stacking gel was discarded. In a tray containing transfer buffer, the gel was carefully removed from the glass plate and laid facing upward onto a 3 mm Whatman filter paper. Prior to using the Polyvinyl difluoride (PVDF) membrane (Immuno-Blot PVDF, BioRad, UK), it was activated by wetting with Methanol before immersion in transfer buffer. The electrotransfer apparatus and the polyacrylamide gel were also equilibrated in the transfer buffer.

The PVDF membrane was laid over the gel, and both were placed in between two 3 mm Whatman filter papers. Any trapped air bubbles between the gel and the membrane were removed carefully. In a transfer cassette, the gel with the PVDF membrane was enclosed between sponge pads then fibre pads. The electrotransfer cassette was assembled and inserted into the transfer tank ensuring that the PVDF membrane faced the anode. Ice pack and stirring flea were placed inside the tank, for cooling by stirring. The tank was filled covering the cassette with transfer buffer. Electrotransfer was carried out at constant voltage 100 Volts for 60 minutes.

2.7.5. Staining the membrane with Ponceau Red

After transfer, staining with Ponceau Red (1 % (w/v) Ponceau Red in 3 % (w/v) Trichloroacetic acid) was done to evaluate the success of the electrotransfer of proteins from the gel to the membrane. The gel was discarded and the PVDF membrane was removed from the transfer apparatus and rinsed in ddH_2O to eliminate all traces of methanol. The membrane was stained with Ponceau Red for 30-60 seconds, then washed gently with a little amount of ddH_2O removing background staining to inspect protein bands for evidence of degradation. The membrane was de-stained by rinsing repeatedly in ddH_2O. It was air dried completely, wrapped in tissue and foil before storing at -20 °C until immunoblotting.

2.7.6. Western blotting

Phosphate Buffer Saline (PBS) solution:

NaCl	137 mM
KCl	2.7 mM
Na_2HPO_4	28 mM
KH_2PO_4	1.5 mM

Blocking, washing and dilution solutions were prepared freshly. The membrane for blotting was warmed to room temperature, reactivated with Methanol, rinsed in ddH_2O and immersed in PBS. All steps were carried out at room temperature.

Immunoblotting for SGLT1:

The PVDF membrane was incubated in 20 ml of blocking solution, as appropriate in table 2.1, at room temperature for 1 hour with constant agitation. Skimmed dried milk was used as a blocking agent to avoid the non-specific binding of the primary antibody to proteins on the PVDF membrane. The blocking solution was removed and the membrane was incubated with the primary polyclonal anti-SGLT1 antibody for 1 hour on a rocking platform. Anti-SGLT1 antibody was diluted in 10 ml of dilution solution in different conditions as shown in table 2.1.

***Table 2.1**: Solutions in PBS, anti-SGLT1 antibodies and its dilutions*

Protein sample	***Blocking solution***	***SGLT1 antibody***	***Dilution***	***Dilution / Washing solution***
Pig tissue	0.5% (w/v) skimmed milk powder + 0.05% (v/v) Tween 20 in PBS	D49/6 SGLT1 (rabbit serum)	1:1000	Same as blocking solution
Rat tissue	5% (w/v) skimmed milk powder + 0.05% (v/v) Tween 20 in PBS	SGLT1 (rabbit serum, terminal bleed)	1:5000	0.5% (w/v) skimmed milk powder + 0.05% (v/v) Tween 20 in PBS

The membrane was then washed three times for 10 minutes in 10 ml of washing solution with constant agitation. The solution was discarded and the membrane was incubated with the secondary antibody- affinity purified polyclonal swine anti-rabbit IgG conjugated to HRP (Dako, UK), (diluted 1:2000) 5 µl in 10 ml of dilution solution for 1 hour on a rocking platform. The membrane was washed again three times for 10 minutes in 10 ml of washing solution. The immunoblots were developed for detection as described below (section 2.7.7).

Immunoblotting for GLUT2

Non-specific protein binding was blocked by incubating the PVDF membrane in 20 ml of blocking solution (5 % (w/v) skimmed milk powder, 0.1 mM EDTA and 0.1 % (v/v) Triton X-100 in PBS) at room temperature for 1 hour on a rocking platform. The blocking solution was removed and the membrane was incubated with the primary rabbit polyclonal anti-GLUT2 antibody diluted 1:500 in dilution solution (1 % (w/v) skimmed milk powder, 0.1 mM EDTA and 0.1 % (v/v) Triton X-100 in PBS) for 1 hour on a rocking platform.

The membrane was washed three times as described above, and incubated with the secondary antibody-affinity purified polyclonal swine anti-rabbit IgG conjugated to HRP (Dako, UK), (diluted 1:2000) 5 µl in 10 ml of dilution solution for 1 hour on a rocking platform. The membrane was washed again three times the immunoblots were developed for detection as described below (section 2.7.7).

Immunoblotting for β-actin

To block non-specific binding of the primary antibodies to the membrane, PVDF membrane was incubated in 20 ml of blocking solution (5% (w/v) skimmed milk powder, 0.5 % (v/v) Triton X-100 and 0.1 mM EDTA in PBS) at room temperature for 1 hour with constant agitation on a rocking platform. The blocking solution was removed and the membrane was incubated with the primary mouse monoclonal anti-β-Actin antibody (clone AC-15 (A5441), Sigma) (diluted 1:20,000)

0.5 µl in 10 ml of dilution solution (0.5 % (v/v) Triton X-100 and 0.1 mM EDTA in PBS) for 1 hour at room temperature on a rocking platform.

The membrane was then washed three times for 10 minutes in 10 ml of washing solution with constant agitation. Then, the membrane was incubated with the secondary antibody- affinity purified rabbit anti-mouse IgG conjugated to horseradish HRP (Dako, UK), (diluted 1:2000) 5µl in 10ml of dilution solution, for 1 hour on a rocking platform. The membrane was washed again three times for 10 minutes in 10 ml of washing solution. The immunoblots were developed for detection as described below (section 2.7.7).

2.7.7. Development of immunoreactive protein blots

Enhanced chemiluminescence is a non-radioactive method for the detection of immobilized specific antigen, conjugated directly or indirectly, with horseradish peroxidase-labelled antibodies. For the detection of the immunoreactive protein bands, an enhanced chemiluminescence spray (WEST-one Western Blot Detection System) was used following the manufacturer's instructions.

PVDF membrane was sprayed three to five times and incubated for 1 minute. Excess solution was dabbed on a paper tissue before immediately being wrapped in Saran wrap and marked with Tracker Tape (Amersham Ltd., UK). Saran-wrapped membrane was exposed to Kodak BioMax-light film (Sigma-Aldrich, UK) and placed into an X-ray cassette (Sigma, UK). The required exposure time was variable between 5 seconds for β-actin band detection, few minutes for GLUT2, while up to 30 minutes for SGLT1 band detection.

The film was developed in a darkroom using GBX developer/replenisher solution (Kodak, Sigma-Aldrich, UK) then stopped in stop solution (2.5 % Glacial acetic acid with acridine orange as indicator). The film was fixed in GBX fixer/replenisher solution (Kodak, Sigma-Aldrich, UK), then rinsed with tap water and allowed to dry.

The intensity of the detected immunoreactive bands was quantified using scanning densitometry software (Phoretix ID Quantifier, Non-Linear Dynamics).

2.7.8. Stripping and re-probing of PVDF membrane

PVDF membranes were sometimes re-probed with different antibodies after the removal of the previous primary and secondary antibodies. Stripping of the membranes was carried out by washing the membrane with cold acidic stripping buffer (137 mM NaCl, 20 mM Glycine, pH 2.5) three times for 10 minutes on a rocking platform. After stripping, membranes were equilibrated for 15 minutes in the blocking buffer and re-probed with a new antibody and subsequently immunoblotted as described previously.

2.8. Tissue fixation and preparation for cryo-sectioning:

2.8.1. Preparation of the solutions used in tissue fixation process:

Phosphate Buffer Saline (PBS)

A litre of 10X PBS solution was prepared, and then diluted 1:10 with distilled water to prepare 1X PBS, which was used for the fixation and immunohistochemical process.

10X PBS solution:	NaCl	1.37 M
	KCl	27 mM
	Na_2HPO_4	81 mM
	KH_2PO_4	14.7 mM

All the chemicals were dissolved on a stirrer and the pH was adjusted to 7.4 with 1 M NaOH. The solution was made-up to a litre with distilled H_2O and stored at 4 °C.

4 % Paraformaldehyde (PFA) solution in PBS

PBS solution was heated to 65−70 °C. In a fume hood, 4 % (w/v) of paraformaldehyde powder was dissolved in PBS solution by stirring. A few drops of 1 M NaOH (0.04 g/ml) were added to clear the cloudy solution while stirring. After dissolving, the solution was filtered through Whatman paper and allowed to cool at 4 °C. Fresh PFA solution was prepared prior to fixation.

20 % Sucrose solution in PBS

20 % (w/v) of sucrose was dissolved in PBS solution by stirring and stored at 4°C.

Gelatine/ Sucrose solution in PBS

PBS solution was heated to 45−50 °C, and 7.5 % (w/v) of gelatine powder (Sigma) was dissolved in PBS solution by stirring. Then, 15 % (w/v) of sucrose was added and dissolved. Sodium azide (NaN_3) was added to the solution to a final concentration of 0.05 % (w/v). The gelatine/sucrose solution was then allowed to cool to 38 °C in an incubator. This solution was prepared fresh on the same day of its use.

2.8.2. Tissue fixation and cryoprotection:

After collection of intestinal tissue samples and biopsies, 1-2 cm pieces were cut and were fixed in 4 % (w/v) PFA/PBS solution for 4 hours at 4 °C. The samples were then cryoprotected by being transferred to 20 % (w/v) sucrose/PBS solution and kept overnight at 4 °C.

2.8.3. Gelatine embedding:

The cryoprotected tissue samples in 20 % sucrose at 4 °C were warmed at 38 °C in an incubator for 1 hour. This is to warm the solution and the tissues to the same temperature of gelatine/sucrose solution. Tissues were transferred from the 20 % sucrose solution to the gelatine/sucrose solution and maintained at 38 °C for 3

hours. In the last 10 minutes of the 3 hours, some gelatine/sucrose solution was poured in the bottom of plastic weighing boats and allowed to semi-dry. Tissue samples were placed on the dried gelatine in the boats and covered with additional gelatine/sucrose solution. The boats were kept at room temperature to allow the gelatine to set and dry. Then, the boats were wrapped and cooled at 4 °C overnight.

2.8.4. Freezing the gelatine embedded tissue samples:

On the following day, the dried gelatine containing the embedded tissue samples was cut into cubes. Each cube was stuck to a labelled cork disc with OCT embedding matrix (Raymond A Lomb Ltd, Eastbourne, East Sussex, UK). The cubes were snap frozen in 2-methylbutane (Sigma-Aldrich Company Ltd, Gillingham, Dorset, UK) that was liquid nitrogen-cooled. The frozen cubes containing the tissues, embedded in gelatine blocks, were immediately stored at -80 °C until used for sectioning.

2.8.5. Cryostat tissue sectioning:

A cryostat device (Leica, CM 1900UV-1-1, Milton Keynes, Buckinghamshire, UK) was used for cryostat tissue sectioning. Frozen gelatine embedded blocks were sectioned at thickness of 10 µm and thaw-mounted onto poly-L-lysine coated slides (Polysine ™, Deisenhofen, Germany) and stored at -80 °C until used for Haematoxylin and Eosin staining or immunohistochemical studies.

2.9. Mayer's Haematoxylin and Eosin staining

Haematoxylin and Eosin staining was performed prior to immunohistochemistry to evaluate the integrity of the tissue. All steps were carried out in a fume hood at room temperature. The vertical incubation of the slides was done in glass staining jars. The slides with tissue sections were allowed to warm at room temperature for 5-10 minutes. Then, for hydration of the tissue sections, the slides were rinsed in tap water for 30 seconds. Slides were incubated vertically, in glass staining jar at volume of 250 ml of solution, in Mayer's Haematoxylin stain for 1 minute followed by washing under running tap water for 5 minutes. Slides were incubated vertically in Eosin stain for 30-60 seconds. Slides were placed in a holding rack to be easily transferred between jars containing different solutions. Slides were incubated in two subsequent 70 % ethanol solutions, then in two subsequent 100 % ethanol solutions, each incubation lasted for 1 minute. Followed by, transferring the slides in three subsequent xylene solutions for 1 minute each. Fluids were tipped off and tissues were mounted with D.P.X., neutral mounting medium (Sigma-Aldrich, UK) and left to dry for 20 minutes at 60 °C. Tissue sections were viewed and photographed using a Nikon microscope (Eclipse E400) equipped with a Nikon digital camera (DXM1200).

2.10. Morphometry

Cross sections, 10 µm were prepared from frozen gelatin embedded tissues of rats. Tissue sections were stained with haematoxylin and eosin. Using an Eclipse E400 microscope and DXM 1200 digital camera (Nikon, Japan), images were captured with a 4X objective using ACT-1 Products Laboratory Software (Version 2.20, Nikon) and stored as 16-bit tiff files.

Using ImageJ software (Wayne Rasband, National institutes of health, Bethesda, USA), a 100 µm gradient slide was calibrated. Villus height was measured as the average distance from crypt-villus junction to villus tip from an average of at least sixteen well-oriented villi per section, from at least eight different cross sections per tissue segment. Crypt depth was measured as the distance from crypt-villus junction to crypt base.

2.11. Immunohistochemistry

After Haematoxylin and Eosin staining, intact tissue samples were used for immunohistochemical studies. The vertical incubation of the slides during washing was carried out in glass staining jars filled with solution to cover the slides. The horizontal incubation of the slides to apply the primary and secondary antibodies was carried out in a Hybaid OmniSlide Humidity Chamber (Thermo, Middlesex, UK).

The slides with tissue sections were allowed to warm at room temperature for 5-10 minutes. Tissue sections were circled with ImmEdge Hydrophobic Pen (Vector Laboratories, Burlingame, USA) and left to dry for 10 minutes. Slides were washed in PBS five times for 5 minutes. To reduce background, non-specific antibody binding sites on the tissues were pre-blocked with 10% of donkey serum in PBS (or in blocking solution according to optimized conditions, as shown in table 2.2) for 1 hour in a humid chamber. Blocking solution was tipped off and sections were incubated overnight with the primary antibody diluted in dilution buffer in a humid chamber at 4 °C. Primary antibodies diluted as optimized and shown in table 2.2. Omission of primary antibody was routinely used as a control.

Table 2.2: *Blocking solutions, Primary antibodies and their dilutions.*

Primary Antibodies	*Blocking solution*	*Dilution*
SGLT 1 (Rabbit serum, terminal bleed)	10% Donkey serum in PBS	1:100 for mouse tissue * 1:500 for rat & human tissue *
GLUT 2 (Rabbit)	10% Donkey serum in PBS	1:100 *
T1R2 (Rabbit)	5% (w/v) sucrose, 3% (w/v) BSA, 0.1% (w/v) NaN_3 and 2% (v/v) donkey serum in PBS	1:100 *
T1R3 (Rabbit)	As T1R2	1:100 *
VIP (Rabbit)	10% Donkey serum in PBS	1:100 in PBS + 5% donkey serum **
Substance P (Mouse)	10% Donkey serum in PBS	1:100 in PBS + 5% donkey serum **

** Dilution solution used was: (2.5 % (v/v) Donkey serum, 0.2 % (v/v) Triton X-100 and 0.02 % (w/v) NaN_3 in PBS).*
*** For VIP and substance P immunostaining: tissue sections were rinsed in 0.1 mol/L PBS, permeabilized in gradient of alcohol and processed for immunohistochemistry.*

After overnight incubation, primary antibody solution was removed and slides were washed in PBS five times for 5 minutes. The tissue sections were incubated with the secondary antibody diluted in dilution solution (2.5 % (v/v) Donkey serum, 0.2 % (v/v) Triton X-100 and 0.02 % (w/v) NaN_3 in PBS) in a humid chamber for 1 hour at room temperature. The secondary antibody was FITC donkey anti-rabbit (Fluorescein isothiocyanate–conjugated affinity purified, Jackson ImmunoResearch laboratories, Suffolk, UK) diluted 1:500 in dilution solution (except for VIP and SP: it was 1:100). Finally, unbounded antibodies were removed by washing the slides in PBS five times for 5 minutes before slides were mounted in mounting medium with 4',6-diamidino-2-phenylindole (DAPI) (Vectashield, Vector Laboratories, Peterborough, UK).

Slides were allowed to dry in the dark for at least 4 hours before viewing. Immunostaining was visualised using an epifluorescence Nikon microscope (Nikon, model: Eclipse E400, Kingston upon Thames, Surrey, UK) and images were captured with Hamamatsu digital camera (C4742-96-12G04, Hamamatsu Photonics K.K, Hamamatsu City, Japan). The photographed tissue sections with immunostaining were coloured and merged using IPL lab imaging software (BioVision Technologies, Exton, PA, USA).

2.12. Isolation of total RNA

2.12.1. Isolation of total RNA from tissue samples:

Qiagen RNeasy Mini Kit (Qiagen Ltd., Crawley, West Sussex, UK) or LABQ kit was used to isolate total RNA from tissue samples as described by the manufacturer's protocol. RNA was isolated from intestinal tissues of rats or from duodenal biopsies of human subjects. The frozen tissues at -80 °C were weighted 30-40 mg and thawed in 600 µl of RLT Lysis Buffer with 6 µl (0.01 volume) of β-Mercaptoethanol.

- *Note:* For q lab RNA kit, tissues were thawed in 600 µl of RLT Lysis Buffer without β-Mercaptoethanol; otherwise, all steps were the same for both kits.

Tissue samples were homogenized using a polytron microprobe (Ystral, Goettingen, Germany) at speed 5 for 1 minute. The lysate was centrifuged at 10,000 x g (14,000 rpm) for 3 minutes to sediment any non-homogenized tissues. The supernatant of lysate was collected and added to 600 µl (equal volume) of 70 % (v/v) molecular biology grade Ethanol and mixed 10 times by pipetting. The solution was loaded onto an RNeasy spin column and centrifuged at 8,000 x g (10,000 rpm) for 30 seconds. The flow-through was discarded and the column silica membrane was washed with 500 µl of Washing Buffer RW1, supplied with the Kit, and centrifuged at 10,000 rpm for 30 seconds. The flow-through was discarded and the DNase was digested using DNase 1 on-membrane digestion kit as illustrated by the manufacturer. This reaction mixture was prepared fresh before RNA isolation. The following components were added for each PerfectBind RNA column and mixed gently:

DNase 1 Digestion Buffer	73.5 µl
RNase-free DNase 1 (20 units/ µl)	1.5 µl

After mixing of the DNase 1 Digestion reaction mixture, 75 µl was applied directly onto the membrane of PerfectBind RNA column and incubated at room temperature for 15 minutes. The membrane was washed again with 400 µl of Washing Buffer RW1 and centrifuged at 10,000 rpm for 30 seconds. The flow-through was discarded and the column membrane was washed twice with Buffer RPE according to the manufacturer's instructions. The column was centrifuged for 2 minutes at 10,000 rpm to remove the excess Ethanol.

In a sterile tube, total RNA was eluted with 35 µl of RNase-free elution buffer added directly to the membrane and centrifuged at 10,000 rpm for 1 minute. RNA samples were stored at -80 °C at least for 1 hour before RNA quantification.

2.12.2. Quantification of RNA concentration:

The concentration of RNA in the samples was determined by measuring the optical density of the nucleic acid using a double-beam ultraviolet spectrophotometer. RNA elution was diluted 1:100 in ddH_2O before reading the absorbance at 260 nm and 280 nm. As an indicative of low protein contamination, the absorbance ratio of 260 nm / 280 nm was determined and a ratio of 1.8 to 2 indicated good purity of the RNA samples.

At 260 nm, one optical density unit equates to 40 µg/ml of single-strand RNA. The concentration of RNA samples was calculated as following:

$$RNA\ concentration\ (\mu g/\mu l) = \frac{40\ \text{X Abs}\ 260\ \text{X}\ 100\ (\text{dilution})}{1000}$$

2.12.3. Qualification of RNA samples by Agarose gel electrophoresis:

TTE Buffer:

Tris Base	(Sigma)	30 mM
TAPS	(Sigma)	30 mM
EDTA	(Sigma)	0.1 mM

To avoid the degradation of RNA and to inhibit the RNase activity, all solutions were prepared using RNase-free ddH_2O, all plastic materials, glassware and electrophoresis tank were sterilized and washed with a detergent (MicroSol[3]) (Anachem, UK) then with ethanol and RNase-free ddH_2O.

Agarose gel preparation and electrophoreses

2 % (w/v) Agarose gel was prepared by adding 0.8 g of agarose powder (molecular grade, BIOLINE chemicals, London, UK) to 40 ml of TTE buffer. The powder was dissolved and melted by heating until boiling in a microwave oven. The solution was allowed to cool to 50 °C before the addition of Ethidium Bromide (Fluka) to a final concentration of 0.25 µg/µl. The gel solution was poured gently into a flat casting tray (Hoefer) avoiding bubbles and a plastic comb was inserted to create the wells. The gel was allowed to set and dry for about 30 minutes at room temperature. When the gel dried, it was placed in the electrophoresis rig and TTE buffer was poured in to cover the gel.

RNA samples were separated by electrophoresis on the Agarose gel. Equal amounts of the RNA samples, 3-5 µg, were mixed with Blue/Orange 5X Loading Dye (Fermentas) before loaded onto the wells of the gel. Electrophoresis was run in 1X TTE buffer at constant 80 V for approximately 40 minutes until the bromophenol-

blue in the loading dye had reached 2/3 the distance along the gel. The RNA bands were visualized and photographed by placing the gel in a UV transilluminator with a camera device system (BioDoc-It™ imaging system, UVP, Cambridge, UK).

Gel electrophoresis for RNA samples was done to ensure that the RNA sample was pure, free from contamination and has sufficient quantity for cDNA synthesis. This was confirmed by visualizing the gel on a UV transilluminator to see two prominant bands, 28S and 18S rRNA bands of the RNA sample. The upper band (28S rRNA) should be approximately twice the brightness of the lower band (18S rRNA). The 2:1 ratio (28S:18S) was a good indication that the RNA was intact.

2.13. First- Strand cDNA synthesis

2.13.1. First- Strand cDNA synthesis:

The isolated total RNA from rat intestinal tissues and human duodenal biopsies were used in First-Strand cDNA synthesis.

In a nuclease-free microcentrifuge thin-walled PCR tube, the following were added:

Total RNA sample	3 µg
Random Hexamer Primers (100 ng/µl) (Invitrogen)	2.5 µl
ddH_2O was added to a final volume of	11.4 µl.

The mixture was incubated at 70 °C for 10 minutes to denature the RNA in GeneAmp PCR System 2700 (Applied Biosystems). PCR tubes were then placed on ice for 1-2 minutes before incubating at 25 °C for 5 seconds for annealing. Samples were heated until reaching 50 °C, then, the following mixture was added to the tube and mixed by pipetting:

First-Strand cDNA Reaction Buffer 5X (Invitrogen)	4 µl
DTT 0.1 mM (Invitrogen)	2 µl
dNTP Mix (10 mM)	1 µl
RNaseOUT **™** (40 Units/µl) (Invitrogen)	0.6 µl
SuperScript III**™** RT (200 Units/µl) (Invitrogen)	0.5 µl

The process was resumed to be incubated at 50 °C for 60 minutes for reverse transcription. Then, incubated at 70 °C for 10 minutes to denature the reverse transcriptase. Once the reaction was cooled to 37 °C, 0.5 µl (2 Units) of RNase H (4 Units/µl, USB Europe GmBH, Staufen, Germany) was added to the tube and incubated at 37 °C for 30 minutes to digest all RNA. Finally, the reaction tubes were cooled at 4 °C. cDNA was purified using QIAquick**™** PCR purification kit (Qiagen).

2.13.2. Purification of cDNA

First-strand cDNA samples were purified using QIAquick PCR purification Kit (Qiagen, Crawley, UK), with the provided buffers and columns, following the Spin protocol according to the manufacturer's instructions.

Briefly, binding buffer was added to the cDNA sample (5 volumes to 1 volume) and mixed well. To bind the DNA, the mixture was applied to the spin column membrane and centrifuged at 18,000 x g (13,000 rpm) for 1 minute. The flow-through was discarded and the column was washed with 750 µl of ethanol-containing PE Buffer and centrifuged at 18,000 x g for 1 minute. To remove residual ethanol from PE Buffer, the flow-through was discarded and the column was centrifuged again at 18,000 x g for 1 minute. cDNA was eluted by adding 36 µl of Elution Buffer EB (10 mM Tris/HCl, pH 8.5) to the centre of the membrane in QIAquick column. The column was allowed to stand for 1 minute then centrifuged at 18,000 x g for 1 minute.

After purification of cDNA samples, they were quantified using a UV spectrophotometer as described in the following section. Aliquots were diluted to make stock of 5, 10 or 50 ng/µl before using in qRT-PCR reactions. Samples were stored at -20 °C until use.

2.13.3. Quantification of cDNA concentration

The concentration of cDNA in the samples was determined by measuring the optical density of the nucleic acid using a double-beam ultraviolet spectrophotometer (Hitachi, U-2000 spectrophotometer, UK). Elution of cDNA was diluted 1:20 in ddH_2O before reading the absorbance at 260 nm and 280 nm. As an indicative of low protein contamination, the absorbance ratio of 260 nm / 280 nm was determined. A ratio of 0.08 to 1 indicated good cDNA purity of the samples.

At 260 nm, one optical density unit equates to 33 µg/ml of single-strand DNA (cDNA). The concentration of DNA in the samples was calculated using the following equations:

$$cDNA\ \text{concentration}\ (\mu g/\mu l) = \frac{33\ \text{X Abs}\ 260\ \text{X}\ 20\ (\text{dilution})}{1000}$$

2.14. Quantitative Real-Time PCR

2.14.1. Primers used for quantitative RT-PCR:

After choosing the sequence of PCR template (mRNA nucleotide sequence from NCBI website), the primer sets were designed using primer-BLAST tool for finding a specific sense (forward) and antisense (reverse) primers at PubMed website (http://www.ncbi.nlm.nih.gov/tools/primer-blast/). The designed primers were saved and checked for their thermodynamic properties to reduce primer dimer formation using the Vector NTI computer software. The selected primers were ordered and manufactured by Eurogentec (Berlin, Germany). All primers used for q Real-Time PCR were designed to be between 18 and 30 bp long, their GC % to be between 45 % and 60 %, their Tm to be very close together for each primer pair. Sequences and characteristics of the designed primers are shown in table 2.3.

Note: Some primers were designed previously for mouse cDNA amplification and they were used for rats as they were working well in the qRT-PCR. Mouse primers for GCG amplification were used with cDNA from rats. After cloning of the PCR amplicon obtained using these primers, the sequenced PCR products were identified typical GCG mRNA using Vector NTI software and NCBI website for nucleotide blast. For mouse GCG forward primer, there was only 1 bp mismatches to the rat GCG sequence; while the mouse GCG reverse primer was 100 % identical with the sequence of rat GCG.

Table 2.3: Designed Primers for qRT-PCR

Gene name		*Primer sequence (5'->3')*	*Accession No.*
rat *SGLT1*	Forward Reverse	*ACACCCAGGGCCGACTCGTT* *CCGAGAGGCATCGCTGCACA*	*NM_013033*
rat *GLUT2*	Forward Reverse	*TCAGCCAAGGACCCCGTCCC* *AAGGCCCGAGGAAGTCCGCA*	*NM_012879.2*
rat *T1R3*	Forward Reverse	*TGGTGCCACAACATGACACT* *CAGATGCAAACAGCACCACC*	*NM_130818*
rat *GLP-2 R*	Forward Reverse	*CTTTCTTCCCCGACGACCAA* *CCACCAGAAATCCGTGGACA*	*NM_021848.1*
mouse *GCG*	Forward Reverse	*CCCAAGATTTTGTGCAGTGGTT* *AGCATGCCTCTCAAATTCATCA*	*NM_008100.3*
rat *VIP*	Forward Reverse	*TCTGCTCTCAGGTTGGGTGA* *AGATGTTACTGCTAACACGTTTTCC*	*NM_053991.1*
rat *PACAP*	Forward Reverse	*CCACTGGTTGCGGGACAAT* *TTCCTTATGGGCTGGGACTC*	*NM_016989.2*
rat *TAC1*	Forward Reverse	*AGTGGCCCTGTTAAAGGCTCT* *TGCCCATTAGTCCAACAAAGGA*	*NM_012666.2*
rat *ACTB*	Forward Reverse	*GGATCAGCAAGCAGGAGTACGA* *AACGCAGCTCAGTAACAGTCCG*	*NM_031144.3*
human *SGLT1*	Forward Reverse	*TAGATTTACCATGGCTGGACTCTTACT* *CACCTGGGCAAAATTTACAACTG*	*NM_000343.3*
human *ACTB*	Forward Reverse	*ACGGCATCGTCACCAACTG* *AGCCACACGCAGCTCATTG*	*NM_001101.3*

2.14.2. Quantitative Real-time PCR preparation:

Quantitative real-time Polymerase Chain Reaction (qRT-PCR) was carried out to quantify the gene expression in samples. It is based on the continuous monitoring of the fluorescent signals that are generated proportionally to the DNA concentration during the amplification of a PCR product.

All preparations were carried out in a clean UV-irradiated PCR hood to avoid any contamination to the samples or non-template controls.

In order to improve the PCR specificity and sensitivity, the Hot Start protocol was used, so the reaction was only started after reaching elevated temperature to control mispriming events. This high temperature incubation step is also essential for the activation of the *Taq* Polymerase enzyme (DNA polymerase originally isolated from bacterium Thermus aquaticus), ensuring that the enzyme is only activated at a temperature where the DNA is fully denatured.

In a PCR micro-tube, each PCR reaction was prepared in a final volume of 20-µl containing the following:

Reaction Buffer *Taq*-Man	12.5 µl
Specific primers 20x assay mix	1.25 µl
ddH_2O	6.25 µl

The master mix was mixed well and 20 µl were aliquoted into the PCR tubes. Then, 5 µl of the cDNA sample, as template (5, 10 or 50 ng/µl), were added to the mixture. While no cDNA was added to the Non-Template Control (NTC) tubes, 5 µl of ddH_2O was added instead. For each primer pair in a PCR run, template samples and NTCs were carried out in triplicate.

The reaction buffer is *Taq*-Man Jump Start Ready Mix SYBR Green (Sigma, UK). The specific primers 20x assay mix consists of 18 µM of each sense and anti-sense primers to a final concentration of 900 nM. Starting material of cDNA samples (25 ng, 50 ng or 250 ng) was modified in some experiments as needed.

PCR tubes were then placed onto the Rotor-Gene 3000 (Corbett Research, Mortlake, NSW, Australia) and set up to run the PCR. Polymerase chain reaction was initiated by Hot-Start incubation step for 2 minutes at 95°C to activate the *Taq* DNA polymerase enzyme. Subsequently, qRT-PCR was carried out with the following program setting:

- Hold temperature at 95 °C for 2 minutes for DNA denaturation
- PCR amplification 35-45 cycles:
  - 15 seconds at 95 °C (for DNA denaturation to form single strand DNA)
  - 60 seconds at 60 °C (based on annealing temperature of the lowest T_m of each primer pair)
  - 60 seconds at 60-95 °C (for the extension step. Time is corresponding to the expected size of the PCR product; 1 minute per kb).
- Then, a final step of 45 °C for 5 seconds and chilled to 4 °C.

Results were analysed using the Rotor-Gene 3000 computer software (Corbett Research, Australia).

2.14.3. Agarose gel electrophoresis for DNA (qRT-PCR product):

Agarose gel preparation

1 % (w/v) Agarose gel was prepared by adding 0.4 g of agarose powder (molecular grad, BIOLINE chemicals) to 40 ml of TTE buffer (30 mM Tris Base, 30 mM TAPS, 0.1 mM EDTA). The gel was performed as described before in Agarose gel electrophoresis for RNA samples. The gel was allowed to dry then placed in the electrophoresis rig and TTE buffer was poured in to cover the gel.

The resulting qRT-PCR products, cDNA amplicons, were separated by electrophoresis on the Agarose gel. The PCR products were mixed 1:5 with Blue/Orange 5X Loading Dye (Fermentas) before loading onto the wells of the gel along with 5 µl of a DNA Ladder (GeneRuler™ 100 bp Plus, 0.1 mg DNA/ml, MBI Fermentas). Electrophoresis was run in 1X TTE buffer at constant 100 V for approximately 40 minutes. The DNA bands in the gel were visualized and photographed by UV transilluminator and a camera device system (BioDoc-It™ imaging system, UVP, Cambridge, UK).

Gel electrophoresis was done to ensure that the primers, which were used in the qRT-PCR, were amplifying only our target cDNA amplicon. This was confirmed by visualizing a single correct band size, with no bands observed in the non-template controls.

2.15. Cloning and sequencing of the PCR products

2.15.1. Preparation of solutions and agar plates:

Lysogeny broth (LB) medium:

In a glass bottle, the following were dissolved in distilled water with stirring:

	For 100 ml
NaCl 1%	1 g
Tryptone (Difco, London,UK) 1%	1 g
Yeast extract (Difco) 0.5 %	0.5 g
ddH_2O to 100 ml	

The pH of the solution was adjusted to 7.0 with NaOH. The lid of the bottle was loosely closed and the solution was autoclaved for 20 min using the liquid cycle. The medium was allowed to cool and stored at room temperature with a securely closed lid.

LB- Ampicillin agar plates (Lysogeny broth)

LB medium was prepared as above in a flask, 1.5 % Bacto-agar (Becton Dickinson, Swindon, UK) was added to the medium before autoclaving, covered with foil, in liquid cycle for 20 minutes. The mixture was cooled to 50 °C before the addition of 10 % ampicillin antibiotic filter sterilized (Sigma) and gently swirled to mix.

For 500 ml: 7.5 g of agar was added to 500 ml of LB medium, then 5 ml of 10 mg/ml ampicillin was added and mixed. Then, the flask mouth was sterilized by flame and LB agar was poured into 10 cm plates, approximately 30 ml per plate, under sterilized conditions. The LB agar in the plates was allowed to set and dry. The plates were stored upside down in a bag, to prevent drying, at 4 °C in the dark.

SOB medium (Super optimal broth)

To prepare SOB medium, the following were mixed in a glass bottle:

	For 250 ml
NaCl 0.04 %	0.1 g
Tryptone 2%	5 g
Yeast extracts 0.5%	1.25 g
ddH_2O	to 250 ml

The pH of the solution was adjusted to 7.0 with NaOH. The lid of the bottle was loosely closed and the solution was autoclaved for 20 minutes. The medium was stored at room temperature with a tightly closed lid.

SOC medium (for catabolic repression)

SOC medium was prepared immediately before use. To prepare 1 ml of SOC medium, the following were mixed under sterilized conditions:

2 M Mg^{2+} (1 M $MgCl_2$, 1 M $MgSO_4$)	10 µl
2 M D-glucose, filtered sterilized	10 µl
SOB medium	980 µl

2.15.2. Extraction and purification of DNA from agarose gel (band preparation):

The QIAquick™ Gel Extraction Kit (Qiagen) was used, as described in the manufacturer's handbook, for the DNA extraction and purification from agarose gel. After running a qRT-PCR using the designed primers with the desired cDNA samples as template, Rotor-Gene software was used to ensure that all melt curves showed the same single peak in all the templates except for the non-template controls.

The qRT-PCR product was loaded with loading dye onto 1 % (w/v) agarose gel electrophoresis and run alongside 5 µl of a DNA Ladder; the DNA was visualized with a UV transilluminator (BioRad Gel DOC 1000) to ensure the correct size of a single band. The band of interest was dissected of the gel with a sterile scalpel under low UV illumination and placed into a sterile Eppendorf tube (UV light exposure was minimized to reduce the formation of pyrimidine dimers). The weight of the agarose gel slice was determined and 3 volumes of Binding Buffer QG (Qiagen) were added to the gel. The gel slice was dissolved in the buffer in a water bath at 50 °C for 10-15 minutes with frequent gentle mixing.

After dissolving the DNA fragment, the mixture was loaded to a silica column provided with the kit. To bind the DNA, the column was centrifuged at 10,000 x g for 1 minute. The flow-through was discarded and 500 µl of Binding Buffer QG was added again to the column and centrifuged at 10,000 x g for 1 minute. The column was washed with 750 µl of Washing Buffer PE and centrifuged at 10,000 x g for 1 minute. The flow-through was discarded followed by centrifugation for 1 minute to remove any residual buffer. The column was then placed into a new 1.5 ml tube and the DNA sample was eluted with 35 µl ddH_2O, collected by centrifugation at 10,000 x g for 1 minute.

2.15.3. Quantification of DNA concentration:

The concentration of purified dsDNA sample was quantified by measuring the absorbance at 260 nm using a Hitachi U-2000 spectrophotometer. The eluted DNA sample was diluted in ddH_2O before reading the absorbance at 260 nm and 280 nm.

At 260 nm, 1 optical density unit equates to 50 µg/ml of double-strand DNA. The concentration of DNA was calculated as follows:

$$DNA\ concentration = Abs_{260} \times 50 \times dilution$$

If the DNA concentration was low, the eluted DNA was concentrated into less volume ~ 15 µl by centrifuging the tube with an open lid in a vacuum spin system and heating (DNA SpinVac 100, Savant) for 10-20 minutes.

2.15.4. 'a-tailing' of blunt ended PCR products for cloning:

This *'a-tailing'* process is optional but gives better results with cloning because it facilitates the ligation and the insertion of the DNA fragment into the plasmid. In a sterile microtube, the following components were mixed and incubated for 30-60 minutes at 70 °C in a standard PCR machine:

Purified PCR product (dsDNA)	6 µl
Taq polymerase reaction buffer IV 10X	1 µl
Taq DNA polymerase (5 U/ µl)	1 µl
$MgCl_2$ (25 mM) (Invitrogen)	1 µl
dATP (2 mM) (Invitrogen)	1 µl

2.15.5. Ligation of cDNA into bacterial plasmid:

DNA ligation process is the joining of two DNA molecule ends together, one is the plasmid (vector) and the other is the insert (DNA fragment). The ligation reaction is catalyzed by DNA ligase enzyme (commonly used T_4 DNA ligase™), which creates a phosphodiester bond between the 3' hydroxyl of one nucleotide and the 5' phosphate of another in ds DNA fragments.

To ensure that the concentration of the purified, gel extracted, DNA is enough for the ligation process, a single product should be detected by gel electrophoresis. 1 % (w/v) agarose gel electrophoresis was run using 1 µl of DNA product with loading dye alongside 5 µl of a DNA Ladder (GeneRuler™ 100 bp Plus, MBI Fermentas) and visualized in a UV transilluminator.
To calculate the amount of PCR product (DNA) needed for ligation, the following equation was used:

$$Amount\ needed = \frac{ng\ of\ vector\ X\ kbp\ size\ of\ insert\ X\ 3}{kbp\ size\ of\ vector}$$

(The optimal ratio of insert to vector is 3:1, vector (plasmid) concentration is 50 ng/µl and vector size is 3 kbp).
To set up the ligation reaction, the following components (all supplied by Rapid Ligation Vector II, Promega) were added and mixed in a sterile tube:

2X Rapid Ligation Buffer	5 µl
pGEM-T Easy™ Vector 50 ng/µl	1 µl
T_4 DNA ligase™ 3U/µl	1 µl
PCR product (purified DNA)	as calculated
ddH_2O	up to 10 µl total volume

The tube was incubated either at room temperature for 1 hour or at 4°C overnight. For optimal ligation results, 3 µl of PCR product after a tailing was added without water, and incubated 4°C overnight.

2.15.6. Transformation of Escherichia coli cells:

Under flame to provide septic conditions, 50 µl of freshly thawed competent JM109 *E.coli* cells (Stratagene) were added gently to 5 µl of the ligation mixture in a sterile tube. The tube was incubated on ice for 20 minutes to allow interaction of the plasmid with the bacterial cell wall. Then, the bacteria was subjected to heat shock in a water bath for 45 seconds at 42 °C before incubation on ice for further 5 minutes to allow recovery time from the heat shock. 450 µl of nutrient-rich SOC medium (prepared freshly as described before) were added to the mixture and incubated at 37 °C in a shaking incubator at 200 rpm/minute for 60-90 minutes.

In the meanwhile, the LB-ampicillin agar plates were equilibrated at room temperature. The LB-ampicillin agar indicator plates for blue/ white colony screening were treated by spreading the following solutions on the surface of the agar under aseptic conditions:

100 mM Isopropyl-β-d-thiogalactopyranoside (IPTG, Promega)	100 µl
50 mg/ml 5-bromo-4-chloro-3-indolyl-β-D-galactosidase (X-Gal, Fermentas)	50 µl

The treated plates were kept in a 37°C incubator for 30 minutes to allow the absorbance of the added materials. Then, 50- 150 µl of the bacterial suspension (transformed cells in SOC medium) were spread on the indicator plates (plates with IPTG/x-Gal) to grow and incubated up-side-down at 37°C overnight. Next day, the plates were placed at 4˚C to intensify the blue colour of the blue colonies and to identify white colonies.

Successful transformation was identified by the appearance of white colonies that were not at the periphery of the plate and not adjacent to blue colonies. White bacterial colonies were considered to be transformed by plasmid (confer resistance to ampicillin and survive on LB-ampicillin agar plate). These bacterial white colonies contained an insert, which disrupts the Lac-Z β-galactosidase gene on the plasmid. While the blue colonies indicating no insert, inappropriate ligation process, so the Lac-Z β-galactosidase is catalysed by X-Gal and gives blue colour.

2.15.7. Culture of transformed E.coli cells:

Under sterile conditions, 5 ml of LB medium and 50 µl of 10 mg/ml Ampicillin (final concentration 100 µg/ml) (Sigma) were mixed in a sterile universal tube. Using a sterile pipette tip, a single white colony from the plate was inoculated into the tube. To allow the growth of bacterial colonies, the universal tube was incubated with orbital shacking at 200 rpm/minute at 37°C for 16 hours. After that, the tubes were placed at 4°C until the colonies containing the DNA insert of interest were identified by standard PCR.

2.15.8. Colony screening by standard PCR:

For screening of the recombinant grown colonies, a standard PCR reaction was performed using the following reagents per PCR reaction tube to a final volume of 50 µl:

10x Thermo-Start PCR Reaction Buffer	5 µl
8 mM (total) dNTP mix	5 µl
10 mM Sense primer	1 µl
10 mM Anti-Sense primer	1 µl
Thermoprime Plus Polymerase (*Taq*, 1 U/ µl)	0.5 µl
25 mM $MgCl_2$	3 µl
Bacterial cell suspension	1 µl
ddH_2O	33 µl

Positive and negative controls were prepared by adding 1 µl of the purified DNA and ddH_2O, respectively, replacing the 1 µl of bacterial cell suspension.
The PCR was run in 25 cycles, which carried out as the following steps:

Reaction was heated	at 94 °C for 15 minutes
PCR amplification	at 94 °C for 20 seconds
	at 55 °C for 20 seconds
	at 72 °C for 1 minute
Final extension step	at 72 °C for 7 minutes

Finally, the reaction was cooled to 4 °C.

Following standard PCR, the PCR products were loaded onto 1 % (w/v) agarose gel and electrophoresis was run, as described previously, alongside the positive control.

If the gel showed that the PCR products had a single band of the correct size, this indicated that the cloned DNA insert was our DNA of interest. Then, plasmid DNA was prepared from that bacterial suspension.

2.15.9. Preparation of plasmid DNA from transformed E.coli cells:

Using the Qiaprep Spin Minikit™ (Qiagen) with the provided buffers, plasmids were prepared by alkaline lysis of bacterial cells followed by absorption of plasmid DNA onto a silica column in the presence of high salt. The universal tubes containing bacterial suspension of successful transformation were centrifuged in a swing-out rotor at 3,000 rpm for 5 minutes at 4 °C (RC5C Plus refrigerated centrifuge, rotor SH3000, Sorvall). The supernatant was discarded and the pellet was resuspended in 250 µl of suspension buffer P1 (containing 0.1 µg/µl RNase A) and transferred to a microcentrifuge tube.

The cells were lysed in 250 µl of lysis buffer P2 (containing NaOH/SDS) and mixed gently by inverting the tube until lysis was completed. The lysate was neutralized in 350 µl of neutralization buffer N3 (containing high salt) leading to the precipitation of genomic DNA, denatured proteins and cellular debris. To remove

precipitates, the tube was centrifuged at 10,000 x g for 10 minutes. Leaving the pellet containing protein, cell debris and chromosomal DNA), the supernatant containing renatured plasmid was transferred to a QIAprep silica column and centrifuged at 10,000 x g for 1 minute. Endotoxin and endonucleases were removed by washing the spin column with the supplied washing buffers (Qiagen). The column was washed with 500 µl of Buffer PB by centrifuging at 10,000 x g for 1 minute and discarding the flow-through. Followed by another wash with 750 µl of ethanol-containing Buffer PE by centrifuging for 1 minute and discarding the flow-through. Further centrifugation for 1 minute was performed to dry the column and remove any residual wash buffer. The column was finally placed in a sterile 1.5 ml microcentrifuge tube and plasmid DNA was eluted with 50 µl of ddH_2O by soaking for 1 minute then centrifuged for 1 minute.

The plasmid DNA concentration was quantified by measuring the absorbance at 260 nm wavelength.

Concentration of plasmid ds DNA (µg/µl) = $\frac{50\ X\ Abs\ at\ 260\ X\ dilution}{1000}$

2.15.10. Sequencing of the plasmid DNA:

Plasmid DNA (2 µg) was placed in an eppendorf tube and dried by centrifugation in a vacuum with heat. Dried DNA samples were submitted to a commercial sequencing service (SourceBioscience) for custom nucleotides sequencing. The sequences were received by emails and aligned to the database in nucleotide blast at NCBI website.

2.16. GLP-2 enzyme immunoassay (EIA)

2.16.1. Preparation of animals:

Diabetes mellitus was experimentally induced in adult male rats (Sprague-Dawley) (four control and four diabetics) by Streptozotocin injection as described before in section 2.2.2. Diabetes was confirmed by assessing the blood glucose, and then the animals were kept for 5 weeks before killing. The blood concentration was measured again on the day before killing by cervical dislocation. The body weight of rats was recorded individually. After dissecting, photos were taken of the small intestine, and after the removal of the intestine, the weight and length of the whole intestine were measured.

2.16.2. Preparation of solutions and tissue collection:

Low glucose DMEM medium was prepared a day before the experiment. Sixty ml of DMEM was mixed with 50 ml of FBS (foetal bovine serum). Five ml of Pencillin/Streptomycin and 5 ml of glutamate were added to the medium. On the same day, the medium was gassed with 95% O_2 and 5% CO_2 for 30 minutes before it was used to prepare the incubation solutions. Incubation solutions were prepared fresh on the same day including DPP IV inhibitor (20 µl/ml) added to either low (control) or high (10 %) glucose concentrations.

From control and diabetic rats, the small intestine was removed and divided into proximal, mid and distal parts. The intestine was cut-open and rinsed in cold normal saline. The intestinal tissue was placed on glass plate and the serosa was gently removed by scalpel under microscopy. Tissue pieces were cut into 2 cm length and placed in microcentrifuge tubes to be incubated with 500 µl of incubation solution at 37 °C for one hour. After incubation, the tubes were centrifuged for 10 seconds to collect the tissue at the bottom of the tubes without damaging the tissue. Aliquots of the incubation medium ~ 250 µl were saved in 0.5 ml tubes and immerged in liquid nitrogen. Tubes of incubation medium and tubes with tissue were stored at -80 °C until use.

2.16.3. GLP-2 enzyme immunoassay protocol:

The EIA kit was purchased from Phoenix Pharmaceuticals, Inc., Burlingame, USA, for the GLP-2 enzyme immunoassay. The assay procedure was carried out as demonstrated by the manufacture's instructions.

All components of the kit and the plate were allowed to warm to room temperature before use (30-45 minutes). The 50 ml of 20x assay buffer concentrate was diluted with 950 ml of distilled water to make 1x assay buffer solution. This assay buffer was used to dilute and reconstitute all other reagents provided in the kit, and used in the washes of the plate. The 1x assay buffer and all prepared solutions were allowed to warm to room temperature and mixed thoroughly just before use.

The standard peptide was centrifuged and diluted with 1 ml of 1x assay buffer and vortex to make a stock solution (concentration of stock: 1,000 ng/ml). The solution was completely dissolved by mixing for 10 minutes at room temperature (20-23 °C).

Peptide standard solutions were prepared as follow:

Standard No.	***Standard volume and preparation***	***Concentration***
Stock	1000 µl	1,000 ng/ml
# 1	100 µl of stock + 900 µl of 1x Assay Buffer	100 ng/ml
# 2	100 µl of # 1 + 900 µl of 1x Assay Buffer	10 ng/ml
# 3	100 µl of # 2 + 900 µl of 1x Assay Buffer	1 ng/ml
# 4	100 µl of # 3 + 900 µl of 1x Assay Buffer	0.1 ng/ml
# 5	100 µl of # 4 + 900 µl of 1x Assay Buffer	0.01 ng/ml

The primary antibody was rehydrated with 5 ml of 1x assay buffer and the biotinylated peptide was also rehydrated with 5 ml of 1x assay buffer. The positive control was centrifuged and rehydrated with 200 µl of 1x assay buffer. All solutions were allowed to sit for 5 minutes at room temperature for complete dissolving then mixed thoroughly.

The provided immunoplate in the kit has 96 wells, the bottom of the wells is pre-coated with secondary antibody (capture antibody) and the non-specific binding sites were blocked. The numbers of the wells are shown below.

The first two wells A-1 and A-2 were left empty as Blanks. 50 µl of 1x assay buffer were added into wells B-1 and B-2 as Total Binding. 50 µl of prepared peptide standards from #5 to #1 (in reverse order of serial dilution) were added into wells from C-1 and C-2 to G-1 and G-2, respectively (Peptide standards were assayed in duplicate). 50 µl of rehydrated positive controls were added into wells H-1 and H-2 (Positive controls were also assayed in duplicate). The previously prepared samples were thawed from -80 °C and 50 µl were added into their allocated wells. 25 µl of rehydrated primary antibody (detection antibody) was added into each well except the Blank wells. Followed by the addition of 25 µl of rehydrated biotinylated peptide into each well except the Blank wells. The rest of the wells were filled with the samples.

The immunoplate was sealed with acetate plate seal (APS) and incubated for 2 hours at room temperature (20-23 °C) with orbital shaking at 300-400 rpm.
The APS was removed from the immunoplate and the contents of the wells were discarded. The wells were washed with 350 µl of 1x assay buffer. The washing buffer was discarded by inverting and blot drying the plate, the wash was repeated 4 times. (A separate multi-channel pipette is recommended for the washes and the next steps using a sterile solution reservoir each time).

The streptavidine-HRP conjugate (SA-HRP) vial provided in the kit was centrifuged at 5,000 rpm for 5 seconds, and 12 µl was added to 12 ml of 1x assay buffer to make SA-HRP solution. 100 µl of SA-HRP solution were added into each well. The immunoplate was resealed with APS and incubated for 1 hour at room temperature (20-23 °C) with orbital shaking at 300-400 rpm. The APS was removed from the immunoplate and the contents of the wells were discarded. The wells were washed with 350 µl of 1x assay buffer. The washing buffer was discarded, as described before, and the wash was repeated 4 times. 100 µl of the provided TMB substrate solution were added into each well and the immunoplate was covered to protect from light. The immunoplate was resealed with APS and incubated for 1 hour at room temperature (20-23 °C) with orbital shaking at 300-400 rpm. The APS was removed from the immunoplate and the reaction was stopped by adding 100 µl of 2N HCl into each well, for a positive result, the colour in the well was changed from blue to yellow. Within 20 minutes, the immunoplate was loaded onto a Microtiter Plate Reader to read the absorbance O.D. at 450 nm.

2.17. Statistical analysis of the data

The data in this study were analysed statistically using Prism 5 software version 5 with unpaired 'student' t-test. The results were considered to be not significant if the p-value was > 0.05, significant if the p-value was ≤ 0.05, very significant if the p-value was ≤ 0.01 and extremely significant if the p-value was ≤ 0.001. Results are expressed as mean ± S.E.M. unless otherwise stated.

Chapter 3

Acquiring relevant techniques using small intestinal tissues of different species

CHAPTER 3

Introduction

The absorptive function of the small intestine occurs through the specialized absorptive cells (enterocytes) lining the small intestinal mucosa. Enterocytes are the prominent type of epithelial cells that cover the surface of the villi. They originate from stem cells located near the base of intestinal crypts and migrate up to villus tip to shed into the lumen for continuous renewal (for further information, see introduction section 1.3.1).

The enterocytes have two membrane domains: the apical side facing the intestinal lumen and known as the brush-border membrane (BBM) due to its characteristic microvilli, and the basal and lateral sides are known as the basolateral membrane (BLM) facing the circulation and adjacent cells. Each membrane has its characteristic surface charges, membrane structure and lipid composition. These specific properties facilitated the selective isolation of BBM and BLM vesicles using Mg^+ precipitation and differential centrifugation techniques (Shirazi-Beechey *et al.*, 1990), (see Methods). This method of BBMV preparation offered several experimental advantages over other procedures, which use tissue or isolated cells (see introduction section 2.1.3).

The pure population of BBM vesicles (BBMV) has aided transport studies across the brush-border membrane via specific transporters like the intestinal Na^+/glucose cotransporter 1, SGLT1, eliminating the effect of the paracellular shunt and sugar metabolism (Kessler *et al.*, 1978). In addition, the vesicles retain their functional polarity after isolation, which makes it possible to address the role of different cell membranes under various conditions (Murer and Kinne, 1980).

The BBM has characteristic transmembrane protein carriers such as SGLT1 and GLUT5 sugar transporters, as well as digestive enzymes such as disaccharidases and alkaline phosphatase (Keelan *et al.*, 1985, Prabhu *et al.*, 2003). These transporters and enzymes are considered as reliable BBM markers. Hence, the purity and membrane origin of the prepared BBMV can be assessed by measuring the specific activities, enrichment and percentage recovery of the enzyme markers in the vesicles over the cellular homogenate. Additionally, the protein abundance of these markers can be assessed in the vesicles and homogenates to identify the membrane origin of the vesicles.

On the luminal domain of the intestine, the BBM digestive disaccharidases include maltase, sucrase and lactase, which breakdown dietary disaccharides into monosaccharides. Maltase splits maltose into two glucose molecules, sucrase splits

sucrose into glucose and fructose and lactase splits lactose into glucose and galactose (Mantei *et al.*, 1988, Nichols *et al.*, 2003, Nichols *et al.*, 1998). Those simple sugars are then absorbed through the intestinal absorptive cells from the gut lumen to the systemic circulation. On the BBM of the enterocyte, monosaccharide carriers SGLT1 and GLUT5 transport glucose/galactose and fructose, respectively, into the enterocytes.

In this study, to avoid wastage of human tissues, I acquired the relevant techniques such as BBMV isolation, disaccharidase assays, glucose uptake test, Western blotting and immunohistochemistry using intestinal tissues from mouse and pig available in our laboratory.

After aquired expertise and confidence in isolating BBMV, the technique was applied to isolate BBMV from i) intestine of rats, healthy and with stretozotocin-induced diabetes (See chapter 4) and ii) human intestinal biopsies of healthy and diabetic subjects (See chapter 5). Subsequently, the BBM origin of membrane vesicles was determined by assessing the enrichment and recovery of BBM marker enzymes, maltase, sucrase, lactase and alkaline phosphatase along small intestinal regions, whenever possible.

Aims:

1- To prepare membrane vesicles using intestinal tissues from mouse and pig.
2- To assess the membrane origin of the membrane vesicles.
3- To estimate SGLT1 protein abundance in BBMV
4- To determine morphological integrity and localize the expression of SGLT1 protein along crypt-villus axis.
5- To practice glucose uptake test in BBMV.

Results

Small intestinal tissues were used from mouse and pig for the isolation of BBMV. To assess the membrane origin of these vesicles, the specific activities of the BBM markers sucrase, lactase and maltase were determined in the BBMV and in their corresponding cellular homogenates. The enrichment and percentage recovery values of these enzymes were calculated as follows:

$$\text{Enrichment} = \frac{specific\ enzyme\ activity\ in\ BBMV}{specific\ enzyme\ activity\ in\ homogenate}$$

$$\text{Recovery}\ (\%) = \frac{Total\ enzyme\ \ activity\ in\ BBMV}{Total\ \ enzyme\ activity\ in\ homogenate} \times 100$$

Having isolated BBMV from the small intestine of different species and determined their membrane origin, enzyme assays and Western blotting were carried out.

3.1. Isolation and characterisation of BBMV isolated from intestinal tissues of mouse and pig

3.1.1. Enrichment and percent recovery of BBM markers in vesicle preparation

- Mouse intestine:

The activity of maltase and sucrase was determined in BBMV isolated from the intestinal tissues of adult mice, maintained on 40% carbohydrate diet. Specific activity in BBMV, enrichments and recoveries in the three intestinal regions (proximal, mid and distal) are shown in table 3.1. Histograms in figure 3.1 represent the enrichment of maltase and sucrase in the proximal intestine of mice.

Table 3.1. ***Specific activity, enrichment and recovery of maltase and sucrase in BBMVs isolated from the intestine of mice.***

	Proximal			***Mid***			***Distal***		
	Specific activity (µmol/min/mg)	Fold Enrichment	Recovery %	Specific activity (µmol/min/mg)	Fold Enrichment	Recovery %	Specific activity (µmol/min/mg)	Fold Enrichment	Recovery %
Maltase	3.8 ± 0.05	22.2 ± 3.7	15.5 ± 7.4	1.3 ± 0.1	5 ± 3	6.5 ± 3.5	0.42 ± 0.08	3.3 ± 0.6	3.6 ± 1.7
Sucrase	0.6 ± 0.06	11.5 ± 3.1	8.2 ± 4.7	0.2 ± 0.07	2.1 ± 1.8	3.2 ± 1.8	0.07 ± 0.01	3.32 ± 1.5	2.32 ± 0.4

Results are expressed as mean ± S.E.M of separate BBMVs preparations (n = 4)

Table 3.2. ***Specific activity, enrichment and recovery of disaccharidases in BBMVs isolated from three small intestinal regions of suckling pigs.***

	Duodenum			***Jejunum***			***Ileum***		
	Specific activity (µmol/min/mg)	Fold Enrichment	Recovery %	Specific activity (µmol/min/mg)	Fold Enrichment	Recovery %	Specific activity (µmol/min/mg)	Fold Enrichment	Recovery %
Maltase	0.24 ± 0.04	10 ± 5	12.8 ± 2.7	0.14 ± 0.04	8.8 ± 1.8	7.3 ± 2.7	0.17 ± 0.03	7.66 ± 2.5	15.46 ± 2.7
Sucrase	0.031 ± 0.004	3.32 ± 1	4.2 ± 2.4	0.05 ± 0.01	3.83 ± 0.9	5 ± 1.4	0.036 ± 0.004	4.2 ± 1.1	8 ± 2.2
Lactase	0.22 ± 0.01	10.44 ± 3.8	11.3 ± 3.4	0.10 ± 0.01	6.3 ± 1.6	6.3 ± 2.3	0.05 ± 0.01	3.2 ± 1.3	4.2 ± 2

Result are expressed as mean ± S.E.M of separate BBMV preparations (n = 6)

In BBMV isolated from the mouse proximal intestinal tissue, results showed that maltase and sucrase were significantly and markedly enriched 22.2 ± 3.7 and 11.5 ± 3.1 -fold, respectively, over their crude homogenates. The percent recovery of maltase and sucrase were 15.5 ± 7.4 % and 8.2 ± 4.7 %, respectively.

In the BBMVs isolated from the mouse mid intestine, maltase and sucrase were enriched 5 ± 3 fold and 2.1 ± 1.8 fold with percent recoveries being 6.5 ± 3.5 % and 3.2 ± 1.8 %, respectively. While in the mouse distal region, maltase and sucrase showed enrichment of 3.3 ± 0.6 and 3.32 ± 1.5-fold, and percent recoveries of 3.6 ± 1.7 % and 2.32 ± 0.4 %, respectively.

<u>Figure 3.1.</u> Specific activity of maltase and sucrase in BBMV isolated from proximal intestine of mice and their original homogenates

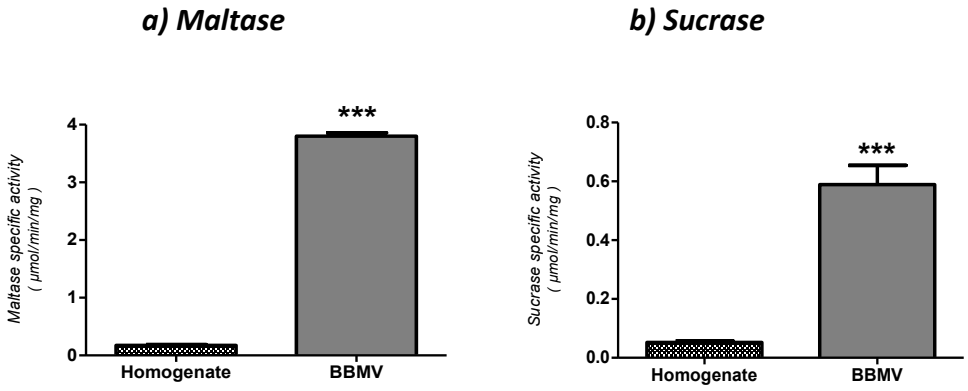

Histograms showing the specific activity of a) maltase and b) sucrase in the original homogenates and the BBMVs isolated from proximal small intestine of mice.
*Values are mean ± S.E.M (n = 4), ***P < 0.001, unpaired t-test.*

- Pig intestine:

In suckling pigs of 28 days old, maltase, sucrase and lactase were assayed in the BBMV isolated from three small intestinal regions. For the assessment of the membrane origin of these vesicles, the specific activities, enrichments and recoveries were determined and reported in table 3.2. Enrichments of BBM markers are represented as histograms in figure 3.2 showing the specific activity of disaccharidases in the BBMVs and their corresponding homogenates.

Generally, the BBM markers were significantly enriched in the BBMV over their cellular homogenates (table 3.2). Maltase and lactase were similarly enriched in the duodenum and jejunum. Maltase, sucrase and lactase showed enrichments of 10 ± 5, 3.32 ± 1 and 10.44 ± 3.8 fold, respectively, over their homogenates in the duodenum region. In the jejunum, they were enriched 8.8 ± 1.8, 3.83 ± 0.9 and 6.3 ± 1.6 fold, respectively. While in the ileum, they were enriched 7.66 ± 2.5, 4.2 ± 1.1 and 3.2 ± 1.3 fold, respectively.

The percent recoveries of maltase, sucrase and lactase were 12.8 ± 2.7 %, 4.2 ± 2.4 % and 11.3 ± 3.4 % , respectively, in the duodenum. They were 7.3 ± 2.7 %, 4.9 ± 1.4 % and 6.3 ± 2.3 % , respectively, in the jejunum. While in the ileum, the recoveries were 15.46 ± 2.7 %, 7.9 ± 2.2 % and 4.2 ± 2 % , respectively.

By comparing the specific activity levels in the BBMVs and the crude homogenates (figure 3.2), maltase showed significantly higher level by 13.5, 9 and 10 fold in the duodenum, jejunum and ileum, respectively. For sucrase, the specific activity is significantly higher by 3.6, 6.2 and 4 fold in the duodenum, jejunum and ileum, respectively. While for lactase, it is significantly increased by 12, 10 and 5 fold in the duodenum, jejunum and ileum, respectively.

<u>Figure 3.2</u>. Specific activity of disaccharidases in original homogenates and BBMVs isolated from intestinal regions of suckling pigs.

a) Maltase

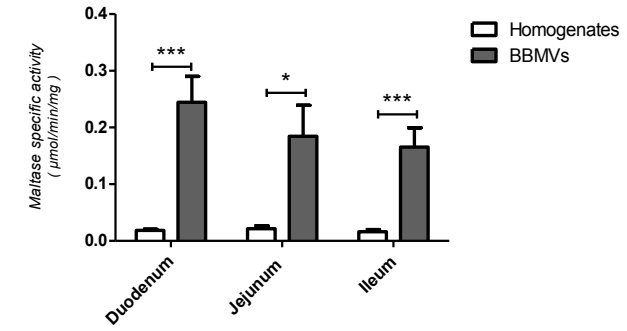

b) Sucrase

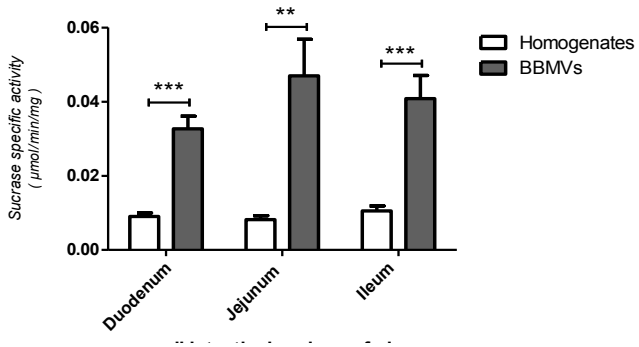

c) Lactase

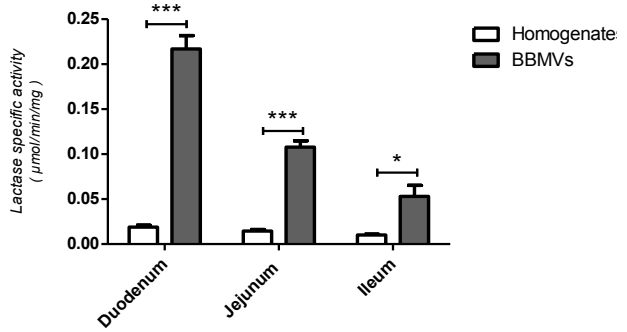

Graphs comparing the specific activities of a) Maltase, b) Sucrase and c) Lactase in the cellular homogenates and the BBMVs isolated from three small intestinal regions of suckling pigs.
*Values are mean ± S.E.M (n = 6); ***P < 0.001, **P < 0.01 and *P < 0.05, unpaired t-test.*

1.1.1. Specific activities of BBM enzymes along the small intestinal length

- Mouse intestine:

a) Maltase

As shown in figure 3.3, maltase specific activity was highest in the proximal region, and declined steeply toward the distal small intestine. Maltase level was 3.8 ± 0.05, 1.3 ± 0.1 and 0.42 ± 0.08 µmol/min/mg protein in the proximal, mid and distal intestinal regions, respectively.

b) Sucrase

As displayed in figure 3.4, sucrase specific activity was highest in the proximal region, and it is significantly lower in the distal progression throughout the small intestine. In the proximal, mid and distal regions, sucrase activity was 0.59 ± 0.06, 0.2 ± 0.07 and 0.07 ± 0.01 µmol/min/mg protein, respectively.

By comparing maltase and sucrase specific activities in mouse intestine, the specific activity of maltase was significantly higher than sucrase in all three small intestinal regions. Data are presented as a histogram in figure 3.5.

c) Lactase

Lactase activity was assayed in the proximal and distal small intestinal regions of the mouse. As shown in figure 3.6, the activity of lactase is barely detected in both regions with slightly higher level in the proximal than the distal small intestine. By comparison, the activity of maltase is much higher than lactase by 17 and 15 fold in the proximal and distal regions, respectively.

Figure 3.3. Maltase specific activity along the small intestine of mice

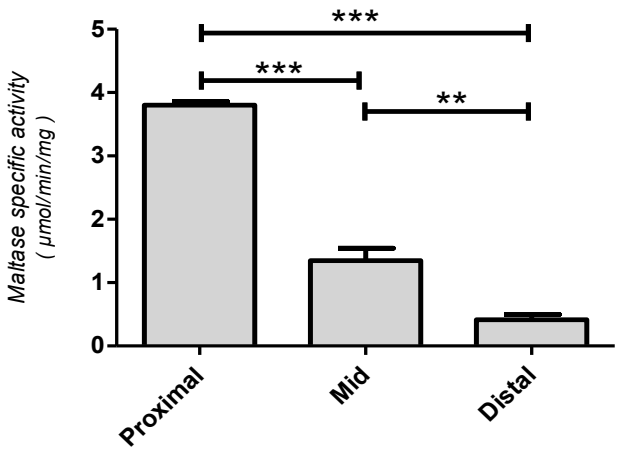

A histogram representing the specific activity of maltase measured in BBMVs isolated from three small intestinal regions of mice.
*Values are mean ± S.E.M (n = 4); ***P < 0.001, unpaired t-test.*

Figure 3.4. Sucrase specific activity along the small intestine of mice

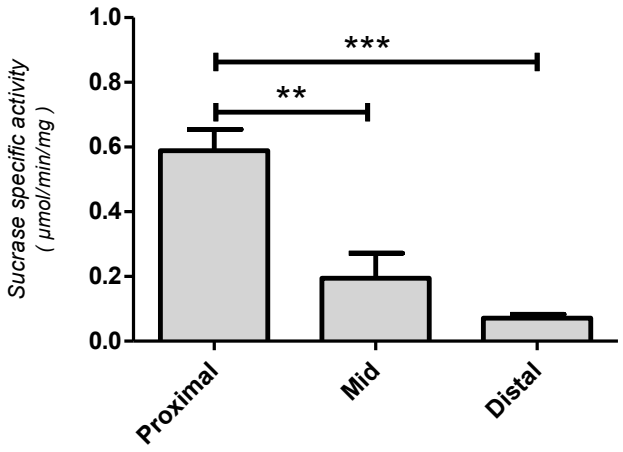

A histogram representing the specific activity of Sucrase measured in BBMVs isolated from three small intestinal regions of mice.
*Values are mean ± S.E.M (n = 4); ***P < 0.001 and **P < 0.01, unpaired t-test.*

Figure 3.5. Comparison of the specific activities of maltase and sucrase along the small intestine of mice

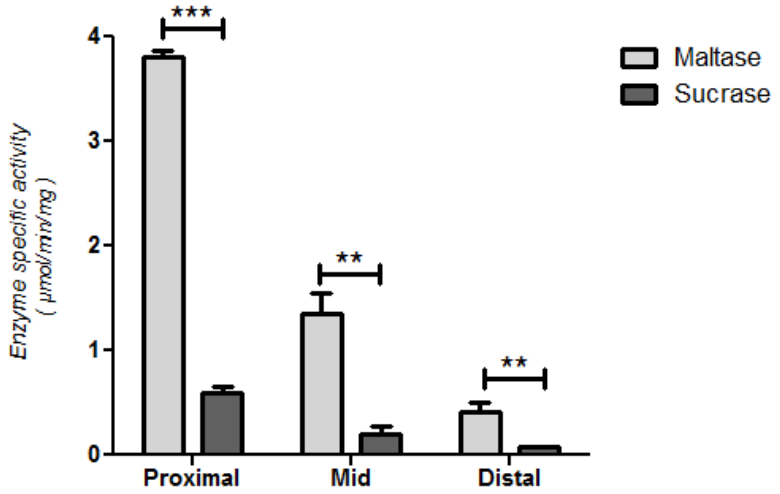

The histogram compares the specific activities of maltase and sucrase among the small intestinal regions of mice.
Values are mean ± S.E.M *(n = 4); ***P < 0.001 and **P < 0.01, unpaired t-test.*

Figure 3.6. Comparison of the specific activities of maltase and lactase along the small intestine of mouse

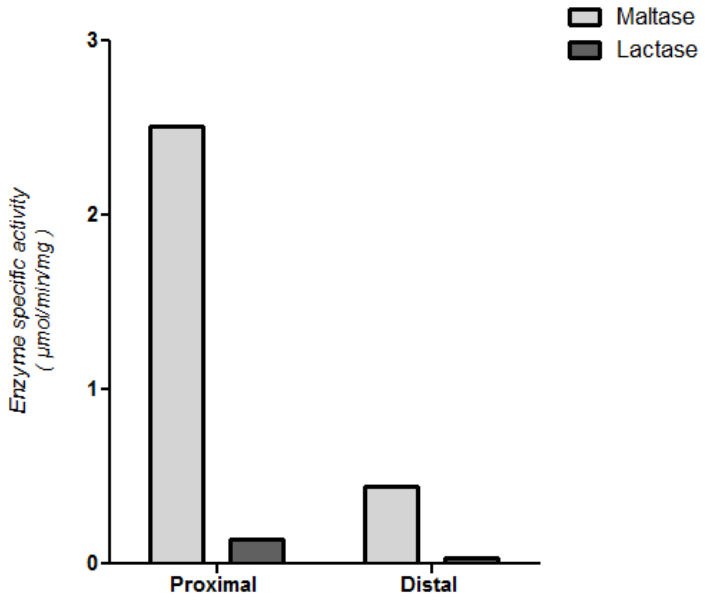

The histogram shows the specific activity of maltase and lactase in the proximal and the distal intestinal regions of mouse. This experiment was carried out using BBMV isolated from intestine of one adult mouse intestine to estimate lactase activity in comparison to maltase.

- Pig intestine:

Along the small intestine of suckling pigs, maltase, sucrase and lactase were assayed in the BBMVs isolated from duodenum, jejunum and ileum. Results are shown in figure 3.7, and the activity of each enzyme along the intestinal length is shown in figure 3.8.

As seen in figure 3.7, maltase has the highest activity level among disaccharidases in all small intestinal regions. Interestingly, lactase has higher specific activity than sucrase by 6.7 fold and 2.3 fold in the duodenum and jejunum, respectively, while, they have similar activity levels in the ileum. However, sucrase did not change with intestinal regions.

The histograms in figure 3.8 demonstrate that the activity of maltase and sucrase does not show great changes throughout the intestine of suckling pigs. In contrast, lactase level is reduced significantly with distal progression along the length of the intestine.

Figure 3.7. Comparison of the specific activity of disaccharidases among intestinal regions of suckling pigs.

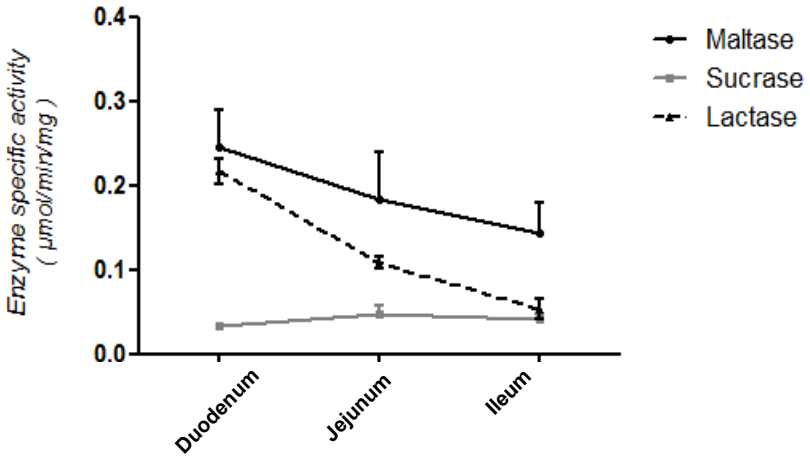

Graphs demonstrating specific activities of maltase, sucrase and lactase in the proximal, mid and distal intestinal regions of suckling pigs.
Results are expressed as mean ± S.E.M. (n = 6).

Figure 3.8. Specific activity of disaccharidases in BBMVs isolated from intestinal regions of suckling pigs.

a) Maltase

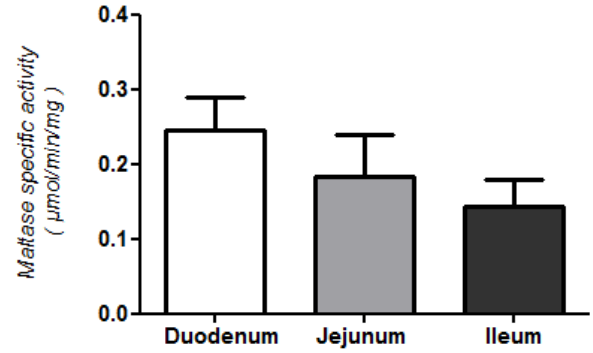

b) Sucrase

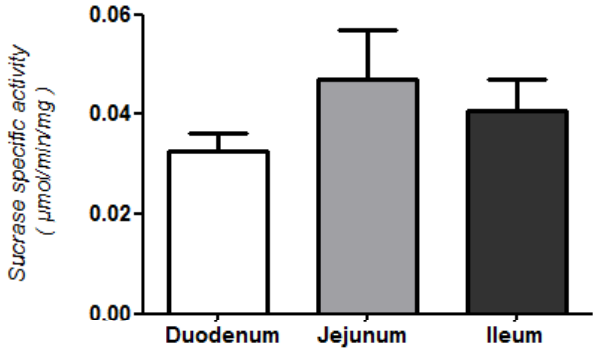

c) Lactase

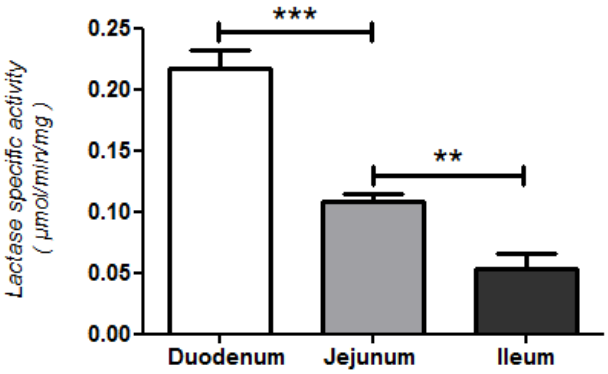

Histograms showing the specific activity levels of a) Maltase, b) Sucrase and c) Lactase in the BBMVs isolated from the three small intestinal regions of suckling pigs.
*Values are mean ± S.E.M (n = 6); ***P < 0.001 and **P < 0.01, unpaired t-test.*

1.2. Development and optimization of immunohistochemical technique using small intestinal tissue of mouse:

Prior to immunohistochemistry, histological analysis of the intestinal tissue sections by haematoxylin and eosin (H & E) staining was routinely carried out to assess the morphology of the intestinal villi and to determine the integrity of the brush-border membrane. As known, Haematoxylin stains the basophilic structures (nuclei) with blue-purple colour, while Eosin stains the eosinophilic structures (the cytoplasm plus the intracellular and extracellular proteins) with varying degrees of pink colour (Fischer *et al.*, 2008).

Immunostaining was carried out using a custom made antibody to SGLT1, which has been used in our laboratory for the past 16 years. The antipeptide antibody was raised in rabbit and made against a synthetic peptide corresponding to amino acids 402-420 of SGLT1 sequence (Wood *et al.*, 2000, Dyer *et al.*, 1997a). This region is a conserved intracellular loop of SGLT1 and has a significant high degree of homology in the amino acid sequencing among various species; having 100 %, 94.7 % and 84.2 % identity with mouse, rat and human, respectively, and 100 % similarity with mouse and 94.7 % with rat and human. Therefore, this antibody was suitable for assessing SGLT1 expression in intestines of mouse, rat and human.

1.2.1. Morphological assessment of mouse intestinal tissues

For morphological analysis, representative images in figure 3.9 shows different sections from the mid intestine of mouse stained with haematoxylin and eosin. It appears that the BBM of the enterocytes is intact and the cells are well-attached to the villi and crypts structures.

Figure 3.9. Analysis of haematoxylin and eosin staining in intestinal tissues of mice

a) *20X magnified*

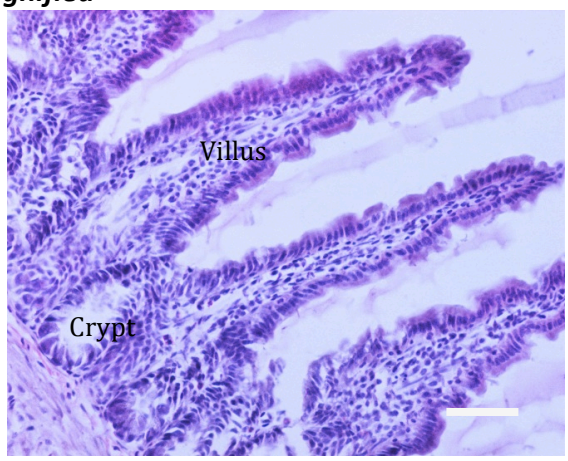

b) *10X magnified*

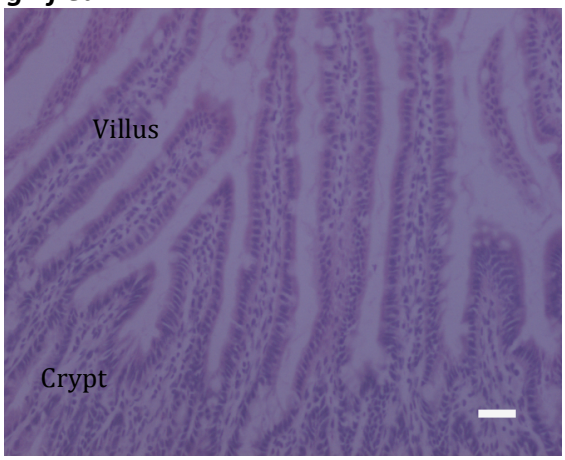

Representative images of H & E staining show different tissue sections of mouse mid intestine for histological examinations (for four animals). Tissues showed good integrity with intact BBM. Bar scale is 20 µm.

1.2.2. Immunohistochemical detection and localization of SGLT1 protein along the crypt/villus axis in mouse intestine.

Skills in immunohistochemistry were developed using mid intestinal tissue from mouse. An anti-peptide primary antibody against SGLT1 was used with the optimized conditions as described in the Methods. The immunohistochemical images in figure 3.10 show promising results of specific labelling without background staining. To ensure specific antibody-antigen binding, omission of the primary antibody was routinely performed as a control. Results show that SGLT1 protein expression is strongly detected in the BBM of the enterocytes along the entire length of the villi, while no staining was detected in the crypts.

Figure 3.10. Developing the immunohistochemical technique to detect SGLT1 protein using intestinal tissues of mice.

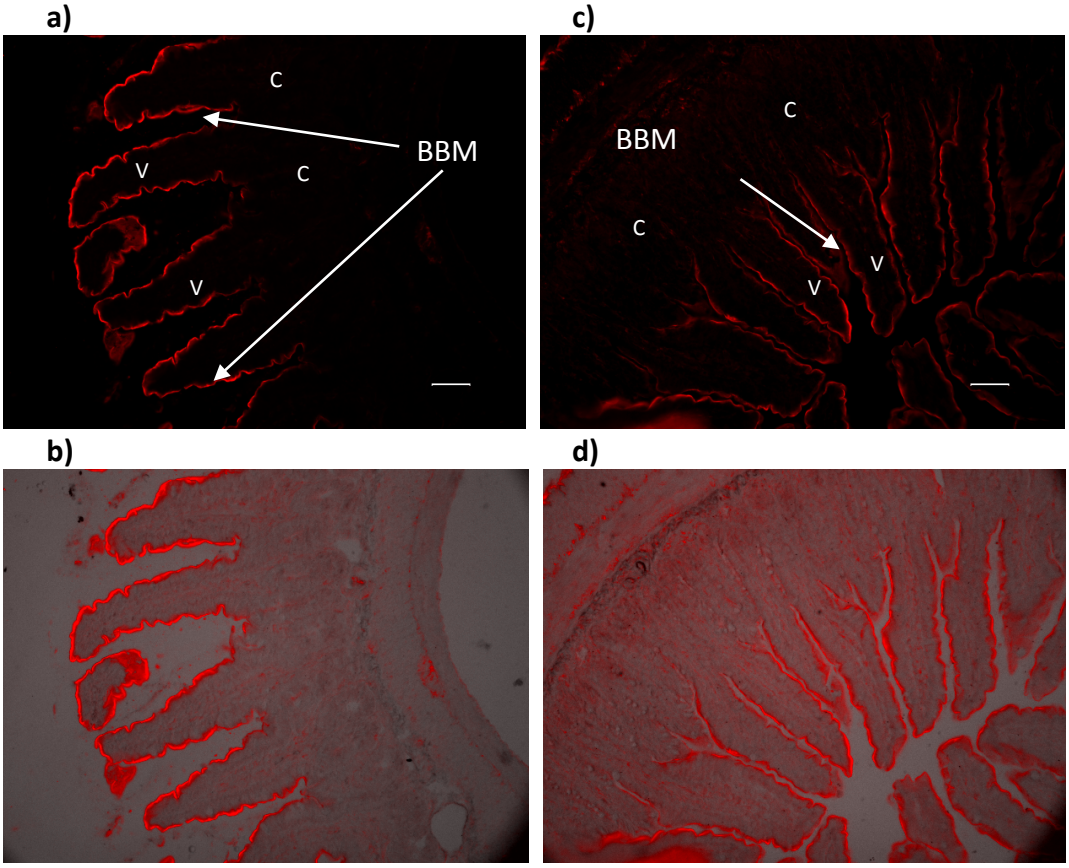

Typical immunofluorescence images show the immunohistochemical detection of SGLT1 protein (red signal) in different sections of the mid intestinal region of mouse (n=4). The immunofluorescence labelling of SGLT1 protein is clearly detected on the BBM of the villus attached enterocytes. There was no backgrounds or non-specific antibody binding.
Both images are 20 X magnified, a) and c) are florescent images, and b) and d) are their corresponding phase images. Bar scale is 20 µm (C: crypts, and V: villus).

1.3. Acquiring and optimizing the technique of Western blotting using pig small intestinal tissue

Western blotting technique was carried out to investigate SGLT1 protein abundance in brush-border membrane vesicles (BBMV) isolated from small intestinal tissues. For immunoblotting, the membrane was probed using a polyclonal anti-SGLT1 primary antibody, raised in rabbit, and then the membrane was re-probed using a monoclonal anti- β-actin primary antibody.

For initial practicing of Western blotting technique, samples of BBMV isolated from the intestine of weaned pigs, on 36 % CHO-containing diet, and suckling pigs, 28 days old, were used for SGLT1 immunoblotting. Figures 3.11 and 3.12 show typical images of the detected bands in the BBMVs samples of weaned and suckling pigs, respectively.

Figure 3.11. Western blotting technique to detect SGLT1 protein using intestinal tissues from weaned pigs.

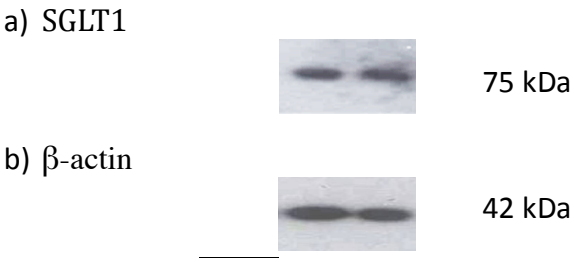

Images of Western blots show the detection of SGLT1 and β-actin proteins in BBMVs isolated from the duodenum of weaned pigs.
a) SGLT1 bands of 75 kDa and b) β-actin bands of 42 kDa.
(Protein in BBMV samples: 20 µg of protein in each lane).

In further experiments, BBMV were isolated from various intestinal regions of 28 day-old suckling pigs for the immunodetection of SGLT1 protein. In figure 3.12, a typical picture is shown of detected 73 kDa immunoreactive bands, corresponding to SGLT1 protein, along the intestinal length. It appears that the bands of the proximal and the mid intestine are more intensive than that of the distal ileum.

Figure 3.12. Immunodetection of SGLT1 protein using intestinal tissue from suckling pigs.

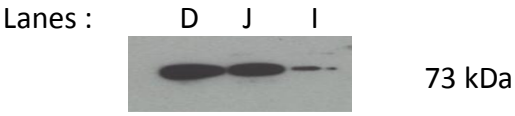

A typical image of immunoblotting shows the detection and characterization of SGLT1 protein, 73 kDa band, in BBMV isolated from three intestinal regions of suckling pigs. Lanes D, J and I are duodenum, jejunum and ileum, respectively. (Protein in BBMV samples: 20 µg of protein in each lane).(n=3).

In an attempt to use frozen rat intestinal tissue, BBMV were isolated from intestinal tissue of adult rats for the immunodetection of SGLT1 protein. In figure 3.13, picture a) shows protein degradation in all the samples. However, as shown in picture b), using fresh rat intestinal tissue to prepare BBMV showed specific immunoreactive bands ~ *75 kDa*, corresponding to SGLT1 protein. This was after optimization of the blotting technique.

Figure 3.13. Immunodetection and characterization of SGLT1 protein using intestinal tissue from rats.

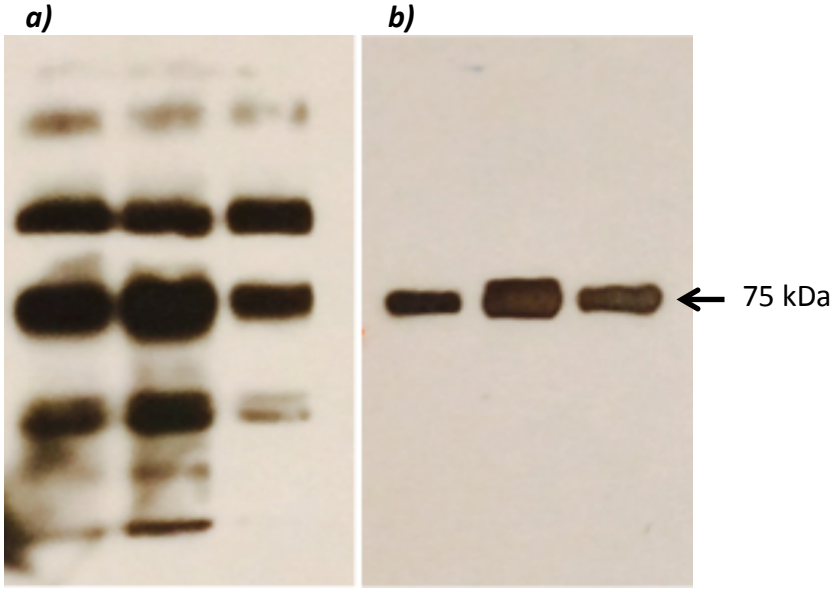

Images of immunoblotting of SGLT1 protein in

a) BBMV isolated from frozen intestinal tissue of rats, showing protein degradation in all samples,

b) BBMV isolated from fresh intestinal tissue of rats showing specific immunoreactive bands ~ 75 kDa, corresponding to SGLT1 protein.

Discussion

Monosaccharides, especially glucose, are essential nutrients for all the physiological functions in the living organisms. Digestion of carbohydrates is accomplished by salivary and pancreatic amylase. The resultant disaccharides sucrose, lactose and maltose are subsequently hydrolysed by the intestinal brush border membrane, sucrase, lactase and maltase, respectively, to monosaccharides: D-glucose, D-galactose and D-fructose (Dyer *et al.*, 2005). These monosaccharides are absorbed from the intestinal lumen to the circulation across the luminal and basolateral membrane of absorptive enterocytes by specific transporters (Shirazi-Beechey, 1995).

Disaccharidases are membrane-bound glycoproteins and SGLT1 and GLUT5 glucose transporters are transmembrane proteins that are all expressed at the apical domain of the enterocytes, hence they are considered reliable brush-border membrane markers.

The apical brush-border membrane (BBM) and the basolateral membrane (BLM) of the enterocyte differ in their structure, composition and surface charge. This permits the selective isolation of BBM and BLM vesicles depending on Mg^{+} precipitation and differential centrifugation (Shirazi-Beechey *et al.*, 1990). It has been demonstrated previously that this procedure yields intact and sealed BBM vesicles, which aided transport studies as they are predominantly oriented right-side-out facing the BBM to the outer (extra-vesicular) compartment (Hearn *et al.*, 1981). Thus, providing an excellent *in-vitro* model to study intestinal nutrient transport across the two membrane domains as it functions *in-vivo*.

The aim of this part of the project was to learn and develop the relevant techniques using available intestinal tissues from pig and mouse, before applying these technologies to intestinal tissues obtained from rats and humans. After isolating BBMV, it was important to confirm the membrane origin of the vesicles. To this end, the activity of BBM marker enzymes was determined using enzyme assays, also aimed to develop expertise in further procedures including: Western blotting and immunohistochemistry.

Pig and mouse intestinal tissues appear to retain their integrity when frozen, therefore, the vesicles were prepared successfully from frozen tissue samples of the small intestine. Tissues from those animals also showed promising results in Western blotting and immunohistochemical techniques. However, protein degradation was observed when BBMV were isolated from frozen rat intestinal

tissue, therefore, the vesicles were prepared successfully from fresh tissue samples of rat small intestine.

The work in this chapter showed that the isolated vesicles, using the described technique by Dyer *et al.*, 2002 (see Methods), originated from the brush-border membrane of the enterocytes. This was confirmed by measuring the enrichment and recovery of the BBM markers, maltase, lactase and sucrase, whenever possible, in the vesicles and comparing to that in the original cellular homogenates. Results here also demonstrated that digestive enzymes are not equally expressed throughout the small intestine, and they are variable between species. That explains the different enrichment values among intestinal regions in various animals.

Enrichment results of maltase and lactase were the highest in the proximal intestine of mice and suckling pigs, respectively. Maltase showed significantly higher activity levels than sucrase in all the intestinal regions of both species. Generally, the digestive enzymes showed higher levels of activity in the proximal intestine that decline dramatically with distal progression throughout the intestine. This can be predicted by the reduction of the luminal substrate through the length of the small intestine because disaccharides are mainly hydrolysed by enzymes in the proximal part and very little reaches the distal part of the intestine. Similar expression patterns of maltase and sucrase along the intestinal length was observed previously in cats and dogs (Batchelor *et al.*, 2011).

Lactase was highly enriched in BBMVs isolated from pig intestine as they were suckling and expected to have high lactase activity levels. Although, the enrichment of lactase is very low in some membrane vesicle samples, this does not reflect a low purity of the BBMVs, but is due to low enzyme expression in some intestinal regions in various animals and different developmental stages. Lactase was assayed in the intestine of different species, but its activity levels were hardly detected in adult animals. This was not surprising as the consumption of milk is markedly reduced in adults, and the intestine is adapting to digest alternative sources of carbohydrate in food. As these pigs are 28 days old, which are the last days in the suckling period before weaning, the activity levels of maltase are just above lactase levels to adapt to the dietary transition from milk to solid food. The results presented here for lactase are consistent with previous reports (Zhang *et al.*, 1997, Montgomery *et al.*, 1991).

The BBMV preparation procedure has been successfully used for many years in our laboratory and been shown to yield pure isolated membrane vesicles originating from the BBM of the enterocytes and not contaminated with BLM or membranes of other intracellular organelles (Murer and Kinne, 1980, Kessler *et al.*, 1978, Shirazi-Beechey *et al.*, 1990). The purity of BBMV has been confirmed, using the isolation technique employed in this thesis, by determining the enrichment and recovery of the BBM markers that were markedly enriched in the vesicles over the original homogenate. In contrast, the classical markers of BLM (Na^+/K^+ ATPase and GLUT2) and other organelles markers like the endoplasmic reticulum (Tris-resistant α-glucosidase) were not detected in the vesicles. This indicates that the vesicles are BBMV and are devoid of any contamination with other membranes (Shirazi-Beechey *et al.*, 1990, Dyer *et al.*, 1997b). In our laboratory, western blot analysis was also used to determine the protein abundance of BBM and BLM marker: SGLT1 and GLUT2 proteins, respectively, further supporting the purity and membrane origin of vesicles using the present procedure (Batchelor *et al.*, 2011). Other studies also confirmed the purification, orientation and integrity of the prepared vesicles by several independent methods: D-glucose uptake, electron-microscopic technique and immunological methods (Haase *et al.*, 1978a, Hearn *et al.*, 1981, Hopfer *et al.*, 1973).

In this part of the study, the technique of immunohistochemistry was acquired after the histological assessment of the mouse intestinal tissue sections from mouse. The morphological analysis by haematoxylin and eosin staining showed good architecture of attached villus enterocytes with intact BBM in mice intestine. By immunohistochemical technique, the anti-SGLT1 antibody used successfully labeled protein on the BBM with no background or non-specific staining. Along the crypt/villus axis, SGLT1 protein is expressed along the BBM of the entire villus length but not in the crypts in mouse mid intestine. That was confirmed by the absence of this expression when the primary antibody was omitted in control slides. These findings were also shown in different species including cats and dogs (Batchelor *et al.*, 2011), horses (Dyer *et al.*, 2009) and pigs (Moran *et al.*, 2010b). This technique was then successfully applied to rat intestinal tissue and human duodenal biopsies (see chapter 4 and 5, respectively).

In this chapter, technical skills of western blotting were developed using BBMV isolated from pig intestinal tissues. SGLT1 protein, between 73-75 kDa, was detected in the BBMVs samples of weaned and suckling pig intestine, with more band intensity proximally than distally in the small intestine.

The anti-SGLT1 antibody has been used successfully in our laboratory in pig tissue (Moran *et al.*, 2010a). The antibody was raised in rabbits (custom synthesis) to a synthetic peptide corresponding to amino acids 402–420 of SGLT1. This antibody identifies a specific immunoreactive band similar to when an antibody raised to the recombinant SGLT1 protein was employed. Both antibodies were also used with several species in our laboratory (Wood *et al.*, 2000, Dyer *et al.*, 1997b, Dyer *et al.*, 2003).

However, glucose transport studies (rapid filtration technique) and the quantitative RT-PCR techniques were applied to rat and human tissues as needed (see chapters 4 and 5).

Chapter 4

SGLT1 expression in the small intestine of control and streptozotocin-induced diabetic rats

Introduction

Dietary carbohydrates are digested in the mouth and duodenum by salivary and pancreatic amylases, respectively, which break down starch and polysaccharides into disaccharides. In the small intestine, brush-border membrane (BBM) disaccharidases: maltase, sucrase and lactase further hydrolyze disaccharides: maltose, sucrose and lactose, respectively, into monosaccharides (D-glucose, D-galactose and D-fructose). The intestinal alkaline phosphatase, a BBM enzyme, dephosphorylates its substrate phosphate esters and is considered as a gut mucosal protection factor limiting inflammation (Tuin *et al.*, 2009).

Following digestion, luminal glucose (and galactose) is actively transported across the BBM into the enterocyte by the sodium/glucose co-transporter 1 (SGLT1). Subsequently, it passively exits from the cell to the systemic circulation via GLUT2, across the basolateral membrane (Shirazi-Beechey, 1995). Intestinal glucose absorption is adapted to dietary carbohydrate contents by regulating SGLT1 expression.

The synthesis of SGLT1 is regulated primarily at the level of mRNA in newly emerged enterocytes in the intestinal crypt. Then, cells migrate along the crypt/villus axis, during their lifespan, before they are shed from the villus tip. Subsequently, SGLT1 protein is incorporated into the BBM resulting in the expression of functional SGLT1 protein (Smith, 1985). Upon cell maturation, the enterocytes are able to maintain an electrochemical gradient and develop their digestive enzymes and absorptive functions.

The profile of SGLT1 expression differs along the small intestinal length according to the site of absorption, and varies between species depending on their dietary habit. Normally, glucose absorption is maintained by basal levels of SGLT1 expression, which is subjected to circadian rhythm and modulated during development and other physiological and pathological situations (Ferraris, 2001, Stearns *et al.*, 2009). This basal SGLT1 expression is independent of luminal sugar concentration. However, when dietary carbohydrates exceed 50%, SGLT1 expression is up-regulated to meet demand (Margolskee *et al.*, 2007, Moran *et al.*, 2010b). In pathological conditions like diabetes and obesity, abnormal expression of intestinal SGLT1 has been observed in various species, including humans (Dyer *et al.*, 1997a, Ferraris, 2001, Batchelor *et al.*, 2013), which appears to be due to deregulation of pathways controlling SGLT1 expression. SGLT1 expression is also influenced by diabetic-induced tissue hypertrophy.

In diabetes mellitus, studies have shown enhanced intestinal capacity to absorb D-glucose, which is not responsive to luminal carbohydrate concentrations, blood glucose or insulin levels (Sharp *et al.*, 1997, Olsen and Rosenberg, 1970). This enhancement is possibly explained by a combination of structural and functional modification in the small intestine that has been observed in diabetic humans and experimentally induced diabetic rats (Dyer *et al.*, 2002b, Dyer *et al.*, 1997c).

Diabetic-associated mucosal hyperplasia expands the intestinal absorptive surface area for all nutrients in general, providing longer villi supporting greater number of absorptive enterocytes with prolonged lifespan (Debnam and Ebrahim, 1990). In addition, diabetes appears to induce earlier maturation of enterocytes and changes in their BBM properties, thus, enhancing their digestive and transport functions (Fedorak *et al.*, 1991, Debnam and Ebrahim, 1989). The activity and expression and activity of BBM disaccharidases are increased in diabetic intestine, providing more available luminal sugars to be absorbed than normal, which exacerbate the situation (Liu *et al.*, 2011). Increased expression and activity of SGLT1 in enterocyte has been reported (Dyer *et al.*, 1997a), in addition to the recruitment of additional SGLT1 onto the BBM of more lower villus enterocytes, where glucose is not usually transported, resulting in more glucose uptake by the diabetic intestine (Fedorak *et al.*, 1987).

It has been claimed by some workers (Kellette and Helliwell, 2000) that the BLM transporter GLUT2 is rapidly trafficked to the BBM of rat enterocytes *in vivo*, when the lumen was perfused with high concentrations of glucose or fructose (Kellett and Helliwell, 2000), and in adaptation to the BBM transport of fructose in diabetes (Corpe *et al.*, 1996), proposing that GLUT2, in addition to SGLT1 and GLUT5, is involved in the apical transport of luminal monosaccharides. However, this is controversial, because mutation in human *SGLT1* gene results in glucose-galactose malabsorption, which is characterized by life-threatening osmotic diarrhea and dehydration, indicating that SGLT1 is the major glucose (and galactose) transporter on the BBM of enterocytes and is not compensated by any apical GLUT2 (Turk *et al.*, 1991). Additionally, it has been reported that *GLUT5* knockout mice are unable to absorb fructose, argues against the existing of GLUT2 on the BBM precipitating in fructose absorption in the absence of GLUT5 (Barone *et al.*, 2009).

Objectives in this chapter:

The main objective was to induce experimental diabetes in rats using streptozotocin (STZ) injection, a potent diabetogenic agent, and to determine any potential diabetes-induced structural and functional changes. To achieve this, the following tasks were undertaken. The aims of this chapter were:

1. To prepare brush-border membrane vesicles from the intestine of control and diabetic rats and determine their membrane origin.
2. To assess the effect of streptozotocin-induced diabetes on whole body parameters.
3. To analyse the morphometric changes in the control and diabetic intestine.
4. To estimate the activity levels of BBM enzymes: maltase, sucrase and intestinal alkaline phosphatase in the small intestine of control and diabetic rats.
5. To investigate the expression pattern of SGLT1 at the mRNA, protein and functional levels along the length of the small intestine of control and diabetic rats using the following methods:
   - Expression and localization of SGLT1 protein along the crypt/villus axis by immunohistochemistry.
   - Assessment of SGLT1 protein abundance by Western blotting.
   - Quantification of *SGLT1* mRNA levels.
   - Determination of Na^+/D-glucose transport rates using rapid uptake filtration technique
6. To determine whether GLUT2 protein is translocated into BBM of enterocytes in the diabetic condition, and, estimate *GLUT2* mRNA levels in control and diabetic intestine.

RESULTS

4.1. Isolation of BBMVs from rat intestine and assessment of their membrane origin:

4.1.1. Enrichment and percentage recovery of BBM markers in vesicle preparations

Maltase, sucrase and lactase are classical markers of the BBM. The activity of sucrase and maltase were measured in membrane vesicles isolated from the intestinal tissue of adult rats. Lactase level is known to be negligible in the intestine of adult animals, so it was not measured. To assess the membrane origin of the membrane vesicles, the specific activity, enrichment and recovery were determined and reported in table 4.1. Maltase showed greater values of enrichment and recoveries than sucrase throughout the intestinal length.

Maltase and sucrase were enriched 20 ± 4.7 and 8.6 ± 1.1 fold, respectively, over their crude homogenates in the proximal intestine. Their recoveries were 22.7 ± 7.8 % and 9.8 ± 2.3 %, respectively. In the mid intestine, they were enriched 14 ± 0.5 and 7.5 ± 1 fold, respectively, with recoveries of 34 ± 11.6 % and 18.6 ± 8 %, respectively. While in the distal part, they were enriched 18.7 ± 2.9 and 6.8 ± 2.4 fold, respectively, and showed recoveries of 33 ± 4.7 % and 12 ± 4.1 %, respectively.

4.1.2. Immunoreactive proteins in BBMV preparation and crude homogenates

As seen in figure 4.1, western blot analysis showed that SGLT1 protein, a BBM protein, is enriched in the purified membrane vesicles with negligible levels in the respective homogenates. However, there was no detectable GLUT2 protein, a classical BLM marker, when the same membrane vesicles were immunoblotted using an antibody to GLUT2 (data not shown). These data indicate that the membrane vesicles originate from the BBM domain with negligible contamination by the BLM.

Figure 4.1. Western blots of SGLT1 and GLUT2 in homogenates and BBMVs isolated from rat intestine

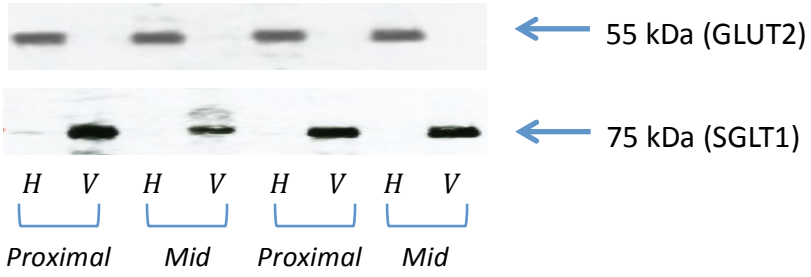

Typical images show GLUT2 protein, ~ 55 kDa bands, in cellular homogenates (H) and SGLT1 protein, ~75 kDa bands, in the purified brush border membrane vesicles (V) isolated from proximal and mid intestinal tissue of rats.

Table 4.1. ***Specific activity, enrichment and recovery of maltase and sucrase in BBMVs isolated from rat tissues.***

	Proximal			***Mid***			***Distal***		
Enzyme	Specific activity (µmol/mg/min)	Fold Enrichment	Recovery %	Specific activity (µmol/mg/min)	Fold Enrichment	Recovery %	Specific activity (µmol/mg/min)	Fold Enrichment	Recovery %
Maltase	3.04 ± 1	20 ± 4.7	22.7 ± 7.8	3.3 ± 0.5	14 ± 0.5	34 ± 11.6	1.22 ± 0.3	18.7 ± 2.9	33 ± 4.7
Sucrase	0.4 ± 0.1	8.6 ± 1.1	9.8 ± 2.3	0.25 ± 0.01	7.5 ± 1	18.6 ± 8	0.07 ± 0.01	6.8 ± 2.4	12 ± 4.1

Results of separate BBMVs preparations from three small intestinal regions of control rats.
Results are expressed as mean ± SD (n = 2).

4.2. Assessment of changes in whole body parameters brought about by streptozotocin (STZ)-induced diabetes

4.2.1. Blood Glucose concentration

To confirm the induction of diabetes, blood glucose concentration was measured in the morning from the tail blood of rats. This was recorded 1-day before and 3-days after STZ treatment, for control and diabetic rats, and then 5 weeks post STZ injection for diabetic rats only. Some of the rats were not diabetic after the first injection of STZ, therefore, those rats were re-injected with a second dose. Blood glucose concentrations in control rats were between 6.9 and 8.9 mmol/l, whereas after 5 weeks, diabetic rats were so hyperglycemic that values could not be determined except for one rat, which was about 29.9 mmol/l.

4.2.2. Body weight and small intestinal weight and length

For both control and STZ-induced diabetic rats, body weight and small intestinal weight and length were measured and recorded in table 4.2.

It was observed that streptozotocin-diabetic rats had a statistically significant body weight loss by 1.3-fold when compared with control rats of the same age (369.3 ± 10.8 g *vs* 500 ± 6.8 g, $p<0.0001$). However, the weight of the small intestine of the diabetic rats was significantly increased compared to that in the controls by 2.7-fold (40.8 ± 3.5 g *vs* 15.1 ± 0.5 g, $p=0.0004$) and it was longer by 1.2-fold (129.5 ± 6.8 cm *vs* 107 ± 3.4 cm, $p=0.02$).

***Table 4.2:* Body weight and small intestinal weight and length in control and diabetic rats.**

	Body weight (gm)	*Intestinal weight (gm)*	*Intestinal length (cm)*
Control rats	*500 ± 6.8*	*15.1 ± 0.5*	*107 ± 3.4*
Diabetic rats	*369.3 ± 10.8*	*40.8 ± 3.5*	*129.5 ± 6.8*

Results are represented as mean ± S.E.M (n = 4), unpaired t-test

4.2.3. Histological and morphometric analysis of the small intestine in control and STZ-induced diabetic rats.

Haematoxylin and eosin (H&E) staining of rat intestinal tissue sections were carried out for: 1) histological analysis prior to immunohistochemistry to assess tissue structure and BBM integrity, and 2) morphometric measurements of villus height and crypt depth.

4.2.3.1. Histological assessment of rat intestinal tissues

Rat intestinal tissue sections were stained with H & E and representative images are shown in figure 4.2. Images a) and b) show that the structure of the rat intestine had a disrupted mucosa, with some enterocytes on the villi being shed, and the BBM being not completely intact. Those rats were killed by phenobarbital injection and tissue were removed in more that 20 minutes later. Therefore, other rats were killed by cervical dislocation and tissues were collected in less than 10 minutes. The latter tissues, as seen in images c) and d), showed good structural integrity with intact BBM and well-attached cells to the mucosa along the villi and crypts.

Figure 4.2. Analysis of haematoxylin and eosin staining in intestinal tissues of rats

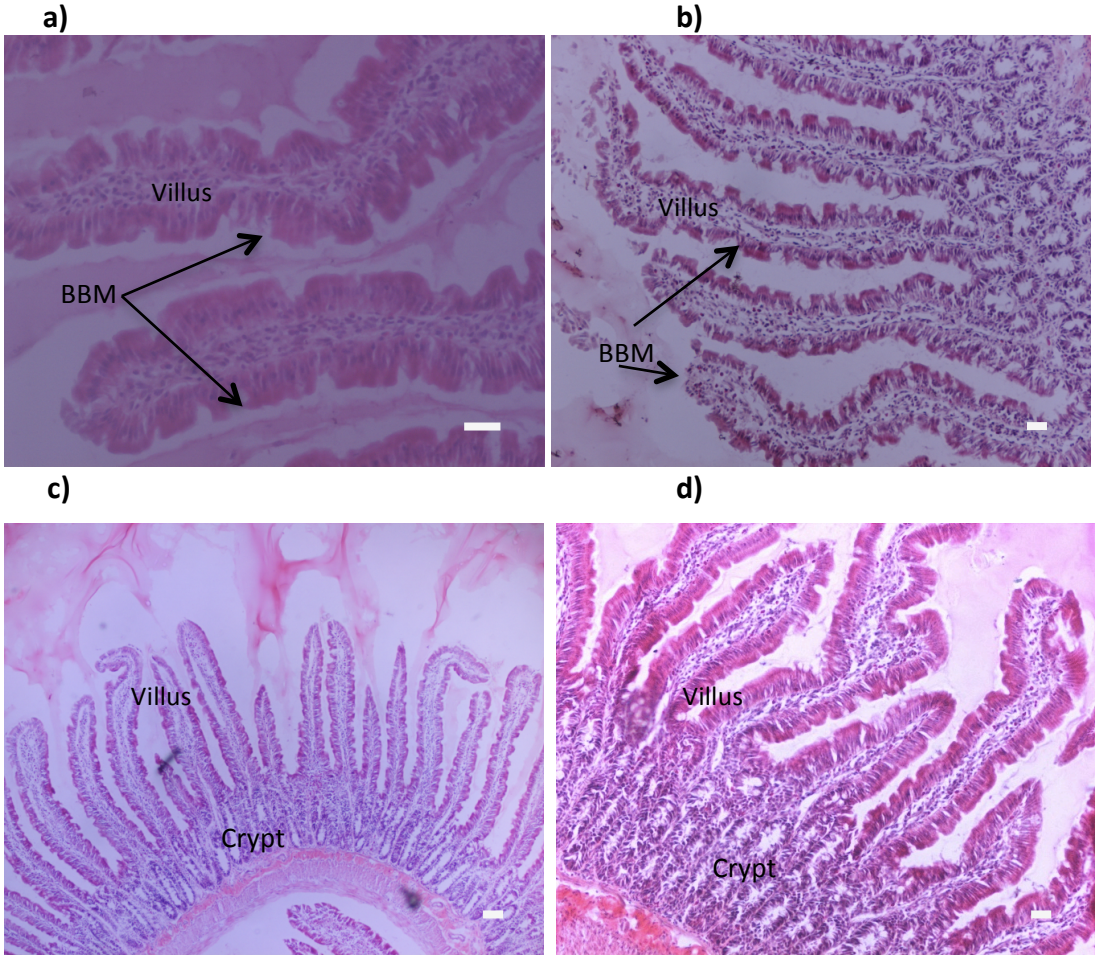

Representative images of haematoxylin and eosin staining show small intestinal tissue sections of rats. The results of histological examination seen in figures a) and b) show that the enterocytes are not well attached to the villus structure and BBM is distorted. However, in c) and d) it appears that the BBM along the villi is intact with good architecture of the enterocytes. a) Proximal region, 20X magnified and b) mid region, 10 X magnified; scale bar is 20 µm for both images. c) Proximal region, 4 X magnified; scale bar is 100 µm, and d) proximal region, 10 X magnified; scale bar is 20 µm.

4.2.3.2. Morphometric measurements of villus height and crypt depth

Several tissue sections from the three small intestinal regions of control and diabetic rats were stained with haematoxylin and eosin to assess any potential intestinal morphometric changes brought about by diabetes. As seen in figure 4.3, it appears that the villi are longer in the intestine of diabetic rats than that in the controls.

Using Image J computer software, villus height was determined by measuring the distance from villus tip to crypt villus junction, and crypt depth was determined by measuring the distance from crypt base to crypt villus junction. Results are depicted in table 4.3 and demonstrated as histograms in figure 4.4.

Generally, the length of the intestinal villi was longest in the proximal part and decreased with distal progression throughout the intestine. Morphometric measurements, represented in table 4.3, showed that the intestinal villi in the diabetic rats were (statistically significant) longer than those of the controls by 1.2 fold in the proximal, mid and distal intestine. However, crypts depths did not changed between the intestine of diabetic and control rats.

Figure 4.3: ***Morphometric analysis of small intestinal sections of control and diabetic rats.***

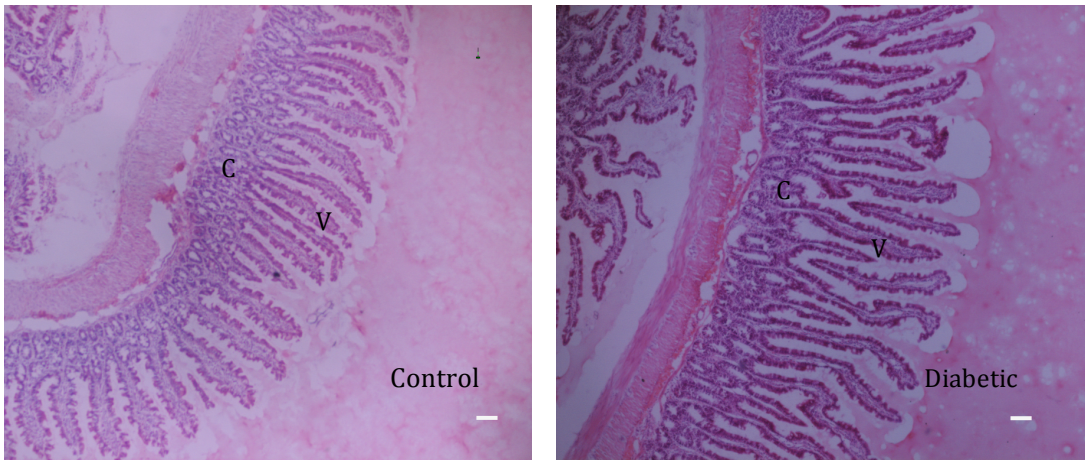

Representative images showing haematoxylin and eosin staining of the distal small intestinal tissue sections. It appears that villi lengths are longer in the intestine of diabetics compared to those in the controls. (V: villus, C: crypt)
Images are 4 X magnified, scale bar is 100 µm.

Table 4.3. : Morphometric measurements of the villus height and crypt depth in the small intestinal regions of control and diabetic rats

	Villus height			*Crypt depth*		
	Proximal	*Mid*	*Distal*	*Proximal*	*Mid*	*Distal*
Control rats	*668.2 ± 19.8*	*461.5 ± 20*	*306.2 ± 14.6*	*206.5 ± 10*	*138.2 ± 8*	*147.1 ± 13.7*
Diabetic rats	*821.3 ± 28.1* *p=0.004*	*597.6 ± 18.3* *p=0.001*	*376.7 ± 15* *p=0.012*	*210.6 ± 11*	*159.5 ± 7*	*153.3 ± 6.6*

Values are measured in µm and expressed as mean ± S.E.M (n = 4), unpaired t-test

Figure 4.4: Morphometric measurements of the villus height and crypt depth in the small intestine of control and diabetic rats

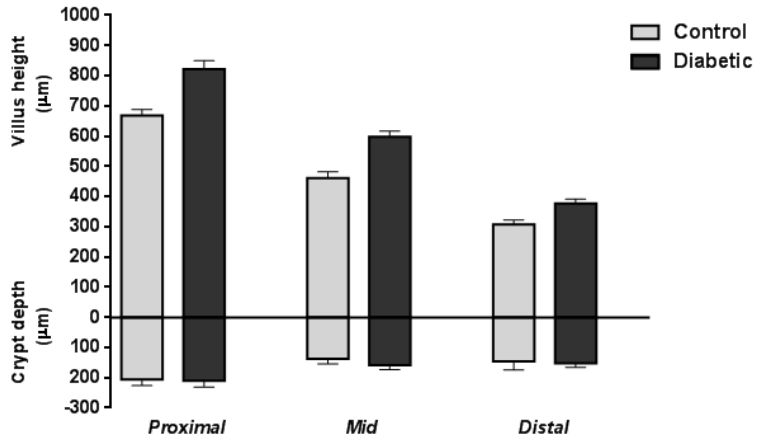

Graphical presentation of morphometric measurements demonstrates the villus height and crypt depth in the small intestinal regions of control and diabetic rats.
Villus height: upward bars above the x axis, and crypt depth: downward bars below the x axis.
Results are expressed as mean ± S.E.M (n = 4).

4.3. Expression of BBM enzymes along the intestine of control and diabetic rats

Digestive BBM enzymes: maltase, sucrase and intestinal alkaline phosphatase (IAP) were assayed in BBMV isolated from the three intestinal regions of control and diabetic rats. Their specific activity levels were determined to identify if i) there were changes in their activity in the diabetic intestine and ii) there was any correlation between the changes in the activity of BBM enzymes to that in SGLT1 expression in the diabetic condition. However, lactase could not be included as it has low expression in the intestine of adult animals.

Table 4.4 represents the specific activity values of alkaline phosphatase, maltase and sucrase along the small intestine of control and diabetic rats. Figure 4.5, displays graphs comparing the activity of each enzyme in the intestine of controls and diabetics. Generally, in each group of control and diabetic rats, the activity levels of alkaline phosphatase and maltase were much higher than sucrase throughout the small intestine. By comparing the diabetic and the control rats, enzyme levels were changed more significantly in the mid and distal than the proximal intestine.

As shown in figure 4.5 a), alkaline phosphatase was significantly elevated by 3 and 3.3 fold in the mid and distal intestine, respectively, in the diabetic rats compared to that in the controls. Figure 4.5 b) shows that maltase levels were increased by 1.1, 1.6 and 2.5 fold in the proximal, mid and distal intestine, respectively, in the diabetic rats compared to that in the controls. While, as seen in figure 4.5 c), sucrase levels were significantly higher by 1.1, 2 and 3.3 fold in the proximal, mid and distal intestine, respectively, in the diabetic than the control rats.

***Table 4.4*: Specific activity of BBM enzymes in BBMVs isolated from intestinal regions of control and diabetic rats.**

	Alkaline Phosphatase *(µmol/ min/ mg)*		***Maltase*** *(µmol/ min/ mg)*		***Sucrase*** *(µmol/ min/ mg)*	
	CNT	***DM***	***CNT***	***DM***	***CNT***	***DM***
Proximal	*3.98 ± 0.74*	*3.28 ± 0.40 (P=0.4)*	*1.91 ± 0.20*	*2.15 ± 0.54 (P=0.6)*	*0.28 ± 0.05*	*0.32 ± 0.06 (P=0.6)*
Mid	*1.06 ± 0.22*	*3.01 ± 0.56 (P=0.03)*	*2.62 ± 0.49*	*4.22 ± 0.09 (P=0.04)*	*0.27 ± 0.02*	*0.53 ± 0.1 (P=0.04)*
Distal	*0.22 ± 0.02*	*0.73 ± 0.13 (P=0.02)*	*0.86 ± 0.15*	*2.12 ± 0.37 (P=0.01)*	*0.06 ± 0.01*	*0.20 ± 0.04 (P=0.02)*

Results are expressed as mean ± S.E.M (n = 4) CNT: Control, DM: Diabetes Mellitus

***Figure 4.5:* Specific activity of BBM enzymes along the intestine of control and diabetic rats**

a) Alkaline phosphatase

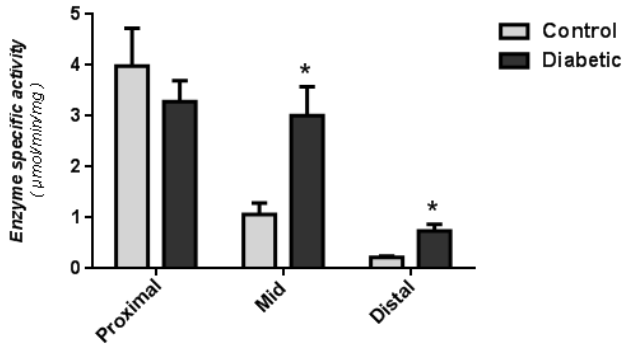

b) Maltase

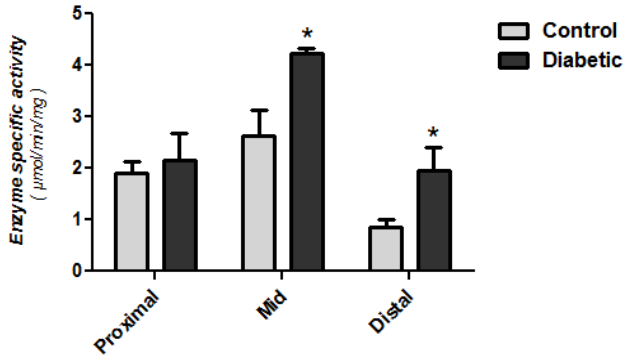

c) Sucrase

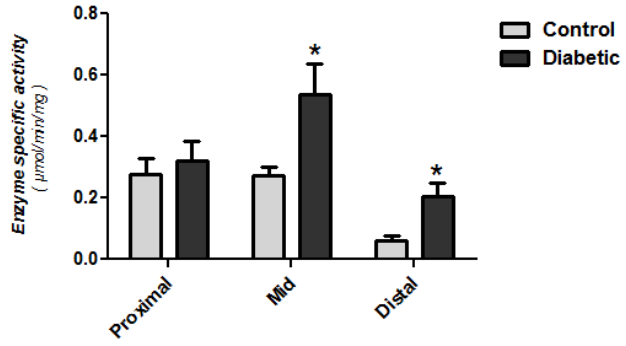

Graphical presentation showing the specific activity of a) Alkaline phosphatase, b) Maltase and c) Sucrase in BBMV isolated from all three small intestinal tissues of control and diabetic rats. Generally, BBM enzymes have significant higher activity levels in mid and distal intestinal regions in the diabetic condition.
*Results are mean ± S.E.M (n = 4); *P < 0.05, unpaired t-test.*

4.4. Expression of SGLT1 in the small intestine of control and STZ-induced diabetic rats.

4.4.1. Immunohistochemical detection and localization of SGLT1 protein along the crypt/villus axis in rat intestine

Immunohistochemical studies were carried out using a custom synthesised antipeptide antibody to SGLT1, which has been successfully used in our laboratory to assess SGLT1 expression in the intestine of different species (Wood *et al.*, 2000, Dyer *et al.*, 1997a). The antibody was raised in rabbit against a synthetic peptide corresponding to amino acids 402-420 of rabbit SGLT1, which has 94.7 % identity and 94.7 % similarity with rat SGLT1.

SGLT1 protein expression was investigated along the crypt/villus length (horizontal axis) as well as among the proximal, mid and distal intestinal regions (longitudinal axis) in diabetic rats after 1 week and 5 weeks induction of diabetes. Representative images for SGLT1 immunostaining are displayed in figures 4.6, 4.7 and 4.8 for the proximal, mid and distal intestine, respectively.

In general, the results revealed that in the small intestine of both control and diabetic rats, SGLT1 protein expression was exclusively expressed on the brush-border membrane of the enterocytes, whereas no staining was detected on the basolateral membrane. However, the expression profile varied along the crypt/villus axis among different intestinal regions of the same group. Furthermore, different expression patterns were observed in the diabetic intestine compared to that in the controls. The profile of SGLT1 expression in the intestine of STZ-induced diabetic rats after one or five weeks induction was similar.

The images in figures 4.6 show that the proximal intestine has a similar SGLT1 protein expression pattern in both control and diabetic rats. SGLT1 protein expression was detected on the BBM of enterocytes along the entire villus length, but not in the crypts. However, images in figures 4.7 and 4.8, show that the mid and distal intestine, respectively, have different SGLT1 protein expression patterns along the crypt-villus axis between control and diabetic rats. In control rats, SGLT1 protein was first detected in the mid villus with increasing intensity toward the villus tip, but little staining was observed in the lower villus and no staining in the crypts. In contrast, in diabetic rats, after one or five weeks of diabetes induction, SGLT1 protein was expressed on the BBM of enterocytes along the whole villus length, but no expression was seen in the crypts.

***Figure 4.6**: Immunohistochemical detection and localization of SGLT1 protein in the proximal intestine of control and diabetic rats*

a) Control rat (10X magnified)

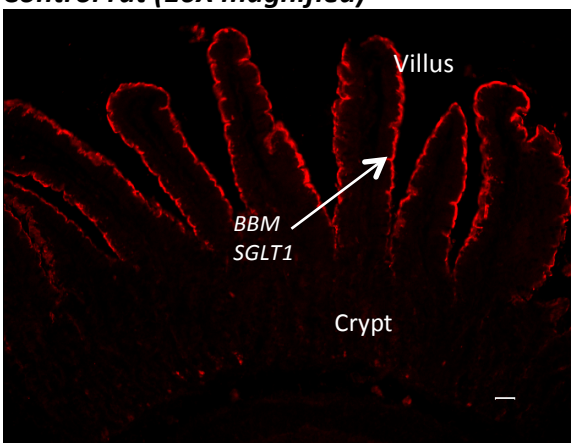

b) One-week post diabetes (10X magnified)

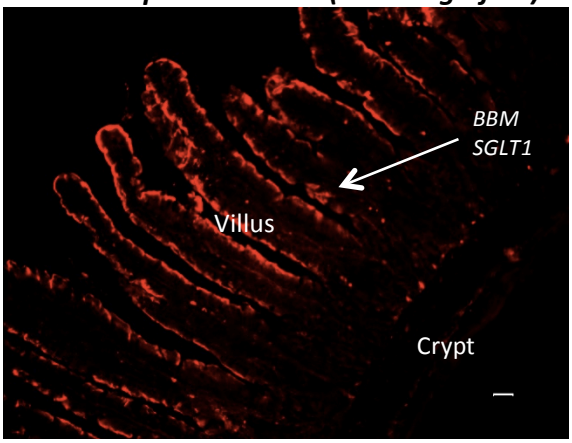

c) Five-weeks post diabetes (20X magnified)

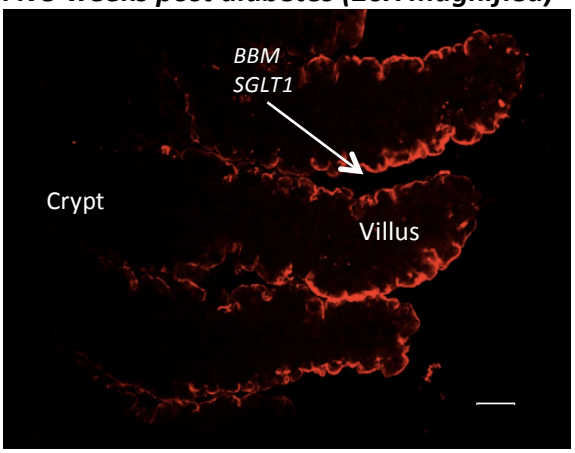

Representative immunofluorescence images (of four animals) show the expression of SGLT1 protein (Red label) on the BBM of the entire villus length in proximal intestine of control and diabetic rats. There was no labelling in the intestinal crypts of both controls and diabetics. Scale bar is 20 µm.

***Figure 4.7*: Immunohistochemical detection and localization of SGLT1 protein in the mid intestine of control and diabetic rats**

a) Control rat

(20X magnified) ***(10X magnified)***

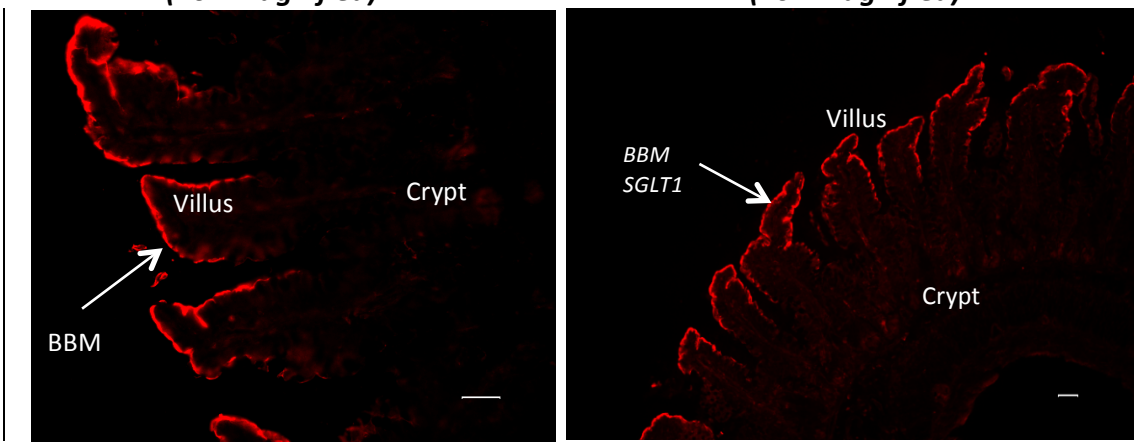

b) One-week post diabetes (10X magnified)

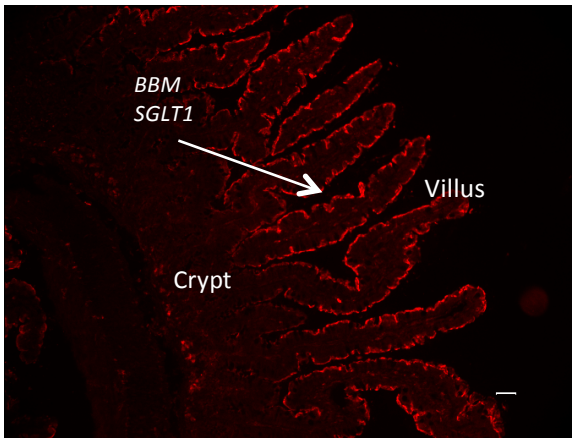

c) Five-weeks post diabetes (10X magnified)

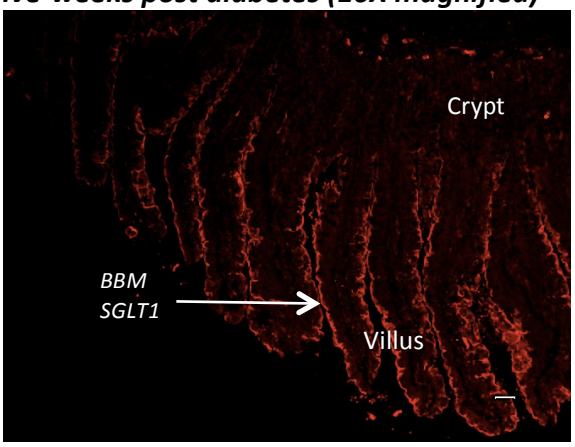

Representative immunofluorescence images (of four animals) show the expression of SGLT1 protein (Red label) in the mid intestine. SGLT1 protein was detected on the BBM of the upper villus and the villus tip in control rats (a), whereas, it was expressed on the BBM of the entire villus length in the diabetic rats (b and c). There was no detected staining in the crypts in all groups. Scale bar is 20 µm.

Figure 4.8: Immunohistochemical detection and localization of SGLT1 protein in the distal intestine of control and diabetic rats

a) Control rat (10X magnified)

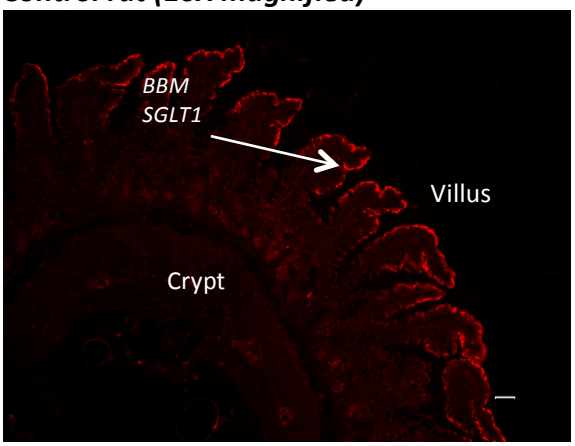

b) One-week post diabetes (20X magnified)

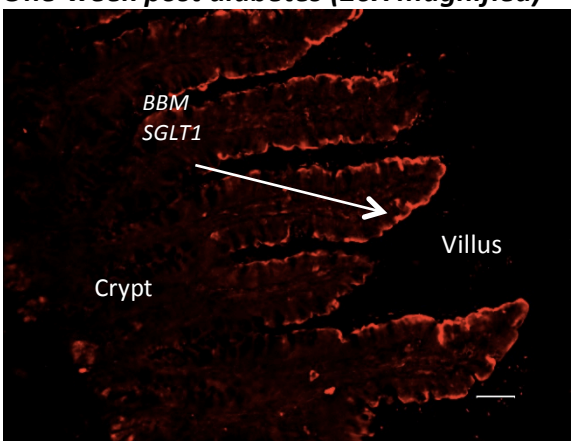

c) Five-weeks post diabetes (20X magnified)

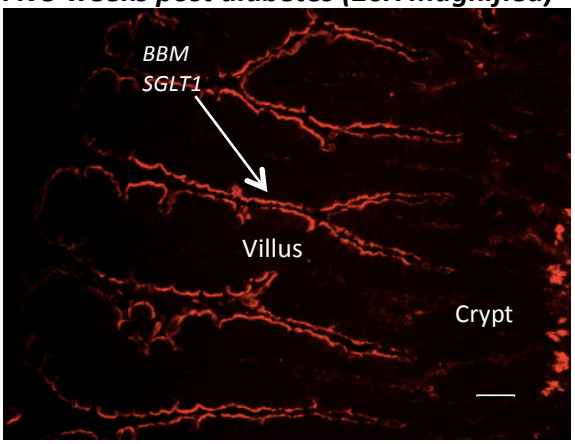

Representative immunofluorescence images (of four animals) show the expression of SGLT1 protein (Red label) in the distal intestine. SGLT1 protein was detected on the BBM of the upper villus enterocytes and the villus tip in the intestine of control rats (a). In contrast, it is detected along the BBM of the entire villus enterocytes in the intestine of diabetic rats (b and c). No staining was observed in the crypts of control or diabetic intestine. Scale bar is 20 µm.

4.4.2. Quantitative RT-PCR analysis of *SGLT1* mRNA levels along the length of the small intestine.

The quantitative real-time PCR was carried out to analyse the intestinal expression of SGLT1 at the mRNA level in control and STZ-induced diabetic rats after one and five weeks induction of diabetes. Rat SGLT1 primer set was used with 25 ng of cDNA of rat intestinal samples. The qPCR product was successfully cloned and sequenced to confirm its identity as the rat *SGLT1* gene, as outlined in Methods.

Figure 4.9 shows the relative abundance of *SGLT1* mRNA, normalized to the *β-actin* gene, along the intestine of control and diabetic rats. In control rats, results demonstrated that *SGLT1* mRNA abundance was similar throughout the intestinal length; with a slight decline distally. Interestingly, in the diabetic rats, the relative *SGLT1* mRNA expression was significantly higher by 2 fold (2.04 ± 0.17 *vs* 1.02 ± 0.05, *P=0.002*), 2.2 fold (1.98 ± 0.2 *vs* 0.91 ± 0.1, *P=0.001*) and 2.3 fold (1.6 ± 0.2 *vs* 0.7 ± 0.08, *P=0.008*) in the proximal, mid and distal intestine, respectively, compared to that in the control rats.

Figure 4.9. ***Expression of SGLT1 mRNA levels in control and diabetic rats determined by qRT-PCR.***

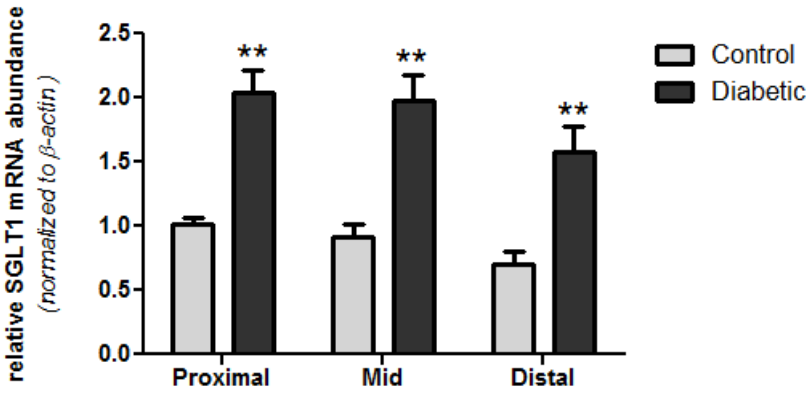

A histogram shows the relative abundance of SGLT1 mRNA expression among the three intestinal regions of control and diabetic rats.
*Results are means ± S.E.M. (n = 6); **P < 0.01, unpaired t-test.*

4.4.3. Immunodetection of SGLT1 protein in BBMV isolated from intestine of control and diabetic rats.

By Western blotting, 75 kDa SGLT1 and 42 kDA β-actin protein bands were clearly detected as shown in figure 4.10.a) and 4.10.b), respectively, in the intestine of control and diabetic rats. A histogram in figure 4.10.c) displays the densitometric analysis of the relative SGLT1 protein abundance, quantified using scanning densitometry (Phoretix).

There was a trend to higher levels of SGLT1 protein abundance in the diabetic rats compared to the controls by 1.5 fold (1.4 ± 0.27 *vs* 0.9 ± 0.2, *P=0.3*), 1.4 fold (1.33 ± 0.2 *vs* 0.9 ± 0.03, *P=0.2*) and 2.2 fold (1.31 ± 0.2 *vs* 0.6 ± 0.06, *P=0.06*) in BBMV isolated from the proximal, mid and distal regions, respectively. SGLT1 protein expression in the intestine of control rats declined with distal progression, whereas it had similar abundance throughout the intestine of diabetics.

Figure 4.10. Immunodetection of SGLT1 protein in BBMV isolated from the intestinal regions of control and STZ-induced diabetic rats

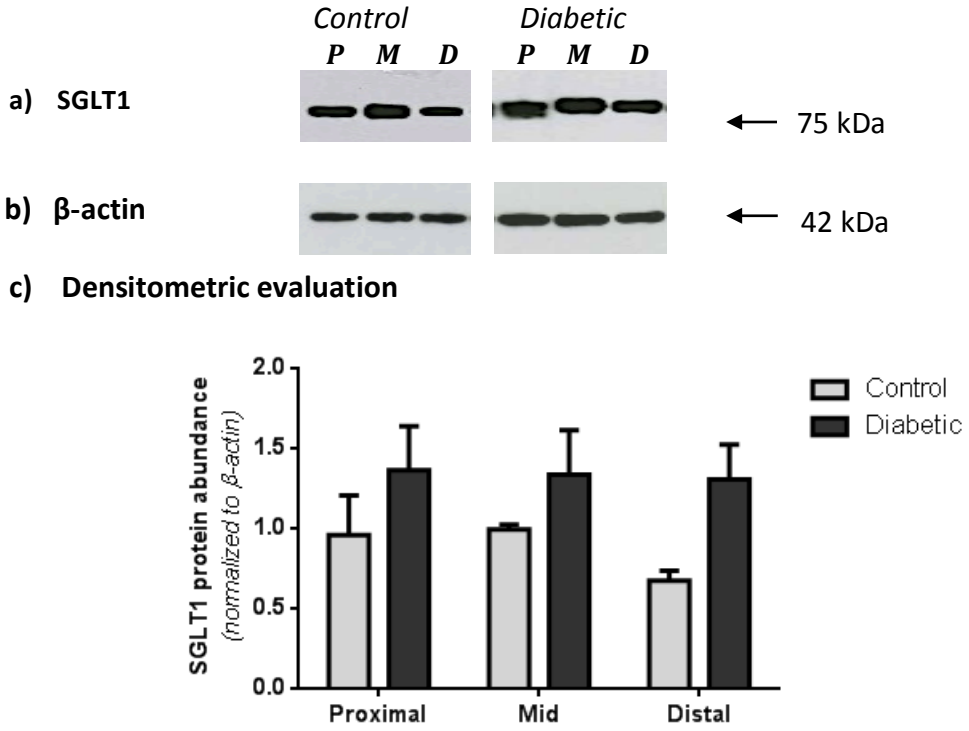

SGLT1 protein abundance determined by Western blotting in BBMV isolated from the intestinal regions of control and STZ-induced diabetic rats. 10 µg of protein was used in each lane. P: proximal, M: mid and D: distal.

a) SGLT1 protein of ~75 kDa.
b) β-actin protein of ~42 kDa.
c) The densitometric analysis of relative protein abundance of SGLT1, normalized to β-actin, in control and diabetic rats. Results are means ± S.E.M (n = 4).

4.4.4. Functional analysis of SGLT1; Na^+-dependent glucose transport rate in BBMV isolated from the intestine of control and diabetic rats.

To analyse the transport function of SGLT1, Na^+-dependent D-glucose uptake rates were determined using the rapid filtration technique, as described in the Methods. For transport studies in rat intestinal tissue, freshly prepared BBMVs were used to avoid protein degradation and vesicular damage as discussed in Methods. The histogram in figure 4.11 shows the initial rate (3 second uptake) of Na^+-dependent D-glucose uptake in BBMV isolated from the intestinal regions of control and diabetic rats.

Results revealed that in both control and diabetic groups, uptake rates were slightly higher in the order of mid > proximal > distal intestine. This is adapting to the bioavailability of the substrate (glucose) in the intestinal lumen, which is digested in the proximal region and mostly absorbed in the mid region, then, little sugars reach the distal small intestine.
However, the rate of D-glucose uptake was significantly higher in the intestine of diabetic rats compared to that in the controls by 2 fold (149 ± 71 *vs* 73.4 ± 50 pmol/mg protein/sec, *P=0.4*), 3.3 fold (274.80 ± 23.3 *vs* 88.61 ± 34.4 pmol/mg protein/sec, *P=0.002*), and 3.5 fold (192.3 ± 30.3 *vs* 45.5 ± 22.5 pmol/mg protein/sec, *P=0.007*) in the BBMVs isolated from the proximal, mid and distal regions, respectively.

Figure 4.11. ***Functional analysis of SGLT1: D-glucose transport rate in the intestine of control and diabetic rats***

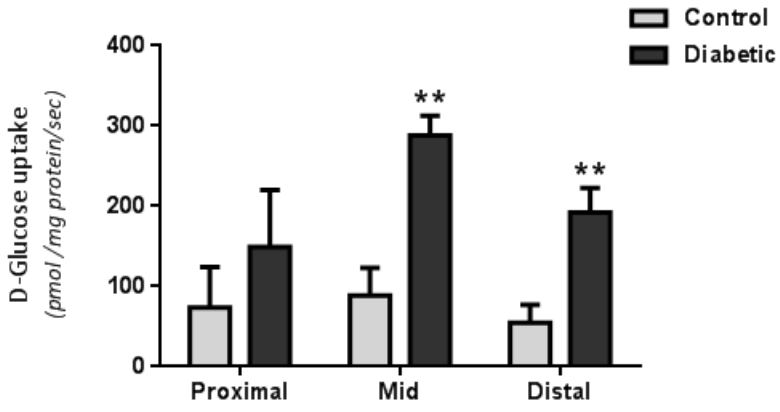

*A representative histogram showing the Na^+-dependent D-glucose transport by SGLT1 into BBMVs isolated from proximal, mid and distal intestinal regions of control and diabetic rats. Results are from separate uptake done in triplicate, and values are means ± S.E.M (n = 4); **P < 0.01, unpaired t-test.*

4.5. Assessment of GLUT2 expression in the intestine of control and diabetic rats.

4.5.1. Immunohistochemical detection and localization of GLUT2 protein in control and diabetic intestine.

Having determined SGLT1 protein expression, the expression of GLUT2 protein was assessed, as it is the facilitated glucose transporter on the basolateral membrane (BLM) of the enterocytes and involved in intestinal glucose absorption.

Immunohistochemistry was carried out as described in the Methods, and two antibodies were employed. The exact GLUT2 expression was observed when using an antibody targeted either to residues 40-55 (the extracellular loop region) of rat GLUT2 or to residues 511-524 (the C- terminus region) of equine GLUT2. As a control, tissue sections were routinely stained with the omission of the primary antibody.

Images in figure 4.12 show that GLUT2 protein was exclusively expressed on the BLM of the enterocytes, whereas no labeling was detected on the BBM even in the diabetic condition. As seen in figure 4.13, the expression of GLUT2 was detected only along the villus enterocytes but not in the crypt compartment. This pattern of expression was similar among the intestinal tissue sections from proximal, mid and distal, of control and diabetic rats.

***Figure 4.12*: Immunohistochemical detection and localization of GLUT2 protein in the intestine of control and diabetic rats**

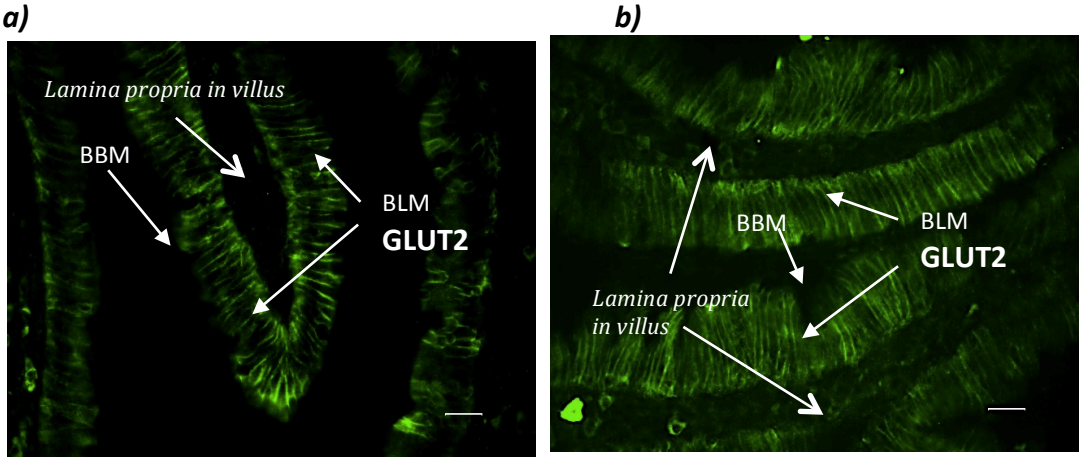

Representative images of the proximal intestinal region show that GLUT2 protein is exclusively localised on the BLM of the enterocytes in both a) control and b) diabetic rats. No labelling was observed on the BBM even in the diabetic intestine using anti-GLUT2 antibody targeted to residues 40-55 (the extracellular loop region).
Both images are 40 X magnified. Scale bar is 10 µm.

***Figure 4.13*: Immunohistochemical detection and localization of GLUT2 protein along the villus in rat intestine**

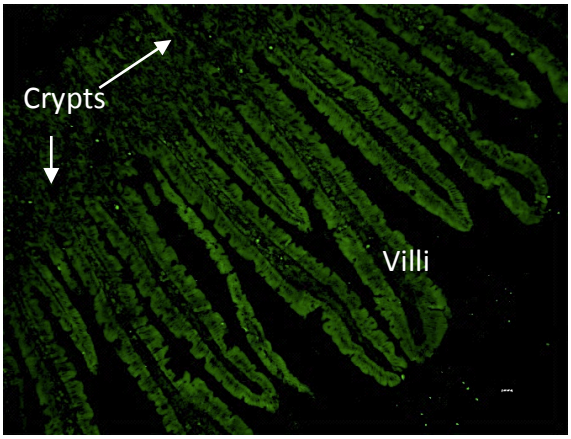

A typical immunohistochemical image of intestinal tissue from control rat showing that GLUT2 protein expression is only seen in the intestinal villi but not the crypts. Image is 10 X magnified; scale bar is 10 µm.

4.5.2. Absence of GLUT2 protein detection in BBMV isolated from the intestine of control and diabetic rats.

By Western blotting, using the same anti-GLUT2 antibodies as employed in immunohistochemistry, it was demonstrated that GLUT2 protein was not detected in BBMV isolated from control and diabetic intestine. In contrast, high expression of SGLT1 was found in those vesicles, see figure 4.1.

4.5.3. Expression of *GLUT2* mRNA levels along the intestinal length of control and diabetic rats.

After determining that GLUT2 protein is exclusively expressed on the BLM of the enterocytes, which is responsible for glucose exit from the enterocyte to the blood circulation, its mRNA level was investigated using quantitative Real-Time PCR analysis.

The graph shown in figure 4.14 demonstrated that for both control and diabetic rats, *GLUT2* mRNA expression was higher proximally than distally. However, the mRNA levels of *GLUT2*, normalized of *β-actin* mRNA, was significantly elevated in the diabetic rats by approximately 1.6 fold (1.61 ± 0.23 *vs* 1.07 ± 0.03, *P=0.04*), 1.8 fold (1.12 ± 0.17 *vs* 0.62 ± 0.06, *P=0.02*) and 2.6 fold (0.7 ± 0.14 *vs* 0.26 ± 0.08, *P=0.02*) in the proximal, mid and distal regions, respectively, compared to that in control rats.

***Figure 4.14*: Expression analysis of GLUT2 mRNA levels in the intestine of control and diabetic rats determined by qRT-PCR.**

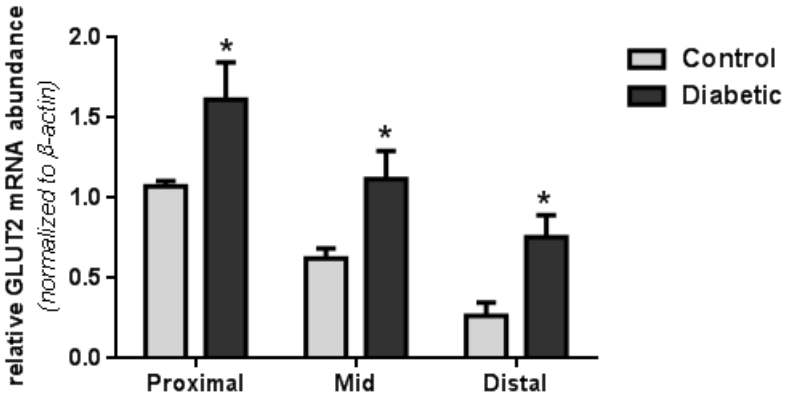

Histograms demonstrating the relative abundance of GLUT2 mRNA, normalized to that of β-actin (control gene), among the three intestinal regions of control rats and diabetic rats.
*Results are means ± S.E.M. (n = 6); *P < 0.05, unpaired t-test.*

Discussion

In this project, streptozotocin injection was used to induce type 1 diabetes in rats and subsequently diabetes was confirmed by measuring blood glucose concentrations. The present work determined the intestinal structural changes, BBM enzymatic activity, the expression and functional levels of SGLT1 along the small intestine of control and STZ-induced diabetic rats. Moreover, the GLUT2 expression was assessed.

Initially in this study, intact BBMV could not be prepared successfully from frozen tissues of rats, and SGLT1 immunoblotting showed degraded proteins in the isolated BBMV (see figure 3.13 page 111, frozen *vs* fresh tissue used for BBMV preparation). The reason for this may be due to the time between killing the animals and removing the tissue, or isolating BBMV from frozen rat intestinal tissues. Considering these factors that may have affected the integrity of the tissue or the vesicles, tissue collection was done very rapidly after killing the rat, and BBMVs were isolated from freshly removed tissues. Additionally, protease inhibitors were included in buffers employed in vesicle preparation to prevent protein degradation. For glucose uptake studies, it was difficult to assess glucose transport function in frozen BBMV isolated from rat intestine, thus the transport study was carried out on the same day of vesicles preparation. For Western blotting, protein samples were mixed with the sample buffer prior to freezing; then, protein separation was processed on another day. It was shown that the isolated vesicles originated from the BBM of the enterocytes by determining the enrichment and percent recovery of BBM markers (maltase and sucrase) in the vesicles and compared to their cellular homogenates. This was further confirmed by the immunoblotting detection of the BBM marker (SGLT1 protein) and the absence of the BLM marker (GLUT2 protein) in the vesicles, reflecting the origin and purity of the BBMV and that they are not contaminated with BLM.

For morphological analysis in this work, it was a challenge to obtain intestinal tissue from rats with good architecture. In initial attempts, it was noticed that some enterocytes were shed from the villi and the BBM was not completely intact. This could have been due to the proteases present in the luminal contents and the slow tissue removal. These were avoided by removal of tissue within ten minutes of sacrifice, and the use of protease inhibitors in fixation solutions. Tissues from the latter animals showed good structural integrity with well-attached cells and intact BBM, which could be used for the morphometric measurements and immunohistochemistry.

Assessing the whole body parameters and the small intestinal morphometric changes in response to diabetes mellitus, statistically significant body weight loss by 1.3-fold was observed in the diabetic rats, although, the gut was enlarged showing increase in intestinal weight and length by 2.7 and 1.2 fold, respectively. This was accompanied by longer villi in the three intestinal regions by 1.2 fold in the diabetic rats compared to that in controls. Results also showed that the activities of intestinal maltase, sucrase and alkaline phosphatase, were increased in the diabetic rats compared to that in the controls. In the proximal intestine, they were higher by 1.1 and 1.1 fold for maltase and sucrase, respectively, but lower alkaline phosphatase. They were significantly higher by 1.6, 2 and 3 fold, respectively, in the mid; and 2.5, 3.3 and 3.3 fold, respectively, in the distal intestine.

The data presented in this chapter clearly show that intestinal *SGLT1* mRNA levels are higher by 2, 2.2 and 2.3 fold in the proximal, mid and distal intestine, respectively, of diabetic rats compared to controls. SGLT1 protein was immune-blotted as a single band of 75 kDa, and showed increased SGLT1 protein abundance by 1.5, 1.4 and 2.2 fold in the proximal, mid and distal intestine, respectively, of diabetic rats compared to controls. However, enhancement of glucose transport rates (SGLT1 function) was higher than increase in *SGLT1* mRNA and protein expression. The function was enhanced by 2, 3.3 and 3.5 in the BBMV isolated from the proximal, mid and distal intestine, respectively, of diabetic rats compared to controls. This disparity between transport rates and protein abundance is likely due to differences in the sensitivity of techniques, glucose uptake studies using radiolabelled glucose appears to be more sensitive than Western blotting. The limitation of Western blot findings could be due to the freezing and defrosting of BBM vesicles leading to SGLT1 protein degradation, as separation of protein was not processed on the same day of vesicle preparation, unlike uptake studies using freshly isolated BBMV.

Immunohistochemistry studies demonstrated that SGLT1 protein was expressed on the BBM of enterocytes along the entire villus length in the proximal intestine of both control and diabetic rats. However, in the mid and distal intestine, SGLT1 expression on the BBM was limited to the upper villus region in control rats, whereas, it was extended to the lower villus in diabetic rats. Negligible SGLT1 protein detection was found in the crypts of both groups. This expression pattern was similar after one and five week post-diabetes indicating the early impact of diabetes on the SGLT1 expression profile.

Moreover, GLUT2 protein was expressed only on the BLM of enterocytes in the intestine of controls and diabetics confirming its exclusive role in the basolateral glucose transport, which is similar to previous observations in our laboratory in many species including humans (Dyer *et al.*, 2009, Dyer *et al.*, 2002b, Moran *et al.*, 2010b). GLUT2 protein is not immunodetected in isolated BBMVs from the intestine of both control and diabetic rats; in contrast, SGLT1 is strongly detected in the same vesicles samples. *GLUT2* mRNA was increased in the diabetic intestine compared to controls by 1.6, 1.8 and 2.6 fold in the proximal, mid and distal intestine, respectively, implying that there is an enhanced increase in trans-cellular transport of glucose from the lumen of the intestine into the circulation.

The morphometric analysis reported here are consistent with previous morphometric analysis (Zhao *et al.*, 2003) and intestinal parameters (Jorgensen *et al.*, 2001). Furthermore in line with the findings reported in this thesis, it has been documented that intestinal growth is localized to the mucosal layer, as the weight of underlying tissue after mucosal scrapping was not significantly changed (Schedl and Wilson, 1971).
Results of enzyme activities seem to be consistent with results in other reports (Caspary *et al.*, 1972, Younoszai and Schedl, 1972), which also found that increased activity of BBM enzymes are not dependent on carbohydrate intake, developmental stage or gut hormones in the diabetic condition (Schedl *et al.*, 1983). Other studies indicated that enhanced digestive activity in diabetes is reversed by insulin treatment (Liu *et al.*, 2011).

Previous studies have also shown more *SGLT1* mRNA level in the intestine of STZ-diabetic rats compared to controls (Burant *et al.*, 1994), and significantly increased in chronic diabetes (30- to 60-day after STZ injection) (Miyamoto *et al.*, 1991). Our Western blotting showed greater changes in SGLT1 protein expression in the ileum than in the duodenum and jejunum, similar to that observed previously with changes in SGLT1 expression being confined to the ileum and jejunum of experimentally induced diabetic rats compared to controls (Burant *et al.*, 1994, Fedorak *et al.*, 1991). At the cellular level, SGLT1 protein was previously found in villus enterocytes of diabetic ileum, but not control ileal tissue (Debnam *et al.*, 1995). Other work showed a recruitment of specific phlorizin binding in the mid to lower villus of chronically diabetic rats (Fedorak *et al.*, 1991, Fedorak *et al.*, 1989). Furthermore, similar results were previously documented by Debnam *et al.*, 1995 that SGLT1 function is significantly higher in the diabetic intestine, and that this enhancement is due to increases in the maximum velocity of glucose uptake through recruitment of additional glucose carriers to the BBM, possibly in enterocytes of the lower villus to crypt region (Fedorak *et al.*, 1987).

In summary, as demonstrated in the table below, the magnitude of changes in the villus morphology and the activity of BBM markers do not entirely match the enhanced expression and function of SGLT1 in the diabetic intestine. In the proximal intestine of diabetic rats compared to controls, there is no change in the villus length and in the activity of the BBM enzymes. However, there is a 2- fold increase in *SGLT1* mRNA expression and function, indicating that increased SGLT1 expression brought about by diabetes may be due to enhancement of the number of SGLT1 transporters per enterocytes. This pattern of expression is different in mid and distal regions of the intestine of diabetic rats. The lower villus enterocytes of control rats do not express SGLT1 protein, whereas in diabetic rats, intestinal SGLT1 expression spreads to lower villus enterocytes. It is likely that the 2- and 3- fold increase in SGLT1 expression is due to a combination of more enterocytes expressing SGLT1 and more SGLT1 being expressed by each enterocyte.

	Proximal ***Diabetic vs. Control***	***Mid*** ***Diabetic vs. Control***	***Distal*** ***Diabetic vs. Control***
Villus length	*1.2 fold*	*1.2 fold*	*1.2 fold*
BBM enzymes -Alkaline phosphatase - Maltase - Sucrase	 - *1.1 fold* *1.1 fold*	 *3 fold* *1.6 fold* *2 fold*	 *3.3 fold* *2.5 fold* *3.3 fold*
***SGLT1* mRNA**	*2 fold*	*2.2 fold*	*2.3 fold*
SGLT1 protein abundance	*1.5 fold*	*1.5 fold*	*2.2 fold*
SGLT1 function (Na/glucose uptake)	*2 fold*	*3.3 fold*	*3.5 fold*
SGLT1 protein expression	*No change:* *SGLT1 expressed on entire villus enterocytes in both C and D.*	*Doubled:* *SGLT1 expressed on* *- Upper villus (C)* *- Upper and lower villus (C and D)*	*Doubled:* *SGLT1 expressed on* *- Upper villus (C)* *- Upper and lower villus (C and D)*
***GLUT2* mRNA** **GLUT2 protein**	*1.6 fold* *No change:* *(GLUT2 expressed exclusively on BLM of enterocytes in both C and D)*	*1.8 fold* *No change*	*2.6 fold* *No change*

C=control, D=diabetes

The table displays the fold increase in villus height, BBM enzymes (markers), SGLT1 expression and function as well as GLUT2 expression in the intestine of diabetic rats compared to controls.

Chapter 5

The expression of SGLT1 in the intestine of non-diabetic (control) humans and patients with type 2 diabetes mellitus

Introduction

In the human digestive system, dietary carbohydrates are digested by intestinal brush-border membrane (BBM) hydrolases into monosaccharides, which are absorbed from the gut lumen to the systemic circulation via transmembrane carriers on the luminal and the serosal sides of the enterocytes.

Intestinal SGLT1 is an integral membrane protein localised in the BBM of the intestinal epithelium. It is a symporter importing glucose, or galactose, coupled to Na^+ and its associated electrochemical gradient from the intestinal lumen into the enterocytes across the BBM. Subsequently, all monosaccharides are passively moved down their concentration gradient out of the cells to the blood stream via GLUT2 across the basolateral membrane (Gould and Bell, 1990, Wright, 1993, Shirazi-Beechey, 1995).

The expression of intestinal SGLT1 has a persistent basal level, which is independent of local luminal nutrients, to maintain the glucose absorption in the gut even in starvation. However, the expression is regulated in response to the fluctuation in luminal carbohydrate, above a threshold exceeding 50 % of dietary contents. It has also been reported that this SGLT1 expression is normally modulated according to the developmental stage and other physiological conditions like pregnancy and lactation (Rhoads *et al.*, 1998, Ferraris, 2001, Dyer *et al.*, 1997a, Dyer *et al.*, 1997b). Interestingly, there are increased levels of SGLT1 protein and mRNA that are independent of luminal sugars and blood glucose or insulin levels observed in diabetes and obesity (Burant *et al.*, 1994). Studies revealed that SGLT1 expression and activity are enhanced in the intestine of human subjects with NIDDM (Dyer *et al.*, 2002b). Limited work, however, has been carried out to explain the molecular basis of the enhanced intestinal capacity for glucose absorption in patients with diabetes mellitus.

Diabetes mellitus (DM) is a chronic metabolic disorder with disturbances in carbohydrate, fat and protein metabolism. It is characterized by chronic hyperglycaemia due to either absolute or relative insulin deficiency, or peripheral tissue resistance to insulin. Diabetes is diagnosed by measuring the plasma glucose levels in fasting ≥ 7.0 mmol/L (126 mg/dL) and 2 hours after 75 g glucose drink ≥ 7.8 mmol/L (140 mg/dL) or random plasma glucose level ≥ 11.1 mmol/L (200 mg/dL) with classical symptoms (Colman *et al.*, 1999, Puavilai *et al.*, 1999). According to the World Health Organization, (WHO 1999), the three most common types of DM are: type 1, insulin-dependent diabetes mellitus (IDDM), type 2, non-insulin dependent diabetes mellitus (NIDDM) and type 3, the gestational diabetes. They all have multiple etiologies plus the genetic predisposition for developing the disease. About 90 % of diabetic cases are considered type 2, which is due to a combination of

tissue resistance to insulin and relative insulin deficiency. This is in contrast to type 1, which results from autoimmune destruction of insulin-producing β-cells of the pancreas, leading to absolute insulin deficiency (Knowler *et al.*, 2002).

The rising prevalence of type 2 diabetes is an epidemic health problem especially in developing countries and causes a financial burden to health authorities. Diabetes can be a life-threatening disease if blood glucose is not managed properly. It has serious long-term complications such as nephropathy, neuropathy and retinopathy due to high blood glucose, which can cause disability or end-stage organ failure. The acute complications include diabetic ketoacidosis and nonketotic hyperosmolar diabetic coma, which could lead to coma or death from severe hypo-glycaemia (Sarwar *et al.*, 2010, American Diabetes Association, 2011).

Therefore, effective management of diabetes is vital to maintain glucose homeostasis and to minimize the risk of complications. In type 1 (IDDM), the definitive treatment is insulin injections, or pancreatic transplants; the latter is rarely done for those with badly uncontrolled diabetes. By contrast, in type 2 (NIDDM), endocrinologist deal with this disorder in different ways, such as modifying diets and lifestyles, reducing body weight and promoting exercise. In addition, oral administrated hypoglycemic agents (OHAs) are generally prescribed to patients with NIDDM, either alone or in combination with insulin injections as needed in some cases. Different classes of OHAs are available, which have various modes of action: they stimulate insulin secretion or its action, reverse insulin resistance, reduce gluconeogenesis by the liver and inhibit the gut enzymes that convert dietary carbohydrates into simple sugars to reduce glucose absorption after meals.

Research is now focused on innovative new treatments for diabetes mellitus. As SGLT1 plays a major role in intestinal glucose transport, it is considered a novel target to control postprandial hyperglycemia. However, better understanding of the mechanisms underlying increased expression of SGLT1 will allow the design of strategies to control rates of glucose uptake in the intestine of patients with diabetes mellitus with therapeutic potential.

Aims:

The aim of the work presented in this chapter was to investigate the enhanced SGLT1 expression in the intestine of human diabetics. To this end, human biopsies were collected by endoscopy from the duodenum of non-diabetic individuals and patients suffering from type 2 diabetes mellitus. The expression pattern of SGLT1 protein and *SGLT1* mRNA levels were assessed in diabetic intestinal biopsies and compared to that of control biopsies from intestine of non-diabetics undergoing routine endoscopy to exclude disease, whose intestine was shown to be histologically normal.

The following strategies were employed:

1. Isolation and characterisation of BBMV isolated from human duodenal biopsies and assessment of their membrane origin.
2. Measurement of the specific activity of the BBM marker, maltase, in post nuclear membrane fractions (PNMF) prepared from duodenal biopsies of control humans and diabetics.
3. Haematoxylin and eosin staining of the tissue sections for morphological assessment.
4. Immunohistochemical detection and localization of SGLT1 protein along the crypt/villus axis in duodenum.
5. Quantitative Real-Time PCR analysis of *SGLT1* mRNA levels.
6. Western blotting to detect SGLT1 protein in PNMF.

RESULTS

5.1. Isolation and characterisation of BBMV from human duodenal biopsies and assessment of their membrane origin.

For the isolation of BBMVs from intestinal biopsies, the microscale procedure was used as described by Shirazi-Beechey *et al.*, (1990). Specific activity, enrichment and percent recovery of maltase, as a brush border membrane marker, were determined to assess the membrane origin of the vesicles. Due to the shortage of human tissue samples, only maltase activity was assayed in the BBMVs isolated from duodenal biopsies of human subjects.

Figure 5.1 demonstrates the level of maltase activity in the BBMVs and their respective homogenates. The specific activity of maltase was 0.34 and 0.37 µmol/min/mg in human samples 1 and 2, respectively. Maltase was enriched 4 fold in the membrane vesicles over cellular homogenates and the recovery was 3.8 %.

Figure 5.1. Specific activity of BBM marker, maltase, in original homogenates and BBMVs isolated from human duodenal biopsies.

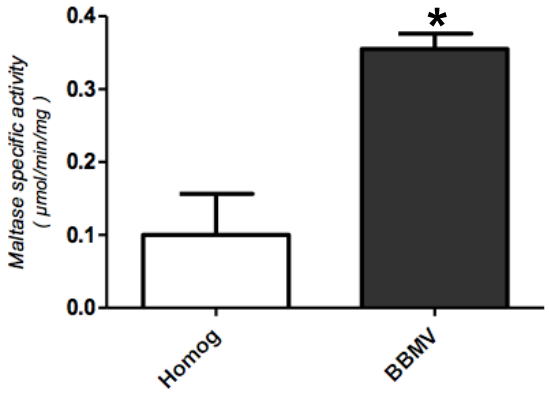

Maltase activity in BBMVs (black bar) and their cellular homogenates (white bar) prepared from human duodenal biopsies.
*Values are mean ± SD (n = 2); *P < 0.05, unpaired t-test.*

5.2. Specific activity of a BBM marker, maltase, in PNMFs prepared from duodenal biopsies of control humans and diabetics

PNMFs were isolated from the duodenal biopsies of control and diabetic humans. The specific activity of maltase was determined to correlate the enhanced expression of BBM enzymes to the expression of SGLT1 in the diabetic condition.

As shown in figure 5.2, maltase had significantly higher activity in the duodenum of diabetic patients by 2.1-fold compared to that in the healthy controls (0.55 ± 0.05 *vs* 0.26 ± 0.05 μmol/min/mg, *p=0.009*)

Figure 5.2. Expression of the BBM marker, maltase, in the duodenal biopsies of control and diabetic humans.

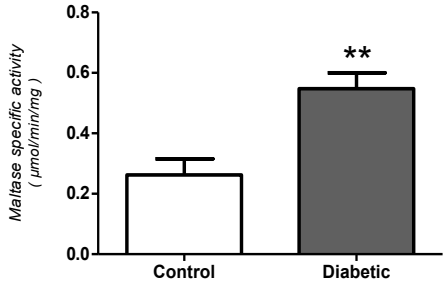

Maltase specific activity in PNMFs prepared from duodenal biopsies of non-diabetic controls and diabetic patients.
*Values are mean ± S.E.M (n = 4), **P < 0.01, unpaired t-test.*

5.3. Comparison of maltase specific activity across species

The opportunity was taken to compare maltase specific activity in the duodenum of human subjects to that measured in other species. As shown in table 5.1, it appears that maltase level in the proximal intestine of rat is close to that in mouse. Similarly, close levels of maltase activity are seen in the duodenum of humans and pigs. Interestingly, maltase activity in the intestine of mice and rats (small mammals) was 10 times higher than that measured in the intestine of humans and pigs (large mammals).

Table 5.1. Maltase specific activity in BBMVs isolated from the proximal small intestine of different species

	Human	***Pigs***	***Mice***	***Rats***
Maltase	0.35	0.24	3.8	3.04
(μmol/min/mg)	± 0.01	± 0.04	± 0.05	± 0.7
	(n=2)	*(n=6)*	*(n=4)*	*(n=4)*

Results are expressed as mean ± S.E.M. (n=4 or 6) or S.D. (n=2).

5.4. Morphological assessment of human duodenal biopsies by haematoxylin and eosin staining.

Human duodenal samples were sectioned and stained with haematoxylin and eosin (H & E) to assess tissue morphology and integrity prior to immunohistochemistry. Representative images of the intestinal tissue sections with H & E staining are shown in figure 5.3. As the human samples used in this study were collected by endoscopy, the duodenal biopsies only contained tissue from the mucosal layer. It appears that the tissue samples retained their integrity with brush-border membrane (BBM) and intact attached enterocytes along the crypt-villus compartment. Obviously, only the epithelium of the gut was seen, not the whole thickness of the intestinal wall.

Figure 5.3. Morphological assessment of human duodenal biopsies

a) **b)**

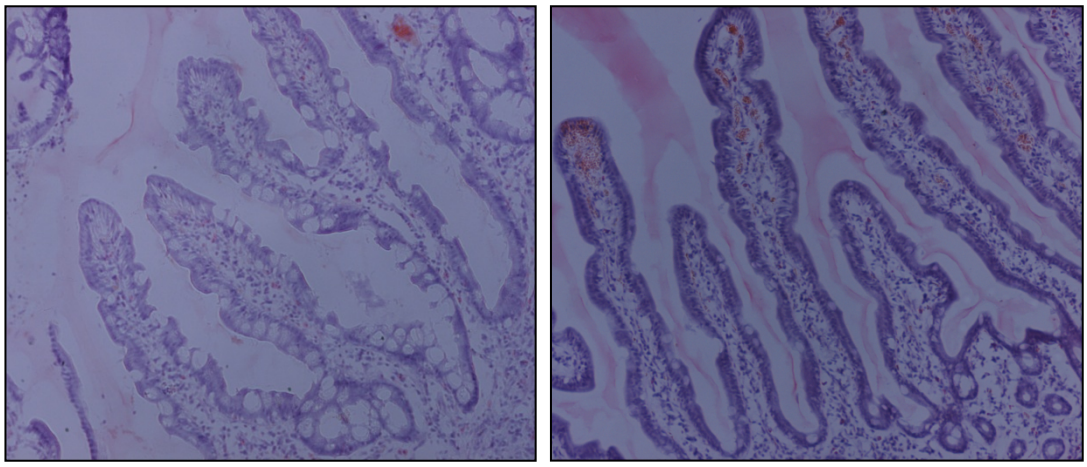

Representative images of Mayer's haematoxylin and eosin staining showing sections of human duodenal biopsies from a) non-diabetic (controls) and b) diabetic humans. Enterocytes are attached to the villus structurse with intact BBM.
Both images are 10 X magnified.

5.5. Immunohistochemical detection of SGLT1 protein and its localization in the duodenum of control and diabetic humans.

The expression of SGLT1 protein was investigated by immunohistochemistry, as described in the Methods, using the primary anti-SGLT1 antibody that was used before in our laboratory. Omission of the primary antibody was routinely carried out as a control to confirm specific antibody binding. As shown in figure 5.4, SGLT1 protein was localized to the BBM of the enterocytes along the entire villus length in the duodenum of non-diabetic controls and diabetic patients. However, in patients with NIDDM, the immunofluorescence staining appeared stronger than that of controls.

Figure 5.4. Immunohistochemical detection and localization of SGLT1 protein in the duodenum of control and diabetic humans

Control human

a) 20 X magnified

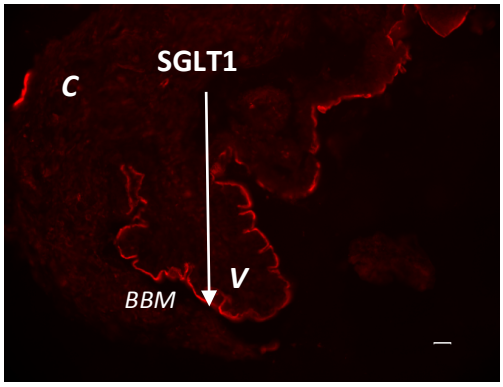

b) 40 X magnified

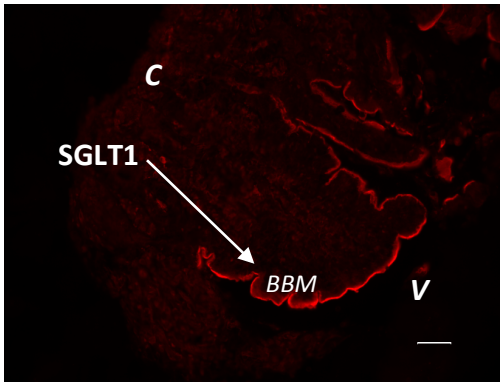

Diabetic human

c) 20 X magnified

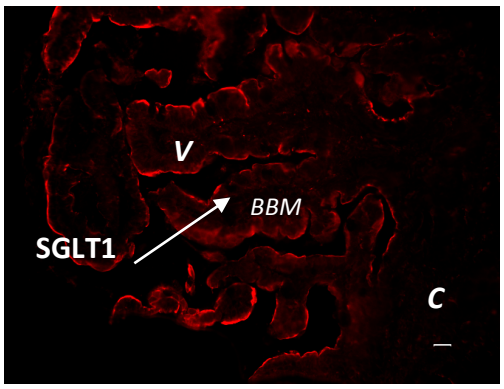

Representative images show the immunostaining of SGLT1 protein in the duodenal biopsies of non-diabetic humans and diabetic patients. The expression of SGLT1 protein, labelled in red colour, is detected on the BBM of enterocytes along the entire villus length, while no staining is seen in the crypts of both the control and the diabetics. Scale bar is 10 µm. V (villus) and C (crypt).

5.6. Analysis of *SGLT1* mRNA in the duodenum of control and diabetic humans

The expression of *SGLT1* mRNA level was analysed using quantitative RT-PCR. The PCR reaction was carried out with 50 ng cDNA generated from duodenal samples of healthy controls and diabetic patients. Figure 5.5 demonstrates that *SGLT1* mRNA expression in the duodenum of diabetic patients was significantly higher, by 2.7-fold, compared to that in the non-diabetic controls (1.7 ± 0.4 *vs* 4.6 ± 0.5, *p=0.008*).

Figure 5.5. ***Expression of SGLT1 mRNA levels in control and diabetic human subjects determined by q RT-PCR.***

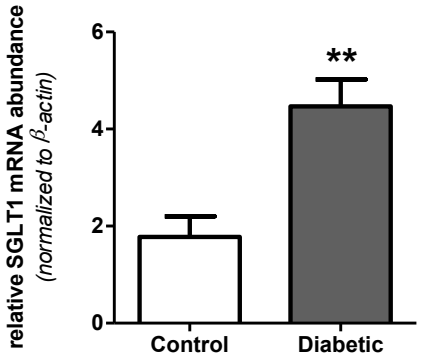

A histogram representing the relative abundance of SGLT1 mRNA, normalized to β-actin, in duodenal biopsies removed from control and diabetic humans.
*Values are means ± S.E.M (n = 4); ** P value < 0.01, unpaired t-test.*

5.7. Immunodetection of SGLT1 protein in human duodenum

Post-nuclear membrane fractions (PNMFs) were isolated from duodenal biopsies of non-diabetic controls and patients with NIDDM for the detection of SGLT1 protein by Western blotting. Proteins in PNMFs were separated by SDS-PAGE gel electrophoresis on acrylamide gels. Isolated proteins were transferred from the gel onto PVDF membranes and immunoblotted with the SGLT1 and β-actin antibodies (The latter used as the control), as described in the Methods.

Typical images of Western blots are shown in figure 5.6. Only in some PNMF samples, a single band of 75 kDa, corresponding to SGLT1 protein, was recognized using the antibody against SGLT1. Unfortunately, in other samples of PNMF isolated from diabetic humans, this band was not detected and hence, protein abundance could not be estimated in all samples. However, the β-actin antibody recognized a single band of 42 kDa, corresponding to β-actin protein, which was detected in all the samples of both diabetics and controls. This indicated that the protein was loaded equally (10 µg) in all the lanes. Concluding that in some samples SGLT1 protein was degraded. The shortage of human biopsies limited the availability of more PNMF samples.

Figure 5.6. Immunodetection of SGLT1 protein in PNMF prepared from the duodenal biopsies of control and diabetic humans

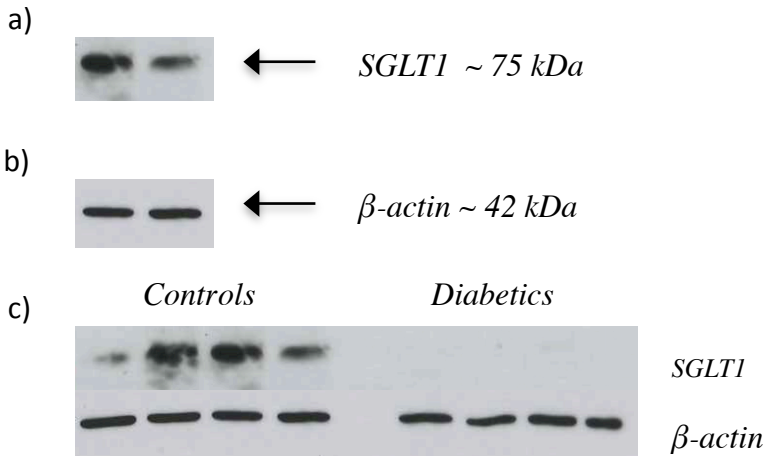

Representative images show the detection of a) SGLT1 protein band of 75 kDa and b) β-actin protein band of 42 kDa in PNMF isolated from the duodenal biopsies of control individuals and diabetic patients. c) bands of SGLT1 protein were detected only in some PNMF samples. While, bands of β-actin protein were detected in all PNMF samples isolated from control and diabetic human intestine.

Discussion

Diabetes mellitus (DM) is a serious common metabolic disease characterized by uncontrolled blood glucose levels, which lead to irreversible chronic complications as well as life-threatening acute complications. Effective treatment of diabetes is thus important, employing multi-strategy medications as well as lifestyle habits, like exercise, maintaining a normal blood pressure and healthy body weight. All forms of diabetes have been managed since insulin became available, and type 2 diabetes can be controlled with diet and medication.

Postprandial hyperglycemia can also be managed by reducing the absorption of dietary sugars from the gut. Researchers can contribute by identifying the factors that control intestinal glucose transport. The main route for glucose uptake from the gut lumen into enterocytes is the glucose transporter SGLT1. Hence, interest has recently focused on the expression of SGLT1 as a new therapeutic target for diabetic patients by modulating intestinal glucose uptake.

It has been documented previously that the small intestine has a higher capacity to absorb monosaccharides in diabetics. This enhancement is independent of dietary sugar load, blood glucose concentration, or insulin level. It was reported that D-glucose is transported mainly in a Na^+- dependent manner at a higher rate, over 3-fold, in BBM vesicles isolated from diabetic intestine than in vesicles isolated from non-diabetics, indicating that the activity of SGLT1 was enhanced in the intestine of humans with type 2 diabetes mellitus (Dyer *et al.*, 2002). Similarly, it was observed that the maximum capacity for intestinal sugar transport is increased in the intestine of Alloxan- or streptozotocin-induced diabetic rats (Fedorak *et al.*, 1989).

In this study, human duodenal biopsies were removed by endoscopy from non-diabetic controls and patients with NIDDM. Brush-border membrane vesicles (BBMVs) or post-nuclear membrane fractions (PNMFs) were isolated successfully from frozen human duodenal biopsies using the microscale technique described by Klett *et al.*, (2004) and Lambert *et al.*, (2002) (see Methods). The membrane origin of the vesicles (BBMVs) was assessed by determining the enrichment and recovery of maltase, as a BBM marker. However, as preparation of PNMFs yields more sample volume than BBMVs, most of the human biopsies were used for PNMF preparation.

Interestingly, maltase specific activity in BBMVs isolated from the duodenum of non-diabetic human biopsies showed similar levels of activity to those in the duodenum of pigs. Similarly, maltase levels in rats were equivalent to those in mice in the proximal intestinal region. The latter (small mammals) showed 10 times more maltase activity than humans and pigs (large mammals); that could be modified depending on the nature of food intake.

Results in this chapter demonstrate that maltase activity, a BBM digestive enzyme, is higher in the diabetic intestine by 2.1 fold than in the controls. *SGLT1* mRNA expression was increased by 2.7-fold in the duodenum of diabetic patients compared to that in control subjects. SGLT1 protein expression was immunodetected on the BBM of the enterocytes along the entire villus length, having similar pattern in the duodenum of both diabetic and non-diabetic humans, with no expression detected in the crypts. This expression was relatively stronger on the BBM of the enterocytes lining the villi in the diabetic intestine. However, there were difficulties immunoblotting SGLT1 protein that could be due to protein degradation in some of the prepared PNMF. The morphological analysis by haematoxylin and eosin staining showed good integrity of the mucosal layer with an intact BBM and absence of submucosal and muscularis externa but not consisting the deeper layers of the gut wall. Unfortunately, morphometric measurements could not be analysed due to the shortage of human duodenal samples and the few villi in the tissue sections.

In this study, it was also aimed to estimate maltase activity and SGLT1 protein abundance in the same post-nuclear membrane fractions (PNMF) isolated from duodenal biopsies of non-diabetic controls and patients with type 2 diabetes mellitus. By immunoblotting, a single band of 75 kDa, corresponding to SGLT1 protein, was detected only in some PNMFs samples. Unfortunately, other immunoblotting experiments failed to detect any bands in the PNMF samples. It seems that the SGLT1 protein was degraded in those samples, and due to the shortage of human samples, this investigation could not be repeated.

However, work was done in our laboratory (using PNMF and BBMV) and reported that the abundance of SGLT1 protein is significantly higher by 3.3-fold and 4.3-fold in the PNMF and the BBMV, respectively, isolated from the duodenal biopsies of diabetic patients compared with that isolated from control subjects (Dyer *et al.*, 2002b). Previous investigations in this laboratory also revealed that the estimated abundance of the structural proteins villin and beta-actin were increased by 2-fold in the intestine of diabetic patients compared to that of controls. Other BBM proteins like sucrase and lactase were also enhanced by 1.5- to 2-fold in the diabetic intestine, which is similar to the fold increase in maltase observed in this

study. The increase in monosaccharide transporters proteins, SGLT1 and GLUT5, is greater by two fold than the increase in the structural proteins and disaccharidase (Dyer *et al.*, 2002b). The qRT-PCR findings that *SGLT1* mRNA expression was increased in the diabetic intestine compared to that in non-diabetic controls were similar to that observed previously in our laboratory by northern blot analysis (Dyer *et al.*, 2002b).

It is known that enterocytes maturate during the migration to the villus tip (Thomson and Wild, 1997). Subsequently, they express the functional SGLT1 protein on their brush-border membrane. It has been published, using microdensitometric analysis of [^{3}H] phlorizin binding, that diabetes lead to increase in the transporter density by 10-fold in enterocytes during early stages of their migration (Fedorak *et al.*, 1991). Diabetes also promotes early cellular induction of the SGLT1 gene in crypt cells and enhances *SGLT1* mRNA stability and protein trafficking from the Golgi compartment leading to increased numbers of SGLT1 protein in each enterocytes (Burant *et al.*, 1994). Furthermore, the recruitment of additional sugar carriers on the BBM probably in the midvillus-to-crypt region, allowing glucose transport across the BBM in enterocytes that do not normally transport glucose (Fedorak *et al.*, 1987, Burant *et al.*, 1994, Fedorak *et al.*, 1989).

Those findings support to data presented here to suggest that the stimulated intestinal capacity to absorb monosaccharides in the diabetic human is caused by a combination of 1) the diabetic-induced tissue hypertrophy expands the absorptive surface area, this provides a greater number of enterocytes along the villus supporting SGLT1 expression, 2) a specific enhancement in the activity and expression of glucose transporters, SGLT1, per enterocyte, 3) diabetes promotes earlier expression of SGLT1 on the BBM of relatively premature enterocytes.

However, the molecular basis of increased intestinal SGLT1 expression in diabetes is not well defined. Fortunately, our laboratory has carried out extensive studies on the pathway regulating expression of intestinal SGLT1. Our hypothesis is that enhanced expression of SGLT1 observed in the intestine of diabetes might be due to dysregulation of the pathways underlying regulation of SGLT1. To this end, this possibility was examined in the following chapter (Chapter 6).

Chapter 6

The molecular basis underlying the enhanced expression of SGLT1 in the diabetic intestine

Introduction

The main route for glucose (and galactose) transport from the intestinal lumen into the enterocyte is SGLT1. Thus, the regulation of this protein is pivotal for provision of glucose to the body and avoidance of intestinal malabsorption. Work in various laboratories has shown that in the majority of species, monosaccharides in the intestinal lumen directly regulate SGLT1 expression (Ferraris and Diamond, 1993, Shirazi-Beechey *et al.*, 1991, Dyer *et al.*, 1997c), and that metabolism of monosaccharides is not required for sugar-induced SGLT1 upregulation (Shirazi-Beechey *et al.*, 1991, Solberg and Diamond, 1987). Furthermore, introduction of membrane-impermeable glucose analogues to the lumen of the intestine also stimulates SGLT1 expression (Dyer *et al.*, 2003a), arguing that there is a glucose sensor on the gut luminal membrane responsible for detecting luminal sugars, to modulate SGLT1 expression (glucose-induced SGLT1 expression).

Further work, using *in vitro* models suggested that sugar mediated up-regulation of SGLT1 is likely to involve a G-protein-coupled second messenger pathway (Dyer *et al.*, 2003a). The discovery that the lingual epithelium sweet taste receptor, a G-protein coupled receptor, is expressed in the intestinal enteroendocrine cells stimulated research to identify if this receptor may act as the intestinal glucose sensor (Dyer *et al.*, 2005). This receptor consists of two subunits taste family 1 receptor 2 and 3 (T1R2-T1R3), and associated with the transducer G-protein gustducin, which are coexpressed in endocrine cells in a variety of species (Margolskee *et al.*, 2007, Batchelor *et al.*, 2011, Moran *et al.*, 2010).

Studies using mice in which the genes for either α-gustducin or T1R3 were deleted (knockout mice) provided convincing evidence for the involvement of the gut-expressed glucose receptor and gustducin in intestinal sweet transduction (Margolskee *et al.*, 2007, Dyer *et al.*, 2007). Abolishing sweet taste transduction in mice by deletion of either α-gustducin or T1R3 prevented the dietary monosaccharide-induced up-regulation of SGLT1 expression observed with wild type mice (Margolskee *et al.*, 2007). In wild type mice maintained on a high-carbohydrate diet (70% sucrose), there was a 2-fold increase in *SGLT1* mRNA, protein abundance and initial rate of Na^+-dependent glucose transport, compared with mice fed an isocaloric low-carbohydrate diet (1.9% sucrose). T1R3-and gustducin-knockout mice, however, showed no change in *SGLT1* mRNA protein and function on either diet (Margolskee *et al.*, 2007). Thus, knocking out either α-gustducin or T1R3 eliminated the ability of the mouse intestine to increase SGLT1 expression in response to increased dietary carbohydrates.

The expression of SGLT1 in both types of knockout mice was identical to that in wild type animals on the low-carbohydrate diet, suggesting that there is a constitutive intestinal SGLT1, independent of luminal sugar sensing by T1R3 and

gustducin that maintains basal SGLT1 expression levels, and an inducible pathway, dependent on T1R3 and gustducin that regulates SGLT1 expression in response to luminal sugars. The data indicated that the intestinal capacity to absorb glucose is maintained via basal levels of SGLT1, although, this capacity becomes limiting when luminal carbohydrate exceeds a certain level.

Further experimental data suggested that T1R2-T1R3, expressed on the luminal membrane of villus endocrine cells, senses luminal glucose concentration. Luminal glucose above a threshold level activates a signaling pathway in endocrine cells involving T1R2-T1R3, gustducin and other signaling elements resulting in the secretion of the gut hormone glucagon like peptide 2 (GLP-2) (Margolskee *et al.*, 2007). GLP-2 binding to its receptor residing on enteric neurons elicits an action potential (Bjerknes and Cheng, 2001), evoking the release of the neuropeptides vasoactive intestinal peptide (VIP) or pituitary adenylate cyclase-activating polypeptide (PACAP). Binding of VIP /PACAP to its receptor VPAC1 expressed on the basolateral membrane of absorptive enterocytes enhances the intracellular concentration of cyclic adenosine monophosphate (cAMP) leading to an increase in half-life of SGLT1 mRNA and enhancement of functional SGLT1 protein in the brush border membrane of absorptive enterocytes (Shirazi-Beechey *et al.*, 2011a, Sternini *et al.*, 2008, Sharp and Debnam, 1994). Other neuropeptides like substance P (SP) and calcitonin gene-related peptide (CGRP) had no effect on SGLT1 up-regulation indicating that the effect is specific to VIP/PACAP. This pathway is depicted in the following figure:

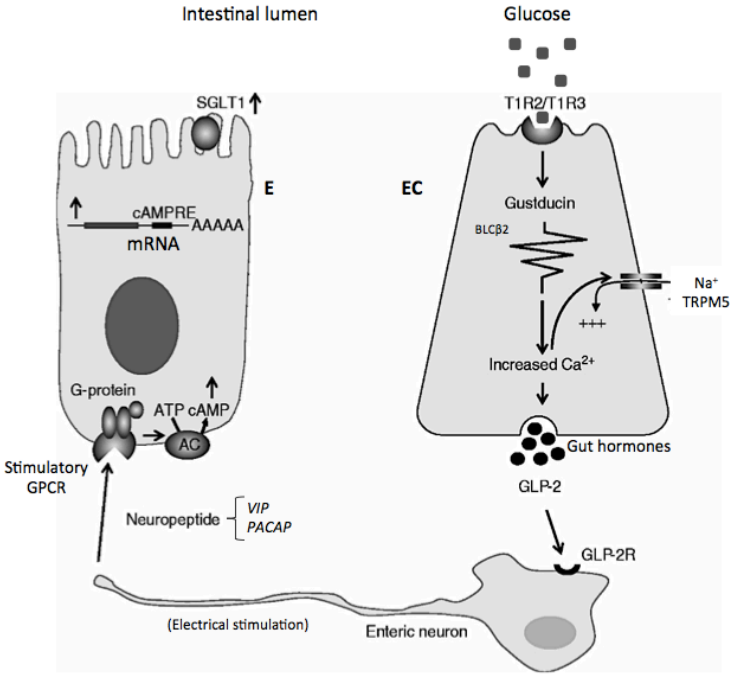

Taken with permission from Shirazi-Beechey et al. Proceedings of Nutrition Society 2011, 79: 185-193 (Shirazi-Beechey et al., 2011a). EC: enteroendocrine cell; E: enterocyte.

However, it has been reported (Dyer *et al.*, 2002) that enhanced expression of SGLT1 in the intestine of diabetic humans is independent of changes in concentrations of glucose in the lumen of the intestine. The expression of SGLT1 remained high in the intestine of human diabetics maintained on either diabetic (low carbohydrate) or normal (high carbohydrate) diets. Furthermore hypoglycemic drugs, sulfonylureas and biguanides did not affect the increased levels of monosaccharide transporters in the intestine of diabetic patients. Sulfonylurea drugs, gliclazide or glibenclamide, act mainly by augmenting insulin secretion. While, the biguanide drug metformin exerts its effect mainly by decreasing gluconeogenesis and by increasing the peripheral utilization of glucose, according to the British National Formulary. This suggests that the enhanced expression of intestinal monosaccharide transporters is independent of any changes in blood glucose or insulin levels. It was hypothesised that enhanced expression of SGLT1 in the intestine of diabetics is due to deregulation of pathway(s) controlling SGLT1 expression (Dyer *et al.*, 2002).

Aims:

In this chapter, the main objective was an attempt in identifying the molecular basis underlying enhanced SGLT1 expression in the diabetic intestine. To this end, potential changes in key components of the pathway underling SGLT1 regulation were determined.

These included assessing levels of:

1. Expression of glucose receptor (sensor) T1R2-T1R3
2. Proglucagon gene encoding GLP-2
3. Secretion of GLP-2 hormone
4. Expression of GLP-2 receptor
5. Expression of neuropeptides VIP and PACAP

RESULTS

6.1. Expression of glucose receptor subunits, T1R2 and T1R3, in the small intestine

Expression of T1R2-T1R3 was determined by immunohistochemistry and qRT-PCR using: i) duodenal biopsies obtained from non-diabetic and diabetic humans ii) intestinal tissue removed from normal and diabetic rats.

6.1.1. Immunohistochemical detection and localization of T1R2 protein in the duodenum of human:

Immunohistochemical studies revealed that T1R2 protein is expressed in the enteroendocrine cells (EEC), which are few scattered cells amongst the absorptive enterocytes. Figure 6.1 shows the flask-shaped EEC stained with T1R2 antibodies in the duodenal biopsies of non-diabetic and diabetic humans. Omission of the primary antibody confirmed specific antibody binding.

***Figure 6.1*: Immunohistochemical detection and localization of T1R2 protein in human intestine**

a) *20X magnified* **b)** *40X magnified*

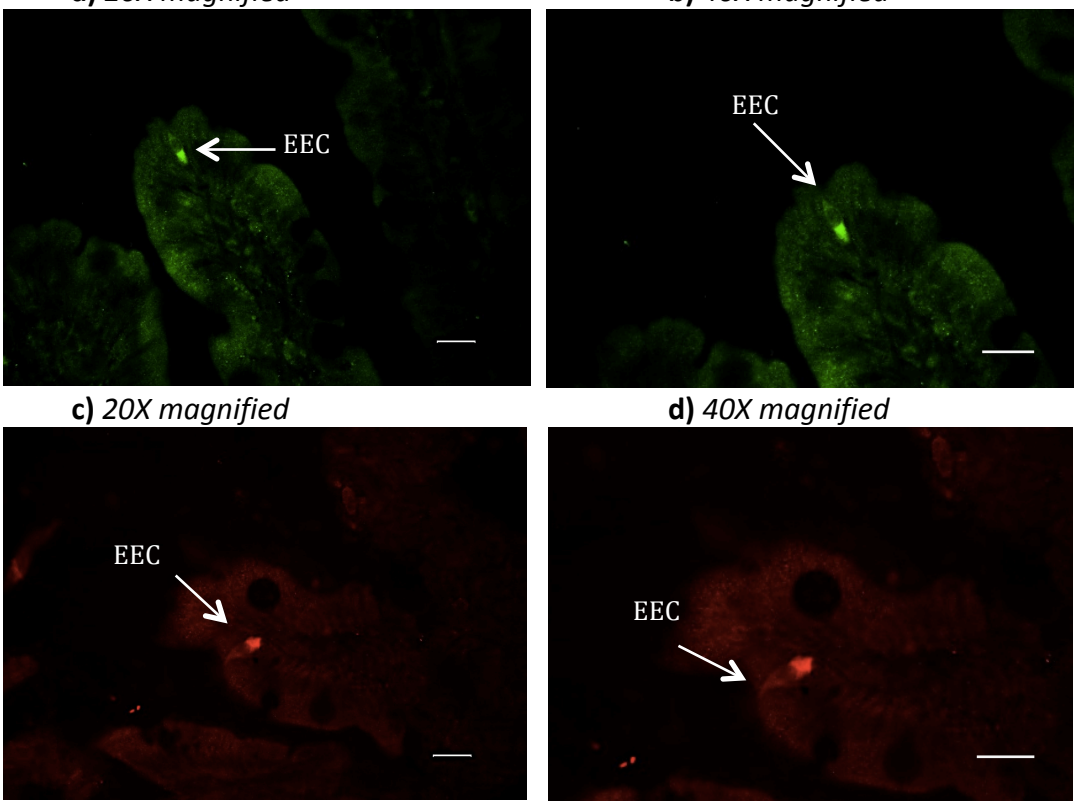

c) *20X magnified* **d)** *40X magnified*

Representative immunostaining images shows that T1R2 protein expression is detected in a few enteroendocrine cells (EEC) in the duodenum of non-diabetic (a and b) and diabetic humans (c and d). Scale bar is 10 µm.

6.1.2. Immunohistochemical detection and localization of T1R2 protein in the intestine of rat:

Immunohistochemistry demonstrated a similar expression pattern for T1R2 being located in enteroendocrine cells, as shown in the human intestine. Furthermore, there were no changes in the number of endocrine cells expressing T1R2 in diabetic rats compared to controls. Figure 6.2 shows the immunohistochemical detection of T1R2 protein in the intestine of a control rat. No satisfactory results were obtained using the antibody to T1R3; therefore T1R3 expression at mRNA level was determined.

Figure 6.2: Immunohistochemical detection and localization of T1R2 protein in rat intestine

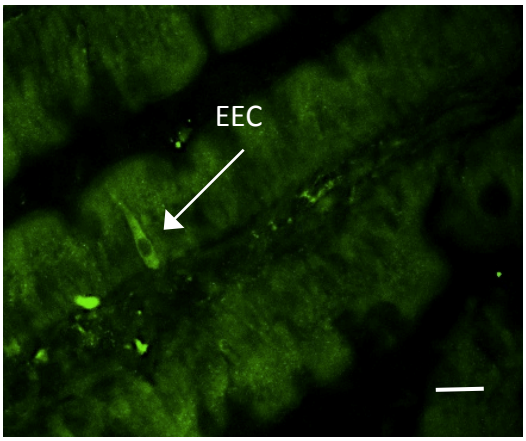

Representative immunofluorescence image of intestinal tissue from a control rat shows that the T1R2 protein is expressed in enteroendocrine cells (EEC).
The image is 40X magnified. Scale bar is 10 µm.

6.1.3. Expression of *T1R3* mRNA in intestinal regions of control and diabetic rats

Expression of *T1R3* was determined in the intestine of control and diabetic rats using quantitative PCR. Figure 6.3 shows no significant changes in the relative abundance of *T1R3* mRNA, normalized to the *β-actin* gene, in any region of the small intestine between control and diabetic rats.

***Figure 6.3*: Expression of T1R3 mRNA levels in the intestine of control and diabetic rats determined by qRT-PCR.**

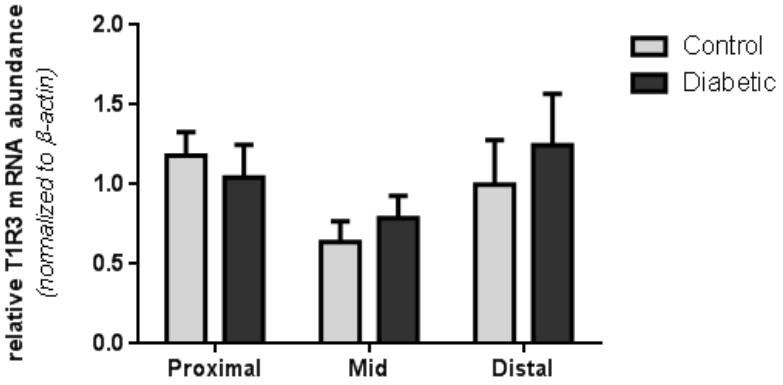

Histogram shows expression levels of the intestinal glucose receptor subunit T1R3 mRNA along the intestine of control and diabetic rats. Results are means ± S.E.M. (n = 6), unpaired t-test.

Unfortunately, expression of *T1R2* mRNA in the intestine of control and diabetics rat could not be investigated by qRT-PCR because all primer pairs for rat T1R2 tested failed to amplify *T1R2* mRNA. The primers were tested with 25, 50 and 250 ng of cDNA generated from rat RNA samples but all without success. This also limited the detection of *T1R2* mRNA in human tissue due to tissue shortage.

6.2. Expression of proglucagon gene mRNA encoding for GLP-2

Proglucagon protein (coded by *GCG* gene), is a precursor of glucagon that gives rise to GLP-1 and GLP-2, gut hormones secreted by the enteroendocrine L-cells (Brubaker, 1991, Bryant and Bloom, 1979). Using qRT-PCR reactions, as shown in figure 6.4, the relative abundance of *GCG* mRNA, normalized to the *β-actin* gene, was determined. Expression levels increased with distal progression through the small intestine for both control and diabetic rats. There was no change in the expression of proglucagon gene in any intestinal region between the control and the diabetic rats.

Figure 6.4: Expression analysis of glucagon gene (GCG) mRNA levels in control and diabetic rats determined by qRT-PCR.

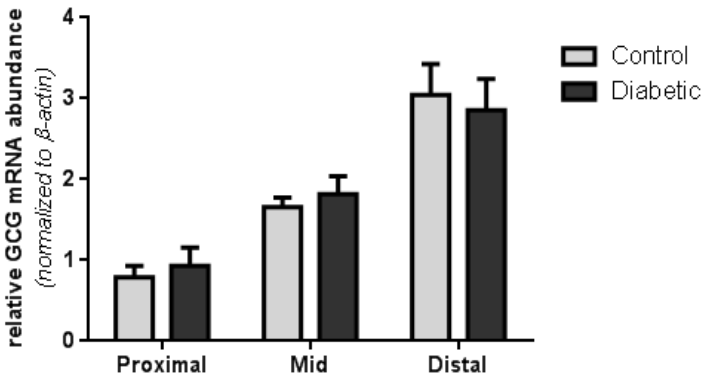

Graph showing the relative abundance of glucagon gene (GCG) mRNA, normalized to β-actin gene, in the intestinal regions of control and diabetic rats. Results are means ± S.E.M. (n = 6), unpaired t-test.

6.3. Expression of intestinal GLP-2 hormone and GLP-2 receptor (GLP-2R)

6.3.1. Intestinal GLP-2 hormone secretion:

Table 6.1 and figure 6.5 demonstrate that in control rats, exposure of intestinal tissue to high (10%) glucose concentrations increased GLP-2 secretion by 1.4 and 1.6 fold in the mid and distal intestine compared to low glucose concentrations. By contrast, the proximal intestine did not secrete more GLP-2 in response to high glucose concentration.

However, diabetic rats showed higher intestinal GLP-2 secretion compared to controls, which was not affected greatly by glucose concentration.

In response to low glucose (LG) concentration, GLP-2 release in the diabetic intestine was higher than that in controls by 1.2, 1.6 and 1.9 fold in the proximal, mid and distal regions, respectively.

In response to high glucose (HG) concentration, GLP-2 release in the intestine of diabetic rats was higher than that in controls by 1.2, 1.4 and 1.4 fold in the proximal, mid and distal intestine, respectively.

Table 6.1: Measurement of GLP-2 release in response to intestinal exposure to low and high glucose concentrations in control and diabetic rats

	Low Glucose (LG)		**High Glucose (HG)**	
	Control	**Diabetic**	**Control**	**Diabetic**
Proximal	305.5 ± 21.75	375.3 ± 16.62 *(P=0.013)*	308.0 ± 24.28	393.4 ± 16.53 *(P= 0.027)*
Mid	241.0 ± 26.74	405.8 ± 14.88 *(P=0.001)*	328.2 ± 13.07	460.4 ± 9.38 *(P=0.001)*
Distal	290.4 ± 37.46	543.7 ± 38.58 *(P=0.001)*	453.1 ± 36.49	660.6 ± 15.49 *(P=0.006)*

Values are in pmol/L. Results are expressed as mean ± SEM (n = 4), unpaired t-test.

***Figure 6.5*: Intestinal GLP-2 secretion in the intestine of control and diabetic rats in response to variable glucose concentrations**

a)

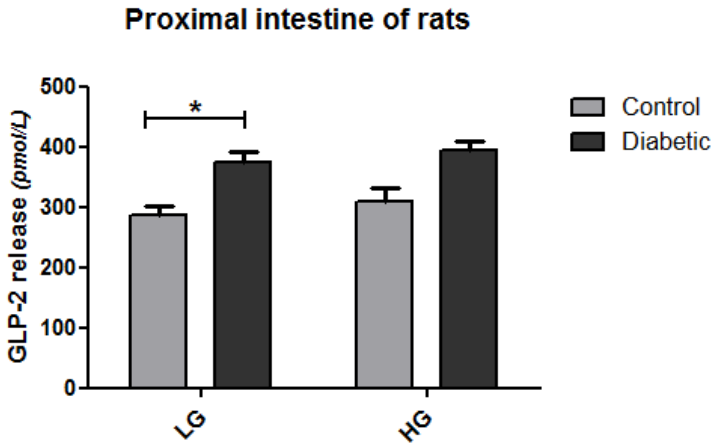

b)

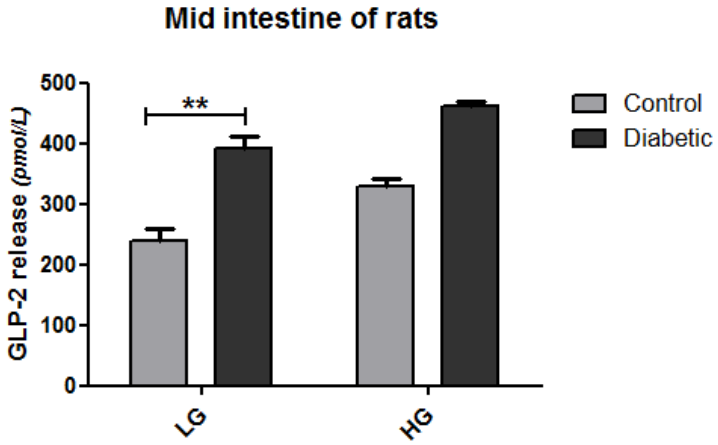

c)

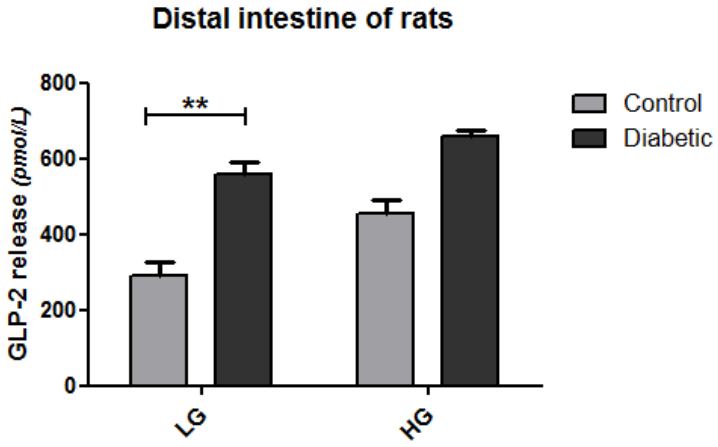

*Graphs show that intestinal exposure to low glucose (LG) and high glucose (HG) concentrations evoke more GLP-2 release in the intestinal regions of diabetic rats compared to those of control rats. GLP-2 was measured in pmol/L and results are means ± S.E.M. (n = 4); *P < 0.05 and **P < 0.01, unpaired t-test.*

6.3.2. Expression analysis of GLP-2 receptor mRNA:

GLP-2 receptor (GLP-2 R) is expressed on the afferent enteric neurones in the submucosal layer of the gut. As a result of substrate-receptor binding, action potentials are generated in the afferent fibres of the enteric nervous system (Drucker, 2002, Shirazi-Beechey *et al.*, 2011a).

Using qRT-PCR, figure 6.6 demonstrates that mRNA expression of GLP-2R in the diabetic intestine is significantly lower by 1.5 fold (*P=0.012)* and 1.4 fold (*P=0.032*) in the proximal and mid regions, respectively, compared to that of controls. However, no expression changes were found in the distal intestine.

Figure 6.6: Expression analysis of GLP-2 receptor mRNA levels in control and diabetic rats determined by qRT-PCR

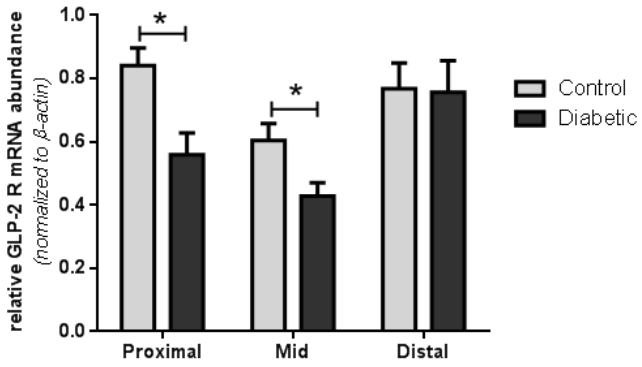

The graph shows the relative abundance of GLP-2 receptor mRNA along the intestinal length of control and diabetic rats.
*Results are means ± S.E.M. (n = 6); *P < 0.05, unpaired t-test.*

6.4. Expression analysis of the neuropeptide VIP in human and rat intestine

VIP (vasoactive intestinal peptide) is one of the neuropeptides that are released from secretory granules at the enteric nerve endings, in response to neuronal activation, for signal transmission to enterocytes. Subsequently, VIP peptides bind to their receptors VPAC1 and VPAC2, which are G-protein coupled receptors, situated on the BLM of enterocytes to transmit signals to the regulatory pathway underlying SGLT1 expression (Shirazi-Beechey *et al.*, 2011b).

6.4.1. Expression of *VIP* mRNA in human duodenum:

Quantitative RT-PCR analysis showed that *VIP* mRNA expression, normalized to *β-actin* gene, was significantly increased by 2.3 fold in the duodenum of diabetic patients compared to non-diabetic individuals (0.054 ± 0.007 *vs* 0.023 ± 0.006, *P = 0.029*), as seen in figure 6.7.

***Figure 6.7*: Analysis of VIP mRNA expression in non-diabetic controls and diabetic patients**

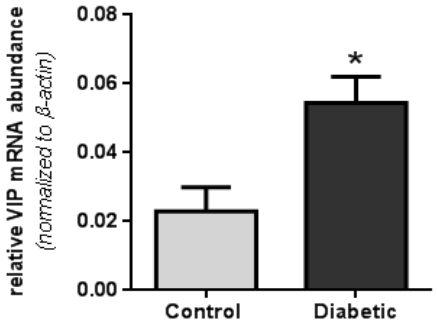

The graph shows the relative abundance of neuropeptide VIP mRNA in the duodenum of control and diabetic humans.
*Results are means ± S.E.M. (n = 4); *P < 0.05, unpaired t-test.*

6.4.2. Expression of *VIP* mRNA in rat intestine:

Using qRT-PCR, the mRNA expression of *VIP*, normalized to *β-actin* gene, is displayed in figure 6.8. In the proximal, mid and distal intestine, *VIP* mRNA abundance was significantly higher by 2.1 fold (0.145 ± 0.02 *vs* 0.07 ± 0.008, *P = 0.03*), 2.5 fold (0.24 ± 0.03 *vs* 0.097 ± 0.01, *P = 0.015*) and 2.3 fold (0.26 ± 0.04 *vs* 0.118 ± 0.007, *P = 0.016*), respectively, in the intestine of diabetic rats compared to that of controls.

***Figure 6.8*: Expression analysis of VIP mRNA levels in the intestine of control and diabetic rats determined by qRT-PCR**

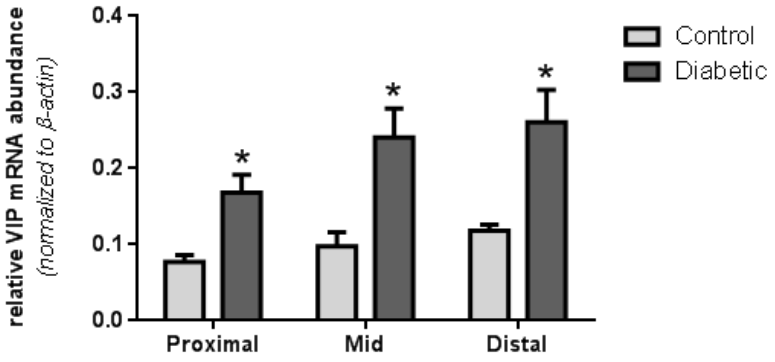

*The relative abundance of VIP mRNA along the intestine of control and diabetic rats. Results are means ± S.E.M. (n = 6); *P < 0.05, unpaired t-test.*

6.4.3. Immunohistochemical expression of VIP protein in rat intestine:

Immunohistochemical results revealed that VIP protein expression is detected in the lamina propria of villus and the nerve fibres of submucosal and myenteric plexuses, as seen in figure 6.9. Expression levels were higher in the intestine of diabetic rats compared to non-diabetic control rats.

***Figure 6.9*: Immunohistochemical detection and localization of VIP protein in rat intestine**

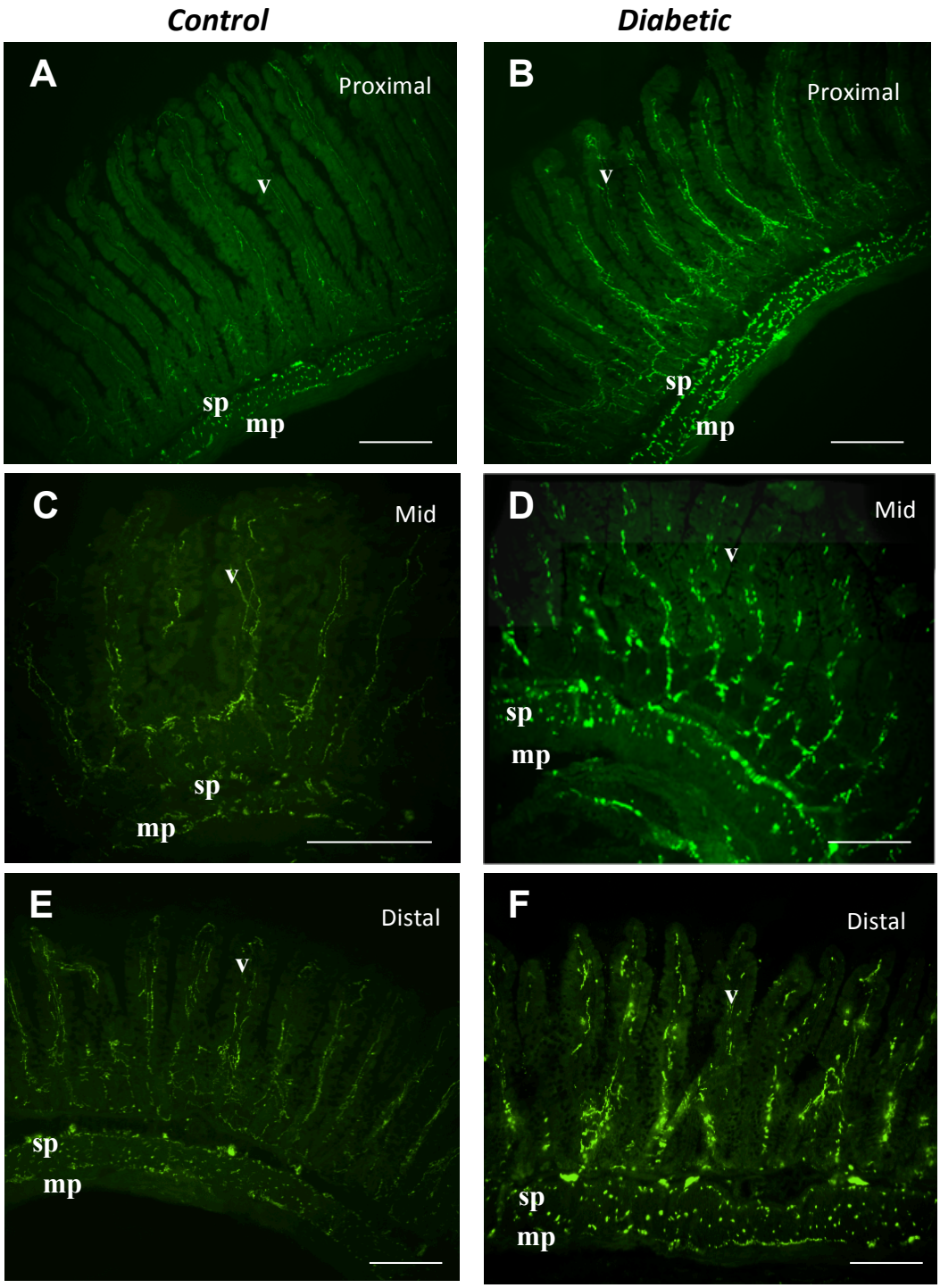

Representative immunofluorescence images show VIP expression in the proximal, mid and distal intestine of control (A, C and E) and diabetic rats (B, D and F). VIP protein expression is detected in the lamina propria of villus (v), submucosal plexus (sp) and myenteric plexus (mp) and axonal projections spreading from submucosal plexus into the villi. Note; Axonal projections run parallel and in close proximity to the basolateral membrane of enterocytes. Scale bar is 100 µm.

6.5. Expression of the neuropeptide *PACAP* mRNA

Pituitary adenylate cyclase-activating polypeptide (PACAP) is another neurotransmitter released from enteric nerve endings. PACAP as well as VIP bind to the same receptor VPAC1 and VPAC2 as well as to additional PAC1 receptors on enterocytes. PACAP potently stimulates adenylate cyclase leading to 'cAMP formation' in target cells beside its neurotransmitter function (Heinemann and Holzer, 1999). qRT-PCR analysis showed a significant increase in *PACAP* mRNA expression in the diabetic intestine compared to controls, as displayed in figure 6.10. *PACAP* mRNA expression was higher by 2.5 fold (0.39 ± 0.07 *vs* 0.157 ± 0.052, *P = 0.033*), 2.6 fold (0.44 ± 0.05 *vs* 0.17 ± 0.06, *P = 0.03*) and 2.1 fold (0.26 ± 0.02 *vs* 0.128 ± 0.03, *P = 0.015*), in the proximal, mid and distal intestine, respectively.

Figure 6.10: ***Expression analysis of PACAP mRNA levels in the intestine of control and diabetic rats determined by qRT-PCR.***

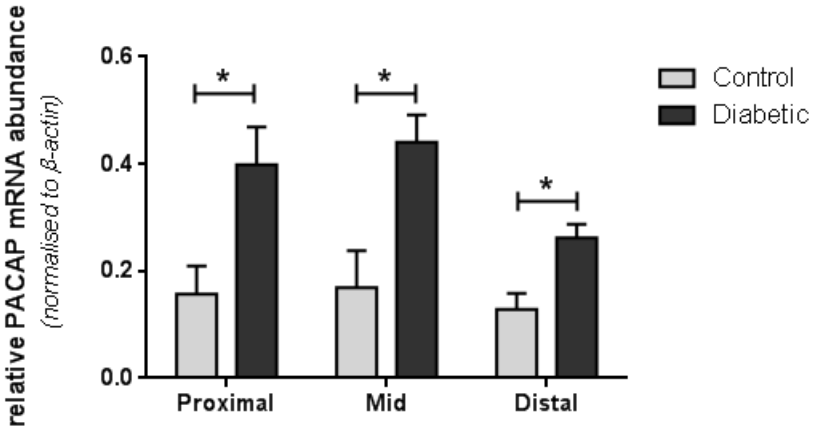

The relative abundance of neuropeptide PACAP mRNA levels along the intestinal length of control and diabetic rats.
*Results are means ± S.E.M. (n = 6); *P < 0.05, unpaired t-test.*

6.6. Expression analysis of the neuropeptide substance P in rat intestine

6.6.1. Expression of the substance P precursor, *TAC1* gene mRNA:

Work in our laboratory has shown that exposure of absorptive enterocytes to VIP and PACAP, but not substance P (SP), enhances SGLT1 expression. Therefore, potential changes in SP expression in the diabetic intestine were assessed. SP acts via a stimulatory GPCR to increase accumulation of cAMP, because the promoter of substance P receptor, NK1R, contains regions that are sensitive to cAMP affecting its intracellular level. However, SP protein expression in intestinal tissue of the diabetic rat was even lower than controls (Belai *et al.*, 1985).

As shown in figure 6.11, mRNA expression of the *TAC1* gene, encoding substance P, was lower in the intestine of diabetic rats compared to that of controls.

***Figure 6.11*: Expression analysis of TAC1 mRNA levels in the intestine of control and diabetic rats determined by q RT-PCR.**

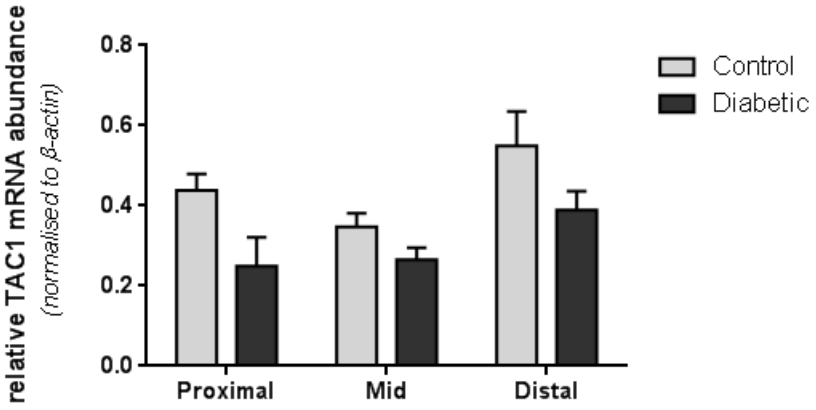

Expression analysis of the neuropeptide precursor TAC1 mRNA levels along the intestinal length of control and diabetic rats.
Results are means ± S.E.M. (n = 6); unpaired t-test.

6.6.2. Immunohistochemical expression of substance P protein:

Results of immunohistochemistry are shown in figure 6.12. It appears that substance P protein expression in enteric neurons and axonal projections in the intestine of diabetic rats was lower than that in of control rats.

***Figure 6.12**: Immunohistochemical localization of substance P protein in rat intestine*

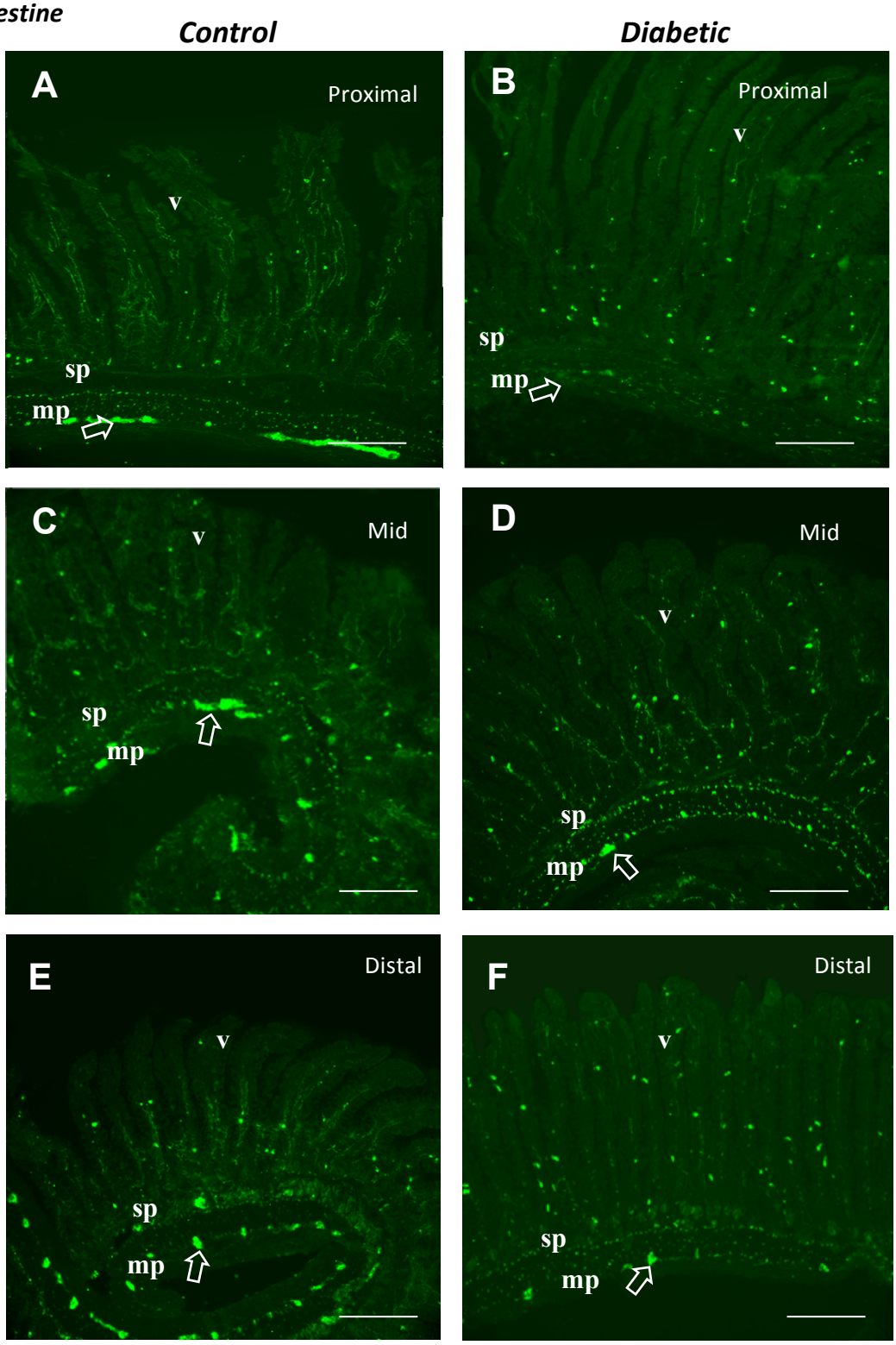

Representative images show the immunostaining of substance P in the intestinal regions of control (A, C and E) and diabetic rats (B, D and F). The fluorescent intensity of SP was lower in myenteric plexus (mp) of the proximal, mid and distal intestine of diabetic rats (opened arrows) compared to the control rats. (v: villi and sp: submucosal plexus); scale bar is 100 µm.

DISCUSSION

In intestinal glucose absorption, SGLT1 is regulated in response to dietary carbohydrates (Dyer *et al.*, 1997a). This process is mediated by sugar activation of intestinal glucose sensors (T1R2-T1R3) in endocrine cells, evoking neuroparacrine signaling mechanism enhancing SGLT1 mRNA stability leading to up-regulation of SGLT1 protein in neighbouring enterocytes (Shirazi-Beechey *et al.*, 2011b, Daly *et al.*, 2012, Dyer *et al.*, 2007, Dyer *et al.*, 2003a, Dyer *et al.*, 2003b).

However, it has been documented that the gut capacity to absorb glucose is enhanced in the intestine of diabetic humans due to increased activity and expression of SGLT1 (Dyer *et al.*, 2002). Similarly, diabetic rats showed increased glucose uptake rates by SGLT1 corresponding to increased *SGLT1* mRNA and protein abundance (Dyer *et al.*, 1997b, Burant *et al.*, 1994).

This enhanced expression of SGLT1 in the diabetic intestine is not dependent on luminal sugars, blood glucose nor insulin levels. It is also not regulated by low or high carbohydrate diets, oral hypoglycemic drugs or insulin injections. Indicating that the mechanism controlling SGLT1 expression is deregulated, leading to enhanced glucose absorption in the diabetic intestine.

Work in this chapter assessed the expression of some key components participating in the pathway underlying SGLT1 regulation in intestinal tissues of diabetics and controls. Due to the shortage of human tissue, the majority of studies were carried out using rat intestine. Results are summarized in the table below:

	Proximal ***Diabetic vs. Control***	***Mid*** ***Diabetic vs. Control***	***Distal*** ***Diabetic vs. Control***
T1R2/T1R3			
Human (protein expression)	*No change*	-	-
Rat (Protein & mRNA expression)	*No change*	*No change*	*No change*
GCG mRNA expression in rat (encoding GLP-2)	*No change*	*No change*	*No change*
GLP-2 secretion in rat intestine			
In response to low glucose	*X 1.2 fold*	*X 1.6 fold*	*X 1.9 fold*
In response to high glucose	*X 1.2 fold*	*X 1.4 fold*	*X 1.4 fold*
GLP-2 receptor mRNA in rat	*Lower*	*Lower*	*No change*
VIP			
Human (mRNA expression)	*X 2.3 fold*	-	-
Rat (Protein expression)	*Higher*	*Higher*	*Higher*
(mRNA expression)	*X 2.1 fold*	*X 2.5 fold*	*X 2.3 fold*
PACAP mRNA in rat	*X 2.5 fold*	*X 2.6 fold*	*X 2.1 fold*
SP in rat			
Protein expression	*Lower*	*Lower*	*Lower*
mRNA expression	*Lower*	*Lower*	*Lower*

Interestingly, it was observed that in the intestine of diabetic rats, GLP-2 is secreted significantly more than that in controls in response to low glucose (and to a lesser extent high glucose) concentrations, indicating that the diabetic intestine secretes more GLP-2 independent of luminal glucose levels. As expected, proglucagon gene mRNA and its product GLP-2 hormone have higher levels, in the distal intestine of both control and diabetic rats, as the number of L-cells increase distally (Larsson *et al.*, 1975).

Work from other laboratories has shown that intestinal mucosal growth in diabetic rats is associated with elevated GLP-2 concentrations in both plasma and ileal tissue (Fischer *et al.*, 1997). However, the level of GLP-2 secretion by diabetic humans is controversial. GLP-2 hormone, besides its intestinal trophic effect (Drucker *et al.*, 1996), is known to increase SGLT1 expression (Ramsanahie *et al.*, 2003, Cheeseman, 1997, Sangild *et al.*, 2006). mRNA levels of GLP-2 receptors, which are located on afferent enteric neurons (Baldassano *et al.*, 2009, Bjerknes and Cheng, 2001), are either decreased or not changed in the intestine of diabetic rats compared to controls. However, several studies strongly support the idea that the enteric nervous system is involved in the up-regulation of SGLT1 expression (Sharp *et al.*, 1996, Debnam, 1985). Unpublished work from our laboratory, using murine intestine, has shown that electric field stimulation of enteric neurons leads to enhanced SGLT1 expression; which was inhibited by the neuronal sodium-channel blocker tetrodotoxin TTX.

It is known that diabetic neuropathy, resulting from excess blood sugar levels injuring the walls of the capillaries that nourish nerves, affects the gut-brain axis and enteric neurons in the diabetic intestine and hence, nerves do not conduct signals normally. As a result, the generated action potentials stimulate nerve endings to release more of the neuropeptides VIP and PACAP as evidenced by significantly higher mRNA expression in the intestine of diabetic rats for VIP/PACAP and humans for VIP. This was consistent with higher expression of VIP protein in the intestine of diabetic rats using immunohistochemistry. However, expression of substance P, which has been shown not to participate in SGLT1 regulatory pathway (unpublished work from our laboratory), was not changed in the diabetic intestine.

Work in our laboratory has shown that *SGLT1* mRNA abundance is increased in response to VIP and PACAP in a dose-dependent manner in the intestinal epithelial cell line, Caco-2 (unpublished data), while substance P, CGRP (Calcitonin gene-related peptide) and CRH (Corticotropin-releasing hormone) neuropeptides had no effect on SGLT1 expression. Other workers have shown that the diabetic intestine with enhanced SGLT1 expression has increased VIP release and express higher VIP in enteric neurons (Belai *et al.*, 1985).

The data obtained in this chapter suggests that secretion of the neuropeptides VIP and PACAP brought about by diabetic neuropathy and possibly increased secretion of GLP-2 are involved in the deregulation of the pathway controlling SGLT1 expression and enhanced intestinal glucose transport. This is depicted in the following diagrams in diabetic rat and human intestine:

Diabetic rat intestine

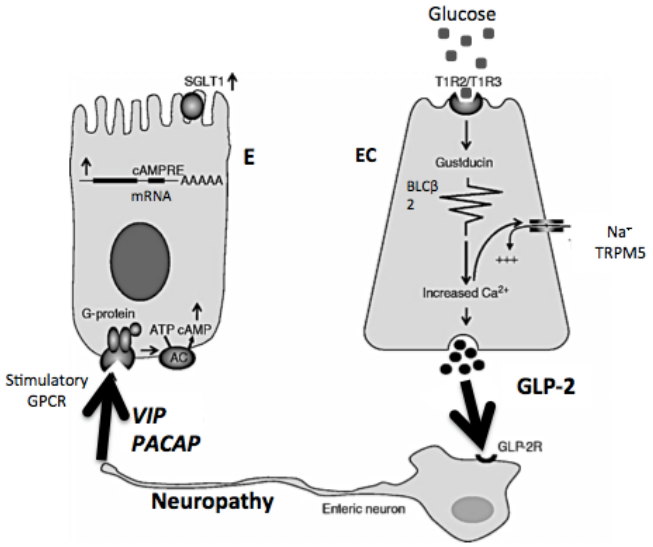

Diabetic human intestine

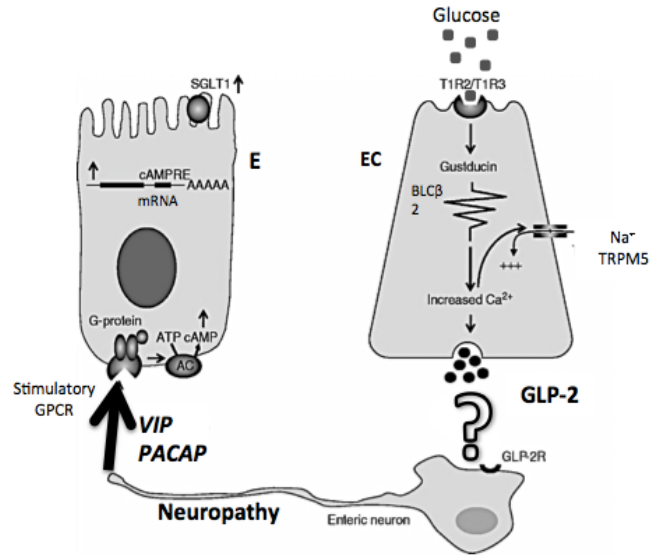

Adapted with permission from Shirazi-Beechey et al. Proceedings of Nutrition Society 2011, 79: 185-193 (Shirazi-Beechey et al., 2011a). EC: enteroendocrine cell; E: enterocyte.

Chapter 7

General Discussion

Summary of the work presented in the thesis:

Chapter 3:

The technical skills needed for the work carried out in this thesis were developed using available intestinal tissues. Membrane vesicles were successfully isolated from frozen intestinal tissues of mice and pigs. The enrichment and recovery values indicated that the membrane vesicles originated from the brush border membrane (BBM). In mouse, sucrase and maltase activity was higher in proximal than distal intestine. While lactase, as expected, showed very low activity in the intestine of adult mice because milk consumption is reduced in adulthood. In contrast, in suckling pigs lactase activity was similar to maltase and more than sucrase. This reflects the adaptive response of the intestinal digestive capacity to be prepared for the transition from milk feeding to solid food in the last days of the suckling period. Generally, in mice and pigs, maltase showed significantly higher activity levels than sucrase in all intestinal regions. These digestive enzymes have the lowest activity in the distal ileum as carbohydrates are mainly hydrolysed in the proximal part of the intestine and very little reaches the distal part.

In the intestine of mouse, SGLT1 protein was expressed on the BBM of enterocytes along the entire villus length, with negligible expression in crypts. This pattern of expression has been shown in the intestine of other mammalian species. SGLT1 protein was detected as a 73-75 kDa immunoreactive band in BBMVs isolated from intestinal tissue of suckling and weaned pigs. In suckling pigs, SGLT1 protein abundance in duodenum is similar to that in jejunum but more than in ileum.

Conclusion:

Disaccharidases activity is modulated by diet and developmental stage, and the expression of SGLT1 protein indicates that all villus enterocytes are capable of absorbing glucose.

Chapter 4

By assessing whole body and small intestinal parameters, STZ-induced diabetic rats had body weight loss by 1.3-fold, compared to control rats. However, the small intestine of diabetic rats was increased in weigh and length by 2.7 and 1.2 fold, respectively. Moreover, villi in the intestine of diabetic rats were 1.2 fold longer than those of controls.

Generally, the activities of intestinal BBM enzymes (maltase, sucrase and alkaline phosphatase) were increased in diabetic rats compared to controls, with more significant changes in the mid and distal intestine. In the proximal, mid and distal intestine of diabetic rats, maltase activity increased by 1.1, 1.6 and 2.5 fold, respectively, and sucrose activity was higher by 1.1, 2 and 3.3 fold, respectively, compared to that in controls. However, alkaline phosphatase was significantly elevated in the diabetic intestine by 3 fold and 3.3 fold only in the mid and distal region, respectively.

SGLT1 protein was expressed on the BBM of enterocytes along the entire villus length in the proximal intestine of both control and diabetic rats. Interestingly, in the mid and distal intestine, SGLT1 expression on the BBM was limited to the upper villus region in control rats, whereas, was extended to the lower villus in diabetic rats. However, negligible SGLT1 detection was found in the crypts. This expression pattern was similar after one and five week post-diabetes indicating that diabetes promptly effect SGLT1 expression.

SGLT1 mRNA levels increased significantly by 2, 2.2 and 2.3 fold in the proximal, mid and distal intestine, respectively, in diabetic rats compared to controls. SGLT1 protein abundance was higher by 1.5, 1.4 and 2 fold in the proximal, mid and distal intestine, respectively, of diabetic rats compared to controls. SGLT1 function (D- glucose transport rate) was enhanced by 2, 3.3 and 3.5 in the BBMV isolated from the proximal, mid and distal intestine, respectively, of diabetic rats compared to controls, showing higher enhancement than increases in *SGLT1* mRNA and protein expression.

GLUT2 protein was exclusively expressed on the basolateral membrane (BLM) of enterocytes in the intestine of control and diabetic rats. Moreover, GLUT2 protein was absent in BBMV isolated from the intestine of control and diabetic rats. This confirms the exclusive role of GLUT2 in glucose transport across the BLM and that GLUT2 is not trafficked to the BBM in the diabetic intestine.

However, *GLUT2* mRNA expression was significantly elevated in the diabetic rats by 1.6, 1.8 and 2.6 fold in the proximal, mid and distal intestine, respectively, compared to that of controls, suggesting enhanced trans-cellular glucose transport from the intestinal lumen into circulation.

Conclusion:

The magnitude of changes in the villus length and the activity of BBM markers did not entirely match the enhanced expression and function of SGLT1 in the diabetic intestine. Hence, the enhanced intestinal glucose absorption in rats may be caused by a combination of:

1) Higher SGLT1 expression per enterocyte, as seen in the proximal intestine.
2) More enterocytes expressing SGLT1, possibly in the mid to lower villus, as seen in the mid and distal diabetic intestine.
3) Recruitment of additional sugar carriers, SGLT1, on the BBM of relatively premature enterocytes that do not normally transport glucose.

However, the underlying molecular basis of this enhancement is discussed in chapter 6.

Chapter 5

Maltase activity, a BBM digestive enzyme, was higher in the duodenum of diabetic patients by 2.1 fold compared to that in non-diabetic controls. *SGLT1* mRNA expression was increased by 2.7-fold in the duodenum of diabetics compared to that in non-diabetics. SGLT1 protein was expressed on the BBM of enterocytes along the entire villus length in the duodenum of both diabetic and non-diabetic individuals, with relatively stronger staining on the BBM lining the villi of the diabetic intestine. However, no expression was detected in the crypts.

Unfortunately, SGLT1 protein abundance in the duodenum of diabetics and controls could not be estimated, as there were difficulties in the immunoblotting of SGLT1 protein, which might be due to protein degradation in some samples of isolated PNMF. The morphological assessment showed good integrity of the duodenal biopsies, but the shortage of human samples and the few villi numbers in the tissue sections limited the morphometric analysis.

Previous work in our laboratory revealed that the increased abundance of glucose transporters, SGLT1, is greater by twofold than the increase in the structural proteins (villin and β-actin) and BBM disaccharidases (sucrase and lactase) in the intestine of diabetic patients compared to that of controls (Dyer *et al.*, 2002).

Conclusion:

The enhanced glucose absorption in the duodenum of diabetic humans (NIDDM) is due to:

1) More cells supporting SGLT1, due to diabetes-induced tissue hypertrophy.
2) In combination with tissue hypertrophy, a specific increase in *SGLT1* mRNA, resulting in more SGLT1 protein expression per each enterocyte.

Chapter 6

Work in this chapter assessed changes in the expression of some key components involved in the mechanism underlying the regulation of SGLT1 expression in the intestine of diabetics and controls.

In humans and rats, the glucose receptor subunits T1R2/T1R3 protein was only expressed in the enteroendocrine cells, with no change in the number of expressing cells between controls and diabetics. No significant change of *T1R3* mRNA in the intestine of control and diabetic rats. No changes seen in proglucagon gene mRNA expression (encoding for GLP-2) between the intestine of control and diabetic rats.

In control rats, exposure of intestinal tissue to high (10%) glucose concentrations evoked significant GLP-2 secretion, which was higher by 1.4 and 1.6 fold in the mid and distal intestine in response to high (10%) glucose compared to low glucose. In contrast, proximal intestine did not respond to glucose concentration. In diabetic rats, intestinal GLP-2 secretion was higher than that in controls, which was more significant in the mid and distal region. However, this increase was not affected greatly by glucose concentration. In response to low glucose, GLP-2 release was significantly higher in the diabetic intestine compared to controls by 1.2, 1.6 and 1.9 fold in the proximal, mid and distal regions, respectively. While, in response to high glucose, it was higher by 1.2, 1.4 and 1.4 fold in the proximal, mid and distal intestine, respectively. Expression of *GLP-2 R* mRNA was slightly lower in the proximal and mid regions of the diabetic intestine compared to that of controls, while no change was found in the distal intestine.

In humans, *VIP* mRNA expression was significantly higher by 2.3 fold in the duodenum of diabetic patients than that in non-diabetic individuals. In rats, *VIP* mRNA expression was significantly higher by 2.1, 2.5 and 2.3 fold in the proximal, mid and distal intestine, respectively, of diabetics compared to controls. VIP protein expression was higher, in the nerve fibres of submucosal and myenteric plexuses and the lamina propria of villi, in the intestine of diabetic rats compared to controls. *PACAP* mRNA expression was significantly increased in the diabetic intestine compared to controls by 2.5, 2.6 and 2.1 fold in the proximal, mid and distal intestine, respectively.

mRNA expression of *TAC1* gene, encoding substance P, was lower in the intestine of diabetic rats compared to that of controls. These data confirm that exposure of absorptive enterocytes to VIP and PACAP, but not substance P (SP), enhances SGLT1 expression, as shown in previous work done in our laboratory. Protein expression of substance P in the proximal, mid and distal intestine of diabetic rats was lower in the enteric neurons and axonal projections compared to that of control rats.

Conclusion:

The enhanced glucose transport in the intestine of diabetic rats (IDDM) is due to deregulated underlying mechanisms regulating the expression of SGLT1 protein on the BBM. The key molecules increase the stability of *SGLT1* mRNA leading to enhanced SGLT1 protein expression per enterocyte, together with mucosal hyperplasia to increase the number of cells supporting SGLT1.

It is suggested that the cause of enhanced glucose absorption in the intestine of rats is different from that of human subjects, as demonstrated in the diagram below; this could be due to different species or different type of diabetes.

Human duodenum **Rat mid and distal intestine:**

Rat proximal intestine:

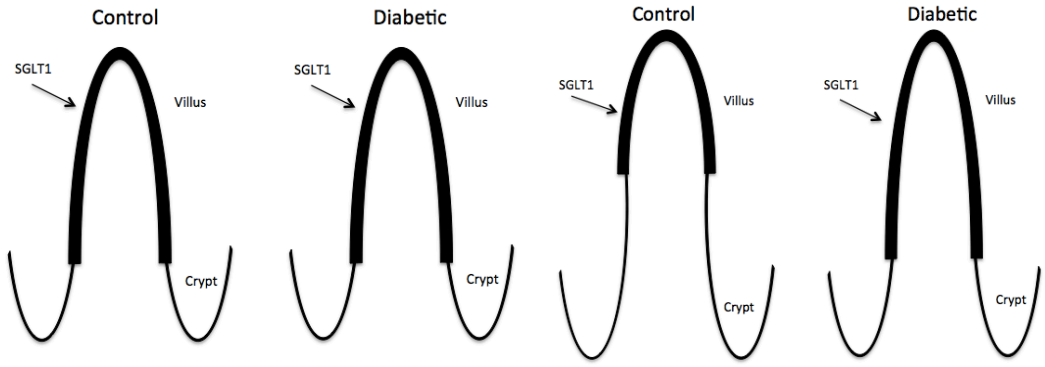

A diagram shows the different expression patterns of SGLT1 protein in rat and human intestine by immunohistochemistry.

Chapter 8

Future work

Future work:

It would be interesting to assess the expression of *SGLT1* mRNA, protein and function plus the immunohistochemical expression of SGLT1 protein along the crypt-villus axis in different animals with type II diabetes mellitus. Furthermore, to identify the involved molecules underlying the enhanced expression of SGLT1 in those diabetic models, as well as the morphometric changes.

It would be worthwhile to use intestinal tissues of mice with type II diabetes mellitus (NIDDM) to determine if the increased expression of SGLT1 varies among species or does it depends on the type of diabetes mellitus. If it is possible to obtain more samples of human duodenal biopsies, it would be helpful to do morphometric measurements, in all intestinal regions, to clarify the hypertrophic effect on SGLT1 up-regulation in NIDDM.

Further investigation is needed to understand the underlying mechanism of SGLT1 up-regulation in humans with type II diabetes mellitus, as that will help to develop a new approach for postprandial glycaemic control.

References

List of references

ABRAHAM, E. J., LEECH, C. A., LIN, J. C., ZULEWSKI, H. & HABENER, J. F. 2002. Insulinotropic hormone glucagon-like peptide-1 differentiation of human pancreatic islet-derived progenitor cells into insulin-producing cells. *Endocrinology,* 143**,** 3152-61.

AFFLECK, J. A., HELLIWELL, P. A. & KELLETT, G. L. 2003. Immunocytochemical detection of GLUT2 at the rat intestinal brush-border membrane. *J Histochem Cytochem,* 51**,** 1567-74.

ALBERTI, K. G. & ZIMMET, P. Z. 1998. Definition, diagnosis and classification of diabetes mellitus and its complications. Part 1: diagnosis and classification of diabetes mellitus provisional report of a WHO consultation. *Diabet Med,* 15**,** 539-53.

ALESSANDRI, J. M., ARFI, T. S., THEVENOUX, J. & LEGER, C. L. 1990. Diet-induced alterations of lipids during cell differentiation in the small intestine of growing rats: effect of an essential fatty acid deficiency. *J Pediatr Gastroenterol Nutr,* 10**,** 504-15.

ALWAKEEL, J. S., AL-SUWAIDA, A., ISNANI, A. C., AL-HARBI, A. & ALAM, A. 2009. Concomitant macro and microvascular complications in diabetic nephropathy. *Saudi J Kidney Dis Transpl,* 20**,** 402-9.

American diabetes association, 2011. Standards of medical care in diabetes. *Diabetes Care,* 34 Suppl 1**,** S11-61.

ANDERSEN, G., ROSE, C. S., HAMID, Y. H., DRIVSHOLM, T., BORCH-JOHNSEN, K., HANSEN, T. & PEDERSEN, O. 2003. Genetic variation of the GLUT10 glucose transporter (SLC2A10) and relationships to type 2 diabetes and intermediary traits. *Diabetes,* 52**,** 2445-8.

ANDRES-BARQUIN, P. J. & CONTE, C. 2004. Molecular basis of bitter taste: the T2R family of G protein-coupled receptors. *Cell Biochem Biophys,* 41**,** 99-112.

ARAKAWA, K., ISHIHARA, T., OKU, A., NAWANO, M., UETA, K., KITAMURA, K., MATSUMOTO, M. & SAITO, A. 2001. Improved diabetic syndrome in C57BL/KsJ-db/db mice by oral administration of the Na(+)-glucose cotransporter inhibitor T-1095. *Br J Pharmacol,* 132**,** 578-86.

ARIMURA, A. & SHIODA, S. 1995. Pituitary adenylate cyclase activating polypeptide (PACAP) and its receptors: neuroendocrine and endocrine interaction. *Front Neuroendocrinol,* 16**,** 53-88.

ARLUISON, M., QUIGNON, M., NGUYEN, P., THORENS, B., LELOUP, C. & PENICAUD, L. 2004. Distribution and anatomical localization of the glucose transporter 2 (GLUT2) in the adult rat brain--an immunohistochemical study. *J Chem Neuroanat,* 28**,** 117-36.

ASAHI, Y., HAYASHI, H., WANG, L. & EBINA, Y. 1999. Fluoromicroscopic detection of myc-tagged GLUT4 on the cell surface. Co-localization of the translocated GLUT4 with rearranged actin by insulin treatment in CHO cells and L6 myotubes. *J Med Invest,* 46**,** 192-9.

ASANO, T., KATAGIRI, H., TAKATA, K., TSUKUDA, K., LIN, J. L., ISHIHARA, H., INUKAI, K., HIRANO, H., YAZAKI, Y. & OKA, Y. 1992. Characterization of GLUT3 protein expressed in Chinese hamster ovary cells. *Biochem J,* 288 (Pt 1)**,** 189-93.

ASHLEY BLACKSHAW, L. & YOUNG, R. L. 2011. Detection and signaling of glucose in the intestinal mucosa--vagal pathway. *Neurogastroenterol Motil,* 23**,** 591-4.

ATTAIX, D. & MESLIN, J. C. 1991. Changes in small intestinal mucosa morphology and cell renewal in suckling, prolonged-suckling, and weaned lambs. *Am J Physiol,* 261**,** R811-8.

AUBRY, M., ZOLLINGER, M., FORTIN, S., VENIEN, C., LEGRIMELLEC, C. & CRINE, P. 1988. Monoclonal antibodies as probes for the transmembrane structure of neutral endopeptidase 24.11 ('enkephalinase'). *Biochimica et biophysica acta,* 967**,** 56-64.

AUGUSTIN, R. 2010. The protein family of glucose transport facilitators: It's not only about glucose after all. *IUBMB Life,* 62**,** 315-33.

BACHMANOV, A. A. & BEAUCHAMP, G. K. 2007. Taste receptor genes. *Annu Rev Nutr,* 27**,** 389-414.

BALDASSANO, S., LIU, S., QU, M. H., MULE, F. & WOOD, J. D. 2009. Glucagon-like peptide-2 modulates neurally evoked mucosal chloride secretion in guinea pig small intestine in vitro. *Am J Physiol Gastrointest Liver Physiol,* 297**,** G800-5.

BARBEZAT, G. O. & GROSSMAN, M. I. 1971. Intestinal secretion: stimulation by peptides. *Science,* 174**,** 422-4.

BARONE, S., FUSSELL, S. L., SINGH, A. K., LUCAS, F., XU, J., KIM, C., WU, X., YU, Y., AMLAL, H., SEIDLER, U., ZUO, J. & SOLEIMANI, M. 2009. Slc2a5 (Glut5) is essential for the absorption of fructose in the intestine and generation of fructose-induced hypertension. *J Biol Chem,* 284**,** 5056-66.

BARRY, P. H. & DIAMOND, J. M. 1984. Effects of unstirred layers on membrane phenomena. *Physiol Rev,* 64**,** 763-872.

BATCHELOR, D. J., AL-RAMMAHI, M., MORAN, A. W., BRAND, J. G., LI, X., HASKINS, M., GERMAN, A. J. & SHIRAZI-BEECHEY, S. P. 2011. Sodium/glucose cotransporter-1, sweet receptor, and disaccharidase expression in the intestine of the domestic dog and cat: two species of different dietary habit. *Am J Physiol Regul Integr Comp Physiol,* 300**,** R67-75.

BATCHELOR, D. J., GERMAN, A. J. & SHIRAZI-BEECHEY, S. P. 2013. Relevance of sodium/glucose cotransporter-1 (SGLT1) to diabetes mellitus and obesity in dogs. *Domest Anim Endocrinol,* 44**,** 139-44.

BATES, J. M., AKERLUND, J., MITTGE, E. & GUILLEMIN, K. 2007. Intestinal alkaline phosphatase detoxifies lipopolysaccharide and prevents inflammation in zebrafish in response to the gut microbiota. *Cell Host Microbe,* 2**,** 371-82.

BATTERHAM, R. L. & BLOOM, S. R. 2003. The gut hormone peptide YY regulates appetite. *Ann N Y Acad Sci,* 994**,** 162-8.

BAYLISS, W. M. & STARLING, E. H. 1902. The mechanism of pancreatic secretion. *J Physiol,* 28**,** 325-53.

BAZALAKOVA, M. H. & BLAKELY, R. D. 2006. The high-affinity choline transporter: a critical protein for sustaining cholinergic signaling as revealed in studies of genetically altered mice. *Handb Exp Pharmacol***,** 525-44.

BECKER, A., SCHLODER, P., STEELE, J. E. & WEGENER, G. 1996. The regulation of trehalose metabolism in insects. *Experientia,* 52**,** 433-9.

BELAI, A., LINCOLN, J., MILNER, P., CROWE, R., LOESCH, A. & BURNSTOCK, G. 1985. Enteric nerves in diabetic rats: increase in vasoactive intestinal polypeptide but not substance P. *Gastroenterology,* 89**,** 967-76.

BELL, D. S. 2004. Type 2 diabetes mellitus: what is the optimal treatment regimen? *Am J Med,* 116 Suppl 5A**,** 23S-29S.

BELL, G. I., BURANT, C. F., TAKEDA, J. & GOULD, G. W. 1993. Structure and function of mammalian facilitative sugar transporters. *J Biol Chem,* 268**,** 19161-4.

BELLUCCI, F., CARINI, F., CATALANI, C., CUCCHI, P., LECCI, A., MEINI, S., PATACCHINI, R., QUARTARA, L., RICCI, R., TRAMONTANA, M., GIULIANI, S. & MAGGI, C. A. 2002. Pharmacological profile of the novel mammalian tachykinin, hemokinin 1. *Br J Pharmacol,* 135**,** 266-74.

BENHAM, F. J. & HARRIS, H. 1979. Human cell lines expressing intestinal alkaline phosphatase. *Proc Natl Acad Sci U S A,* 76**,** 4016-9.

BENTO, J. L., BOWDEN, D. W., MYCHALECKYJ, J. C., HIRAKAWA, S., RICH, S. S., FREEDMAN, B. I. & SEGADE, F. 2005. Genetic analysis of the GLUT10 glucose transporter (SLC2A10) polymorphisms in Caucasian American type 2 diabetes. *BMC Med Genet,* 6**,** 42.

BERTELOOT, A. & SEMENZA, G. 1990. Advantages and limitations of vesicles for the characterization and the kinetic analysis of transport systems. *Methods Enzymol,* 192**,** 409-37.

BIANCHI, L. & DIEZ-SAMPEDRO, A. 2010. A single amino acid change converts the sugar sensor SGLT3 into a sugar transporter. *PLoS One,* 5**,** e10241.

BIBER, J., STIEGER, B., HAASE, W. & MURER, H. 1981. A high yield preparation for rat kidney brush border membranes. Different behaviour of lysosomal markers. *Biochim Biophys Acta,* 647**,** 169-76.

BJERKNES, M. & CHENG, H. 2001. Modulation of specific intestinal epithelial progenitors by enteric neurons. *Proc Natl Acad Sci U S A,* 98**,** 12497-502.

BLAKEMORE, S. J., ALEDO, J. C., JAMES, J., CAMPBELL, F. C., LUCOCQ, J. M. & HUNDAL, H. S. 1995. The GLUT5 hexose transporter is also localized to the basolateral membrane of the human jejunum. *Biochem J,* 309 (Pt 1)**,** 7-12.

BOISEN, K. A. & HJELT, K. 1999. [Glucose-galactose malabsorption. The first reported case in Denmark]. *Ugeskr Laeger,* 161**,** 4008-9.

BOLZAN, A. D. & BIANCHI, M. S. 2002. Genotoxicity of streptozotocin. *Mutat Res,* 512**,** 121-34.

BRADFORD, M. M. 1976. A rapid and sensitive method for the quantitation of microgram quantities of protein utilizing the principle of protein-dye binding. *Anal Biochem,* 72**,** 248-54.

BRASITUS, T. A. & DUDEJA, P. K. 1985. Alterations in the physical state and composition of brush border membrane lipids of rat enterocytes during differentiation. *Arch Biochem Biophys,* 240**,** 483-8.

BREER, H., EBERLE, J., FRICK, C., HAID, D. & WIDMAYER, P. 2012. Gastrointestinal chemosensation: chemosensory cells in the alimentary tract. *Histochem Cell Biol*.

BRENTJENS, R. & SALTZ, L. 2001. Islet cell tumors of the pancreas: the medical oncologist's perspective. *Surg Clin North Am,* 81**,** 527-42.

BROWN, M. & VALE, W. 1976. Effects of neurotensin and substance P on plasma insulin, glucagon and glucose levels. *Endocrinology,* 98**,** 819-22.

BRUBAKER, P. L. 1991. Regulation of intestinal proglucagon-derived peptide secretion by intestinal regulatory peptides. *Endocrinology,* 128**,** 3175-82.

BRYANT, M. G. & BLOOM, S. R. 1979. Distribution of the gut hormones in the primate intestinal tract. *Gut,* 20**,** 653-9.

BRYANT, M. G., POLAK, M. M., MODLIN, I., BLOOM, S. R., ALBUQUERQUE, R. H. & PEARSE, A. G. 1976. Possible dual role for vasoactive intestinal peptide as gastrointestinal hormone and neurotransmitter substance. *Lancet,* 1**,** 991-3.

BUDDINGTON, R. K. 1987. Does the natural diet influence the intestine's ability to regulate glucose absorption? *J Comp Physiol B,* 157**,** 677-88.

BUDDINGTON, R. K., CHEN, J. W. & DIAMOND, J. 1987. Genetic and phenotypic adaptation of intestinal nutrient transport to diet in fish. *J Physiol,* 393**,** 261-81.

BUDDINGTON, R. K. & DIAMOND, J. 1992. Ontogenetic development of nutrient transporters in cat intestine. *Am J Physiol,* 263**,** G605-16.

BURANT, C. F., FLINK, S., DEPAOLI, A. M., CHEN, J., LEE, W. S., HEDIGER, M. A., BUSE, J. B. & CHANG, E. B. 1994. Small intestine hexose transport in experimental diabetes. Increased transporter mRNA and protein expression in enterocytes. *J Clin Invest,* 93**,** 578-85.

BURANT, C. F., TAKEDA, J., BROT-LAROCHE, E., BELL, G. I. & DAVIDSON, N. O. 1992. Fructose transporter in human spermatozoa and small intestine is GLUT5. *J Biol Chem,* 267**,** 14523-6.

BURRIN, D. G., STOLL, B. & GUAN, X. 2003. Glucagon-like peptide 2 function in domestic animals. *Domest Anim Endocrinol,* 24**,** 103-22.

CARAYANNOPOULOS, M. O., CHI, M. M., CUI, Y., PINGSTERHAUS, J. M., MCKNIGHT, R. A., MUECKLER, M., DEVASKAR, S. U. & MOLEY, K. H. 2000. GLUT8 is a glucose transporter responsible for insulin-stimulated glucose uptake in the blastocyst. *Proc Natl Acad Sci U S A,* 97**,** 7313-8.

CARTER, M. S. & KRAUSE, J. E. 1990. Structure, expression, and some regulatory mechanisms of the rat preprotachykinin gene encoding substance P, neurokinin A, neuropeptide K, and neuropeptide gamma. *J Neurosci,* 10**,** 2203-14.

CASPARY, W. F., RHEIN, A. M. & CREUTZFELDT, W. 1972. Increase of intestinal brush border hydrolases in mucosa of streptozotocin-diabetic rats. *Diabetologia,* 8**,** 412-4.

CASTANEDA, F., BURSE, A., BOLAND, W. & KINNE, R. K. 2007. Thioglycosides as inhibitors of hSGLT1 and hSGLT2: potential therapeutic agents for the control of hyperglycemia in diabetes. *Int J Med Sci,* 4**,** 131-9.

CASTANEDA-SCEPPA, C. & CASTANEDA, F. 2011. Sodium-dependent glucose transporter protein as a potential therapeutic target for improving glycemic control in diabetes. *Nutr Rev,* 69**,** 720-9.

CASTELLO, A., GUMA, A., SEVILLA, L., FURRIOLS, M., TESTAR, X., PALACIN, M. & ZORZANO, A. 1995. Regulation of GLUT5 gene expression in rat intestinal mucosa: regional distribution, circadian rhythm, perinatal development and effect of diabetes. *Biochem J,* 309 (Pt 1)**,** 271-7.

CHANDRASHEKAR, J., HOON, M. A., RYBA, N. J. & ZUKER, C. S. 2006. The receptors and cells for mammalian taste. *Nature,* 444**,** 288-94.

CHANG, L., CHIANG, S. H. & SALTIEL, A. R. 2004. Insulin signaling and the regulation of glucose transport. *Mol Med,* 10**,** 65-71.

CHEESEMAN, C. 2008. GLUT7: a new intestinal facilitated hexose transporter. *Am J Physiol Endocrinol Metab,* 295**,** E238-41.

CHEESEMAN, C. I. 1997. Upregulation of SGLT-1 transport activity in rat jejunum induced by GLP-2 infusion in vivo. *Am J Physiol,* 273**,** R1965-71.

CHEESEMAN, C. I. & TSANG, R. 1996. The effect of GIP and glucagon-like peptides on intestinal basolateral membrane hexose transport. *Am J Physiol,* 271**,** G477-82.

CHEN, K. T., MALO, M. S., MOSS, A. K., ZELLER, S., JOHNSON, P., EBRAHIMI, F., MOSTAFA, G., ALAM, S. N., RAMASAMY, S., WARREN, H. S., HOHMANN, E. L. & HODIN, R. A. 2010. Identification of specific targets for the gut mucosal defense factor intestinal alkaline phosphatase. *Am J Physiol Gastrointest Liver Physiol,* 299**,** G467-75.

CHEN, X., GABITTO, M., PENG, Y., RYBA, N. J. & ZUKER, C. S. 2011. A gustotopic map of taste qualities in the mammalian brain. *Science,* 333**,** 1262-6.

CHENG, H. & LEBLOND, C. P. 1974a. Origin, differentiation and renewal of the four main epithelial cell types in the mouse small intestine. III. Entero-endocrine cells. *Am J Anat,* 141**,** 503-19.

CHENG, H. & LEBLOND, C. P. 1974b. Origin, differentiation and renewal of the four main epithelial cell types in the mouse small intestine. V. Unitarian Theory of the origin of the four epithelial cell types. *Am J Anat,* 141**,** 537-61.

CHERRINGTON, A. D., MOORE, M. C., SINDELAR, D. K. & EDGERTON, D. S. 2007. Insulin action on the liver in vivo. *Biochem Soc Trans,* 35**,** 1171-4.

CHO, Y. M. & KIEFFER, T. J. 2010. K-cells and glucose-dependent insulinotropic polypeptide in health and disease. *Vitam Horm,* 84**,** 111-50.

CHRISTOPHI, C. A., RESNICK, H. E., RATNER, R. E., TEMPROSA, M., FOWLER, S., KNOWLER, W. C., SHAMOON, H., BARRETT-CONNOR, E. & KAHN, S. E. 2013. Confirming glycemic status in the Diabetes Prevention Program: implications for diagnosing diabetes in high risk adults. *J Diabetes Complications,* 27**,** 150-7.

CIARALDI, T. P., KOLTERMAN, O. G. & OLEFSKY, J. M. 1981. Mechanism of the postreceptor defect in insulin action in human obesity. Decrease in glucose transport system activity. *J Clin Invest,* 68**,** 875-80.

COLMAN, P. G., THOMAS, D. W., ZIMMET, P. Z., WELBORN, T. A., GARCIA-WEBB, P. & MOORE, M. P. 1999. New classification and criteria for diagnosis of diabetes mellitus. The Australasian Working Party on Diagnostic Criteria for Diabetes Mellitus. *N Z Med J,* 112**,** 139-41.

CONKLIN, K. A., YAMASHIRO, K. M. & GRAY, G. M. 1975. Human intestinal sucrase-isomaltase. Identification of free sucrase and isomaltase and cleavage of the hybrid into active distinct subunits. *J Biol Chem,* 250**,** 5735-41.

CORPE, C. P., BASALEH, M. M., AFFLECK, J., GOULD, G., JESS, T. J. & KELLETT, G. L. 1996. The regulation of GLUT5 and GLUT2 activity in the adaptation of intestinal brush-border fructose transport in diabetes. *Pflugers Arch,* 432**,** 192-201.

CORPE, C. P., BOVELANDER, F. J., MUNOZ, C. M., HOEKSTRA, J. H., SIMPSON, I. A., KWON, O., LEVINE, M. & BURANT, C. F. 2002. Cloning and functional characterization of the mouse fructose transporter, GLUT5. *Biochim Biophys Acta,* 1576**,** 191-7.

CROSNIER, C., STAMATAKI, D. & LEWIS, J. 2006. Organizing cell renewal in the intestine: stem cells, signals and combinatorial control. *Nat Rev Genet,* 7**,** 349-59.

CUI, X. L., SCHLESIER, A. M., FISHER, E. L., CERQUEIRA, C. & FERRARIS, R. P. 2005. Fructose-induced increases in neonatal rat intestinal fructose transport involve the PI3-kinase/Akt signaling pathway. *Am J Physiol Gastrointest Liver Physiol,* 288**,** G1310-20.

DAHLQVIST, A. 1964. Method for Assay of Intestinal Disaccharidases. *Anal Biochem,* 7**,** 18-25.

DALY, K., AL-RAMMAHI, M., ARORA, D. K., MORAN, A. W., PROUDMAN, C. J., NINOMIYA, Y. & SHIRAZI-BEECHEY, S. P. 2012. Expression of sweet receptor components in equine small intestine: relevance to intestinal glucose transport. *Am J Physiol Regul Integr Comp Physiol,* 303**,** R199-208.

DAVIDSON, N. O., HAUSMAN, A. M., IFKOVITS, C. A., BUSE, J. B., GOULD, G. W., BURANT, C. F. & BELL, G. I. 1992. Human intestinal glucose transporter expression and localization of GLUT5. *Am J Physiol,* 262**,** C795-800.

DE JONGE, W. J. 2013. The Gut's Little Brain in Control of Intestinal Immunity. *ISRN Gastroenterol,* 2013**,** 630159.

DEACON, C. F. 2004. Circulation and degradation of GIP and GLP-1. *Horm Metab Res,* 36**,** 761-5.

DEBNAM, E. S. 1985. Adaptation of hexose uptake by the rat jejunum induced by the perfusion of sugars into the distal ileum. *Digestion,* 31**,** 25-30.

DEBNAM, E. S. & EBRAHIM, H. Y. 1989. Diabetes mellitus and the sodium electrochemical gradient across the brush border membrane of rat intestinal enterocytes. *J Endocrinol,* 123**,** 453-9.

DEBNAM, E. S. & EBRAHIM, H. Y. 1990. Autoradiographic localization of Na(+)-dependent L-valine uptake by the jejunum of streptozotocin-diabetic rats. *Eur J Clin Invest,* 20**,** 61-5.

DEBNAM, E. S., SMITH, M. W., SHARP, P. A., SRAI, S. K., TURVEY, A. & KEABLE, S. J. 1995. The effects of streptozotocin diabetes on sodium-glucose transporter (SGLT1) expression and function in rat jejunal and ileal villus-attached enterocytes. *Pflugers Arch,* 430**,** 151-9.

DELEZAY, O., BAGHDIGUIAN, S. & FANTINI, J. 1995. The development of Na(+)-dependent glucose transport during differentiation of an intestinal epithelial cell clone is regulated by protein kinase C. *J Biol Chem,* 270**,** 12536-41.

DELGADO, M. & GANEA, D. 2013. Vasoactive intestinal peptide: a neuropeptide with pleiotropic immune functions. *Amino Acids,* 45**,** 25-39.

DELGADO, M., POZO, D. & GANEA, D. 2004a. The significance of vasoactive intestinal peptide in immunomodulation. *Pharmacol Rev,* 56**,** 249-90.

DELGADO, M., REDUTA, A., SHARMA, V. & GANEA, D. 2004b. VIP/PACAP oppositely affects immature and mature dendritic cell expression of CD80/CD86 and the stimulatory activity for CD4(+) T cells. *J Leukoc Biol,* 75**,** 1122-30.

DESIMONE, J. A. & LYALL, V. 2006. Taste receptors in the gastrointestinal tract III. Salty and sour taste: sensing of sodium and protons by the tongue. *Am J Physiol Gastrointest Liver Physiol,* 291**,** G1005-10.

DI DANIEL, E., KEW, J. N. & MAYCOX, P. R. 2009. Investigation of the H(+)-myo-inositol transporter (HMIT) as a neuronal regulator of phosphoinositide signalling. *Biochem Soc Trans,* 37**,** 1139-43.

DIEZ-SAMPEDRO, A., HIRAYAMA, B. A., OSSWALD, C., GORBOULEV, V., BAUMGARTEN, K., VOLK, C., WRIGHT, E. M. & KOEPSELL, H. 2003. A glucose sensor hiding in a family of transporters. *Proc Natl Acad Sci U S A,* 100**,** 11753-8.

DOCKRAY, G. J. 2012. Cholecystokinin. *Curr Opin Endocrinol Diabetes Obes,* 19**,** 8-12.

DOEGE, H., BOCIANSKI, A., JOOST, H. G. & SCHURMANN, A. 2000. Activity and genomic organization of human glucose transporter 9 (GLUT9), a novel member of the family of sugar-transport facilitators predominantly expressed in brain and leucocytes. *Biochem J,* 350 Pt 3**,** 771-6.

DONG, R., SRAI, S. K., DEBNAM, E. & SMITH, M. 1997. Transcriptional and translational control over sodium-glucose-linked transporter (SGLT1) gene expression in adult rat small intestine. *FEBS Lett,* 406**,** 79-82.

DOUARD, V. & FERRARIS, R. P. 2008. Regulation of the fructose transporter GLUT5 in health and disease. *Am J Physiol Endocrinol Metab,* 295**,** E227-37.

DROZDOWSKI, L. A. & THOMSON, A. B. 2006. Intestinal sugar transport. *World J Gastroenterol,* 12**,** 1657-70.

DRUCKER, D. J. 1999. Glucagon-like Peptide 2. *Trends Endocrinol Metab,* 10**,** 153-156.

DRUCKER, D. J. 2001a. Glucagon-like peptide 2. *J Clin Endocrinol Metab,* 86**,** 1759-64.

DRUCKER, D. J. 2001b. Minireview: the glucagon-like peptides. *Endocrinology,* 142**,** 521-7.

DRUCKER, D. J. 2002a. Biological actions and therapeutic potential of the glucagon-like peptides. *Gastroenterology,* 122**,** 531-44.

DRUCKER, D. J. 2002b. Gut adaptation and the glucagon-like peptides. *Gut,* 50**,** 428-35.

DRUCKER, D. J. 2003. Glucagon-like peptides: regulators of cell proliferation, differentiation, and apoptosis. *Mol Endocrinol,* 17**,** 161-71.

DRUCKER, D. J. 2006. The biology of incretin hormones. *Cell Metab,* 3**,** 153-65.

DRUCKER, D. J. 2007. The role of gut hormones in glucose homeostasis. *J Clin Invest,* 117**,** 24-32.

DRUCKER, D. J., ERLICH, P., ASA, S. L. & BRUBAKER, P. L. 1996. Induction of intestinal epithelial proliferation by glucagon-like peptide 2. *Proc Natl Acad Sci U S A,* 93**,** 7911-6.

DRUCKER, D. J., MOJSOV, S. & HABENER, J. F. 1986. Cell-specific post-translational processing of preproglucagon expressed from a metallothionein-glucagon fusion gene. *J Biol Chem,* 261**,** 9637-43.

DUCKWORTH, W. C., BENNETT, R. G. & HAMEL, F. G. 1998. Insulin degradation: progress and potential. *Endocr Rev,* 19**,** 608-24.

DYER, J., AL-RAMMAHI, M., WATERFALL, L., SALMON, K. S., GEOR, R. J., BOURE, L., EDWARDS, G. B., PROUDMAN, C. J. & SHIRAZI-BEECHEY, S. P. 2009. Adaptive response of equine intestinal Na+/glucose co-transporter (SGLT1) to an increase in dietary soluble carbohydrate. *Pflugers Arch,* 458**,** 419-30.

DYER, J., BARKER, P. J. & SHIRAZI-BEECHEY, S. P. 1997a. Nutrient regulation of the intestinal Na+/glucose co-transporter (SGLT1) gene expression. *Biochem Biophys Res Commun,* 230**,** 624-9.

DYER, J., DALY, K., SALMON, K. S., ARORA, D. K., KOKRASHVILI, Z., MARGOLSKEE, R. F. & SHIRAZI-BEECHEY, S. P. 2007. Intestinal glucose sensing and regulation of intestinal glucose absorption. *Biochem Soc Trans,* 35**,** 1191-4.

DYER, J., FERNANDEZ-CASTANO MEREDIZ, E., SALMON, K. S., PROUDMAN, C. J., EDWARDS, G. B. & SHIRAZI-BEECHEY, S. P. 2002a. Molecular characterisation of carbohydrate digestion and absorption in equine small intestine. *Equine Vet J,* 34**,** 349-58.

DYER, J., GARNER, A., WOOD, I. S., SHARMA, A. K., CHANDRANATH, I. & SHIRAZI-BEECHEY, S. P. 1997b. Changes in the levels of intestinal Na+/glucose co-transporter (SGLT1) in experimental diabetes. *Biochem Soc Trans,* 25**,** 479S.

DYER, J., HOSIE, K. B. & SHIRAZI-BEECHEY, S. P. 1997c. Nutrient regulation of human intestinal sugar transporter (SGLT1) expression. *Gut,* 41**,** 56-9.

DYER, J., SALMON, K. S., ZIBRIK, L. & SHIRAZI-BEECHEY, S. P. 2005. Expression of sweet taste receptors of the T1R family in the intestinal tract and enteroendocrine cells. *Biochem Soc Trans,* 33**,** 302-5.

DYER, J., VAYRO, S., KING, T. P. & SHIRAZI-BEECHEY, S. P. 2003a. Glucose sensing in the intestinal epithelium. *Eur J Biochem,* 270**,** 3377-88.

DYER, J., VAYRO, S. & SHIRAZI-BEECHEY, S. P. 2003b. Mechanism of glucose sensing in the small intestine. *Biochem Soc Trans,* 31**,** 1140-2.

DYER, J., WOOD, I. S., PALEJWALA, A., ELLIS, A. & SHIRAZI-BEECHEY, S. P. 2002b. Expression of monosaccharide transporters in intestine of diabetic humans. *Am J Physiol Gastrointest Liver Physiol,* 282**,** G241-8.

EISSELE, R., GOKE, R., WILLEMER, S., HARTHUS, H. P., VERMEER, H., ARNOLD, R. & GOKE, B. 1992. Glucagon-like peptide-1 cells in the gastrointestinal tract and pancreas of rat, pig and man. *Eur J Clin Invest,* 22**,** 283-91.

ELFEBER, K., KOHLER, A., LUTZENBURG, M., OSSWALD, C., GALLA, H. J., WITTE, O. W. & KOEPSELL, H. 2004. Localization of the Na+-D-glucose cotransporter SGLT1 in the blood-brain barrier. *Histochem Cell Biol,* 121**,** 201-7.

EMOTO, C., YAMAZAKI, H., YAMASAKI, S., SHIMADA, N., NAKAJIMA, M. & YOKOI, T. 2000. Use of everted sacs of mouse small intestine as enzyme sources for the study of drug oxidation activities in vitro. *Xenobiotica,* 30**,** 971-82.

ENGLE, M. J., MAHMOOD, A. & ALPERS, D. H. 1995. Two rat intestinal alkaline phosphatase isoforms with different carboxyl-terminal peptides are both membrane-bound by a glycan phosphatidylinositol linkage. *J Biol Chem,* 270**,** 11935-40.

ESTALL, J. L. & DRUCKER, D. J. 2006. Glucagon-like Peptide-2. *Annu Rev Nutr,* 26**,** 391-411.

FAHRENKRUG, J. & EMSON, P. C. 1982. Vasoactive intestinal polypeptide: functional aspects. *Br Med Bull,* 38**,** 265-70.

FEDORAK, R. N., CHANG, E. B., MADARA, J. L. & FIELD, M. 1987. Intestinal adaptation to diabetes. Altered Na-dependent nutrient absorption in streptozocin-treated chronically diabetic rats. *J Clin Invest,* 79**,** 1571-8.

FEDORAK, R. N., CHEESEMAN, C. I., THOMSON, A. B. & PORTER, V. M. 1991. Altered glucose carrier expression: mechanism of intestinal adaptation during streptozocin-induced diabetes in rats. *Am J Physiol,* 261**,** G585-91.

FEDORAK, R. N., GERSHON, M. D. & FIELD, M. 1989. Induction of intestinal glucose carriers in streptozocin-treated chronically diabetic rats. *Gastroenterology,* 96**,** 37-44.

FEHMANN, H. C., GOKE, R. & GOKE, B. 1995. Cell and molecular biology of the incretin hormones glucagon-like peptide-I and glucose-dependent insulin releasing polypeptide. *Endocr Rev,* 16**,** 390-410.

FERRARIS, R. P. 2001. Dietary and developmental regulation of intestinal sugar transport. *Biochem J,* 360**,** 265-76.

FERRARIS, R. P. & DIAMOND, J. 1992. Crypt-villus site of glucose transporter induction by dietary carbohydrate in mouse intestine. *Am J Physiol,* 262**,** G1069-73.

FERRARIS, R. P. & DIAMOND, J. 1997. Regulation of intestinal sugar transport. *Physiol Rev,* 77**,** 257-302.

FERRARIS, R. P. & DIAMOND, J. M. 1989. Specific regulation of intestinal nutrient transporters by their dietary substrates. *Annu Rev Physiol,* 51**,** 125-41.

FERRARIS, R. P. & DIAMOND, J. M. 1993. Crypt/villus site of substrate-dependent regulation of mouse intestinal glucose transporters. *Proc Natl Acad Sci U S A,* 90**,** 5868-72.

FERRARIS, R. P., VILLENAS, S. A., HIRAYAMA, B. A. & DIAMOND, J. 1992. Effect of diet on glucose transporter site density along the intestinal crypt-villus axis. *Am J Physiol,* 262**,** G1060-8.

FERRARIS, R. P., YASHARPOUR, S., LLOYD, K. C., MIRZAYAN, R. & DIAMOND, J. M. 1990. Luminal glucose concentrations in the gut under normal conditions. *Am J Physiol,* 259**,** G822-37.

FIELD, M. 2003. Intestinal ion transport and the pathophysiology of diarrhea. *J Clin Invest,* 111**,** 931-43.

FINGER, T. E., DANILOVA, V., BARROWS, J., BARTEL, D. L., VIGERS, A. J., STONE, L., HELLEKANT, G. & KINNAMON, S. C. 2005. ATP signaling is crucial for communication from taste buds to gustatory nerves. *Science,* 310**,** 1495-9.

FIORE, MARIANO S. H. DI. & SCHMIDT, I. G. 1981. Atlas of Human Histology. 5th ed. Philadelphia: Lea & Febiger.

FISCHER, K. D., DHANVANTARI, S., DRUCKER, D. J. & BRUBAKER, P. L. 1997. Intestinal growth is associated with elevated levels of glucagon-like peptide 2 in diabetic rats. *Am J Physiol,* 273**,** E815-20.

FISHER, R. B. & PARSONS, D. S. 1949. A preparation of surviving rat small intestine for the study of absorption. *J Physiol,* 110**,** 36-46, pl.

FOLWACZNY, C., RIEPL, R., TSCHOP, M. & LANDGRAF, R. 1999a. Gastrointestinal involvement in patients with diabetes mellitus: Part I (first of two parts). Epidemiology, pathophysiology, clinical findings. *Z Gastroenterol,* 37**,** 803-15.

FOLWACZNY, C., RIEPL, R., TSCHOP, M. & LANDGRAF, R. 1999b. Gastrointestinal involvement in patients with diabetes mellitus: Part II (second of two parts). Diagnostic procedures, pharmacological and nonpharmacological therapy. *Z Gastroenterol,* 37**,** 817-26.

FORMULARY, B. N. 2001. *British National Formulary 41. (British Medical Association and Royal Pharmaceutical Society of Great Britain, London).* London: British National Formulary.

FREEMAN, H. J. 2008. Crypt region localization of intestinal stem cells in adults. *World J Gastroenterol,* 14**,** 7160-2.

FREEMAN, H. J., JOHNSTON, G. & QUAMME, G. A. 1987. Sodium-dependent D-glucose transport in brush-border membrane vesicles from isolated rat small intestinal villus and crypt epithelial cells. *Can J Physiol Pharmacol,* 65**,** 1213-9.

FREEMAN, T. C., WOOD, I. S., SIRINATHSINGHJI, D. J., BEECHEY, R. B., DYER, J. & SHIRAZI-BEECHEY, S. P. 1993. The expression of the Na+/glucose cotransporter (SGLT1) gene in lamb small intestine during postnatal development. *Biochim Biophys Acta,* 1146**,** 203-12.

FUKUMOTO, H., SEINO, S., IMURA, H., SEINO, Y., EDDY, R. L., FUKUSHIMA, Y., BYERS, M. G., SHOWS, T. B. & BELL, G. I. 1988. Sequence, tissue distribution, and chromosomal localization of mRNA encoding a human glucose transporter-like protein. *Proc Natl Acad Sci U S A,* 85**,** 5434-8.

FUKUZAWA, T., FUKAZAWA, M., UEDA, O., SHIMADA, H., KITO, A., KAKEFUDA, M., KAWASE, Y., WADA, N. A., GOTO, C., FUKUSHIMA, N., JISHAGE, K., HONDA, K., KING, G. L. & KAWABE, Y. 2013. SGLT5 reabsorbs fructose in the kidney but its deficiency paradoxically exacerbates hepatic steatosis induced by fructose. *PLoS One,* 8**,** e56681.

FURNESS, J. B. 2008. The enteric nervous system: normal functions and enteric neuropathies. *Neurogastroenterol Motil,* 20 Suppl 1**,** 32-8.

GAI, W., SCHOTT-OHLY, P., SCHULTE IM WALDE, S. & GLEICHMANN, H. 2004. Differential target molecules for toxicity induced by streptozotocin and alloxan in pancreatic islets of mice in vitro. *Exp Clin Endocrinol Diabetes,* 112**,** 29-37.

GAINETDINOV, R. R., PREMONT, R. T., BOHN, L. M., LEFKOWITZ, R. J. & CARON, M. G. 2004. Desensitization of G protein-coupled receptors and neuronal functions. *Annu Rev Neurosci,* 27**,** 107-44.

GAJDOSIK, A., GAJDOSIKOVA, A., STEFEK, M., NAVAROVA, J. & HOZOVA, R. 1999. Streptozotocin-induced experimental diabetes in male Wistar rats. *Gen Physiol Biophys,* 18 Spec No**,** 54-62.

GALLIGAN, J. J., LEPARD, K. J., SCHNEIDER, D. A. & ZHOU, X. 2000. Multiple mechanisms of fast excitatory synaptic transmission in the enteric nervous system. *J Auton Nerv Syst,* 81**,** 97-103.

GAMMELTOFT, S. & VAN OBBERGHEN, E. 1986. Protein kinase activity of the insulin receptor. *Biochem J,* 235**,** 1-11.

GANEA, D. & DELGADO, M. 2002. Vasoactive intestinal peptide (VIP) and pituitary adenylate cyclase-activating polypeptide (PACAP) as modulators of both innate and adaptive immunity. *Crit Rev Oral Biol Med,* 13**,** 229-37.

GANONG.W.F 2003. *Review of medical physiology* new york, New York Lange Medical Books / McGraw-Hill companies.

GERARDI-LAFFIN, C., DELQUE-BAYER, P., SUDAKA, P. & POIREE, J. C. 1993. Oligomeric structure of the sodium-dependent phlorizin binding protein from kidney brush-border membranes. *Biochim Biophys Acta,* 1151**,** 99-104.

GHATEI, M. A., TAKAHASHI, K., SUZUKI, Y., GARDINER, J., JONES, P. M. & BLOOM, S. R. 1993. Distribution, molecular characterization of pituitary adenylate cyclase-activating polypeptide and its precursor encoding messenger RNA in human and rat tissues. *J Endocrinol,* 136**,** 159-66.

GILMAN, A. G. 1987. G proteins: transducers of receptor-generated signals. *Annu Rev Biochem,* 56**,** 615-49.

GOESTEMEYER, A. K., MARKS, J., SRAI, S. K., DEBNAM, E. S. & UNWIN, R. J. 2007. GLUT2 protein at the rat proximal tubule brush border membrane correlates with protein kinase C (PKC)-betal and plasma glucose concentration. *Diabetologia,* 50**,** 2209-17.

GOLDBERG, R. F., AUSTEN, W. G., JR., ZHANG, X., MUNENE, G., MOSTAFA, G., BISWAS, S., MCCORMACK, M., EBERLIN, K. R., NGUYEN, J. T., TATLIDEDE, H. S., WARREN, H. S., NARISAWA, S., MILLAN, J. L. & HODIN, R. A. 2008. Intestinal alkaline phosphatase is a gut mucosal defense factor maintained by enteral nutrition. *Proc Natl Acad Sci U S A,* 105**,** 3551-6.

GORBOULEV, V., SCHURMANN, A., VALLON, V., KIPP, H., JASCHKE, A., KLESSEN, D., FRIEDRICH, A., SCHERNECK, S., RIEG, T., CUNARD, R., VEYHL-WICHMANN, M., SRINIVASAN, A., BALEN, D., BRELJAK, D., REXHEPAJ, R., PARKER, H. E., GRIBBLE, F. M., REIMANN, F., LANG, F., WIESE, S., SABOLIC, I., SENDTNER, M. & KOEPSELL, H. 2012. Na(+)-D-glucose cotransporter SGLT1 is pivotal for intestinal glucose absorption and glucose-dependent incretin secretion. *Diabetes,* 61**,** 187-96.

GOULD, G. W. & BELL, G. I. 1990. Facilitative glucose transporters: an expanding family. *Trends Biochem Sci,* 15**,** 18-23.

GOULD, G. W. & HOLMAN, G. D. 1993. The glucose transporter family: structure, function and tissue-specific expression. *Biochem J,* 295 (Pt 2)**,** 329-41.

GOUYON, F., CAILLAUD, L., CARRIERE, V., KLEIN, C., DALET, V., CITADELLE, D., KELLETT, G. L., THORENS, B., LETURQUE, A. & BROT-LAROCHE, E. 2003. Simple-sugar meals target GLUT2 at enterocyte apical membranes to improve sugar absorption: a study in GLUT2-null mice. *J Physiol,* 552**,** 823-32.

GOVERS, R., COSTER, A. C. & JAMES, D. E. 2004. Insulin increases cell surface GLUT4 levels by dose dependently discharging GLUT4 into a cell surface recycling pathway. *Mol Cell Biol,* 24**,** 6456-66.

GOZES, I. & BRENNEMAN, D. E. 1989. VIP: molecular biology and neurobiological function. *Mol Neurobiol,* 3**,** 201-36.

GRIDER, J. R. & MAKHLOUF, G. M. 1988. Vasoactive intestinal peptide. Transmitter of inhibitory motor neurons of the gut. *Ann N Y Acad Sci,* 527**,** 369-77.

GRIDER, J. R. & MAKHLOUF, G. M. 1990. Regulation of the peristaltic reflex by peptides of the myenteric plexus. *Arch Int Pharmacodyn Ther,* 303**,** 232-51.

GROSS, K. J. & POTHOULAKIS, C. 2007. Role of neuropeptides in inflammatory bowel disease. *Inflamm Bowel Dis,* 13**,** 918-32.

GUNTHER, R. D. & WRIGHT, E. M. 1983. Na+, Li+, and Cl- transport by brush border membranes from rabbit jejunum. *J Membrane Biol.* 74**,** 85-94.

HAASE, W., SCHAFER, A., MURER, H. & KINNE, R. 1978a. Studies on the orientation of brush-border membrane vesicles. *The Biochemical journal,* 172**,** 57-62.

HAASE, W., SCHAFER, A., MURER, H. & KINNE, R. 1978b. Studies on the orientation of brush-border membrane vesicles. *Biochem J,* 172**,** 57-62.

HAJDUCH, E., DARAKHSHAN, F. & HUNDAL, H. S. 1998. Fructose uptake in rat adipocytes: GLUT5 expression and the effects of streptozotocin-induced diabetes. *Diabetologia,* 41**,** 821-8.

HAJDUCH, E., LITHERLAND, G. J., TURBAN, S., BROT-LAROCHE, E. & HUNDAL, H. S. 2003. Insulin regulates the expression of the GLUT5 transporter in L6 skeletal muscle cells. *FEBS Lett,* 549**,** 77-82.

HAMID, R., KHAN, M. A., AHMAD, M., AHMAD, M. M., ABDIN, M. Z., MUSARRAT, J. & JAVED, S. 2013. Chitinases: An update. *J Pharm Bioallied Sci,* 5**,** 21-9.

HAN, S., HAGAN, D. L., TAYLOR, J. R., XIN, L., MENG, W., BILLER, S. A., WETTERAU, J. R., WASHBURN, W. N. & WHALEY, J. M. 2008. Dapagliflozin, a selective SGLT2 inhibitor, improves glucose homeostasis in normal and diabetic rats. *Diabetes,* 57**,** 1723-9.

HANEY, P. M., SLOT, J. W., PIPER, R. C., JAMES, D. E. & MUECKLER, M. 1991. Intracellular targeting of the insulin-regulatable glucose transporter (GLUT4) is isoform specific and independent of cell type. *J Cell Biol,* 114**,** 689-99.

HANSEN, M. B. 2003. The enteric nervous system I: organisation and classification. *Pharmacol Toxicol,* 92**,** 105-13.

HARRIS, D. M., COHN, H. I., PESANT, S. & ECKHART, A. D. 2008. GPCR signalling in hypertension: role of GRKs. *Clin Sci (Lond),* 115**,** 79-89.

HARRISON, S. & GEPPETTI, P. 2001. Substance p. *Int J Biochem Cell Biol,* 33**,** 555-76.

HARVEY, C. B., FOX, M. F., JEGGO, P. A., MANTEI, N., POVEY, S. & SWALLOW, D. M. 1993. Regional localization of the lactase-phlorizin hydrolase gene, LCT, to chromosome 2q21. *Ann Hum Genet,* 57**,** 179-85.

HAURI, H. P., QUARONI, A. & ISSELBACHER, K. J. 1979. Biogenesis of intestinal plasma membrane: posttranslational route and cleavage of sucrase-isomaltase. *Proc Natl Acad Sci U S A,* 76**,** 5183-6.

HAURI, H. P., WACKER, H., RICKLI, E. E., BIGLER-MEIER, B., QUARONI, A. & SEMENZA, G. 1982. Biosynthesis of sucrase-isomaltase. Purification and NH2-terminal amino acid

sequence of the rat sucrase-isomaltase precursor (pro-sucrase-isomaltase) from fetal intestinal transplants. *J Biol Chem,* 257**,** 4522-8.

HEARN, P. R., RUSSELL, R. G. & FARMER, J. 1981. The formation and orientation of brush border vesicles from rat duodenal mucosa. *J Cell Sci,* 47**,** 227-36.

HEDIGER, M. A., BUDARF, M. L., EMANUEL, B. S., MOHANDAS, T. K. & WRIGHT, E. M. 1989a. Assignment of the human intestinal Na+/glucose cotransporter gene (SGLT1) to the q11.2----qter region of chromosome 22. *Genomics,* 4**,** 297-300.

HEDIGER, M. A., COADY, M. J., IKEDA, T. S. & WRIGHT, E. M. 1987. Expression cloning and cDNA sequencing of the Na+/glucose co-transporter. *Nature,* 330**,** 379-81.

HEDIGER, M. A. & RHOADS, D. B. 1994. Molecular physiology of sodium-glucose cotransporters. *Physiol Rev,* 74**,** 993-1026.

HEDIGER, M. A., TURK, E., PAJOR, A. M. & WRIGHT, E. M. 1989b. Molecular genetics of the human Na+/glucose cotransporter. *Klin Wochenschr,* 67**,** 843-6.

HEIJBOER, A. C., PIJL, H., VAN DEN HOEK, A. M., HAVEKES, L. M., ROMIJN, J. A. & CORSSMIT, E. P. 2006. Gut-brain axis: regulation of glucose metabolism. *J Neuroendocrinol,* 18**,** 883-94.

HEINEMANN, A. & HOLZER, P. 1999. Stimulant action of pituitary adenylate cyclase-activating peptide on normal and drug-compromised peristalsis in the guinea-pig intestine. *Br J Pharmacol,* 127**,** 763-71.

HELLIWELL, P. A., RICHARDSON, M., AFFLECK, J. & KELLETT, G. L. 2000. Regulation of GLUT5, GLUT2 and intestinal brush-border fructose absorption by the extracellular signal-regulated kinase, p38 mitogen-activated kinase and phosphatidylinositol 3-kinase intracellular signalling pathways: implications for adaptation to diabetes. *Biochem J,* 350 Pt 1**,** 163-9.

HERBAI, G. & LUNDIN, A. 1976. Treatment of malignant metastatic pancreatic insulinoma with streptozotocin. Review of 21 cases described in detail in the literature and report of complete remission of a new case. *Acta Med Scand,* 200**,** 447-52.

HERTEL, S., HEINZ, F. & VOGEL, M. 2000. Hydrolysis of low-molecular-weight oligosaccharides and oligosaccharide alditols by pig intestinal sucrase/isomaltase and glucosidase/maltase. *Carbohydr Res,* 326**,** 264-76.

HIRAYAMA, B. A., LOO, D. D. & WRIGHT, E. M. 1994. Protons drive sugar transport through the Na+/glucose cotransporter (SGLT1). *J Biol Chem,* 269**,** 21407-10.

HOLST, J. J., FAHRENKRUG, J., KNUHTSEN, S., JENSEN, S. L., POULSEN, S. S. & NIELSEN, O. V. 1984. Vasoactive intestinal polypeptide (VIP) in the pig pancreas: role of VIPergic nerves in control of fluid and bicarbonate secretion. *Regul Pept,* 8**,** 245-59.

HOLST, J. J. & ORSKOV, C. 2001. Incretin hormones--an update. *Scand J Clin Lab Invest Suppl,* 234**,** 75-85.

HOON, M. A., ADLER, E., LINDEMEIER, J., BATTEY, J. F., RYBA, N. J. & ZUKER, C. S. 1999. Putative mammalian taste receptors: a class of taste-specific GPCRs with distinct topographic selectivity. *Cell,* 96**,** 541-51.

HOPFER, U., NELSON, K., PERROTTO, J. & ISSELBACHER, K. J. 1973. Glucose transport in isolated brush border membrane from rat small intestine. *J Biol Chem,* 248**,** 25-32.

HUANG, A. L., CHEN, X., HOON, M. A., CHANDRASHEKAR, J., GUO, W., TRANKNER, D., RYBA, N. J. & ZUKER, C. S. 2006. The cells and logic for mammalian sour taste detection. *Nature,* 442**,** 934-8.

HWANG, E. S., HIRAYAMA, B. A. & WRIGHT, E. M. 1991. Distribution of the SGLT1 Na+/glucose cotransporter and mRNA along the crypt-villus axis of rabbit small intestine. *Biochem Biophys Res Commun,* 181**,** 1208-17.

IDRIS, I. & DONNELLY, R. 2009. Sodium-glucose co-transporter-2 inhibitors: an emerging new class of oral antidiabetic drug. *Diabetes Obes Metab,* 11**,** 79-88.

INGRAM, D. G. & BACHRACH, B. E. 2012. Validation of HbA1c of 6.5% for diagnosing diabetes mellitus via the use of taxometric analysis. *Ann Epidemiol,* 22**,** 66-9.

INUKAI, K., ASANO, T., KATAGIRI, H., ISHIHARA, H., ANAI, M., FUKUSHIMA, Y., TSUKUDA, K., KIKUCHI, M., YAZAKI, Y. & OKA, Y. 1993. Cloning and increased expression with fructose feeding of rat jejunal GLUT5. *Endocrinology,* 133**,** 2009-14.

ISHII, S., MISAKA, T., KISHI, M., KAGA, T., ISHIMARU, Y. & ABE, K. 2009. Acetic acid activates PKD1L3-PKD2L1 channel--a candidate sour taste receptor. *Biochem Biophys Res Commun,* 385**,** 346-50.

ITO, M., KONDO, Y., NAKATANI, A. & NARUSE, A. 1999. New model of progressive non-insulin-dependent diabetes mellitus in mice induced by streptozotocin. *Biol Pharm Bull,* 22**,** 988-9.

JABBOUR, S. A. & GOLDSTEIN, B. J. 2008. Sodium glucose co-transporter 2 inhibitors: blocking renal tubular reabsorption of glucose to improve glycaemic control in patients with diabetes. *Int J Clin Pract,* 62**,** 1279-84.

JAMES, D. E., BROWN, R., NAVARRO, J. & PILCH, P. F. 1988. Insulin-regulatable tissues express a unique insulin-sensitive glucose transport protein. *Nature,* 333**,** 183-5.

JANG, H. J., KOKRASHVILI, Z., THEODORAKIS, M. J., CARLSON, O. D., KIM, B. J., ZHOU, J., KIM, H. H., XU, X., CHAN, S. L., JUHASZOVA, M., BERNIER, M., MOSINGER, B., MARGOLSKEE, R. F. & EGAN, J. M. 2007. Gut-expressed gustducin and taste receptors regulate secretion of glucagon-like peptide-1. *Proc Natl Acad Sci U S A,* 104**,** 15069-74.

JANSSEN, S. & DEPOORTERE, I. 2013. Nutrient sensing in the gut: new roads to therapeutics? *Trends Endocrinol Metab,* 24**,** 92-100.

JASO, M. J., VIAL, M. & MORETO, M. 1995. Hexose accumulation by enterocytes from the jejunum and rectum of chickens adapted to high and low NaCl intake. *Pflugers Arch,* 429**,** 511-6.

JIANG, L., DAVID, E. S., ESPINA, N. & FERRARIS, R. P. 2001. GLUT-5 expression in neonatal rats: crypt-villus location and age-dependent regulation. *Am J Physiol Gastrointest Liver Physiol,* 281**,** G666-74.

JOOST, H. G., BELL, G. I., BEST, J. D., BIRNBAUM, M. J., CHARRON, M. J., CHEN, Y. T., DOEGE, H., JAMES, D. E., LODISH, H. F., MOLEY, K. H., MOLEY, J. F., MUECKLER, M., ROGERS, S., SCHURMANN, A., SEINO, S. & THORENS, B. 2002. Nomenclature of the GLUT/SLC2A family of sugar/polyol transport facilitators. *Am J Physiol Endocrinol Metab,* 282**,** E974-6.

JOOST, H. G. & THORENS, B. 2001. The extended GLUT-family of sugar/polyol transport facilitators: nomenclature, sequence characteristics, and potential function of its novel members (review). *Mol Membr Biol,* 18**,** 247-56.

JORGENSEN, C. S., AHRENSBERG, J. M., GREGERSEN, H. & FLYVBERG, A. 2001. Tension-strain relations and morphometry of rat small intestine in experimental diabetes. *Dig Dis Sci,* 46**,** 960-7.

JUNOD, A., LAMBERT, A. E., ORCI, L., PICTET, R., GONET, A. E. & RENOLD, A. E. 1967. Studies of the diabetogenic action of streptozotocin. *Proc Soc Exp Biol Med,* 126**,** 201-5.

JUNQUEIRA, C. & CARNEIRO, J. 1971. *Basic Histology,* Los Altos, CA, Lange Medical Publication.

KANAI, Y., LEE, W. S., YOU, G., BROWN, D. & HEDIGER, M. A. 1994. The human kidney low affinity Na+/glucose cotransporter SGLT2. Delineation of the major renal reabsorptive mechanism for D-glucose. *J Clin Invest,* 93**,** 397-404.

KARYLOWSKI, O., ZEIGERER, A., COHEN, A. & MCGRAW, T. E. 2004. GLUT4 is retained by an intracellular cycle of vesicle formation and fusion with endosomes. *Mol Biol Cell,* 15**,** 870-82.

KASKE, S., KRASTEVA, G., KONIG, P., KUMMER, W., HOFMANN, T., GUDERMANN, T. & CHUBANOV, V. 2007. TRPM5, a taste-signaling transient receptor potential ion-channel, is a ubiquitous signaling component in chemosensory cells. *BMC Neurosci,* 8**,** 49.

KATAOKA, S., YANG, R., ISHIMARU, Y., MATSUNAMI, H., SEVIGNY, J., KINNAMON, J. C. & FINGER, T. E. 2008. The candidate sour taste receptor, PKD2L1, is expressed by type III taste cells in the mouse. *Chem Senses,* 33**,** 243-54.

KAYANO, T., BURANT, C. F., FUKUMOTO, H., GOULD, G. W., FAN, Y. S., EDDY, R. L., BYERS, M. G., SHOWS, T. B., SEINO, S. & BELL, G. I. 1990. Human facilitative glucose transporters. Isolation, functional characterization, and gene localization of cDNAs encoding an isoform (GLUT5) expressed in small intestine, kidney, muscle, and adipose tissue and an unusual glucose transporter pseudogene-like sequence (GLUT6). *J Biol Chem,* 265**,** 13276-82.

KEELAN, M., WALKER, K. & THOMSON, A. B. 1985. Intestinal morphology, marker enzymes and lipid content of brush border membranes from rabbit jejunum and ileum: effect of aging. *Mech Ageing Dev,* 31**,** 49-68.

KELLETT, G. L. 2001. The facilitated component of intestinal glucose absorption. *J Physiol,* 531**,** 585-95.

KELLETT, G. L. & BROT-LAROCHE, E. 2005. Apical GLUT2: a major pathway of intestinal sugar absorption. *Diabetes,* 54**,** 3056-62.

KELLETT, G. L., BROT-LAROCHE, E., MACE, O. J. & LETURQUE, A. 2008. Sugar absorption in the intestine: the role of GLUT2. *Annu Rev Nutr,* 28**,** 35-54.

KELLETT, G. L. & HELLIWELL, P. A. 2000. The diffusive component of intestinal glucose absorption is mediated by the glucose-induced recruitment of GLUT2 to the brush-border membrane. *Biochem J,* 350 Pt 1**,** 155-62.

KELLEY, D. E., MINTUN, M. A., WATKINS, S. C., SIMONEAU, J. A., JADALI, F., FREDRICKSON, A., BEATTIE, J. & THERIAULT, R. 1996. The effect of non-insulin-dependent diabetes mellitus and obesity on glucose transport and phosphorylation in skeletal muscle. *J Clin Invest,* 97**,** 2705-13.

KESSLER, M., ACUTO, O., STORELLI, C., MURER, H., MULLER, M. & SEMENZA, G. 1978. A modified procedure for the rapid preparation of efficiently transporting vesicles from small intestinal brush border membranes. Their use in investigating some properties of D-glucose and choline transport systems. *Biochim Biophys Acta,* 506**,** 136-54.

KHAN, A. H. & PESSIN, J. E. 2002. Insulin regulation of glucose uptake: a complex interplay of intracellular signalling pathways. *Diabetologia,* 45**,** 1475-83.

KIDO, Y., NAKAE, J. & ACCILI, D. 2001. Clinical review 125: The insulin receptor and its cellular targets. *J Clin Endocrinol Metab,* 86**,** 972-9.

KIEFFER, T. J. & HABENER, J. F. 1999. The glucagon-like peptides. *Endocr Rev,* 20**,** 876-913.

KIEFFER, T. J., MCINTOSH, C. H. & PEDERSON, R. A. 1995. Degradation of glucose-dependent insulinotropic polypeptide and truncated glucagon-like peptide 1 in vitro and in vivo by dipeptidyl peptidase IV. *Endocrinology,* 136**,** 3585-96.

KIMMICH, G. A. & CARTER-SU, C. 1978. Membrane potentials and the energetics of intestinal Na+-dependent transport systems. *Am J Physiol,* 235**,** C73-81.

KIMMICH, G. A., CARTER-SU, C. & RANDLES, J. 1977. Energetics of Na+-dependent sugar transport by isolated intestinal cells: evidence for a major role for membrane potentials. *Am J Physiol,* 233**,** E357-62.

KINNAMON, S. C. 2012. Taste receptor signalling - from tongues to lungs. *Acta Physiol (Oxf),* 204**,** 158-68.

KINNAMON, S. C. & VANDENBEUCH, A. 2009. Receptors and transduction of umami taste stimuli. *Ann N Y Acad Sci,* 1170**,** 55-9.

KINNE, R. K. & CASTANEDA, F. 2011. SGLT inhibitors as new therapeutic tools in the treatment of diabetes. *Handb Exp Pharmacol***,** 105-26.

KLETT, E. L., LEE, M. H., ADAMS, D. B., CHAVIN, K. D. & PATEL, S. B. 2004. Localization of ABCG5 and ABCG8 proteins in human liver, gall bladder and intestine. *BMC Gastroenterol,* 4**,** 21.

KNOWLER, W. C., BARRETT-CONNOR, E., FOWLER, S. E., HAMMAN, R. F., LACHIN, J. M., WALKER, E. A. & NATHAN, D. M. 2002. Reduction in the incidence of type 2 diabetes with lifestyle intervention or metformin. *N Engl J Med,* 346**,** 393-403.

KOGA, M., MURAI, J., SAITO, H., MUKAI, M. & KASAYAMA, S. 2010. Habitual intake of dairy products influences serum 1,5-anhydroglucitol levels independently of plasma glucose. *Diabetes Res Clin Pract,* 90**,** 122-5.

KOKRASHVILI, Z., MOSINGER, B. & MARGOLSKEE, R. F. 2009. T1r3 and alpha-gustducin in gut regulate secretion of glucagon-like peptide-1. *Ann N Y Acad Sci,* 1170**,** 91-4.

KOMODA, T., SAKAGISHI, Y. & SEKINE, T. 1981. Multiple forms of human intestinal alkaline phosphatase: chemical and enzymatic properties, and circulating clearances of the fast- and slow-moving enzymes. *Clin Chim Acta,* 117**,** 167-87.

KONG, C. T., YET, S. F. & LEVER, J. E. 1993. Cloning and expression of a mammalian Na+/amino acid cotransporter with sequence similarity to Na+/glucose cotransporters. *J Biol Chem,* 268**,** 1509-12.

KOON, H. W. & POTHOULAKIS, C. 2006. Immunomodulatory properties of substance P: the gastrointestinal system as a model. *Ann N Y Acad Sci,* 1088**,** 23-40.

KORN, T., KUHLKAMP, T., TRACK, C., SCHATZ, I., BAUMGARTEN, K., GORBOULEV, V. & KOEPSELL, H. 2001. The plasma membrane-associated protein RS1 decreases transcription of the transporter SGLT1 in confluent LLC-PK1 cells. *J Biol Chem,* 276**,** 45330-40.

KRAMER, J., MOELLER, E. L., HACHEY, A., MANSFIELD, K. G. & WACHTMAN, L. M. 2009. Differential expression of GLUT2 in pancreatic islets and kidneys of New and Old World nonhuman primates. *Am J Physiol Regul Integr Comp Physiol,* 296**,** R786-93.

KRAUSE, J. E., MACDONALD, M. R. & TAKEDA, Y. 1989. The polyprotein nature of substance P precursors. *Bioessays,* 10**,** 62-9.

KUOKKANEN, M., KOKKONEN, J., ENATTAH, N. S., YLISAUKKO-OJA, T., KOMU, H., VARILO, T., PELTONEN, L., SAVILAHTI, E. & JARVELA, I. 2006. Mutations in the translated region of the lactase gene (LCT) underlie congenital lactase deficiency. *Am J Hum Genet,* 78**,** 339-44.

KUROKAWA, T., HASHIDA, F., KAWABATA, S. & ISHIBASHI, S. 1995. Evidence for the regulation of small intestinal Na+/glucose cotransporter by insulin. *Biochemistry and Molecular Biology International,* 37**,** 33-38.

LABURTHE, M., COUVINEAU, A. & TAN, V. 2007. Class II G protein-coupled receptors for VIP and PACAP: structure, models of activation and pharmacology. *Peptides,* 28**,** 1631-9.

LACHAAL, M., SPANGLER, R. A. & JUNG, C. Y. 2001. Adenosine and adenosine triphosphate modulate the substrate binding affinity of glucose transporter GLUT1 in vitro. *Biochim Biophys Acta,* 1511**,** 123-33.

LALLES, J. P. 2010. Intestinal alkaline phosphatase: multiple biological roles in maintenance of intestinal homeostasis and modulation by diet. *Nutr Rev,* 68**,** 323-32.

LAM, J. T., MARTIN, M. G., TURK, E., HIRAYAMA, B. A., BOSSHARD, N. U., STEINMANN, B. & WRIGHT, E. M. 1999. Missense mutations in SGLT1 cause glucose-galactose malabsorption by trafficking defects. *Biochim Biophys Acta,* 1453**,** 297-303.

LAMBERT, D. W., WOOD, I. S., ELLIS, A. & SHIRAZI-BEECHEY, S. P. 2002. Molecular changes in the expression of human colonic nutrient transporters during the transition from normality to malignancy. *Br J Cancer,* 86**,** 1262-9.

LANE, J. S., WHANG, E. E., RIGBERG, D. A., HINES, O. J., KWAN, D., ZINNER, M. J., MCFADDEN, D. W., DIAMOND, J. & ASHLEY, S. W. 1999. Paracellular glucose transport plays a minor role in the unanesthetized dog. *Am J Physiol,* 276**,** G789-94.

LAPUERTA, P., ROSENSTOCK, J., ZAMBROWICZ, B., POWELL, D. R., OGBAA, I., FREIMAN, J., CEFALU, W. T., BANKS, P., FRAZIER, K., KELLY, M. & SANDS, A. 2013. Study Design and Rationale of a Dose-Ranging Trial of LX4211, a Dual Inhibitor of SGLT1 and SGLT2, in Type 2 Diabetes Inadequately Controlled on Metformin Monotherapy. *Clin Cardiol*.

LARANCE, M., RAMM, G. & JAMES, D. E. 2008. The GLUT4 code. *Mol Endocrinol,* 22**,** 226-33.

LARSSON, L. I., HOLST, J., HAKANSON, R. & SUNDLER, F. 1975. Distribution and properties of glucagon immunoreactivity in the digestive tract of various mammals: an immunohistochemical and immunochemical study. *Histochemistry,* 44**,** 281-90.

LECETA, J., GOMARIZ, R. P., MARTINEZ, C., ABAD, C., GANEA, D. & DELGADO, M. 2000. Receptors and transcriptional factors involved in the anti-inflammatory activity of VIP and PACAP. *Ann N Y Acad Sci,* 921**,** 92-102.

LEE, W. Y., LOFLIN, P., CLANCEY, C. J., PENG, H. & LEVER, J. E. 2000. Cyclic nucleotide regulation of Na+/glucose cotransporter (SGLT1) mRNA stability. Interaction of a nucleocytoplasmic protein with a regulatory domain in the 3'-untranslated region critical for stabilization. *J Biol Chem,* 275**,** 33998-4008.

LEE, Y. C., HUANG, H. Y., CHANG, C. J., CHENG, C. H. & CHEN, Y. T. 2010. Mitochondrial GLUT10 facilitates dehydroascorbic acid import and protects cells against oxidative stress: mechanistic insight into arterial tortuosity syndrome. *Hum Mol Genet,* 19**,** 3721-33.

LI, H., PAKSTIS, A. J., KIDD, J. R. & KIDD, K. K. 2011. Selection on the human bitter taste gene, TAS2R16, in Eurasian populations. *Hum Biol,* 83**,** 363-77.

LI, Q., MANOLESCU, A., RITZEL, M., YAO, S., SLUGOSKI, M., YOUNG, J. D., CHEN, X. Z. & CHEESEMAN, C. I. 2004. Cloning and functional characterization of the human GLUT7 isoform SLC2A7 from the small intestine. *Am J Physiol Gastrointest Liver Physiol,* 287**,** G236-42.

LI, W. M. & MCNEILL, J. H. 1997. Quantitative methods for measuring the insulin-regulatable glucose transporter (Glut4). *J Pharmacol Toxicol Methods,* 38**,** 1-10.

LI, X., STASZEWSKI, L., XU, H., DURICK, K., ZOLLER, M. & ADLER, E. 2002. Human receptors for sweet and umami taste. *Proc Natl Acad Sci U S A,* 99**,** 4692-6.

LINDEN, K. C., DEHAAN, C. L., ZHANG, Y., GLOWACKA, S., COX, A. J., KELLY, D. J. & ROGERS, S. 2006. Renal expression and localization of the facilitative glucose transporters GLUT1 and GLUT12 in animal models of hypertension and diabetic nephropathy. *Am J Physiol Renal Physiol,* 290**,** F205-13.

LITHERLAND, G. J., HAJDUCH, E., GOULD, G. W. & HUNDAL, H. S. 2004. Fructose transport and metabolism in adipose tissue of Zucker rats: diminished GLUT5 activity during obesity and insulin resistance. *Mol Cell Biochem,* 261**,** 23-33.

LIU, L., YU, Y. L., LIU, C., WANG, X. T., LIU, X. D. & XIE, L. 2011. Insulin deficiency induces abnormal increase in intestinal disaccharidase activities and expression under diabetic states, evidences from in vivo and in vitro study. *Biochem Pharmacol,* 82**,** 1963-70.

LIU, S., ZHAO, Y., HEMPE, J. M., FONSECA, V. & SHI, L. 2012. Economic burden of hypoglycemia in patients with Type 2 diabetes. *Expert Rev Pharmacoecon Outcomes Res,* 12**,** 47-51.

LJUNGMANN, K., HARTMANN, B., KISSMEYER-NIELSEN, P., FLYVBJERG, A., HOLST, J. J. & LAURBERG, S. 2001. Time-dependent intestinal adaptation and GLP-2 alterations after small bowel resection in rats. *Am J Physiol Gastrointest Liver Physiol,* 281**,** G779-85.

LOFLIN, P. & LEVER, J. E. 2001. HuR binds a cyclic nucleotide-dependent, stabilizing domain in the 3' untranslated region of Na(+)/glucose cotransporter (SGLT1) mRNA. *FEBS Lett,* 509**,** 267-71.

LOMBARDI, M. S., KAVELAARS, A. & HEIJNEN, C. J. 2002. Role and modulation of G protein-coupled receptor signaling in inflammatory processes. *Crit Rev Immunol,* 22**,** 141-63.

LOO, D. D., HIRAYAMA, B. A., GALLARDO, E. M., LAM, J. T., TURK, E. & WRIGHT, E. M. 1998. Conformational changes couple Na+ and glucose transport. *Proceedings of the National Academy of Sciences of the United States of America,* 95**,** 7789-94.

LOO, D. D., HIRAYAMA, B. A., KARAKOSSIAN, M. H., MEINILD, A. K. & WRIGHT, E. M. 2006. Conformational dynamics of hSGLT1 during Na+/glucose cotransport. *J Gen Physiol,* 128**,** 701-20.

LOO, D. D., WRIGHT, E. M. & ZEUTHEN, T. 2002. Water pumps. *J Physiol,* 542**,** 53-60.

LOO, D. D., ZEUTHEN, T., CHANDY, G. & WRIGHT, E. M. 1996. Cotransport of water by the Na+/glucose cotransporter. *Proc Natl Acad Sci U S A,* 93**,** 13367-70.

LOREN, I., EMSON, P. C., FAHRENKRUG, J., BJORKLUND, A., ALUMETS, J., HAKANSON, R. & SUNDLER, F. 1979. Distribution of vasoactive intestinal polypeptide in the rat and mouse brain. *Neuroscience,* 4**,** 1953-76.

LORENZ-MEYER, H., THIEL, F., MENGE, H., GOTTESBUREN, H. & RIECKEN, E. O. 1977. Structural and functional studies on the transformation of the intestinal mucosa in rats with experimental diabetes. *Res Exp Med (Berl),* 170**,** 89-99.

MACE, O. J., MORGAN, E. L., AFFLECK, J. A., LISTER, N. & KELLETT, G. L. 2007. Calcium absorption by Cav1.3 induces terminal web myosin II phosphorylation and apical GLUT2 insertion in rat intestine. *J Physiol,* 580**,** 605-16.

MADARA, J. L., NEUTRA, M. R. & TRIER, J. S. 1981. Junctional complexes in fetal rat small intestine during morphogenesis. *Dev Biol,* 86**,** 170-8.

MAHRAOUI, L., TAKEDA, J., MESONERO, J., CHANTRET, I., DUSSAULX, E., BELL, G. I. & BROT-LAROCHE, E. 1994. Regulation of expression of the human fructose transporter (GLUT5) by cyclic AMP. *Biochem J,* 301 (Pt 1)**,** 169-75.

MANTEI, N., VILLA, M., ENZLER, T., WACKER, H., BOLL, W., JAMES, P., HUNZIKER, W. & SEMENZA, G. 1988. Complete primary structure of human and rabbit lactase-phlorizin hydrolase: implications for biosynthesis, membrane anchoring and evolution of the enzyme. *EMBO J,* 7**,** 2705-13.

MARGOLSKEE, R. F., DYER, J., KOKRASHVILI, Z., SALMON, K. S., ILEGEMS, E., DALY, K., MAILLET, E. L., NINOMIYA, Y., MOSINGER, B. & SHIRAZI-BEECHEY, S. P. 2007. T1R3 and gustducin in gut sense sugars to regulate expression of Na+-glucose cotransporter 1. *Proc Natl Acad Sci U S A,* 104**,** 15075-80.

MARTIN, M. G., LOSTAO, M. P., TURK, E., LAM, J., KREMAN, M. & WRIGHT, E. M. 1997. Compound missense mutations in the sodium/D-glucose cotransporter result in trafficking defects. *Gastroenterology,* 112**,** 1206-12.

MARTIN, M. G., TURK, E., LOSTAO, M. P., KERNER, C. & WRIGHT, E. M. 1996. Defects in Na+/glucose cotransporter (SGLT1) trafficking and function cause glucose-galactose malabsorption. *Nat Genet,* 12**,** 216-20.

MARTINEZ, I. M., MORALES, I., GARCIA-PINO, G., CAMPILLO, J. E. & TORMO, M. A. 2003. Experimental type 2 diabetes induces enzymatic changes in isolated rat enterocytes. *Exp Diabesity Res,* 4**,** 119-23.

MARTINI, F. H., OBER, W. C. & GARRISON, C. W. 2001. Fundamentals of anatomy and physiology. 5th ed. Prentic Hall, USA

MATE, A., DE LA HERMOSA, M. A., BARFULL, A., PLANAS, J. M. & VAZQUEZ, C. M. 2001. Characterization of D-fructose transport by rat kidney brush-border membrane vesicles: changes in hypertensive rats. *Cell Mol Life Sci,* 58**,** 1961-7.

MATHER, A. & POLLOCK, C. 2011. Glucose handling by the kidney. *Kidney Int Suppl***,** S1-6.

MATSUTANI, A., HING, A., STEINBRUECK, T., JANSSEN, R., WEBER, J., PERMUTT, M. A. & DONIS-KELLER, H. 1992. Mapping the human liver/islet glucose transporter (GLUT2) gene within a genetic linkage map of chromosome 3q using a (CA)n dinucleotide repeat polymorphism and characterization of the polymorphism in three racial groups. *Genomics,* 13**,** 495-501.

MCCONALOGUE, K. & FURNESS, J. B. 1994. Gastrointestinal neurotransmitters. *Baillieres Clin Endocrinol Metab,* 8**,** 51-76.

MCVIE-WYLIE, A. J., LAMSON, D. R. & CHEN, Y. T. 2001. Molecular cloning of a novel member of the GLUT family of transporters, SLC2a10 (GLUT10), localized on chromosome 20q13.1: a candidate gene for NIDDM susceptibility. *Genomics,* 72**,** 113-7.

MEDDINGS, J. B., DESOUZA, D., GOEL, M. & THIESEN, S. 1990. Glucose transport and microvillus membrane physical properties along the crypt-villus axis of the rabbit. *J Clin Invest,* 85**,** 1099-107.

MEINILD, A., KLAERKE, D. A., LOO, D. D., WRIGHT, E. M. & ZEUTHEN, T. 1998. The human Na+-glucose cotransporter is a molecular water pump. *J Physiol,* 508**,** 15-21.

MENG, W., ELLSWORTH, B. A., NIRSCHL, A. A., MCCANN, P. J., PATEL, M., GIROTRA, R. N., WU, G., SHER, P. M., MORRISON, E. P., BILLER, S. A., ZAHLER, R., DESHPANDE, P. P., PULLOCKARAN, A., HAGAN, D. L., MORGAN, N., TAYLOR, J. R., OBERMEIER, M. T., HUMPHREYS, W. G., KHANNA, A., DISCENZA, L., ROBERTSON, J. G., WANG, A., HAN, S., WETTERAU, J. R., JANOVITZ, E. B., FLINT, O. P., WHALEY, J. M. & WASHBURN, W. N. 2008. Discovery of dapagliflozin: a potent, selective renal sodium-dependent glucose cotransporter 2 (SGLT2) inhibitor for the treatment of type 2 diabetes. *J Med Chem,* 51**,** 1145-9.

MEREDIZ, E. F., DYER, J., SALMON, K. S. & SHIRAZI-BEECHEY, S. P. 2004. Molecular characterisation of fructose transport in equine small intestine. *Equine Vet J,* 36**,** 532-8.

MERIGHI, A., SALIO, C., FERRINI, F. & LOSSI, L. 2011. Neuromodulatory function of neuropeptides in the normal CNS. *J Chem Neuroanat,* 42**,** 276-87.

MICHEL, V., YUAN, Z., RAMSUBIR, S. & BAKOVIC, M. 2006. Choline transport for phospholipid synthesis. *Exp Biol Med (Maywood),* 231**,** 490-504.

MIGUEL-ALIAGA, I. 2012. Nerveless and gutsy: intestinal nutrient sensing from invertebrates to humans. *Semin Cell Dev Biol*.

MILLER, D. L., HANSON, W., SCHEDL, H. P. & OSBORNE, J. W. 1977. Proliferation rate and transit time of mucosal cells in small intestine of the diabetic rat. *Gastroenterology,* 73**,** 1326-32.

MILLER, P. J., FINUCANE, K. A., HUGHES, M. & ZHAO, F. Q. 2005. Cloning and expression of bovine glucose transporter GLUT12. *Mamm Genome,* 16**,** 873-83.

MIURA, T., SUZUKI, W., ISHIHARA, E., ARAI, I., ISHIDA, H., SEINO, Y. & TANIGAWA, K. 2001. Impairment of insulin-stimulated GLUT4 translocation in skeletal muscle and adipose tissue in the Tsumura Suzuki obese diabetic mouse: a new genetic animal model of type 2 diabetes. *Eur J Endocrinol,* 145**,** 785-90.

MIYAMOTO, K., HASE, K., TAKAGI, T., FUJII, T., TAKETANI, Y., MINAMI, H., OKA, T. & NAKABOU, Y. 1993. Differential responses of intestinal glucose transporter mRNA transcripts to levels of dietary sugars. *Biochem J,* 295 (Pt 1)**,** 211-5.

MIYAMOTO, K., HASE, K., TAKETANI, Y., MINAMI, H., OKA, T., NAKABOU, Y. & HAGIHIRA, H. 1991. Diabetes and glucose transporter gene expression in rat small intestine. *Biochem Biophys Res Commun,* 181**,** 1110-7.

MIYAMOTO, K., TATSUMI, S., MORIMOTO, A., MINAMI, H., YAMAMOTO, H., SONE, K., TAKETANI, Y., NAKABOU, Y., OKA, T. & TAKEDA, E. 1994. Characterization of the rabbit intestinal fructose transporter (GLUT5). *Biochem J,* 303 (Pt 3)**,** 877-83.

MIYATA, A., ARIMURA, A., DAHL, R. R., MINAMINO, N., UEHARA, A., JIANG, L., CULLER, M. D. & COY, D. H. 1989. Isolation of a novel 38 residue-hypothalamic polypeptide which stimulates adenylate cyclase in pituitary cells. *Biochem Biophys Res Commun,* 164**,** 567-74.

MIYATA, A., JIANG, L., DAHL, R. D., KITADA, C., KUBO, K., FUJINO, M., MINAMINO, N. & ARIMURA, A. 1990. Isolation of a neuropeptide corresponding to the N-terminal 27 residues of the pituitary adenylate cyclase activating polypeptide with 38 residues (PACAP38). *Biochem Biophys Res Commun,* 170**,** 643-8.

MOCHIZUKI, K., SAKAGUCHI, N. & GODA, T. 2007. Triiodothyronine (T3) and fructose coordinately enhance expression of the GLUT5 gene in the small intestine of rats during weaning period. *Biosci Biotechnol Biochem,* 71**,** 1345-7.

MOHLKE, K. L., SKOL, A. D., SCOTT, L. J., VALLE, T. T., BERGMAN, R. N., TUOMILEHTO, J., BOEHNKE, M. & COLLINS, F. S. 2005. Evaluation of SLC2A10 (GLUT10) as a candidate gene for type 2 diabetes and related traits in Finns. *Mol Genet Metab,* 85**,** 323-7.

MOJSOV, S., HEINRICH, G., WILSON, I. B., RAVAZZOLA, M., ORCI, L. & HABENER, J. F. 1986. Preproglucagon gene expression in pancreas and intestine diversifies at the level of post-translational processing. *J Biol Chem,* 261**,** 11880-9.

MONTES, R. G., GOTTAL, R. F., BAYLESS, T. M., HENDRIX, T. R. & PERMAN, J. A. 1992. Breath hydrogen testing as a physiology laboratory exercise for medical students. *Am J Physiol,* 262**,** S25-8.

MONTGOMERY, R. K., BULLER, H. A., RINGS, E. H. & GRAND, R. J. 1991. Lactose intolerance and the genetic regulation of intestinal lactase-phlorizin hydrolase. *FASEB journal : official publication of the Federation of American Societies for Experimental Biology,* 5**,** 2824-32.

MORAN, A. W., AL-RAMMAHI, M. A., ARORA, D. K., BATCHELOR, D. J., COULTER, E. A., DALY, K., IONESCU, C., BRAVO, D. & SHIRAZI-BEECHEY, S. P. 2010a. Expression of Na+/glucose co-transporter 1 (SGLT1) is enhanced by supplementation of the diet of weaning piglets with artificial sweeteners. *Br J Nutr,* 104**,** 637-46.

MORAN, A. W., AL-RAMMAHI, M. A., ARORA, D. K., BATCHELOR, D. J., COULTER, E. A., IONESCU, C., BRAVO, D. & SHIRAZI-BEECHEY, S. P. 2010b. Expression of Na+/glucose co-transporter 1 (SGLT1) in the intestine of piglets weaned to different concentrations of dietary carbohydrate. *Br J Nutr,* 104**,** 647-55.

MORTENSEN, K., CHRISTENSEN, L. L., HOLST, J. J. & ORSKOV, C. 2003. GLP-1 and GIP are colocalized in a subset of endocrine cells in the small intestine. *Regul Pept,* 114**,** 189-96.

MUECKLER, M. 1994. Facilitative glucose transporters. *Eur J Biochem,* 219**,** 713-25.

MUNROE, D. G., GUPTA, A. K., KOOSHESH, F., VYAS, T. B., RIZKALLA, G., WANG, H., DEMCHYSHYN, L., YANG, Z. J., KAMBOJ, R. K., CHEN, H., MCCALLUM, K., SUMNER-SMITH, M., DRUCKER, D. J. & CRIVICI, A. 1999. Prototypic G protein-coupled receptor for the intestinotrophic factor glucagon-like peptide 2. *Proc Natl Acad Sci U S A,* 96**,** 1569-73.

MURER, H. & HOPFER, U. 1974. Demonstration of electrogenic Na+-dependent D-glucose transport in intestinal brush border membranes. *Proc Natl Acad Sci U S A,* 71**,** 484-8.

MURER, H. & KINNE, R. 1980. The use of isolated membrane vesicles to study epithelial transport processes. *J Membr Biol,* 55**,** 81-95.

MURRAY-LYON, I. M., EDDLESTON, A. L., WILLIAMS, R., BROWN, M., HOGBIN, B. M., BENNETT, A., EDWARDS, J. C. & TAYLOR, K. W. 1968. Treatment of multiple-hormone-producing malignant islet-cell tumour with streptozotocin. *Lancet,* 2**,** 895-8.

MUTT, V. & SAID, S. I. 1974. Structure of the porcine vasoactive intestinal octacosapeptide. The amino-acid sequence. Use of kallikrein in its determination. *Eur J Biochem,* 42**,** 581-9.

NAFTALIN, R. J. 2008. Osmotic water transport with glucose in GLUT2 and SGLT. *Biophys J,* 94**,** 3912-23.

NAIM, H. Y., JACOB, R., NAIM, H., SAMBROOK, J. F. & GETHING, M. J. 1994. The pro region of human intestinal lactase-phlorizin hydrolase. *J Biol Chem,* 269**,** 26933-43.

NAIM, H. Y., STERCHI, E. E. & LENTZE, M. J. 1988. Biosynthesis of the human sucrase-isomaltase complex. Differential O-glycosylation of the sucrase subunit correlates with its position within the enzyme complex. *J Biol Chem,* 263**,** 7242-53.

NAKAGAWA, Y., NAGASAWA, M., YAMADA, S., HARA, A., MOGAMI, H., NIKOLAEV, V. O., LOHSE, M. J., SHIGEMURA, N., NINOMIYA, Y. & KOJIMA, I. 2009. Sweet taste receptor expressed in pancreatic beta-cells activates the calcium and cyclic AMP signaling systems and stimulates insulin secretion. *PLoS One,* 4**,** e5106.

NASSAR, C. F., ABDALLAH, L. E., BARADA, K. A., ATWEH, S. F. & SAADE, N. E. 1995. Effects of intravenous vasoactive intestinal peptide injection on jejunal alanine absorption and gastric acid secretion in rats. *Regul Pept,* 55**,** 261-7.

NELSON, G., HOON, M. A., CHANDRASHEKAR, J., ZHANG, Y., RYBA, N. J. & ZUKER, C. S. 2001. Mammalian sweet taste receptors. *Cell,* 106**,** 381-90.

NICHOLS, B. L., AVERY, S., SEN, P., SWALLOW, D. M., HAHN, D. & STERCHI, E. 2003. The maltase-glucoamylase gene: common ancestry to sucrase-isomaltase with complementary starch digestion activities. *Proc Natl Acad Sci U S A,* 100**,** 1432-7.

NICHOLS, B. L., ELDERING, J., AVERY, S., HAHN, D., QUARONI, A. & STERCHI, E. 1998. Human small intestinal maltase-glucoamylase cDNA cloning. Homology to sucrase-isomaltase. *J Biol Chem,* 273**,** 3076-81.

NICHOLS, B. L., QUEZADA-CALVILLO, R., ROBAYO-TORRES, C. C., AO, Z., HAMAKER, B. R., BUTTE, N. F., MARINI, J., JAHOOR, F. & STERCHI, E. E. 2009. Mucosal maltase-glucoamylase plays a crucial role in starch digestion and prandial glucose homeostasis of mice. *J Nutr,* 139**,** 684-90.

NOBIGROT, T., CHASALOW, F. I. & LIFSHITZ, F. 1997. Carbohydrate absorption from one serving of fruit juice in young children: age and carbohydrate composition effects. *J Am Coll Nutr,* 16**,** 152-8.

NOREN, O., SJOSTROM, H., COWELL, G. M., TRANUM-JENSEN, J., HANSEN, O. C. & WELINDER, K. G. 1986. Pig intestinal microvillar maltase-glucoamylase. Structure and membrane insertion. *J Biol Chem,* 261**,** 12306-9.

O'CONNOR, J. C., JOHNSON, D. R. & FREUND, G. G. 2006. Psychoneuroimmune implications of type 2 diabetes. *Neurol Clin,* 24**,** 539-59.

O'CONNOR, T. M., O'CONNELL, J., O'BRIEN, D. I., GOODE, T., BREDIN, C. P. & SHANAHAN, F. 2004. The role of substance P in inflammatory disease. *J Cell Physiol,* 201**,** 167-80.

OKU, A., UETA, K., ARAKAWA, K., KANO-ISHIHARA, T., MATSUMOTO, T., ADACHI, T., YASUDA, K., TSUDA, K., IKEZAWA, K. & SAITO, A. 2000. Correction of hyperglycemia and insulin sensitivity by T-1095, an inhibitor of renal Na+-glucose cotransporters, in streptozotocin-induced diabetic rats. *Jpn J Pharmacol,* 84**,** 351-4.

OLSEN, W. A. & ROSENBERG, I. H. 1970. Intestinal transport of sugars and amino acids in diabetic rats. *J Clin Invest,* 49**,** 96-105.

OLSON, A. L. & PESSIN, J. E. 1996. Structure, function, and regulation of the mammalian facilitative glucose transporter gene family. *Annu Rev Nutr,* 16**,** 235-56.

OTIENO, C. F., HUHO, A. N., OMONGE, E. O., AMAYO, A. A. & NJAGI, E. 2008. Type 2 diabetes mellitus: clinical and aetiologic types, therapy and quality of glycaemic control of ambulatory patients. *East Afr Med J,* 85**,** 24-9.

OUELLETTE, A. J., SATCHELL, D. P., HSIEH, M. M., HAGEN, S. J. & SELSTED, M. E. 2000. Characterization of luminal paneth cell alpha-defensins in mouse small intestine. Attenuated antimicrobial activities of peptides with truncated amino termini. *J Biol Chem,* 275**,** 33969-73.

PALMER, R. 2004. An overview of diabetic ketoacidosis. *Nurs Stand,* 19**,** 42-4.

PESSIN, J. E. & BELL, G. I. 1992. Mammalian facilitative glucose transporter family: structure and molecular regulation. *Annu Rev Physiol,* 54**,** 911-30.

PHAY, J. E., HUSSAIN, H. B. & MOLEY, J. F. 2000. Cloning and expression analysis of a novel member of the facilitative glucose transporter family, SLC2A9 (GLUT9). *Genomics,* 66**,** 217-20.

PHILLIPS, L. K. & PRINS, J. B. 2011. Update on incretin hormones. *Ann N Y Acad Sci,* 1243**,** E55-74.

PILCH, P. F. 2008. The mass action hypothesis: formation of Glut4 storage vesicles, a tissue-specific, regulated exocytic compartment. *Acta Physiol (Oxf),* 192**,** 89-101.

PINTO, A. B., CARAYANNOPOULOS, M. O., HOEHN, A., DOWD, L. & MOLEY, K. H. 2002. Glucose transporter 8 expression and translocation are critical for murine blastocyst survival. *Biol Reprod,* 66**,** 1729-33.

POWLEY, T. L., SPAULDING, R. A. & HAGLOF, S. A. 2011. Vagal afferent innervation of the proximal gastrointestinal tract mucosa: chemoreceptor and mechanoreceptor architecture. *J Comp Neurol,* 519**,** 644-60.

PRABHU, R., PERAKATH, B. & BALASUBRAMANIAN, K. A. 2003. Isolation of human small intestinal brush border membranes using polyethylene glycol and effect of exposure to various oxidants in vitro. *Dig Dis Sci,* 48**,** 995-1001.

PREITNER, F., BONNY, O., LAVERRIERE, A., ROTMAN, S., FIRSOV, D., DA COSTA, A., METREF, S. & THORENS, B. 2009. Glut9 is a major regulator of urate homeostasis and its genetic inactivation induces hyperuricosuria and urate nephropathy. *Proc Natl Acad Sci U S A,* 106**,** 15501-6.

PRIETO, R. M., FERRER, M., RAYO, J. M. & TUR, J. A. 1994. Disaccharidase activities in pregnant and lactating rats. *Comp Biochem Physiol A Physiol,* 109**,** 741-7.

PUAVILAI, G., CHANPRASERTYOTIN, S. & SRIPHRAPRADAENG, A. 1999. Diagnostic criteria for diabetes mellitus and other categories of glucose intolerance: 1997 criteria by the Expert Committee on the Diagnosis and Classification of Diabetes Mellitus (ADA), 1998 WHO consultation criteria, and 1985 WHO criteria. World Health Organization. *Diabetes Res Clin Pract,* 44**,** 21-6.

QUEZADA-CALVILLO, R., ROBAYO-TORRES, C. C., OPEKUN, A. R., SEN, P., AO, Z., HAMAKER, B. R., QUARONI, A., BRAYER, G. D., WATTLER, S., NEHLS, M. C., STERCHI, E. E. & NICHOLS, B. L. 2007. Contribution of mucosal maltase-glucoamylase activities to mouse small intestinal starch alpha-glucogenesis. *J Nutr,* 137**,** 1725-33.

RAMSANAHIE, A., DUXBURY, M. S., GRIKSCHEIT, T. C., PEREZ, A., RHOADS, D. B., GARDNER-THORPE, J., OGILVIE, J., ASHLEY, S. W., VACANTI, J. P. & WHANG, E. E. 2003. Effect of GLP-2 on mucosal morphology and SGLT1 expression in tissue-engineered neointestine. *Am J Physiol Gastrointest Liver Physiol,* 285**,** G1345-52.

RASOAMANANA, R., DARCEL, N., FROMENTIN, G. & TOME, D. 2012. Nutrient sensing and signalling by the gut. *Proc Nutr Soc***,** 1-10.

RAYBOULD, H. E. 2007. Sensing of glucose in the gastrointestinal tract. *Auton Neurosci,* 133**,** 86-90.

REHFELD, J. F. 1998. The new biology of gastrointestinal hormones. *Physiol Rev,* 78**,** 1087-108.

REHFELD, J. F. 2004. A centenary of gastrointestinal endocrinology. *Horm Metab Res,* 36**,** 735-41.

REID, T. W., MURPHY, C. J., IWAHASHI, C. K., FOSTER, B. A. & MANNIS, M. J. 1993. Stimulation of epithelial cell growth by the neuropeptide substance P. *J Cell Biochem,* 52**,** 476-85.

REN, L., QIN, X., CAO, X., WANG, L., BAI, F., BAI, G. & SHEN, Y. 2011. Structural insight into substrate specificity of human intestinal maltase-glucoamylase. *Protein Cell,* 2**,** 827-36.

RHOADS, D. B., ROSENBAUM, D. H., UNSAL, H., ISSELBACHER, K. J. & LEVITSKY, L. L. 1998. Circadian periodicity of intestinal Na+/glucose cotransporter 1 mRNA levels is transcriptionally regulated. *J Biol Chem,* 273**,** 9510-6.

RINDI, G., LEITER, A. B., KOPIN, A. S., BORDI, C. & SOLCIA, E. 2004. The "normal" endocrine cell of the gut: changing concepts and new evidences. *Ann N Y Acad Sci,* 1014**,** 1-12.

ROSE, R. C., CHOI, J. L. & KOCH, M. J. 1988. Intestinal transport and metabolism of oxidized ascorbic acid (dehydroascorbic acid). *Am J Physiol,* 254**,** G824-8.

ROSS, M., KAYE, G. & PAWLINA, W. 2003. *Histology: a text and atlas*, Baltimore: Lippincott Williams & Wilkins.

ROWLAND, A. F., FAZAKERLEY, D. J. & JAMES, D. E. 2011. Mapping insulin/GLUT4 circuitry. *Traffic,* 12**,** 672-81.

ROZENGURT, E. 2006. Taste receptors in the gastrointestinal tract. I. Bitter taste receptors and alpha-gustducin in the mammalian gut. *Am J Physiol Gastrointest Liver Physiol,* 291**,** G171-7.

SABINO-SILVA, R., MORI, R. C., DAVID-SILVA, A., OKAMOTO, M. M., FREITAS, H. S. & MACHADO, U. F. 2010. The Na(+)/glucose cotransporters: from genes to therapy. *Braz J Med Biol Res,* 43**,** 1019-26.

SALTIEL, A. R. & KAHN, C. R. 2001. Insulin signalling and the regulation of glucose and lipid metabolism. *Nature,* 414**,** 799-806.

SANGILD, P. T., TAPPENDEN, K. A., MALO, C., PETERSEN, Y. M., ELNIF, J., BARTHOLOME, A. L. & BUDDINGTON, R. K. 2006. Glucagon-like peptide 2 stimulates intestinal nutrient absorption in parenterally fed newborn pigs. *J Pediatr Gastroenterol Nutr,* 43**,** 160-7.

SANTER, R., HILLEBRAND, G., STEINMANN, B. & SCHAUB, J. 2003. Intestinal glucose transport: evidence for a membrane traffic-based pathway in humans. *Gastroenterology,* 124**,** 34-9.

SANTER, R., STEINMANN, B. & SCHAUB, J. 2002. Fanconi-Bickel syndrome--a congenital defect of facilitative glucose transport. *Curr Mol Med,* 2**,** 213-27.

SARWAR, N., GAO, P., SESHASAI, S. R., GOBIN, R., KAPTOGE, S., DI ANGELANTONIO, E., INGELSSON, E., LAWLOR, D. A., SELVIN, E., STAMPFER, M., STEHOUWER, C. D., LEWINGTON, S., PENNELLS, L., THOMPSON, A., SATTAR, N., WHITE, I. R., RAY, K. K. & DANESH, J. 2010. Diabetes mellitus, fasting blood glucose concentration, and risk of vascular disease: a collaborative meta-analysis of 102 prospective studies. *Lancet,* 375**,** 2215-22.

SASSELLI, V., PACHNIS, V. & BURNS, A. J. 2012. The enteric nervous system. *Dev Biol,* 366**,** 64-73.

SCHAAPER, W. M. & BEYERMAN, H. C. 1984. Synthesis of vasoactive intestinal peptide (VIP) via the mixed anhydride method. *Peptides,* 5**,** 167-8.

SCHEDL, H. P., AL-JURF, A. S. & WILSON, H. D. 1983. Elevated intestinal disaccharidase activity in the streptozotocin-diabetic rat is independent of enteral feeding. *Diabetes,* 32**,** 265-70.

SCHEDL, H. P. & WILSON, H. D. 1971. Effects of diabetes on intestinal growth in the rat. *J Exp Zool,* 176**,** 487-95.

SCHEEPERS, A., JOOST, H. G. & SCHURMANN, A. 2004. The glucose transporter families SGLT and GLUT: molecular basis of normal and aberrant function. *JPEN J Parenter Enteral Nutr,* 28**,** 364-71.

SCHEEPERS, A., SCHMIDT, S., MANOLESCU, A., CHEESEMAN, C. I., BELL, A., ZAHN, C., JOOST, H. G. & SCHURMANN, A. 2005. Characterization of the human SLC2A11 (GLUT11) gene: alternative promoter usage, function, expression, and subcellular distribution of three isoforms, and lack of mouse orthologue. *Mol Membr Biol,* 22**,** 339-51.

SCHLIENGER, J. L. 2013. [Type 2 diabetes complications]. *Presse Med,* 42**,** 839-48.

SCHMIDT, G. H., WILKINSON, M. M. & PONDER, B. A. 1985. Cell migration pathway in the intestinal epithelium: an in situ marker system using mouse aggregation chimeras. *Cell,* 40**,** 425-9.

SCHMITZ, J., PREISER, H., MAESTRACCI, D., GHOSH, B. K., CERDA, J. J. & CRANE, R. K. 1973. Purification of the human intestinal brush border membrane. *Biochim Biophys Acta,* 323**,** 98-112.

SCHNEDL, W. J., FERBER, S., JOHNSON, J. H. & NEWGARD, C. B. 1994. STZ transport and cytotoxicity. Specific enhancement in GLUT2-expressing cells. *Diabetes,* 43**,** 1326-33.

SCHNEIDER, A. J., KINTER, W. B. & STIRLING, C. E. 1966. Glucose-galactose malabsorption. Report of a case with autoradiographic studies of a mucosal biopsy. *N Engl J Med,* 274**,** 305-12.

SCHURMANN, A., AXER, H., SCHEEPERS, A., DOEGE, H. & JOOST, H. G. 2002. The glucose transport facilitator GLUT8 is predominantly associated with the acrosomal region of mature spermatozoa. *Cell Tissue Res,* 307**,** 237-42.

SCHWARTZ, C. J., KIMBERG, D. V., SHEERIN, H. E., FIELD, M. & SAID, S. I. 1974. Vasoactive intestinal peptide stimulation of adenylate cyclase and active electrolyte secretion in intestinal mucosa. *J Clin Invest,* 54**,** 536-44.

SEATTER, M. J. & GOULD, G. W. 1999. The mammalian facilitative glucose transporter (GLUT) family. *Pharm Biotechnol,* 12**,** 201-28.

SEGADE, F., ALLRED, D. C. & BOWDEN, D. W. 2005. Functional characterization of the promoter of the human glucose transporter 10 gene. *Biochim Biophys Acta,* 1730**,** 147-58.

SESTI, G., FEDERICI, M., HRIBAL, M. L., LAURO, D., SBRACCIA, P. & LAURO, R. 2001. Defects of the insulin receptor substrate (IRS) system in human metabolic disorders. *FASEB J,* 15**,** 2099-111.

SHARP, P. A., BOYER, S., SRAI, S. K., BALDWIN, S. A. & DEBNAM, E. S. 1997. Early diabetes-induced changes in rat jejunal glucose transport and the response to insulin. *J Endocrinol,* 154**,** 19-25.

SHARP, P. A. & DEBNAM, E. S. 1994. The role of cyclic AMP in the control of sugar transport across the brush-border and basolateral membranes of rat jejunal enterocytes. *Exp Physiol,* 79**,** 203-14.

SHARP, P. A., DEBNAM, E. S. & SRAI, S. K. 1996. Rapid enhancement of brush border glucose uptake after exposure of rat jejunal mucosa to glucose. *Gut,* 39**,** 545-50.

SHEPHERD, P. R., GIBBS, E. M., WESSLAU, C., GOULD, G. W. & KAHN, B. B. 1992. Human small intestine facilitative fructose/glucose transporter (GLUT5) is also present in insulin-responsive tissues and brain. Investigation of biochemical characteristics and translocation. *Diabetes,* 41**,** 1360-5.

SHIN, E. D., ESTALL, J. L., IZZO, A., DRUCKER, D. J. & BRUBAKER, P. L. 2005. Mucosal adaptation to enteral nutrients is dependent on the physiologic actions of glucagon-like peptide-2 in mice. *Gastroenterology,* 128**,** 1340-53.

SHIRAZI, S. P., BEECHEY, R. B. & BUTTERWORTH, P. J. 1981a. Potent inhibition of membrane-bound rat intestinal alkaline phosphatase by a new series of phosphate analogues. *Biochem J,* 194**,** 797-802.

SHIRAZI, S. P., BEECHEY, R. B. & BUTTERWORTH, P. J. 1981b. The use of potent inhibitors of alkaline phosphatase to investigate the role of the enzyme in intestinal transport of inorganic phosphate. *Biochem J,* 194**,** 803-9.

SHIRAZI-BEECHEY, S. P. 1995. Molecular biology of intestinal glucose transport. *Nutr Res Rev,* 8**,** 27-41.

SHIRAZI-BEECHEY, S. P., DAVIES, A. G., TEBBUTT, K., DYER, J., ELLIS, A., TAYLOR, C. J., FAIRCLOUGH, P. & BEECHEY, R. B. 1990. Preparation and properties of brush-border membrane vesicles from human small intestine. *Gastroenterology,* 98**,** 676-85.

SHIRAZI-BEECHEY, S. P., GORVEL, J. P. & BEECHEY, R. B. 1988. Phosphate transport in intestinal brush-border membrane. *J Bioenerg Biomembr*, 20**,** 273-88.

SHIRAZI-BEECHEY, S. P., HIRAYAMA, B. A., WANG, Y., SCOTT, D., SMITH, M. W. & WRIGHT, E. M. 1991. Ontogenic development of lamb intestinal sodium-glucose co-transporter is regulated by diet. *J Physiol,* 437**,** 699-708.

SHIRAZI-BEECHEY, S. P., MORAN, A. W., BATCHELOR, D. J., DALY, K. & AL-RAMMAHI, M. 2011a. Glucose sensing and signalling; regulation of intestinal glucose transport. *Proc Nutr Soc,* 70**,** 185-93.

SHIRAZI-BEECHEY, S. P., MORAN, A. W., BRAVO, D. & AL-RAMMAHI, M. 2011b. Intestinal glucose sensing and regulation of glucose absorption: implications for swine nutrition. *J Anim Sci*.

SHIRAZI-BEECHEY, S. P., MORAN, A. W., BRAVO, D. & AL-RAMMAHI, M. 2011c. Nonruminant Nutrition Symposium: intestinal glucose sensing and regulation of glucose absorption: implications for swine nutrition. *J Anim Sci,* 89**,** 1854-62.

SIMA, A. A. 2006. Pathological mechanisms involved in diabetic neuropathy: can we slow the process? *Curr Opin Investig Drugs,* 7**,** 324-37.

SIMILA, S., KOKKONEN, J. & KOUVALAINEN, K. 1982. Use of lactose-hydrolyzed human milk in congenital lactase deficiency. *J Pediatr,* 101**,** 584-5.

SINGH, N., VRONTAKIS, M., PARKINSON, F. & CHELIKANI, P. 2011. Functional bitter taste receptors are expressed in brain cells. *Biochem Biophys Res Commun,* 406**,** 146-51.

SINGH, S. K., BARTOO, A. C., KRISHNAN, S., BOYLAN, M. O., SCHWARTZ, J. H. & MICHAEL WOLFE, M. 2008. Glucose-dependent insulinotropic polypeptide (GIP) stimulates transepithelial glucose transport. *Obesity (Silver Spring),* 16**,** 2412-6.

SJOLUND, K., SANDEN, G., HAKANSON, R. & SUNDLER, F. 1983. Endocrine cells in human intestine: an immunocytochemical study. *Gastroenterology,* 85**,** 1120-30.

SKOVBJERG, H., SJOSTROM, H. & NOREN, O. 1981. Purification and characterisation of amphiphilic lactase/phlorizin hydrolase from human small intestine. *Eur J Biochem,* 114**,** 653-61.

SMITH, M. W. 1985. Expression of digestive and absorptive function in differentiating enterocytes. *Annu Rev Physiol,* 47**,** 247-60.

SMITH, M. W., PEACOCK, M. A. & JAMES, P. S. 1991. Galactose increases microvillus development in mouse jejunal enterocytes. *Comp Biochem Physiol A Comp Physiol,* 100**,** 489-93.

SOLBERG, D. H. & DIAMOND, J. M. 1987. Comparison of different dietary sugars as inducers of intestinal sugar transporters. *Am J Physiol,* 252**,** G574-84.

SORENSEN, S. H., NOREN, O., SJOSTROM, H. & DANIELSEN, E. M. 1982. Amphiphilic pig intestinal microvillus maltase/glucoamylase. Structure and specificity. *Eur J Biochem,* 126**,** 559-68.

SPECIAN, R. D. & OLIVER, M. G. 1991. Functional biology of intestinal goblet cells. *Am J Physiol,* 260**,** C183-93.

STEARNS, A. T., BALAKRISHNAN, A., RHOADS, D. B., ASHLEY, S. W. & TAVAKKOLIZADEH, A. 2009. Diurnal expression of the rat intestinal sodium-glucose cotransporter 1 (SGLT1) is independent of local luminal factors. *Surgery,* 145**,** 294-302.

STEARNS, A. T., BALAKRISHNAN, A., RHOADS, D. B. & TAVAKKOLIZADEH, A. 2010. Rapid upregulation of sodium-glucose transporter SGLT1 in response to intestinal sweet taste stimulation. *Ann Surg,* 251**,** 865-71.

STERNINI, C., ANSELMI, L. & ROZENGURT, E. 2008. Enteroendocrine cells: a site of 'taste' in gastrointestinal chemosensing. *Curr Opin Endocrinol Diabetes Obes,* 15**,** 73-8.

STEVENS, B. R., FERNANDEZ, A., HIRAYAMA, B., WRIGHT, E. M. & KEMPNER, E. S. 1990. Intestinal brush border membrane Na+/glucose cotransporter functions in situ as a homotetramer. *Proc Natl Acad Sci U S A,* 87**,** 1456-60.

STEVENS, B. R., KAUNITZ, J. D. & WRIGHT, E. M. 1984. Intestinal transport of amino acids and sugars: advances using membrane vesicles. *Annu Rev Physiol,* 46**,** 417-33.

STONER, G. D. 2005. Hyperosmolar hyperglycemic state. *Am Fam Physician,* 71**,** 1723-30.

STUMPEL, F., BURCELIN, R., JUNGERMANN, K. & THORENS, B. 2001. Normal kinetics of intestinal glucose absorption in the absence of GLUT2: evidence for a transport pathway requiring glucose phosphorylation and transfer into the endoplasmic reticulum. *Proc Natl Acad Sci U S A,* 98**,** 11330-5.

SUNDLER, F., EKBLAD, E., ABSOOD, A., HAKANSON, R., KOVES, K. & ARIMURA, A. 1992. Pituitary adenylate cyclase activating peptide: a novel vasoactive intestinal peptide-like neuropeptide in the gut. *Neuroscience,* 46**,** 439-54.

SURRENTI, C., RENZI, D., GARCEA, M. R., SURRENTI, E. & SALVADORI, G. 1993. Colonic vasoactive intestinal polypeptide in ulcerative colitis. *J Physiol Paris,* 87**,** 307-11.

SZKUDELSKI, T. 2001. The mechanism of alloxan and streptozotocin action in B cells of the rat pancreas. *Physiol Res,* 50**,** 537-46.

TAHRANI, A. A., BARNETT, A. H. & BAILEY, C. J. 2013. SGLT inhibitors in management of diabetes. *Lancet Diabetes Endocrinol,* 1**,** 140-51.

TAKATA, K. 1996. Glucose transporters in the transepithelial transport of glucose. *J Electron Microsc (Tokyo),* 45**,** 275-84.

TAKATA, K., KASAHARA, T., KASAHARA, M., EZAKI, O. & HIRANO, H. 1992. Immunohistochemical localization of Na(+)-dependent glucose transporter in rat jejunum. *Cell Tissue Res,* 267**,** 3-9.

TAKEDA, J., KAYANO, T., FUKOMOTO, H. & BELL, G. I. 1993. Organization of the human GLUT2 (pancreatic beta-cell and hepatocyte) glucose transporter gene. *Diabetes,* 42**,** 773-7.

TAKEDA, J., SEINO, Y., TANAKA, K., FUKUMOTO, H., KAYANO, T., TAKAHASHI, H., MITANI, T., KURONO, M., SUZUKI, T., TOBE, T. & ET AL. 1987. Sequence of an intestinal cDNA encoding human gastric inhibitory polypeptide precursor. *Proc Natl Acad Sci U S A,* 84**,** 7005-8.

TARPEY, P. S., WOOD, I. S., SHIRAZI-BEECHEY, S. P. & BEECHEY, R. B. 1995. Amino acid sequence and the cellular location of the Na(+)-dependent D-glucose symporters (SGLT1) in the ovine enterocyte and the parotid acinar cell. *Biochem J,* 312 (Pt 1)**,** 293-300.

TAVARES, W., DRUCKER, D. J. & BRUBAKER, P. L. 2000. Enzymatic- and renal-dependent catabolism of the intestinotropic hormone glucagon-like peptide-2 in rats. *Am J Physiol Endocrinol Metab,* 278**,** E134-9.

TAZAWA, S., YAMATO, T., FUJIKURA, H., HIRATOCHI, M., ITOH, F., TOMAE, M., TAKEMURA, Y., MARUYAMA, H., SUGIYAMA, T., WAKAMATSU, A., ISOGAI, T. & ISAJI, M. 2005. SLC5A9/SGLT4, a new Na+-dependent glucose transporter, is an essential transporter for mannose, 1,5-anhydro-D-glucitol, and fructose. *Life Sci,* 76**,** 1039-50.

THEODORSSON, E., SMEDFORS, B., HELLSTROM, P., SODER, O., ALY, A., MUSAT, A., PANJA, A. B. & JOHANSSON, C. 1991. Aspects on the role of tachykinins and vasoactive intestinal polypeptide in control of secretion, motility and blood flow in the gut. *Adv Exp Med Biol,* 298**,** 233-40.

THOMPSON, C. S. & DEBNAM, E. S. 1986. Hyperglucagonaemia: effects on active nutrient uptake by the rat jejunum. *J Endocrinol,* 111**,** 37-42.

THOMSON, A. B., CHEESEMAN, C. I., KEELAN, M., FEDORAK, R. & CLANDININ, M. T. 1994. Crypt cell production rate, enterocyte turnover time and appearance of transport along the jejunal villus of the rat. *Biochim Biophys Acta,* 1191**,** 197-204.

THOMSON, A. B. & WILD, G. 1997. Adaptation of intestinal nutrient transport in health and disease. Part I. *Dig Dis Sci,* 42**,** 453-69.

THORENS, B., CHARRON, M. J. & LODISH, H. F. 1990a. Molecular physiology of glucose transporters. *Diabetes Care,* 13**,** 209-18.

THORENS, B., CHENG, Z. Q., BROWN, D. & LODISH, H. F. 1990b. Liver glucose transporter: a basolateral protein in hepatocytes and intestine and kidney cells. *Am J Physiol,* 259**,** C279-85.

THORENS, B. & MUECKLER, M. 2010. Glucose transporters in the 21st Century. *Am J Physiol Endocrinol Metab,* 298**,** E141-5.

THULESEN, J. 2004. Glucagon-like peptide 2 (GLP-2), an intestinotrophic mediator. *Curr Protein Pept Sci,* 5**,** 51-65.

TIEDGE, M. & LENZEN, S. 1991. Regulation of glucokinase and GLUT-2 glucose-transporter gene expression in pancreatic B-cells. *Biochem J,* 279 (Pt 3)**,** 899-901.

TIZZANO, M., GULBRANSEN, B. D., VANDENBEUCH, A., CLAPP, T. R., HERMAN, J. P., SIBHATU, H. M., CHURCHILL, M. E., SILVER, W. L., KINNAMON, S. C. & FINGER, T. E. 2010. Nasal chemosensory cells use bitter taste signaling to detect irritants and bacterial signals. *Proc Natl Acad Sci U S A,* 107**,** 3210-5.

TOLHURST, G., REIMANN, F. & GRIBBLE, F. M. 2012. Intestinal sensing of nutrients. *Handb Exp Pharmacol***,** 309-35.

TOLOZA, E. M. & DIAMOND, J. 1992. Ontogenetic development of nutrient transporters in rat intestine. *Am J Physiol,* 263**,** G593-604.

TORNIAINEN, S., SAVILAHTI, E. & JARVELA, I. 2009. [Congenital lactase deficiency--a more common disease than previously thought?]. *Duodecim,* 125**,** 766-70.

TORTOR G. J. AND DERRICKSON B 2006. principles of anatomy and physiology. *In:* SONS, J. W. A. (ed.) *principles of anatomy and physiology.* 11 ed. USA: John wiley and Sons.

TUIN, A., POELSTRA, K., DE JAGER-KRIKKEN, A., BOK, L., RAABEN, W., VELDERS, M. P. & DIJKSTRA, G. 2009. Role of alkaline phosphatase in colitis in man and rats. *Gut,* 58**,** 379-87.

TURK, E., KLISAK, I., BACALLAO, R., SPARKES, R. S. & WRIGHT, E. M. 1993. Assignment of the human Na+/glucose cotransporter gene SGLT1 to chromosome 22q13.1. *Genomics,* 17**,** 752-4.

TURK, E., MARTIN, M. G. & WRIGHT, E. M. 1994. Structure of the human Na+/glucose cotransporter gene SGLT1. *J Biol Chem,* 269**,** 15204-9.

TURK, E. & WRIGHT, E. M. 1997. Membrane topology motifs in the SGLT cotransporter family. *J Membr Biol,* 159**,** 1-20.

TURK, E., ZABEL, B., MUNDLOS, S., DYER, J. & WRIGHT, E. M. 1991. Glucose/galactose malabsorption caused by a defect in the Na+/glucose cotransporter. *Nature,* 350**,** 354-6.

TURNER, N. C., STRAUSS, S. J., SARKER, D., GILLMORE, R., KIRKWOOD, A., HACKSHAW, A., PAPADOPOULOU, A., BELL, J., KAYANI, I., TOUMPANAKIS, C., GRILLO, F., MAYER, A., HOCHHAUSER, D., BEGENT, R. H., CAPLIN, M. E. & MEYER, T. 2010. Chemotherapy with 5-fluorouracil, cisplatin and streptozocin for neuroendocrine tumours. *Br J Cancer,* 102**,** 1106-12.

UCHIDA, N., SAKAMOTO, O., IRIE, M., ABUKAWA, D., TAKEYAMA, J., KURE, S. & TSUCHIYA, S. 2012. Two novel mutations in the lactase gene in a Japanese infant with congenital lactase deficiency. *Tohoku J Exp Med,* 227**,** 69-72.

UDDMAN, R., LUTS, A., ARIMURA, A. & SUNDLER, F. 1991. Pituitary adenylate cyclase-activating peptide (PACAP), a new vasoactive intestinal peptide (VIP)-like peptide in the respiratory tract. *Cell Tissue Res,* 265**,** 197-201.

UETA, K., ISHIHARA, T., MATSUMOTO, Y., OKU, A., NAWANO, M., FUJITA, T., SAITO, A. & ARAKAWA, K. 2005. Long-term treatment with the Na+-glucose cotransporter inhibitor T-1095 causes sustained improvement in hyperglycemia and prevents diabetic neuropathy in Goto-Kakizaki Rats. *Life Sci,* 76**,** 2655-68.

ULDRY, M., IBBERSON, M., HORISBERGER, J. D., CHATTON, J. Y., RIEDERER, B. M. & THORENS, B. 2001. Identification of a mammalian H(+)-myo-inositol symporter expressed predominantly in the brain. *Embo j,* 20**,** 4467-77.

ULDRY, M., IBBERSON, M., HOSOKAWA, M. & THORENS, B. 2002. GLUT2 is a high affinity glucosamine transporter. *FEBS Lett,* 524**,** 199-203.

VADLAPUDI, A. D., VADLAPATLA, R. K. & MITRA, A. K. 2012. Sodium dependent multivitamin transporter (SMVT): a potential target for drug delivery. *Curr Drug Targets,* 13**,** 994-1003.

VAIDEHI, N., FLORIANO, W. B., TRABANINO, R., HALL, S. E., FREDDOLINO, P., CHOI, E. J., ZAMANAKOS, G. & GODDARD, W. A., 3RD 2002. Prediction of structure and function of G protein-coupled receptors. *Proc Natl Acad Sci U S A,* 99**,** 12622-7.

VAISHNAVA, S. & HOOPER, L. V. 2007. Alkaline phosphatase: keeping the peace at the gut epithelial surface. *Cell Host Microbe,* 2**,** 365-7.

VALENKEVICH, L. N. & IAKHONTOVA, O. I. 1996. [Carbohydrate hydrolysis and absorption in the human small intestine in aging]. *Fiziol Zh Im I M Sechenova,* 82**,** 111-6.

VAN CAUTER, E., POLONSKY, K. S. & SCHEEN, A. J. 1997. Roles of circadian rhythmicity and sleep in human glucose regulation. *Endocr Rev,* 18**,** 716-38.

VAVRA, J. J., DEBOER, C., DIETZ, A., HANKA, L. J. & SOKOLSKI, W. T. 1959. Streptozotocin, a new antibacterial antibiotic. *Antibiot Annu,* 7**,** 230-5.

VAYRO, S., LO, B. & SILVERMAN, M. 1998. Functional studies of the rabbit intestinal Na+/glucose carrier (SGLT1) expressed in COS-7 cells: evaluation of the mutant A166C indicates this region is important for Na+-activation of the carrier. *Biochem J,* 332 (Pt 1)**,** 119-25.

VAYRO, S., WOOD, I. S., DYER, J. & SHIRAZI-BEECHEY, S. P. 2001. Transcriptional regulation of the ovine intestinal Na+/glucose cotransporter SGLT1 gene. Role of HNF-1 in glucose activation of promoter function. *Eur J Biochem,* 268**,** 5460-70.

VAZQUEZ, C. M., ROVIRA, N., RUIZ-GUTIERREZ, V. & PLANAS, J. M. 1997. Developmental changes in glucose transport, lipid composition, and fluidity of jejunal BBM. *Am J Physiol,* 273**,** R1086-93.

VENIEN, C., AUBRY, M., CRINE, P. & LE GRIMELLEC, C. 1988. Determination of brush border membrane vesicle orientation using monoclonal antibodies recognizing extracytoplasmic and cytoplasmic domains of neutral endopeptidase-24.11. *Analytical biochemistry,* 174**,** 325-30.

VERA, J. C., RIVAS, C. I., FISCHBARG, J. & GOLDE, D. W. 1993. Mammalian facilitative hexose transporters mediate the transport of dehydroascorbic acid. *Nature,* 364**,** 79-82.

VERNE, G. N. & SNINSKY, C. A. 1998. Diabetes and the gastrointestinal tract. *Gastroenterol Clin North Am,* 27**,** 861-74, vi-vii.

VINCENZINI, M. T., IANTOMASI, T., STIO, M., FAVILLI, F., VANNI, P., TONELLI, F. & TREVES, C. 1989. Glucose transport during ageing by human intestinal brush-border membrane vesicles. *Mech Ageing Dev,* 48**,** 33-41.

WADDELL, I. D., ZOMERSCHOE, A. G., VOICE, M. W. & BURCHELL, A. 1992. Cloning and expression of a hepatic microsomal glucose transport protein. Comparison with liver plasma-membrane glucose-transport protein GLUT 2. *Biochem J,* 286 (Pt 1)**,** 173-7.

WAGMAN, A. S. & NUSS, J. M. 2001. Current therapies and emerging targets for the treatment of diabetes. *Curr Pharm Des,* 7**,** 417-50.

WANG, Z. & GLEICHMANN, H. 1995. Glucose transporter 2 expression: prevention of streptozotocin-induced reduction in beta-cells with 5-thio-D-glucose. *Exp Clin Endocrinol Diabetes,* 103 Suppl 2**,** 83-97.

WANG, Z. & GLEICHMANN, H. 1998. GLUT2 in pancreatic islets: crucial target molecule in diabetes induced with multiple low doses of streptozotocin in mice. *Diabetes,* 47**,** 50-6.

WASHBURN, W. N. 2012. Sodium glucose co-transporter 2 (SGLT2) inhibitors: novel antidiabetic agents. *Expert Opin Ther Pat,* 22**,** 483-94.

WEINSTEIN, S. P., O'BOYLE, E., FISHER, M. & HABER, R. S. 1994. Regulation of GLUT2 glucose transporter expression in liver by thyroid hormone: evidence for hormonal regulation of the hepatic glucose transport system. *Endocrinology,* 135**,** 649-54.

WELLS, R. G., MOHANDAS, T. K. & HEDIGER, M. A. 1993. Localization of the Na+/glucose cotransporter gene SGLT2 to human chromosome 16 close to the centromere. *Genomics,* 17**,** 787-9.

WILCOX, G. 2005. Insulin and insulin resistance. *Clin Biochem Rev,* 26**,** 19-39.

WILSON, G. L., PATTON, N. J., MCCORD, J. M., MULLINS, D. W. & MOSSMAN, B. T. 1984. Mechanisms of streptozotocin- and alloxan-induced damage in rat B cells. *Diabetologia,* 27**,** 587-91.

WILSON, T. H. & WISEMAN, G. 1954. The use of sacs of everted small intestine for the study of the transference of substances from the mucosal to the serosal surface. *J Physiol,* 123**,** 116-25.

WILSON-O'BRIEN, A. L., PATRON, N. & ROGERS, S. 2010. Evolutionary ancestry and novel functions of the mammalian glucose transporter (GLUT) family. *BMC Evol Biol,* 10**,** 152.

WOOD, I. S., DYER, J., HOFMANN, R. R. & SHIRAZI-BEECHEY, S. P. 2000. Expression of the Na+/glucose co-transporter (SGLT1) in the intestine of domestic and wild ruminants. *Pflugers Arch,* 441**,** 155-62.

WOOD, I. S. & TRAYHURN, P. 2003. Glucose transporters (GLUT and SGLT): expanded families of sugar transport proteins. *Br J Nutr,* 89**,** 3-9.

WRIGHT, E. 2006. Sugar absorption. . *In:* LR JOHNSON, K. B., FK GHISHAN, JL MERCHANT, HM SAID, AND JD WOOD (ed.) *In physiology of the gastrointestinal tract* 4 th ed. San Diego: Elsevier Academic Press.

WRIGHT, E. M. 1993. The intestinal Na+/glucose cotransporter. *Annu Rev Physiol,* 55**,** 575-89.

WRIGHT, E. M. 1998. I. Glucose galactose malabsorption. *Am J Physiol,* 275**,** G879-82.

WRIGHT, E. M. 2001. Renal Na(+)-glucose cotransporters. *Am J Physiol Renal Physiol,* 280**,** F10-8.

WRIGHT, E. M., HIRAYAMA, B. A. & LOO, D. F. 2007. Active sugar transport in health and disease. *J Intern Med,* 261**,** 32-43.

WRIGHT, E. M., HIRSCH, J. R., LOO, D. D. & ZAMPIGHI, G. A. 1997. Regulation of Na+/glucose cotransporters. *J Exp Biol,* 200**,** 287-93.

WRIGHT, E. M. & LOO, D. D. 2000. Coupling between Na+, sugar, and water transport across the intestine. *Ann N Y Acad Sci,* 915**,** 54-66.

WRIGHT, E. M., LOO, D. D., HIRAYAMA, B. A. & TURK, E. 2004. Surprising versatility of Na+-glucose cotransporters: SLC5. *Physiology (Bethesda),* 19**,** 370-6.

WRIGHT, E. M., LOO, D. D., PANAYOTOVA-HEIERMANN, M., HIRAYAMA, B. A., TURK, E., ESKANDARI, S. & LAM, J. T. 1998. Structure and function of the Na+/glucose cotransporter. *Acta Physiol Scand Suppl,* 643**,** 257-64.

WRIGHT, E. M., MARTIN, M. G. & TURK, E. 2003. Intestinal absorption in health and disease--sugars. *Best Pract Res Clin Gastroenterol,* 17**,** 943-56.

WRIGHT, E. M. & TURK, E. 2004. The sodium/glucose cotransport family SLC5. *Pflugers Arch,* 447**,** 510-8.

WRIGHT, E. M., TURK, E., HAGER, K., LESCALE-MATYS, L., HIRAYAMA, B., SUPPLISSON, S. & LOO, D. D. 1992. The Na+/glucose cotransporter (SGLT1). *Acta Physiol Scand Suppl,* 607**,** 201-7.

WRIGHT, E. M., TURK, E. & MARTIN, M. G. 2002. Molecular basis for glucose-galactose malabsorption. *Cell Biochem Biophys,* 36**,** 115-21.

WU, S. V., ROZENGURT, N., YANG, M., YOUNG, S. H., SINNETT-SMITH, J. & ROZENGURT, E. 2002a. Expression of bitter taste receptors of the T2R family in the gastrointestinal tract and enteroendocrine STC-1 cells. *Proc Natl Acad Sci U S A,* 99**,** 2392-7.

WU, X. & FREEZE, H. H. 2002. GLUT14, a duplicon of GLUT3, is specifically expressed in testis as alternative splice forms. *Genomics,* 80**,** 553-7.

WU, X., LI, W., SHARMA, V., GODZIK, A. & FREEZE, H. H. 2002b. Cloning and characterization of glucose transporter 11, a novel sugar transporter that is alternatively spliced in various tissues. *Mol Genet Metab,* 76**,** 37-45.

XIAO, Q., BOUSHEY, R. P., DRUCKER, D. J. & BRUBAKER, P. L. 1999. Secretion of the intestinotropic hormone glucagon-like peptide 2 is differentially regulated by nutrients in humans. *Gastroenterology,* 117**,** 99-105.

YABE, D. & SEINO, Y. 2011. Two incretin hormones GLP-1 and GIP: comparison of their actions in insulin secretion and beta cell preservation. *Prog Biophys Mol Biol,* 107**,** 248-56.

YADA, T., SAKURADA, M., IHIDA, K., NAKATA, M., MURATA, F., ARIMURA, A. & KIKUCHI, M. 1994. Pituitary adenylate cyclase activating polypeptide is an extraordinarily potent intra-pancreatic regulator of insulin secretion from islet beta-cells. *J Biol Chem,* 269**,** 1290-3.

YANG, C., ALBIN, D. M., WANG, Z., STOLL, B., LACKEYRAM, D., SWANSON, K. C., YIN, Y., TAPPENDEN, K. A., MINE, Y., YADA, R. Y., BURRIN, D. G. & FAN, M. Z. 2010. Apical Na+-D-glucose co-transporter 1 (SGLT1) activity and protein abundance are expressed along the jejunal crypt-villus axis in the neonatal pig. *Am J Physiol Gastrointest Liver Physiol*.

YANG, C., ALBIN, D. M., WANG, Z., STOLL, B., LACKEYRAM, D., SWANSON, K. C., YIN, Y., TAPPENDEN, K. A., MINE, Y., YADA, R. Y., BURRIN, D. G. & FAN, M. Z. 2011. Apical Na+-D-glucose cotransporter 1 (SGLT1) activity and protein abundance are expressed along the jejunal crypt-villus axis in the neonatal pig. *Am J Physiol Gastrointest Liver Physiol,* 300**,** G60-70.

YOUNOSZAI, M. K. & SCHEDL, H. P. 1972. Effect of diabetes on intestinal disaccharidase activities. *J Lab Clin Med,* 79**,** 579-86.

ZAMBROWICZ, B., FREIMAN, J., BROWN, P. M., FRAZIER, K. S., TURNAGE, A., BRONNER, J., RUFF, D., SHADOAN, M., BANKS, P., MSEEH, F., RAWLINS, D. B., GOODWIN, N. C., MABON, R., HARRISON, B. A., WILSON, A., SANDS, A. & POWELL, D. R. 2012. LX4211, a dual SGLT1/SGLT2 inhibitor, improved glycemic control in patients with type 2 diabetes in a randomized, placebo-controlled trial. *Clin Pharmacol Ther,* 92**,** 158-69.

ZECCA, L., MESONERO, J. E., STUTZ, A., POIREE, J. C., GIUDICELLI, J., CURSIO, R., GLOOR, S. M. & SEMENZA, G. 1998. Intestinal lactase-phlorizin hydrolase (LPH): the two catalytic sites; the role of the pancreas in pro-LPH maturation. *FEBS Lett,* 435**,** 225-8.

ZEUTHEN, T., MEINILD, A. K., KLAERKE, D. A., LOO, D. D., WRIGHT, E. M., BELHAGE, B. & LITMAN, T. 1997. Water transport by the Na+/glucose cotransporter under isotonic conditions. *Biol Cell,* 89**,** 307-12.

ZHANG, H., MALO, C. & BUDDINGTON, R. K. 1997. Suckling induces rapid intestinal growth and changes in brush border digestive functions of newborn pigs. *The Journal of nutrition,* 127**,** 418-26.

ZHANG, Y., HOON, M. A., CHANDRASHEKAR, J., MUELLER, K. L., COOK, B., WU, D., ZUKER, C. S. & RYBA, N. J. 2003. Coding of sweet, bitter, and umami tastes: different receptor cells sharing similar signaling pathways. *Cell,* 112**,** 293-301.

ZHAO, F. Q. & KEATING, A. F. 2007a. Expression and regulation of glucose transporters in the bovine mammary gland. *J Dairy Sci,* 90 Suppl 1**,** E76-86.

ZHAO, F. Q. & KEATING, A. F. 2007b. Functional properties and genomics of glucose transporters. *Curr Genomics,* 8**,** 113-28.

ZHAO, F. Q., MILLER, P. J., WALL, E. H., ZHENG, Y. C., DONG, B., NEVILLE, M. C. & MCFADDEN, T. B. 2004. Bovine glucose transporter GLUT8: cloning, expression, and developmental regulation in mammary gland. *Biochim Biophys Acta,* 1680**,** 103-13.

ZHAO, F. Q., ZHENG, Y. C., WALL, E. H. & MCFADDEN, T. B. 2005. Cloning and expression of bovine sodium/glucose cotransporters. *J Dairy Sci,* 88**,** 182-94.

ZHAO, J., YANG, J. & GREGERSEN, H. 2003. Biomechanical and morphometric intestinal remodelling during experimental diabetes in rats. *Diabetologia,* 46**,** 1688-97.

ZHOU, L., CRYAN, E. V., D'ANDREA, M. R., BELKOWSKI, S., CONWAY, B. R. & DEMAREST, K. T. 2003. Human cardiomyocytes express high level of Na+/glucose cotransporter 1 (SGLT1). *J Cell Biochem,* 90**,** 339-46.